DEPARTAMENTO DE INGENIERÍA TEXTIL Y PAPELERA

UNIVERSIDAD POLITÉCNICA DE VALENCIA

DESARROLLO Y CARACTERIZACIÓN DE ELECTRODOS CATALÍTICOS BASADOS EN POLÍMEROS CONDUCTORES DE POLIPIRROL Y POLIANILINA SOBRE DIFERENTES SUSTRATOS

TESIS DOCTORAL

Autor: Javier Molina Puerto

Directores de Tesis: Dr. D. Francisco Javier Cases Iborra (U.P.V.)

Dr. D. José Antonio Bonastre Cano (U.P.V.)

Marzo 2011

Agradecimientos

En primer lugar deseo manifestar mi gratitud al Director del Departamento de Ingeniería Textil y Papelera, Dr. D. Francisco Cases Iborra, por introducirme en el mundo de la ciencia y poder llevar a cabo mi labor investigadora.

Mis agradecimientos a mis directores de Tesis Doctoral, Dr. D. Francisco Cases Iborra y Dr. D. José Antonio Bonastre Cano del Departamento de Ingeniería Textil y Papelera de Universidad Politécnica de Valencia por su apoyo incondicional y guía a la hora de llevar a cabo el presente trabajo de investigación. Al Dr. D. Francisco Cases Iborra por su dirección, indicaciones, explicaciones, rigurosidad y metodología. Al Dr. D. José Antonio Bonastre Cano por su ayuda y dirección, con sus valiosas aportaciones en todos los ámbitos y más concretamente en el estudio de la Espectroscopía de Impedancia Electroquímica y Espectroscopía Fotoelectrónica de Rayos-X.

Agradecer a la Generalitat Valenciana (Conselleria d'Educació) la concesión de la beca de formación de personal investigador (F.P.I.) sin la cual no habría podido realizar la tesis doctoral. Agradecer también a la Generalitat Valenciana (Conselleria d'Educació) la concesión de las ayudas para realizar estancias de investigación en el Centro Nacional de Investigaciones Metalúrgicas (CENIM-CSIC). Agradecer al Ministerio Ciencia y Tecnología y los Fondos de la Unión Europea (FEDER) (contrato CTM2007-66570-C02-02 y CTM2010-18842-C02-02) y la Universidad Politécnica de Valencia (Primeros Proyectos de Investigación (PAID-06-10)) por la financiación de los trabajos realizados.

Al Dr. D. Juan Carlos Galván Sierra, investigador científico del CENIM (Centro Nacional de Investigaciones Metalúrgicas) del CSIC por permitirme realizar dos estancias en el CENIM e introducirme en el mundo de la Espectroscopía de Impedancia Electroquímica, y por sus lecciones y apoyo en la investigación con dicha técnica electroquímica. Como no agradecer la grata acogida a todas las personas del CENIM, en especial de Juan Carlos Galván, Blanca Casal y Amir el Hadad.

Agradecer la confianza y ayuda de mis padres y mi familia durante todos estos años de estudiante, sin la cual no hubiera podido llegar a realizar esta tesis.

Agradecer a Javier Fernández la realización de las pruebas con Microscopía Electroquímica de Barrido. Agradecer a Juan López la realización de los análisis térmicos. Agradecer también a Manolo Zamorano la ayuda prestada a la hora de realizar los ensayos de lavado y resistencia al frote. A Rocío Lapuente por permitirnos realizar las medidas de XPS en la Universidad de Alicante. Al Servicio de Microscopía de Valencia por la ayuda prestada en los análisis de Microscopía Electrónica de Barrido.

Como no agradecer la compañía y amistad de todas las personas que han pasado por el laboratorio, por hacer más amena la estancia allí: Ana Isabel del Río, María José Benimeli, Javier Fernández, Eduardo Romero, Ángel García, Enrique Duval, Mireia Sala, Ana García, Lucas Santos-Juanes, Antonio Bernabéu, Juan Soler, y de las personas que me olvido.

Agradecer en especial a María José Benimeli su amistad y por compartir la mayoría del camino de la tesis, y por escucharme siempre que le hablaba de la tesis.

Agradecer como no a todos mis amigos su apoyo e interés por la tesis, aunque a veces no se enteraran de lo que les contaba.

Como es difícil nombrar a todas las personas que me han ayudado en estos años dedicados a la investigación, deseo expresar mi gratitud al Departamento de Ingeniería Textil y Papelera de la Universidad Politécnica de Valencia cuyo programa de doctorado he realizado y que me ha permitido desarrollar el trabajo experimental en sus instalaciones. Agradecer también toda la ayuda de Macu de Mora durante todos estos años. Agradecer también al Centro Nacional de Investigaciones Metalúrgicas por su grata acogida durante mis estancias en el CENIM-CSIC.

Finalmente agradecer a todas las personas que directa o indirectamente me han conducido por este camino.

A mis padres.

DESARROLLO Y CARACTERIZACIÓN DE ELECTRODOS CATALÍTICOS BASADOS EN POLÍMEROS CONDUCTORES DE POLIPIRROL Y POLIANILINA SOBRE DIFERENTES SUSTRATOS

Durante los últimos años el desarrollo de tejidos con nuevas propiedades ha sido un campo muy activo. Por ejemplo se han creado tejidos con propiedades termorreguladoras a partir de microcápsulas con materiales que cambian de fase, tejidos autolimpiables, tejidos con acabados hidrófobos, etc. Otro de los campos que se ha estado explorando es el de los tejidos conductores de la electricidad; sobre el cual trata la presente tesis. Se han desarrollado productos basados en tejidos conductores de la electricidad como por ejemplo: un MP3 integrado en una chaqueta, trajes con LEDS, camisetas para monitorizar el estado de los pacientes en los hospitales, etc. Este tipo de modificaciones en los tejidos crea un valor añadido en el producto final además de un creciente mercado que los hace muy interesantes dada la situación actual del sector textil. Se estimó que para el 2008 el campo de los tejidos para monitorizar el estado de los pacientes podía representar un mercado de entre 100 y 1000 millones de dólares.

Para la obtención de tejidos conductores de la electricidad, se han empleado tradicionalmente fibras metálicas integradas en los tejidos. El problema que plantean las fibras metálicas es que los movimientos de flexión, torsión y estiramiento que se dan en un tejido acaban por romper las fibras metálicas. Los polímeros conductores se plantean como una alternativa debido a su flexibilidad y su fácil síntesis sobre los tejidos. La polimerización química del pirrol en presencia de sustratos textiles produce una capa uniforme sobre todo el tejido de un espesor menor de 1 μm.

En el presente trabajo se han obtenido tejidos de poliéster recubiertos con polipirrol/ antraquinona sulfonato (AQSA) y polipirrol/ fosfotungstato ($PW_{12}O_{40}^{3-}$). El empleo de contraiones grandes como son el AQSA (orgánico) y el $PW_{12}O_{40}^{3-}$ (inorgánico) impediría la salida de los mismos de la estructura (desdopado) del polímero evitando la pérdida de propiedades eléctricas y electroquímicas. Una vez se obtiene un sustrato conductor (tejido conductor), se puede realizar la síntesis electroquímica de polímeros conductores (polipirrol y polianilina). El recubrimiento electroquímico mejora las propiedades eléctricas y electroquímicas del material. Los polímeros conductores han sido empleados en electrocatálisis para la eliminación de determinados

contaminantes, por lo que estos materiales podrían ser empleados en el tratamiento electroquímico de contaminantes como los colorantes orgánicos.

Tanto los tejidos conductores obtenidos químicamente como los recubiertos electroquímicamente se caracterizaron química, morfológica, eléctrica y electroquímicamente mediante las siguientes técnicas: Espectroscopía Infrarroja por Transformada de Fourier por Reflectancia Total Atenuada (FTIR-ATR), Energía Dispersiva de Rayos X (EDX), Espectroscopía Fotoelectrónica de Rayos X (XPS), Microscopía Electrónica de Barrido (SEM), medidas de resistividad superficial, Voltametría Cíclica (CV), Espectroscopía de Impedancia Electroquímica (EIS) y Microscopía Electroquímica de Barrido (SECM). La estabilidad de los recubrimientos de polipirrol sobre los tejidos fue evaluada mediante ensayos de abrasión y lavado. Se realizaron también pruebas de estabilidad de los recubrimientos con el pH para estudiar el cambio de sus propiedades y ver su rango de pH operacional donde mantiene unas propiedades eléctricas y electroquímicas aceptables.

Además, los polvos de polipirrol no depositados sobre los tejidos fueron caracterizados adicionalmente mediante las siguientes técnicas para estudiar su estabilidad frente a la temperatura: Espectroscopía de Impedancia Electroquímica con la temperatura, Termogravimetría (TG), Calorimetría Diferencial de Barrido (DSC), Pirólisis/ Cromatografía de Gases/ Espectrometría de Masas (Py-GC-MS).

Los tejidos conductores obtenidos mostraron una resistividad superficial en el rango de los 10^2 Ω/□, frente a >10^{10} Ω/□ que presenta el poliéster; lo que significa una disminución de ocho órdenes de magnitud. La caracterización química y morfológica demostró un recubrimiento uniforme y con buenas propiedades. En general los tejidos conductores presentaron una buena estabilidad al lavado así como con el pH. El ensayo de abrasión produjo una pérdida de parte del recubrimiento aunque sólo produjo un aumento de la resistividad superficial menor de lo que se podía esperar. La caracterización electroquímica demostró que la síntesis electroquímica produce recubrimientos más electroactivos. En la síntesis electroquímica de la polianilina se observó además la influencia del método de síntesis (potenciostático o potenciodinámico) en la microestructura del recubrimiento obtenido. En la síntesis potenciodinámica la velocidad de barrido se mostró también como una variable muy importante. A velocidades de barrido altas (50 mV·s^{-1} y 5 mV·s^{-1}) se ha podido

monitorizar con detalle el crecimiento del polímero. Así en las primeras etapas se ha detectado una morfología en forma de ciempiés para la polianilina, que no ha sido obtenida en bibliografía para los polímeros conductores.

DESENVOLUPAMENT I CARACTERITZACIÓ D'ELECTRODES CATALÍTICS BASATS EN POLÍMERS CONDUCTORS DE POLIPIRROL I POLIANILINA SOBRE DIFERENTS SUBSTRATS

Durant els últims anys el desenvolupament de teixits amb noves propietats ha sigut un camp molt actiu. Per exemple s'han creat teixits amb propietats termoreguladores a partir de microcràpsules amb materials que canvien de fase, teixits autonetejables, teixits amb acabats hidròfobs, etc. Un altre dels camps que s'ha estat explorant es el dels teixits conductors de l'electricitat; sobre el qual tracta la present tesi. S'han desenvolupat teixits conductors de l'electricitat com per exemple: un MP3 integrat en una jaqueta, vestits amb LEDS, camisetes per monitoritzar l'estat dels pacients a l'hospital, etc. Aquest tipus de modificacions en els teixits crea un valor afegit en el producte final a més a més d'un creixent mercat que els fa molt interessants donada la situació actual del sector tèxtil. Es va estimar que per a l'any 2008 el camp dels teixits per monitoritzar l'estat dels pacients podia representar un mercat d'entre 100 y 1000 milions de dòlars.

Per a l'obtenció de teixits conductors de l'electricitat, s'han emprat tradicionalment fibres metàl·liques integrades en els teixits. El problema que plantegen les fibres metàl·liques és que els moviments de flexió, torsió i estirament que es donen en un teixit acaben per trencar les fibres metàl·liques. Els polímers conductors es plantegen com una alternativa degut a la seua flexibilitat i la seua fàcil síntesi sobre els teixits. La polimerització química de pirrol en presència de substrats tèxtils produeix una capa uniforme sobre tot el teixit d'un espessor menor d'1 μm.

En el present treball s'han obtingut teixits de polièster recoberts amb polipirrol/ antraquinona sulfonat (AQSA) y polipirrol/ fosfotungstat ($PW_{12}O_{40}^{3-}$). L'ús de contraions grans como són l'AQSA (orgànic) y el $PW_{12}O_{40}^{3-}$ (inorgànic) impediria l'eixida dels mateixos de l'estructura (desdopat) del polímer evitant la pèrdua de propietats elèctriques i electroquímiques. Una vegada s'obté un substrat conductor (teixit conductor), es pot realitzar la síntesis electroquímica de polímers conductors (polipirrol i polianilina). El recobriment electroquímic millora les propietats elèctriques i electroquímiques del material. Els polímers conductors han sigut usats en electrocatàlisi per a l'eliminació de determinats contaminants, pel que aquests materials podrien ser usats en el tractament electroquímic de contaminants com són els colorants orgànics.

Tant els teixits conductors obtinguts químicament com els recoberts electroquímicament s'han caracteritzat química, morfològica, elèctrica i electroquímicament mitjançant les següents tècniques: Espectroscopia Infrarroja per Transformada de Fourier amb Reflectància Total Atenuada (FTIR-ATR), Energia Dispersiva de Raigs X (EDX), Espectroscopia Fotoelectrònica de Raigs X (XPS), Microscopia Electrònica d'Escaneig (SEM), mesures de resistivitat superficial, Voltametria Cíclica (CV), Espectroscopia d'Impedància Electroquímica (EIS) i Microscopia Electroquímica d'Escaneig (SECM). L'estabilitat dels recobriments de polipirrol fou avaluada mitjançant assajos d'abrasió i llavat. Es realitzaren proves d'estabilitat dels recobriments amb el pH per estudiar el canvi de les seues propietats i veure el seu rang de pH operacional on manté unes propietats elèctriques i electroquímiques acceptables.

A més a més, la pols de polipirrol no depositada sobre els teixits va ser caracteritzada addicionalment mitjançant les següents tècniques per estudiar la seua estabilitat front a la temperatura: Espectroscopia d'Impedància Electroquímica amb la temperatura, Termogravimetria (TG), Calorimetria Diferencial d'Escaneig (DSC), Piròlisi/ Cromatografia de Gasos/ Espectrometria de Mases (Py-GC-MS).

El teixits conductors que es varen obtindre mostraren una resistivitat superficial en el rang dels 10^2 $\Omega/\square$, front a $>10^{10}$ $\Omega/\square$ que presenta el polièster; el que significa una disminució de huit ordres de magnitud. La caracterització química i morfològica va demostrar un recobriment uniforme i amb bones propietats. En general els teixits conductors varen presentar una bona estabilitat al llavat així com al pH. L'assaig d'abrasió va produir una pèrdua de part del recobriment encara que sols va produir un augment de la resistivitat superficial menor del que es podia esperar. La caracterització electroquímica va demostrar que la síntesi electroquímica produeix recobriments més electroactius. En la síntesi electroquímica de polianilina es va observar a més a més la influència del mètode de síntesi (potenciostàtic o potenciodinàmic) en la microestructura del recobriment obtingut. En la síntesi potenciodinàmica la velocitat d'escaneig es va mostrar també com una variable molt important. A velocitats d'escaneig altes (50 mV·s^{-1} y 5 mV·s^{-1}) s'ha pogut monitoritzar amb detall el creixement del polímer. Així en les primeres etapes s'ha detectat una morfologia amb forma de centpeus per a la polianilina, que no ha sigut obtinguda en bibliografia per als polímers conductors.

DEVELOPMENT AND CHARACTERIZATION OF CATALYTIC ELECTRODES BASED ON CONDUCTING POLYMERS OF POLYPYRROLE AND POLYANILINE ON DIFFERENTS SUBSTRATES

During the last years the development of textiles with new properties has been a very active field. For example textiles with thermoregulative properties have been created with microcapsules containing phase change materials, autocleaning textiles, textiles with hydrophobic coatings, etc. Another field that is being explored is the field of conducting textiles, which the present thesis treats about. Products based on conducting textiles have been created, for instance: a MP3 integrated in a jacket, dresses with LEDS, shirts to monitoring the conditions of the patients in the hospitals, etc. This sort of modifications in the textiles creates an extra value in the final product in addition to an increasing market that makes them very interesting in the present situation of the textile sector. It was estimated that for the year 2008, the field of the textiles to monitoring the conditions of the patients could represent a market between 100 and 1000 million dollars.

To obtain conducting textiles, metallic fibers integrated in the textiles have been traditionally employed. The problem with the metallic fibers is that the movements of bending, twisting and stretching that take place in a textile break the fibers. The conducting polymers are employed as an alternative due to its flexibility and ease of synthesis above the fabrics. The chemical polymerization of pyrrole in the presence of textile substrates produce a uniform coating on the textile with a thickness of less than 1 μm.

In the present work textiles of polyester covered with polypyrrole/ anthraquinone sulfonate (AQSA) and polypyrrole/ phosphotungstate ($PW_{12}O_{40}{}^{3-}$) have been obtained. The employment of counter ions with high size like the AQSA (organic) or the $PW_{12}O_{40}{}^{3-}$ (inorganic) would prevent the expulsion of the counter ions (dedoping) from the polypyrrole structure, avoiding the loss of electrical and electrochemical properties. Once a conducting substrate was obtained (conducting textile), an electrochemical synthesis of conducting polymers (polypyrrole and polyaniline) could be performed. The electrochemical coating improves the electrical and electrochemical properties of the material. Conducting polymers have been employed in electrocatalysis for the removal of

certain pollutants; this is why these materials could be employed in the electrochemical treatment of pollutants like organic dyes.

The conducting textiles obtained either chemically or electrochemically were characterized chemically, morphologically, electrically and electrochemically with the following techniques: Fourier Transform Infrared Spectroscopy with Attenuated Total Reflection (FTIR-ATR), Energy Dispersive X-Ray (EDX), X-Ray Photoelectron Spectroscopy (XPS), Scanning Electron Microscopy (SEM), measurements of surface resistivity, Cyclic Voltammetry (CV), Electrochemical Impedance Spectroscopy (EIS) and Scanning Electrochemical Microscopy (SECM). The stability of the coatings was tested with washing and friction tests. Tests of the stability in different pH solutions were also performed to study the changes of the properties and to see the operational range where the conducting textiles maintain an acceptable electrical and electrochemical properties.

Moreover, polypyrrole powders not deposited on the textiles were characterized additionally with the following techniques to study its stability with the temperature: Electrochemical Impedance Spectroscopy with the temperature, Termogravimetry (TG), Differential Scanning Calorimetry (DSC), Pyrolisis/ Gas Chromatography/ Mass Spectrometry (Py-GC-MS).

The conducting textiles showed values of surface resistivity in the range of 10^2 $\Omega/\square$, polyester presents values higher than 10^{10} $\Omega/\square$; what represents a decrease of eight orders of magnitude in the surface resistivity. The chemical and morphological characterization demonstrated the presence of a uniform layer with good properties. In general the conducting textiles presented a good stability with washing tests and with the pH. The friction assay produced a loss of part of the coating, however only an increase of the surface resistivity lower than the expected was obtained. The electrochemical characterization demonstrated that the electrochemical synthesis produces more electroactive coatings. Moreover in the electrochemical synthesis of polyaniline it was observed that the method of synthesis (potentiodynamic or potentiostatic) influences the microstructure of the coating obtained. It was demonstrated that in the potentiodynamic synthesis the scan rate was an important parameter. With high scan rates (50 mV·s^{-1} y 5 mV·s^{-1}) the polymer growth has been monitored with detail. In the first steps a coating with centipede-like morphology has been detected for polyaniline, this sort of morphology has not been obtained in bibliography for conducting polymers.

No entiendes realmente algo a menos que seas capaz de explicárselo a tu abuela.

Albert Einstein (1879-1955)

ÍNDICE

1.- PRESENTACIÓN

1.- PRESENTACIÓN

El presente estudio trata sobre la síntesis de polímeros conductores sobre materiales textiles y la evaluación de sus propiedades y sus posibles aplicaciones. La tesis se estructura en 17 capítulos principalmente. En el primer capítulo de "Presentación" se indica la estructura y contenido de la presente memoria.

En el segundo capítulo de "Introducción" se expone el estado del arte en referencia a la investigación llevada a cabo hasta la fecha en cuanto a los polímeros conductores y la síntesis de polímeros conductores sobre sustratos textiles. Se presentan también las diferentes variables que pueden influir en el proceso de síntesis, tales como tipos de sustrato, método de síntesis, oxidante, tipo de contraión, temperatura de síntesis, etc. Se presenta también bibliografía relacionada con la síntesis electroquímica de polímeros conductores y las microestructuras obtenidas en la síntesis de polímeros conductores.

En el capítulo tercero, "Hipótesis de Trabajo" se exponen las hipótesis de partida propuestas según los antecedentes y resultados previos concernientes a la presente investigación. Los objetivos de la investigación se detallan en el capítulo cuarto, presentándose a continuación en el capítulo quinto la metodología de trabajo empleada para llevar a cabo dichos objetivos.

En el capítulo sexto, "Diseño Experimental y Métodos" se exponen todas las técnicas experimentales utilizadas en la presente investigación así como los métodos y procedimientos empleados. Las técnicas empleadas han sido: Voltametría Cíclica (CV), medidas de resistividad superficial, Espectroscopía Infrarroja por Transformada de Fourier por Reflectancia Total Atenuada (FTIR-ATR), Microscopía Electrónica de Barrido (SEM), Energía Dispersiva de Rayos X (EDX), Espectroscopía Fotoelectrónica de Rayos-X (XPS), Espectroscopía de Impedancia Electroquímica (EIS), Espectroscopía de Impedancia Electroquímica con la temperatura, Microscopía Electroquímica de Barrido (SECM), Termogravimetría (TG), Calorimetría Diferencial de Barrido (DSC), Pirolisis/ Cromotografía de Gases/ Espectrometría de Masas (Py-GC-MS). Además de los ensayos de abrasión y lavado que fueron llevados a cabo para medir la durabilidad de las capas de polipirrol.

En el capítulo séptimo, octavo, noveno, décimo, undécimo, duodécimo y decimotercero, se presentan parte de los resultados obtenidos en la presente tesis. Los resultados se presentan en forma de artículos (5 publicados y 2 enviados), que han sido los siguientes:

1. Chemical and electrochemical polymerisation of pyrrole on polyester textiles in presence of phosphotungstic acid. **European Polymer Journal 44 (2008) 2087-2098.**

2. Chemical, electrical and electrochemical characterization of hybrid organic/inorganic polypyrrole/$PW_{12}O_{40}^{3-}$ coating deposited on polyester fabrics. **Artículo enviado a Applied Surface Science**.

3. Stability of conducting polyester/polypyrrole fabrics in different pH solutions. Chemical and electrochemical characterization. **Polymer Degradation and Stability 95 (2010) 2574-2583.**

4. Monitoring the polymerization process of polypyrrole films by thermogravimetric and X-ray analysis. **Journal of Thermal Analysis and Calorimetry 102 (2010) 695-701.**

5. Electrochemical characterization and influence of the temperature in the electrical properties of polypyrrole discs doped with organic and inorganic counter ions. **Artículo enviado a Materials Letters.**

6. Electrochemical polymerisation of aniline on conducting textiles of polyester covered with polypyrrole/AQSA. **European Polymer Journal 45 (2009) 1302-1315.**

7. Influence of the scan rate on the morphology of polyaniline grown on conducting fabrics. Centipede-like morphology. **Synthetic Metals 160 (2010) 99-107.**

En el capítulo decimocuarto se presenta un resumen de los resultados obtenidos. En el capítulo decimoquinto se exponen las conclusiones generales y en el

capítulo decimosexto se presenta el trabajo actualmente en curso, así como las experiencias futuras y nuevas líneas de trabajo surgidas a partir de la presente Tesis Doctoral.

Finalmente en el capítulo decimoséptimo se presentan las diferentes aportaciones a las que ha dado lugar la Tesis Doctoral.

Dado que los resultados de la tesis se presentan como artículos, con el fin de clarificar el contenido de cada artículo y poder seguir mejor los resultados de la tesis se presenta un breve resumen de cada artículo a continuación:

1. *Chemical and electrochemical polymerisation of pyrrole on polyester textiles in presence of phosphotungstic acid.* **European Polymer Journal 44 (2008) 2087-2098.**

    Resumen: En este artículo se presentan los resultados de la polimerización química de polipirrol/$PW_{12}O_{40}^{3-}$ y polipirrol/AQSA sobre tejidos de poliéster. Se realiza la caracterización de ambos tejidos conductores (PES-PPy/AQSA y PES-PPy/$PW_{12}O_{40}^{3-}$) mediante FTIR-ATR, SEM y EDX. Con el tejido de PES-PPy/$PW_{12}O_{40}^{3-}$ se realizan además ensayos de resistencia al lavado y al frote. Se realiza también la síntesis electroquímica de PPy/$PW_{12}O_{40}^{3-}$ sobre tejidos de PES-PPy/$PW_{12}O_{40}^{3-}$.

2. *Chemical, electrical and electrochemical characterization of hybrid organic/inorganic polypyrrole/$PW_{12}O_{40}^{3-}$ coating deposited on polyester fabrics.* **Artículo enviado a Applied Surface Science.**

    Resumen: En este artículo se presentan los resultados de caracterización del tejido de PES-PPy/$PW_{12}O_{40}^{3-}$ después de estar en contacto el tejido con disoluciones con diferente pH (1, 7, 13) y después de realizar ensayos de lavado. El fin del trabajo es comprobar la estabilidad del contraión en la estructura del polímero. Si el contraión es expulsado del polímero hay una pérdida de propiedades eléctricas. Mediante XPS se determinó el

contenido del contraión, así como el grado de dopaje (N$^+$/N) que nos da una indicación del grado de oxidación del polímero en los tejidos conductores. Las propiedades eléctricas después de cada ensayo se midieron mediante Espectroscopía de Impedancia Electroquímica (EIS). Se realizaron también medidas de electroactividad mediante Microscopía Electroquímica de Barrido después de los diferentes tests.

3. *Stability of conducting polyester/polypyrrole fabrics in different pH solutions. Chemical and electrochemical characterization.* **Polymer Degradation and Stability 95 (2010) 2574-2583.**

Resumen: En este artículo se presentan los resultados de caracterización del tejido de PES-PPy/AQSA después de estar en contacto el tejido con disoluciones con diferente pH (1, 7, 13) y después de realizar ensayos de lavado. El fin del trabajo es comprobar la estabilidad del AQSA en la estructura del polipirrol. Si el contraión es expulsado del polímero, hay una pérdida de propiedades eléctricas. Mediante XPS se determinó el contenido del contraión, así como el grado de dopaje (N$^+$/N) que nos da una indicación del grado de oxidación del polímero en los tejidos conductores. En este caso, mediante FTIR-ATR también se pudo obtener el contenido del contraión debido a la presencia de una banda atribuida al AQSA a 1670 cm^{-1}. Las propiedades eléctricas del tejido después de cada ensayo se midieron mediante Espectroscopía de Impedancia Electroquímica (EIS). Se realizaron también medidas de electroactividad mediante Microscopía Electroquímica de Barrido después de los diferentes test.

4. *Monitoring the polymerization process of polypyrrole films by thermogravimetric and X-ray analysis.* **Journal of Thernal Analysis and Calorimetry 102 (2010) 695-701.**

Resumen: En este artículo se presentan los resultados de caracterización de los polvos sobrantes de la síntesis química de polipirrol sobre los tejidos

(polvos de PPy/AQSA y PPy/$PW_{12}O_{40}{}^{3-}$). Se realiza la caracterización térmica mediante Termogravimetría, Calorimetría Diferencial de Barrido y Pirólisis/Cromatografía de Gases/Espectrometría de Masas. El empleo de un contraión inorgánico con alta estabilidad frente a la temperatura ($PW_{12}O_{40}{}^{3-}$) permite caracterizar la descomposición del polipirrol sin la interferencia de la degradación del contraión como ocurriría en el caso de emplear un contraión orgánico (por ejemplo AQSA). Mediante termogravimetría se puede obtener el contenido de contraión del polímero (sólo en el caso de empleo del $PW_{12}O_{40}{}^{3-}$), obteniendo resultados similares a los obtenidos mediante XPS.

5. *Electrical and electrochemical characterization of polypyrrole doped with organic and inorganic counter ions.* **Artículo enviado a Materials Letters.**

Resumen: En este artículo se presentan los resultados de caracterización de los polvos sobrantes de la síntesis química de polipirrol sobre los tejidos (polvos de PPy/AQSA y PPy/$PW_{12}O_{40}{}^{3-}$). Con los polvos sobrantes se obtienen discos de polipirrol después de realizar una compactación de los polvos con 10 toneladas. Se realiza un estudio de la influencia de la temperatura sobre la conductividad mediante Espectroscopía de Impedancia Electroquímica. La caracterización electroquímica se realizó mediante Microscopía Electroquímica de Barrido a partir de la obtención de curvas de aproximación. Los resultados se ajustaron a los modelos teóricos de un material conductor.

6. *Electrochemical polymerisation of aniline on conducting textiles of polyester covered with polypyrrole/AQSA.* **European Polymer Journal 45 (2009) 1302-1315.**

Resumen: En este artículo se estudia la obtención de dobles capas de polímeros conductores sobre tejidos de PES-PPy/AQSA. Para ello se deposita polianilina mediante síntesis potenciodinámica o mediante síntesis potenciostática. Los materiales obtenidos se caracterizaron

mediante FTIR-ATR, SEM, EDX, XPS, Voltametría Cíclica y Espectroscopía de Impedancia Electroquímica. Mediante síntesis potenciostática se obtuvo morfología globular. En cambio, mediante la síntesis potenciodinámica se observó la formación de polianilina con morfología fibrilar, lo que dio lugar al estudio del efecto de los parámetros de síntesis en el siguiente artículo.

7. *Influence of the scan rate on the morphology of polyaniline grown on conducting fabrics. Centipede-like morphology.* **Synthetic Metals 160 (2010) 99-107.**

Resumen: En este artículo se estudia la obtención de dobles capas de polímeros conductores sobre tejidos de PES-PPy/AQSA. Para ello se deposita polianilina mediante síntesis potenciodinámica y se estudia el efecto de la velocidad de barrido (1, 5 y 50 mV·s^{-1}) y el número de barrido en la morfología obtenida mediante síntesis potenciodinámica. Mediante SEM se ha podido observar la morfología de los depósitos obtenidos y además se ha podido monitorizar el crecimiento de la polianilina y proponer un mecanismo de crecimiento. Al principio se produce un crecimiento en una dimensión con la formación de microfibras, posteriormente se empieza a producir el crecimiento en dos dimensiones con la formación de polianilina en forma de ciempiés y finalmente en tres dimensiones con la formación de polianilina globular. La formación de polianilina con forma de ciempiés sólo se ha observado con altas velocidades de barrido (50 y 5 mV·s^{-1}), debido a la formación de un menor número de sitios de nucleación. Cuando el número de barridos aumenta, la aparición de un mayor número de sitios de nucleación hace predominar la polianilina con morfología globular. Con velocidades de barrido bajas (1 mV·s^{-1}), desde el principio se crean un mayor número de sitios de nucleación lo que hace predominar la polianilina con morfología fibrilar al principio y morfología globular después de un mayor número de barridos. Se realizó también la caracterización mediante voltametría cíclica y FTIR-ATR de los materiales obtenidos.

2.- INTRODUCCIÓN

2.- INTRODUCCIÓN

2.1. POLÍMEROS CONDUCTORES

Los polímeros han sido concebidos tradicionalmente como materiales aislantes y por ejemplo se usan para aislar los cables conductores en las instalaciones eléctricas [1]. Sin embargo el descubrimiento de los polímeros conductores de la electricidad cambió totalmente esta concepción. Los polímeros conductores son capaces de conducir la electricidad a través de su estructura debido a los enlaces conjugados que presentan.

Fruto de ello se concedió el premio Nobel de Química del año 2000 a los científicos Alan J. Heeger, Alan G. MacDiarmid y Hideki Shirakawa por "el descubrimiento y desarrollo de polímeros eléctricamente conductores" [1]. Realmente los polímeros conductores fueron descubiertos anteriormente, pero fue el descubrimiento del poliacetileno por parte de éstos científicos el que produjo un gran impulso en el campo de los polímeros conductores [2-5], al conseguir conductividades cercanas a las de los metales. La primera vez que se mencionaron las propiedades eléctricas de un polímero fue por parte de Letheby, en un trabajo de 1862 [6]. Letheby produjo polianilina a partir de la oxidación de anilina sobre una lámina de Pt. Posteriormente, las propiedades eléctricas del polipirrol fueron también descritas por Weiss y colaboradores en un estudio completo del año 1963 [7-9]. Sin embargo el año de la primera publicación en la que es considerado como polímero conductor es posterior para ambos polímeros como se puede observar en la Tabla 2.1. Durante las últimas tres décadas los estudios sobre polímeros conductores han experimentado un creciente interés como nuevos materiales revolucionarios. En la Tabla 2.1 se pueden observar los principales polímeros conductores, el año de la primera publicación como polímero conductor y la estructura de los principales polímeros conductores [10].

En la tabla 2.2. [11] se puede observar la conductividad de los principales polímeros conductores, así como su estabilidad en el estado dopado y su procesabilidad. El poliacetileno es el polímero más conductor, con una conductividad entre 10^3-10^5 Ω^{-1} cm^{-1}, cerca de la conductividad de los metales. Sin embargo el poliacetileno no es estable en el estado dopado y presenta limitaciones en el procesado.

Es por ello que polímeros menos conductores como el polipirrol y la polianilina son más empleados debido a su mayor estabilidad y procesabilidad.

El dopado de estos polímeros implica la introducción de huecos (dopado tipo-p) o de electrones (dopado tipo-n) en las cadenas conjugadas. La mayoría de los estudios realizados están relacionados con el comportamiento de los polímeros dopados tipo-p, como son: polianilina, polipirrol, politiofeno y sus derivados.
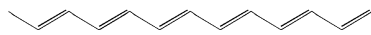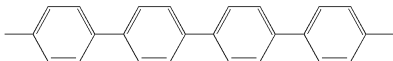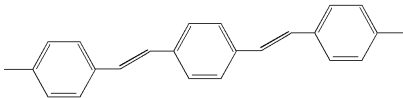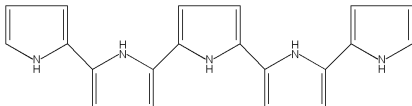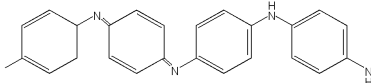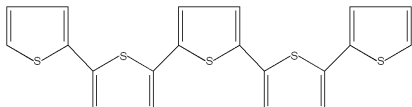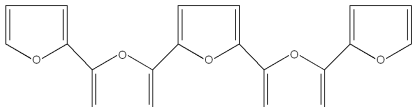
Polímero	Año	Estructura
Poliacetileno	1977	
Poli(p-fenileno)	1979	
Poli(p-fenilenovinileno)	1979	
Polipirrol	1979	
Polianilina	1980	
Politiofeno	1981	
Polifurano	1981	

Tabla 2.1. Estructuras esquemáticas y cronología de los principales polímeros conductores. (a) Año de la primera publicación como polímero conductor. (b) Estructuras lineales idealizadas, protonación, variaciones conformacionales, y a veces la ramificación añaden complejidad a estos polímeros.

Polímero	Conductividad $(\Omega^{-1} cm^{-1})$	Estabilidad en el estado dopado	Procesabilidad
Poliacetileno	10^3-10^5	Pobre	Limitada
Poli(p-fenileno)	10^3	Pobre	Limitada
Polipirrol	10^2	Buena	Buena
Politiofeno	10^2	Buena	Excelente
Polianilina	10^1	Buena	Buena

Tabla 2.2. Conductividad, estabilidad y procesabilidad de los principales polímeros conductores.

2.2. TEJIDOS CONDUCTORES DE LA ELECTRICIDAD [12]

La integración de la electrónica y los textiles empezó hace 80 años cuando se empleaban mantas eléctricas en medicina para que los pacientes de tuberculosis pudieran dormir en el exterior y respirar aire fresco. Las mantas eran una simple resistencia que calentaba el tejido. Sin embargo, los tejidos conductores hoy en día se obtienen tejiendo hilos conductores en el tejido, haciendo los tejidos conductores indistinguibles de un tejido tradicional.

En una versión actualizada de la antigua idea de las mantas eléctricas, el inventor británico Robert Rix, ha creado una línea de textiles conductores basados en carbono (Gorix), que ha sido incorporada por ejemplo desde los trajes de buceo hasta en los asientos de los coches. El tejido lleva una pequeña corriente eléctrica que se convierte en calor.

En 1996, Park y Sundaresan Jayaraman (ingeniero textil de Georgia Tech), lanzaron el campo de los tejidos médicos. Incorporaron fibras conductoras para que sensores de respiración, temperatura y ritmo cardiaco incorporados en el tejido pudieran funcionar. Crearon una camiseta en la que los sensores de monitorización pudieran ser conectados y desconectados para así poder lavarlas. Un estudio de DuPont realizado en el año 2003 estimó que la producción de tejidos conductores para monitorizar las constantes de los pacientes podría representar un mercado entre 100 y 1000 millones de dólares en el año 2008. La tecnología fue cedida a Sensatex, que posteriormente desarrolló una camiseta que podía transmitir la información sin la necesidad de cables. Esta nueva camiseta podría ser utilizada en el campo de la medicina, para monitorizar las constantes vitales de los bomberos, de los soldados durante la guerra o de los atletas de élite.

Otras aplicaciones que han sido desarrolladas son por ejemplo una chaqueta con un reproductor MP3 donde desde la manga de la chaqueta se controla el volumen, etc. Basado en el mismo principio, se ha desarrollado un teclado de piano sobre un tejido o vestidos iluminados con LEDS.

También se han desarrollado aplicaciones militares, por ejemplo para eliminar las antenas de 3 metros que hacían visibles a los soldados frente al enemigo; para ello se ha incorporado la antena en la ropa. Se ha desarrollado también un tejido que es capaz de localizar a los vehículos enemigos y calcular su posición basado en sensores acústicos. Con cables de cobre y sensores de sonido incorporados en el tejido, se calcula la diferencia de tiempos de llegada de un sonido y a partir de los datos un chip procesa los datos y triangula la posición de los vehículos enemigos.

En la mayoría de las aplicaciones mencionadas, se emplean fibras metálicas, debido a que son capaces de transportar una gran corriente eléctrica. El problema con las fibras metálicas es que los movimientos de doblado, extensión y torsión que se dan en los tejidos pueden producir la rotura de éstas produciendo un fallo en la alimentación o en los sensores. Para ello se utilizan circuitos redundantes, es decir en vez de colocar solo un cable, se colocan cuatro por ejemplo, haciendo que si uno se rompe queden otros tres que puedan hacer funcionar el tejido. Además del empleo de fibras metálicas mezclada con fibras no metálicas, otros métodos que han sido empleados para producir tejidos conductores han sido en empleo de fibras metalizadas [13], fibras extruidas con

partículas conductoras como carbono o el empleo de fibras o tejidos recubiertos por polímeros conductores. El último es el método que se ha empleado en la presente tesis para obtener tejidos conductores de la electricidad. Los conductores orgánicos son capaces de aguantar los movimientos de torsión, flexión o estiramiento, aunque la electricidad que son capaces de conducir es menor que con los conductores metálicos. Por ejemplo el empleo de conductores orgánicos para crear circuitos eléctricos ha sido desarrollado por diferentes investigadores [14-17].

2.3. TEJIDOS CONDUCTORES DE LA ELECTRICIDAD BASADOS EN POLÍMEROS CONDUCTORES

Aunque diversos polímeros conductores han sido utilizados para recubrir tejidos, la mayoría de las referencias en bibliografía emplean el polipirrol. Diferentes trabajos han empleado polianilina [18-21], politiofeno [22], poli-3-alquilpirrol [23, 24], nanotubos de carbono [25] o incluso grafeno [26] (el Premio Nobel de Física 2010, ha sido concedido a A.K. Geim y K.S. Novoselov por el descubrimiento del grafeno). El polipirrol posee una buena conductividad que lo hace apto para ser depositado sobre los sustratos textiles. En la referencia [27] se puede observar la evolución de las patentes de polimerización de pirrol sobre sustratos textiles desde su descubrimiento por Kuhn y colaboradores [28, 29]. A partir de estos trabajos diferentes artículos han sido publicados relacionados con la síntesis de polipirrol sobre sustratos textiles [30-73].

2.4. APLICACIONES DE LOS TEJIDOS CONDUCTORES DE LA ELECTRICIDAD BASADOS EN POLÍMEROS CONDUCTORES

Las aplicaciones de los tejidos conductores basados en el recubrimiento de polipirrol son variadas y numerosas; como aplicaciones antiestáticas [30], sensores de gases [31], sensores biomecánicos [43], electroterapia [49], dispositivos de calentamiento [52, 59, 71], atenuación de microondas [32], eliminación de colorantes [72], recuperación de metales [42, 73], etc.

Para la aplicación de los tejidos conductores en aplicaciones antiestáticas se deben conseguir resistividades superficiales por debajo de $5 \cdot 10^9$ $\Omega/\square$ [74]. La

resistividad superficial del poliéster es mayor de 10^{11} $\Omega/\square$ y cuando se realizan los recubrimientos de polipirrol, se consiguen resistividades superficiales en el rango de los 10^1-10^4 $\Omega/\square$ [16], dependiendo de las condiciones de síntesis, etc. Incluso después de realizar un tratamiento con bases en el que se produce una pérdida importante de conductividad; la resistividad superficial continúa siendo bastante baja para actuar como material antiestático. Lo mismo ocurre con la pérdida de conductividad del polipirrol con el tiempo. Las aplicaciones para tejidos antiestáticos son variadas, como: alfombras, tapicería, uniformes, guantes, filtración, rodillos de composites de alta velocidad, etc.

El rango de resistencia de los tejidos también los hace apropiados para su uso en dispositivos de calentamiento. La ventaja de los tejidos conductores frente a los dispositivos tradicionales que presentan cables es que son flexibles y ello permite un mejor diseño de los dispositivos de calentamiento. Otra de las ventajas es que al no presentar cables, la conducción se produce sobre toda la superficie y si se produce un rasgón en una zona, no impide la circulación de la corriente como ocurriría con un circuito tradicional, donde la rotura de un cable impide el paso de la corriente. Los usos de los tejidos conductores basados en polímeros conductores son paneles calefactores en suelo y paredes, asientos calefactables, guantes calefactables, etc. La temperatura que se puede alcanzar con los tejidos conductores depende del voltaje que se aplica, de la conductividad del tejido, etc.

2.5. INFLUENCIA DEL SUSTRATO

Diferentes sustratos textiles han sido empleados para realizar la síntesis química de polipirrol sobre los mismos, como: poliéster [19-31], nylon [39-51], algodón [52-54], seda [53, 55], derivados de la celulosa [56-58], poliéster-nylon [39, 59], nylon-poliuretano [60], poliaramida [61] y lana [62]. El sustrato tiene poca influencia a la hora de realizar la síntesis de polipirrol. Sólo la polaridad de la superficie puede tener un efecto en la adhesión del polímero conductor. La adhesión del polipirrol es peor con fibras que no tienen grupos polares (polietileno por ejemplo) [27]. En nuestro caso elegimos el poliéster ya que es un polímero que contiene grupos polares y además ha sido empleado habitualmente en bibliografía para obtener tejidos conductores basados en recubrimiento mediante polipirrol. Además, se realizaron también síntesis electroquímicas de polianilina sobre los tejidos conductores obtenidos. La síntesis

electroquímica de polianilina se realiza en medio ácido, por lo que se descartaron las fibras naturales debido a la degradación que presentan en los medios ácidos en los que se realiza la síntesis (pH~0). El poliéster es un polímero resistente al ataque químico de los ácidos [63, 64], por lo que es adecuado para ser empleado en la obtención de tejidos conductores.

2.6. MÉTODOS DE SÍNTESIS

Los métodos de síntesis de polipirrol sobre sustratos textiles empleados en bibliografía han sido principalmente:

- Polimerización in-situ [31, 45, 62], donde todos los reactivos son añadidos al mismo tiempo y la reacción de polimerización tiene lugar.
- Polimerización en dos fases [32-44, 46-53, 56-61, 63-66], donde hay una fase de adsorción de reactivos (normalmente monómero y dopante) y una segunda fase donde se añade el oxidante y tiene lugar la polimerización.
- Polimerización en fase gaseosa [53, 56, 60, 65, 66] donde tiene lugar una fase de adsorción de ciertos reactivos y una fase de reacción donde se añaden el resto de los reactivos. Normalmente en la primera fase se adsorben el contraión y el oxidante sobre el sustrato textil y en la segunda fase se expone el sustrato textil a los vapores de pirrol, dando lugar a la polimerización sobre la fibra. La polimerización en fase gaseosa se ha empleado como un método que puede ser automatizado.

Para el presente trabajo se ha empleado el método de polimerización en dos fases, la fase de adsorción permitiría que el monómero se adsorbiera sobre la superficie del sustrato textil y por tanto se obtendría un mejor recubrimiento de polipirrol.

2.7. ELECCIÓN DEL OXIDANTE

A la hora de elegir el oxidante se deben tener en cuenta las siguientes consideraciones [67]:

- El potencial de electrodo debe estar próximo al del pirrol: 1.2 V frente al electrodo de calomelanos saturado.
- La reacción redox no debe acompañarse de reacciones secundarias perturbantes.
- La forma oxidada y reducida del oxidante han de ser separadas fácilmente del polímero sintetizado.

Por todo ello las sales de Fe^{3+}, Cu^{2+} y los persulfatos son los reactivos más apropiados. En este trabajo hemos empleado el $FeCl_3$ como oxidante químico ya que el potencial de semi-reacción del $FeCl_3$ es suficiente para producir la oxidación del pirrol.

Lin y colaboradores [33] estudiaron la cinética de reacción del pirrol y el $FeCl_3$ y obtuvieron que era de primer orden con respecto al pirrol y de segundo orden con respecto al $FeCl_3$ [33]. Se observó también que una baja temperatura favorece la reducción de la velocidad de reacción [33], lo que conseguiría una estructura más ordenada del polímero y por tanto con mayor conductividad y estabilidad [67]. En nuestro caso realizamos también las síntesis de PPy/AQSA y PPy/$PW_{12}O_{40}^{3-}$ con baños de hielo con el fin de bajar la temperatura de síntesis.

2.8. INFLUENCIA DEL CONTRAIÓN

Durante la formación del polipirrol, se generan cargas positivas en la estructura del polipirrol (polarones y bipolarones). Estas especies son responsables de la conducción electrónica en los polímeros conductores. Las cargas positivas deben ser contrarrestadas por cargas negativas para mantener el principio de electroneutralidad. Estas cargas negativas son aportadas por un contraión.

Kuhn y colaboradores emplearon aniones de tamaño pequeño como los Cl^-, aunque su estabilidad es baja [32]. Si el contraión es expulsado de la estructura del polímero (desdopado) se produce una gran pérdida de sus propiedades eléctricas. Para prevenir este fenómeno, se han empleado aniones voluminosos con un alto tamaño molecular. Cuando el tamaño del contraión es grande, su difusión está impedida y permanece en la estructura del polímero [68]. Cuanto mayor es el tamaño del contraión, más difícil es la expulsión del contraión de la estructura del polímero. Los aniones que

más se han empleado para obtener tejidos conductores, son aniones orgánicos con gran tamaño como por ejemplo:

- Ácido antraquinona sulfónico (AQSA) [31-33, 46, 59, 69],
- Ácido antraquinona disulfónico [56, 58].
- Ácido naftalen sulfónico (NSA) [32, 45],
- Ácido naftalen disulfónico (NDSA) [32, 43, 46],
- Ácido dodecilbenzeno sulfónico (DBSA) [30, 46],
- Ácido p-tolueno sulfónico (PTSA) [31, 32, 45],
- Ácido benzeno sulfónico (BSA) [44, 61],

Avlyanov y colaboradores documentaron la influencia de la estructura del contraión (estructura 2D o 3D) en la conductividad del polímero obtenido. Se ha demostrado que los contraiones orgánicos producen polímeros conductores con mejores propiedades eléctricas debido a que su estructura es plana. Cuánto más plana es la estructura del contraión, el polímero conductor obtenido es más conductor [70].

En este trabajo se han empleado un contraión orgánico tradicional (AQSA) y un contraión de naturaleza inorgánica ($PW_{12}O_{40}^{3-}$) que no ha sido empleado en bibliografía en la obtención de tejidos conductores de la electricidad. El $PW_{12}O_{40}^{3-}$ presenta una estructura tridimensional que a priori producirá un polímero menos conductor que el AQSA por ejemplo; pero es muy interesante realizar la síntesis y medir sus propiedades debido a las propiedades electrocatalíticas que presenta el $PW_{12}O_{40}^{3-}$ [10].

2.9. $PW_{12}O_{40}^{3-}$

Los polioxometalatos o heteropolianiones como el $H_3PW_{12}O_{40}$, son clústeres de óxidos metálicos con una estructura perfectamente conocida que es estable en disolución. Aunque existe una gran variedad de polioxometalatos, el número de ellos que ha sido utilizado como electrocatalizador es limitado. Su estructura presenta una simetría Td. El tetraedro interno representa un átomo de P rodeado por cuatro átomos de oxígeno. Los octaedros representan átomos de W. Los 12 octaedros forman triadas que están unidas entre ellas por las esquinas. El diámetro de la molécula es de 10 Å [75].
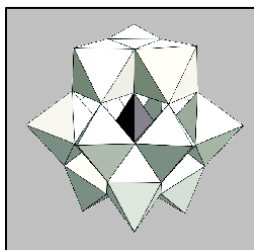
Fig. 2.1. Estructura del $PW_{12}O_{40}^{3-}$

Los heteropolianiones se reducen reversiblemente (tomando uno o dos electrones) para dar un compuesto azul característico. Posteriores reducciones son irreversibles y dan lugar a la descomposición del heteropolianión [76].

Los polioxometalatos son buenos conductores iónicos pero su conductividad electrónica es nula y sus usos se habían limitado a aplicaciones químicas, como catalizadores. En este sentido son complementarios con los polímeros conductores que presentan una buena conductividad electrónica pero con un mecanismo de inserción de aniones que presenta serias desventajas. Por ello, los materiales híbridos están formados por una combinación de una matriz polimérica conductora con componentes activos inorgánicos dispersos en aquella. La presencia de especies iónicas activas inmovilizadas en la estructura polimérica fuerza a los cationes (en vez de los aniones) a entrar o salir de la estructura para compensar cargas cuando se produce una reducción o una oxidación, respectivamente. Al ser aniones de gran tamaño y con gran carga, su coeficiente de difusión es bajo y el intercambio con aniones presentes en disolución es prevenido.

Estos materiales pueden poseer al mismo tiempo propiedades magnéticas, eléctricas, fotoquímicas y electroquímicas. Por esto sus aplicaciones pueden ser muy variadas [10]:

- Aplicaciones en sistemas de almacenamiento de carga.
- Electrocatálisis.
- Materiales con propiedades electrocrómicas y fotoelectrocrómicas.
- Aplicaciones en dispositivos de pantalla ("display").

- Sistemas fotovoltaicos y otros sistemas de conversión de energía de última generación.
- Electrodos que funcionan como bombas de protones.
- Sensores.
- Detectores químicamente resistentes.
- Recubrimientos anticorrosión.

2.10. SÍNTESIS ELECTROQUÍMICA DE POLÍMEROS CONDUCTORES SOBRE SUSTRATOS TEXTILES

Aunque los métodos de síntesis química de polipirrol sobre sustratos textiles son los más empleados en bibliografía; los métodos electroquímicos también han sido empleados en menor medida. La polimerización electroquímica es un método más controlado de síntesis, que sólo produce el polímero en la superficie deseada del electrodo, aunque no se pueden recubrir superficies tan grandes como en la síntesis química. La polimerización electroquímica puede ser realizada directamente o indirectamente, dependiendo de la conductividad del sustrato empleado como electrodo. Si el sustrato es aislante, sólo la polimerización indirecta puede ser llevada a cabo. Sólo unos cuantos trabajos relacionados con la síntesis electroquímica sobre sustratos textiles pueden ser encontrados en bibliografía y la mayoría de ellos realizan una polimerización indirecta [77-80]. Diferentes investigadores han realizado la síntesis de polipirrol [77-79] y de polianilina [80]. Bhadani y colaboradores [77] realizaron una síntesis electroquímica de polipirrol indirecta, en la cual cubrieron un ánodo de Pt con fibra de algodón. Después se realizó una electrolisis a 40 mA en una disolución con polipirrol y PTSA. El resultado fue la formación indirecta de polipirrol en las fibras de algodón. Kim y colaboradores [78] recubrieron una tela de nylon/spandex con polipirrol químicamente y luego realizaron una síntesis electroquímica indirecta similar a la de Bhadani y colaboradores [77]. El tejido recubierto químicamente se colocó entre dos placas de acero inoxidable y la electropolimerización tuvo lugar indirectamente. Babu y colaboradores [79] realizaron la síntesis electroquímica indirecta de polipirrol sobre tejido de algodón. Sobre un ánodo de Pt, se enrolló el tejido de algodón y se realizó una electrolisis con una densidad de corriente de 2 mA·cm^{-2}.

En el presente trabajo se ha realizado una síntesis electroquímica directa. Primero se obtiene un sustrato conductor a través de la síntesis química de polipirrol sobre tejidos de poliéster. Una vez el sustrato es conductor, se utiliza el tejido conductor como ánodo y se puede realizar la síntesis electroquímica sobre el tejido conductor. En este trabajo se ha realizado la síntesis electroquímica directa de polipirrol y polianilina.

2.11. POLÍMEROS CONDUCTORES NANOESTRUCTURADOS

En la tesis se han obtenido también nanoestructuras de polianilina al realizar la síntesis electroquímica de polianilina sobre tejidos conductores, por lo que es interesante introducir el tema de los polímeros nanoestructurados.

Durante los últimos años, el desarrollo de nanoestructuras de polímeros ha sido un importante campo de trabajo dentro de los polímeros conductores. Las nanoestructuras tienen propiedades diferentes a las del polímero sin forma definida. Por ejemplo, las nanofibras de polianilina han demostrado tener mayor sensibilidad y menor tiempo de respuesta que los films tradicionales cuando son usados como sensores de gases [81]. Diferentes nanoestructuras 1-D han sido obtenidas en bibliografía por métodos de oxidación química, como por ejemplo: estructuras en forma de plato [82], en forma de hoja [83], nanocopos [84], nanofibras [84-90], nanotubos [91, 92], nanoesferas [83, 88, 93] o rectángulos recubiertos con formas nanoestructuradas [94]. La agregación o el crecimiento de diferentes micro o nanoestructuras puede crear estructuras 3-D. Estructuras en forma de flor [82, 86], en forma de champiñón [92], en forma de caja compuesta de nanofibras [85] y microesterillas de nanofibras [87] han sido obtenidas. Zhou y colaboradores también obtuvieron nanoláminas, nanocilindros y microcilindros mediante la síntesis de polianilina en disolución alcalina [83].

La morfología obtenida por medio de síntesis electroquímica es menos variada que la obtenida mediante síntesis química. La morfología más observada en bibliografía para la polianilina obtenida electroquímicamente, son las nanofibras de polianilina [95-100] que en algunos caso forma redes 3-D de nanoalambres. La morfología en forma de coral también ha sido obtenida [100].

En la presente tesis se han obtenido nanofibras de polianilina y estructuras en forma de ciempiés. La estructura en forma de ciempiés no ha sido obtenida en bibliografía para polímeros conductores. El concepto de arquitectura molecular en forma de ciempiés puede ser encontrado en bibliografía [101, 102]. Ciempiés "comb-g-comb" han sido obtenidos en bibliografía en síntesis paso a paso [103]. Estructuras similares a las obtenidas en la tesis han sido obtenidas en bibliografía para films inorgánicos, tales como: nitrofosfatos de boro [104] o films de CdTe [105]. Sólo Hsieh y colaboradores mencionaron la aparición de la morfología en forma de ciempiés [91]. Sin embargo, la morfología obtenida por estos autores era una acumulación de nanofibras de polianilina. Nanofibras de polianilina ramificadas también han sido obtenidas, pero la estructura obtenida era como una estructura en forma de árbol [106]. La estructura no era igual de ordenada que la que ha sido obtenida en esta tesis. Otro tipo de estructura similar es la estructura "shish-kebab" que ha sido obtenida para polietileno de alta densidad [107] y nanotubos de carbono [108].

2.12. EMPLEO DE LOS POLÍMEROS CONDUCTORES EN EL TRATAMIENTO DE CONTAMINANTES

Los polímeros conductores también han sido empleados en el campo de la catálisis para realizar el tratamiento de diferentes contaminantes en disolución acuosa. Malinauskas escribió un review [109] en el que se describía el empleo de los polímeros conductores en electrocatálisis.

Alguna de las aplicaciones ambientales que se presentan en bibliografía son por ejemplo la reducción de Cr^{6+} (tóxico y cancerígeno) a Cr^{3+} (inocuo) [110] o la electroreducción de nitritos [111]. También han sido empleados para la recuperación de metales preciosos como por ejemplo la plata. Para ello se han empleado polvos de polipirrol y polianilina, membranas, tejidos y electrodos de carbón vítreo recubierto con ambos polímeros conductores [112]. La recuperación de Ag es selectiva ya que el alto potencial redox del par Ag^+/Ag^0 (+0.8 V) comparado con los pares de otros metales, hace que la reducción de la plata sea la reacción más probable [112]

En el campo del tratamiento de los colorantes también hay bibliografía al respecto; como el empleo de un catalizador de polianilina/MnO_2 y H_2O_2 para degradar

los colorantes orgánicos Direct Red 81, Indigo Carmine y Acid Blue 92 [113, 114]. Lopes y colaboradores también emplearon un tejido conductor basado en el recubrimiento de polipirrol para lograr precipitar el colorante C. I. Direct Red 80 [72].

2.13. BIBLIOGRAFÍA:

[1] The Nobel Prize in Chemistry, 2000: Conductive polymers. The Royal Swedish Academy of Sciences.

http://nobelprize.org/nobel_prizes/chemistry/laureates/2000/macdiarmid-lecture.html

[2] T. Ito, H. Shirakawa, S. Ikeda, J. Polym. Sci, Polym. Chem. 12 (1974) 11.

[3] H. Shirakawa, E.J. Louis, A.G. MacDiarmid, C.K. Chiang, A.J. Heeger, J. Chem. Soc. Chem. Comm. (1977) 579.

[4] C.K. Chiang, C.R. Fischer, Y.W. Park, A.J. Heeger, H. Shirakawa, E.J. Louis, S.C. Gau, A.G. MacDiarmid, Phys. Rev. Letters 39 (1977) 1098.

[5] C.K. Chiang, M.A. Druy, S.C. Gau, A.J. Heeger, E.J. Louis, A.G. MacDiarmid, Y.W. Park, H. Shirakawa, J. Am. Chem. Soc. 100 (1978) 1013.

[6] H. Letheby, J. Chem. Soc. 15 (1862) 161.

[7] R. McNeill, R. Siudak, J.H. Wardlaw, D.E. Weiss, Aust. J. Chem. 16 (1963) 1056.

[8] B.A. Bolto, D.E. Weiss, Aust. J. Chem. 16 (1963) 1076.

[9] B.A. Bolto, R. McNeill, D.E. Weiss, Aust. J. Chem. 16 (1963) 1090.

[10] P. Gómez-Romero, Adv. Mater. 13 (2001) 163.

[11] J.V. Masi, Polymers: Conductors, insulators and active devices. Electrical Insulation Conference and Electrical Manufacturing & Coil Winding Technology Conference, 2003, Proceedings.

http://ieeexplore.ieee.org/xpls/abs_all.jsp?arnumber=1247883&tag=1

[12] R.F. Service, Science 301 (2003) 909.

[13] D. Akbarov, B. Baymuratov, P. Westbroek, R. Akbarov, K. Declerck, P. Kiekens, J. Appl. Electrochem. 36 (2006) 411.

[14] D. De Rossi, Nat. Mater. 6 (2007) 328.

[15] M. Hamedi, R. Forchheimer, O. Inganäs, Nat. Mater. 6 (2007) 357.

[16] J.B. Lee, V. Subramanian, IEEE T. Electron Dev. 52 (2005) 269.

[17] J.B. Lee, V. Subramanian, Electron Devices Meeting, 2003. IEDM ´03 Technical Digest, IEEE International, pag. 8.3.1.

[18] D.C. Trivedi, S.K. Dhawan, J. Mater. Chem. 2 (1992) 1091.

[19] R. Fryczkowski, M. Rom, B. Fryczkowska, Fibres Text. East. Eur. 13 (2005) 141.

[20] K.W. Oh, S.H. Kim, E.A. Kim, J. Appl. Polym. Sci. 81 (2001) 684.

[21] S.K. Dhawan, N. Singh, S. Venkatachalam, Synth. Met. 125 (2002) 389.

[22] C.Y. Wang, A.M. Ballantyne, S.B. Hall, C.O. Too, D.L. Officer, G.G. Wallace, J. Power Sources 156 (2006) 610.

[23] R.C. Foitzik, A. Kaynak, J. Beckmann, F.M. Pfeffer, Synth. Met. 155 (2005) 185.

[24] R.C. Foitzik, A. Kaynak, F.M. Pfeffer, Synth. Met. 156 (2006) 637.

[25] M. Panhuis, J. Wu, S.A. Ashraf, G.G. Wallace, Synth. Met. 157 (2007) 358.

[26] B. Fugetsu, E. Sano, H. Yu, K. Mori, T. Tanaka, Carbon 48 (2010) 3340.

[27] H.H. Kuhn, A.D. Child. Electrically conducting textiles. In: Handbook of Conducting Polymers, T.A. Skotheim, R.L. Elsenbaumer, J.R. Reynolds editors. New York; Marcel Dekker, Inc., 1998. p. 993-1013.

[28] R.V. Gregory, W.C. Kimbrell, H.H. Kuhn, Synth. Met. 28 (1989) C823.

[29] H.H. Kuhn, W.C. Kimbrell, J.E. Fowler, C.N. Barry, Synth. Met. 55-57 (1993) 3707.

[30] P. Lekpittaya, N. Yanumet, B.P. Grady, E.A. O'Rear, J. Appl. Polym. Sci. 92 (2004) 2629.

[31] D. Kincal, A. Kumar, A. Child, J. Reynolds, Synth. Met. 92 (1998) 53.

[32] H. Kuhn, A. Child, W. Kimbrell, Synth. Met. 71 (1995) 2139.

[33] T. Lin, L. Wang, X. Wang, A. Kaynak, Thin Solid Films 479 (2005) 77.

[34] A. Kaynak, E. Håkansson, Synth. Met. 158 (2008) 350.

[35] E. Håkansson, A. Amiet, A. Kaynak, Synth. Met. 156 (2006) 917.

[36] H. Tavanai, A. Kaynak, Synth. Met. 157 (2007) 764.

[37] M.S. Kim, H.K. Kim, S.W. Byun, S.H. Jeong, Y.K. Hong, J.S. Joo, K.T. Songe, J.K. Kim, C.J. Lee, J.Y. Lee, Synth. Met. 126 (2002) 233.

[38] S.K. Dhawan, N. Singh, S. Venkatachalam, Synth. Met. 129 (2002) 261.

[39] A. Kaynak, E. Häkansson, Adv. Polym. Tech. 24 (2005) 194.

[40] R.V. Gregory, W.C. Kimbrell, H.H. Kuhn, J. Ind. Tex. 20 (1991) 167.

[41] C.L. Heisey, J.P. Wightman, E.H. Pittman, H.H. Kuhn, Text. Res. J. 63 (1993) 247.

[42] G. Tsekouras, S.F. Ralph, W.E. Price, G.G. Wallace, Fibers Polym. 5 (2004) 1.

[43] J. Wu, D. Zhou, C.O. Too, G.G. Wallace, Synth. Met. 155 (2005) 698.

[44] K. Wha, H. Jin, S. Hun, J. Appl. Polym. Sci. 88 (2003) 1225.

[45] H.S. Lee, J. Hong, Synth. Met. 113 (2000) 115.

[46] F. Ferrero, L. Napoli, C. Tonin, A. Varesano, J. Appl. Polym. Sci. 102 (2006) 4121.

[47] J. Ding, V. Misoska, W.E. Price, S.F. Ralph, G. Tsekouras, G.G. Wallace, Synth. Met. 135-136 (2003) 35.

[48] A. Kaynak, E. Håkansson, A. Amiet, Synth. Met. 159 (2009) 1373.

[49] T.E. Campbell, B.J. Munro, G.G. Wallace, J.R. Steele, J. Biomech. 40 (2007) 3056.

[50] E. Hakansson, A. Amiet, A. Kaynak. Synth. Met. 157 (2007) 1054.

[51] A. Varesano, B. Antognozzi, C. Tonin, Synth. Met. 160 (2010) 1683.

[52] N.V. Bhat, D.T. Seshadri, M.N. Nate, A.V. Gore, J. Appl. Polym. Sci. 102 (2006) 4690.

[53] S.H. Hosseini, A. Pairovi, Iran. Polym. J. 14 (2005) 934.

[54] A. Varesano, A. Aluigi, L. Florio, R. Fabris, 159 (2009) 1082.

[55] I. Cucchia, A. Boschib, C. Arosiob, F. Bertini, G. Freddib, M. Catellani, Synth. Met. 159 (2009) 246.

[56] L. Dall'Acqua, C. Tonin, A. Varesano, M. Canetti, W. Porzio, M. Catellani, Synth. Met. 156 (2006) 379.

[57] D. Beneventi, S. Alila, S. Boufi, D. Chaussy, P. Nortier, Cellulose 13 (2006) 725.

[58] L. Dall'Acqua, C. Tonin, R. Peila, F. Ferrero, M. Catellani, Synth. Met. 146 (2004) 213.

[59] E. Hakansson, A. Kaynak, T. Lin, S. Nahavandi, T. Jones, E. Hu, Synth. Met. 144 (2004) 21.

[60] P. Xue, X.M. Tao, H.Y. Tsang, Appl. Surf. Sci. 253 (2007) 3387.

[61] E. Gasana, P. Westbroek, J. Hakuzimana, K. De Clerck, G. Priniotakis, P. Kiekens, D. Tseles, Surf. Coat. Tech. 201 (2006) 3547.

[62] A. Varesano, L. Dall'Acqua, C. Tonin, Polym. Degrad. Stabil. 89 (2005) 125.

[63] www.lenntech.com/Chem-physical-resistance-data-fibres.htm

[64]www.engineeringtoolbox.com/chemical-resistance-polyester d 784.html

[65] S.S. Najar, A. Kaynak, R.C. Foitzik, Synth. Met. 157 (2007) 1.

[66] A. Kaynak, S.S. Najar, R.C. Foitzik, Synth. Met. 158 (2008) 1.

[67] Tesis Doctoral Carmen Arribas Arribas (UCM). Investigación de nuevos materiales conductores: Polipirrol crecido en polímeros sulfonados (1991).

[68] K.G. Neoh, T.T. Young, E.T. Kang, K.L. Tan, J. Appl. Polym. Sci. 64 (1997) 519.

[69] S. Garg, C. Hurren, A. Kaynak, Synth. Met. 157 (2007) 41.

[70] J.K. Avlyanov, H.H. Kuhn, J.Y. Josefowicz, A.G. MacDiarmid, Synth. Met. 84 (1997) 153.

[71] J.P. Boutrois, R. Jolly, C. Pétrescu, Synth. Met. 85 (1997) 1405.

[72] A. Lopes, S. Martins, A. Moraö, M. Magrinho, I. Gonçalves, Portugaliae Electrochim. Acta 22 (2004) 279.

[73] R. Dimeska, P.S. Murray, S.F. Ralph, G.G. Wallace, Polymer 47 (2006) 4520.

[74] T. Textor, B. Mahltig, Appl. Surf. Sci. 256 (2010) 1668.

[75] P. Gómez-Romero, N. Casan-Pastor, J. Phys. Chem. 100 (1996) 12448.

[76] M. Sadakane, E. Steckhan, Chem. Rev. 98 (1998) 219.

[77] S.N. Bhadani, M. Kumari, S.K. Sen Gupta, G.C. Sahu, J. Appl. Polym. Sci. 64 (1997) 1073.

[78] S.H. Kim, K.W. Oh, J.H. Bahk, J. Appl. Polym. Sci. 91 (2004) 4064.

[79] K.F. Babu, R. Senthilkumar, M. Noel, M.A. Kulandainathan, Synth. Met. 159 (2009) 1353.

[80] R. Hirase, M. Hasegawa, M. Shirai, J. Appl. Polym. Sci. 87 (2003) 1073.

[81] J. Huang, S. Virji, B.H. Weiller, R.B. Kaner, J. Am. Chem. Soc. 125 (2003) 314.

[82] C. Zhou, J. Han, R. Guo, Macromolecules 41 (2008) 6473.

[83] C. Zhou, J. Han, G. Song, R. Guo, Eur. Polym. J. 44 (2008) 2850.

[84] C.A. Amarnath, J. Kim, K. Kim, J. Choi, D. Sohn, Polymer 49 (2008) 432.

[85] Y. Zhu, J. Li, M. Wan, L. Jiang, Polymer 49 (2008) 3419.

[86] Z. Zhang, J. Deng, L. Yu, M. Wan, Synth. Met. 158 (2008) 712.

[87] C. Zhou, J. Han, G. Song, R. Guo, Macromolecules 40 (2007) 7075.

[88] P. Anilkumar, M. Jayakannan, Macromolecules 40 (2007) 7311.

[89] S.P. Surwade, N. Manohar, S.K. Manohar, Macromolecules 42 (2009) 1792.

[90] G. Li, L. Jiang, H. Peng, Macromolecules 40 (2007) 7890.

[91] B.-Z. Hsieh, H.-Y. Chuang, L. Chao, Y.-J. Li, Y.-J. Huang, P.-H. Tseng, T.-H. Hsieh, K.-S. Ho, Polymer 49 (2008) 4218.

[92] Q. Sun, Y. Deng, Mater. Lett. 62 (2008) 1831.

[93] Y. He, J. Lu, React. Funct. Polym. 67 (2007) 476.

[94] C. Zhou, J. Han, R. Guo, Macromolecules 42 (2009) 1252.

[95] V. Gupta, N. Miura, Electrochem. Solid-State Lett. 8 (2005) A630.

[96] Y. Guo, Y. Zhou, Eur. Polym. J. 43 (2007) 2292.

[97] H. Zhang, J. Wang, Z. Wang, Z. Zhang, S. Wang, Synth. Met. 159 (2009) 277.

[98] H.H. Zhou, S.Q. Jiao, J.H. Chen, W.Z. Wei, Y.F. Kuang, Thin Solid Films 450 (2004) 233.

[99] S.J. Choi, S.M. Park, J. Electrochem. Soc. 149 (2002) E26.

[100] L.J. Duić, Z. Mandić, F. Kovačiček, J. Polym. Sci. Part A: Polym. Chem. 32 (1994) 105.

[101] J. Mijovi, M. Sun, S. Pejanovi, J.W. Mays, Macromolecules 36 (2003) 7640.

[102] L. Gu, Z. Shen, S. Zhang, G. Lu, X. Zhang, X. Huang, Macromolecules 40 (2007) 4486.

[103] M. Schappacher, A. Deffieux, Macromolecules 38 (2005) 7209.

[104] X.W. Zhang, S.Y. Xu, G.R. Han, Phys. Status Solidi A 201 (2004) 2922.

[105] Y. Wang, Z. Tang, X. Liang, L.-M. Liz-Marzán, N.A. Koto, Nano Lett. 4 (2004) 225.

[106] X.-S. Du, C.-F. Zhou, G.-T. Wang, Y.-W. Mai, Chem. Mater. 20 (2008) 3806.

[107] G.-Q. Zheng, L. Huang, W. Yang, B. Yang, M.-B. Yang, Q. Li, C.-S. Shen, Polymer 48 (2007) 5486.

[108] L. Li, Y.C. Li, C. Ni, J. Am. Chem. Soc. 128 (2006) 1692.

[109] A. Malinauskas, Synth. Met. 107 (1999) 75.

[110] F.J. Rodríguez, S. Gutiérrez, J.S. Ibanez, J.L. Bravo, N. Batina, Environ. Sci. Technol. 34 (2000) 2018.

[111] Y. Tian, J. Wang, Z. Wang, S. Wang, Synth. Met. 143 (2004) 309.

[112] R. Dimeska, P.S. Murray, S.F. Ralph, G.G. Wallace. Polymer 47 (2006) 4520.

[113] A.H. Gemeay, R.G. El-Sharkawy, I.A. Mansour, A.B. Zaki, Appl. Catal. B 80 (2008) 106.

[114] A.H. Gemeay, R.G. El-Sharkawy, I.A. Mansour, A.B. Zaki, J. Colloid Interface Sci. 308 (2007) 385.

3.- HIPÓTESIS DE TRABAJO

3.- HIPÓTESIS DE TRABAJO

Los antecedentes y resultados previos permiten formular las siguientes hipótesis de trabajo:

1.- Se pueden obtener recubrimientos de polipirrol/AQSA y de material híbrido polipirrol/$PW_{12}O_{40}^{3-}$ sobre tejidos de poliéster mediante la síntesis por oxidación química del monómero de pirrol.

2.- El polímero conductor sintetizado químicamente recubre adecuadamente toda la superficie del tejido o hilo, por lo que se obtienen tejidos conductores de la electricidad con propiedades homogéneas: con un espesor y adherencia adecuados.

3.- La estabilidad del recubrimiento de polímero conductor en disolución depende del pH. A pH básico se produce la desprotonación del polímero conductor con la consiguiente pérdida de conductividad eléctrica y la pérdida de contraiones. Al emplear contraiones grandes ($PW_{12}O_{40}^{3-}$ o AQSA), el contraión sólo se perdería parcialmente de la estructura del polímero.

4.- Una vez se obtiene un sustrato conductor de la electricidad, se puede realizar la síntesis electroquímica de otros polímeros conductores (polipirrol o polianilina) sobre el tejido conductor de PES-PPy/$PW_{12}O_{40}^{3-}$ o PES-PPy/AQSA. De este modo se obtiene una doble capa de polímeros conductores; la primera capa sintetizada químicamente y la segunda sintetizada electroquímicamente. El polímero conductor obtenido electroquímicamente, sería más electroactivo que el sintetizado químicamente.

5.- Los métodos de síntesis electroquímicos (potenciostático o potenciodinámico) y las condiciones de síntesis influyen en la morfología del recubrimiento del polímero conductor.

Por ello se plantean una serie de objetivos, proponiéndose para su consecución una metodología y plan de trabajo que se detallan en los dos siguientes apartados.

4.- OBJETIVOS DEL TRABAJO

4.- OBJETIVOS DEL TRABAJO

Los objetivos de esta investigación se exponen a continuación:

1.- Evaluar las condiciones experimentales óptimas que permiten la síntesis química de PPy/AQSA y PPy/PW$_{12}$O$_{40}$$^{3-}$ sobre tejidos de poliéster.

2.- Desarrollar y preparar recubrimientos de PPy/AQSA y PPy/PW$_{12}$O$_{40}$$^{3-}$ sobre tejidos de poliéster.

3.- Estudiar la naturaleza y las características químicas, morfológicas y electroquímicas de los recubrimientos de PPy/AQSA y PPy/PW$_{12}$O$_{40}$$^{3-}$ obtenidos sobre materiales textiles.

4.- Evaluar las propiedades mecánicas (ensayo lavado y resistencia al desgaste) del recubrimiento de PPy/PW$_{12}$O$_{40}$$^{3-}$ sobre tejidos de poliéster.

5.- Evaluar la estabilidad de los tejidos conductores de PES-PPy/AQSA y PES-PPy/PW$_{12}$O$_{40}$$^{3-}$ en disoluciones con diferente pH y la estabilidad de sus propiedades eléctricas y electroquímicas.

6.- Desarrollar y caracterizar dobles capas de polímeros conductores a partir de la síntesis electroquímica de polianilina o polipirrol sobre tejidos de PES-PPy/AQSA o PES-PPy/PW$_{12}$O$_{40}$$^{3-}$.

7.- Determinar la influencia del método de síntesis (potenciostático o potenciodinámico y sus variables) en la morfología del recubrimiento obtenido. Estudio de la cinética y del mecanismo de crecimiento de la polianilina sobre los tejidos conductores.

8.- Estudiar las propiedades morfológicas, químicas, térmicas, eléctricas y electroquímicas de los polvos no depositados de PPy/PW$_{12}$O$_{40}$$^{3-}$ y PPy/AQSA obtenidos durante la síntesis de los polímeros sobre los tejidos.

5.- JUSTIFICACIÓN GENERAL DE LA METODOLOGÍA DE TRABAJO

5.- JUSTIFICACIÓN GENERAL DE LA METODOLOGÍA DE TRABAJO

La metodología de trabajo se presenta a continuación para cada uno de los objetivos propuestos en el capítulo anterior:

1.- Evaluar las condiciones experimentales óptimas que permiten la síntesis química de PPy/AQSA y PPy/PW$_{12}$O$_{40}$$^{3-}$ sobre tejidos de poliéster.

1.1. Búsqueda bibliográfica de trabajos relacionados con el recubrimiento de tejidos con polipirrol.

1.2. Evaluación de las mejores condiciones de síntesis de polipirrol sobre tejidos de poliéster: pre-tratamiento, método de síntesis, tipo de contraión, concentraciones de los reactivos, tiempo de síntesis, temperatura de síntesis, etc.

1.3. Pruebas iniciales de polimerización química de PPy/PW$_{12}$O$_{40}$$^{3-}$ y PPy/AQSA sobre tejidos de poliéster.

2.- Desarrollar y preparar recubrimientos de PPy/AQSA y PPy/PW$_{12}$O$_{40}$$^{3-}$ sobre tejidos de poliéster.

2.1. Síntesis química de recubrimientos de PPy/AQSA y PPy/PW$_{12}$O$_{40}$$^{3-}$ sobre los tejidos de poliéster con las condiciones de síntesis óptimas encontradas a partir de la búsqueda bibliográfica.

3.- Estudiar la naturaleza y las características morfológicas, químicas, eléctricas y electroquímicas de los recubrimientos de PPy/AQSA y PPy/PW$_{12}$O$_{40}$$^{3-}$ obtenidos sobre tejidos de poliéster.

3.1. La topografía y uniformidad del recubrimiento sobre el tejido de poliéster se evalúa mediante Microscopía Electrónica de Barrido (SEM); empleando electrones secundarios y también mediante electrones retrodispersados. Los electrones secundarios permiten estudiar la morfología del recubrimiento. La presencia de elementos con un alto peso atómico en el contraión (W en el caso del PW$_{12}$O$_{40}$$^{3-}$) permite la obtención de micrografías mediante electrones retrodispersados en donde las zonas donde se encuentra el contraión aparecen como zonas blancas en las micrografías.

3.2. La estructura y composición superficial de los recubrimientos se determina mediante Espectroscopía de Infrarrojos por Transformada de Fourier y

Reflectancia Total Atenuada (FTIR-ATR), Espectroscopía Fotoelectrónica de Rayos-X (XPS) y Energía Dispersiva de Rayos-X (EDX). Los análisis de FTIR-ATR permiten determinar los enlaces existentes en las muestras a partir de las energías de vibración. Los análisis de XPS permiten determinar la composición superficial y los diferentes grupos funcionales de las muestras analizadas (análisis cuantitativo, % atómico y % másico de los diferentes elementos). Los análisis de EDX permiten determinar la presencia de los diferentes elementos así como una idea aproximada de su composición (análisis semi-cuantitativo).

3.3. A partir de los análisis XPS también es posible determinar los estados de oxidación de los elementos del recubrimiento (C, O, N, W, S), lo que permite obtener información de su estructura molecular. Otro parámetro importante en los polímeros conductores es el grado de dopaje, que se obtiene a partir de la relación entre las moléculas de nitrógeno cargas positivamente y el número total de moléculas de nitrógeno (N^+/N). Esta relación nos da una indicación del grado de oxidación del polímero y por tanto de su conductividad.

3.4. La resistividad superficial de los tejidos conductores se mide mediante el método de las 4 puntas y mediante Espectroscopía de Impedancia Electroquímica (EIS).

3.5. La electroactividad de los tejidos conductores en disoluciones con diferentes pHs (1, 7, 13) se mide mediante Voltametría Cíclica (CV) y Espectroscopía de Impedancia Electroquímica (EIS). La caracterización voltamétrica se realizó a diferentes velocidades de barrido (50, 5 y 1 mV·s^{-1}), ya que se observó la influencia de este parámetro en la respuesta obtenida mediante esta técnica. Mediante Microscopía Electroquímica de Barrido (SECM) se evalúa también la electroactividad de los recubrimientos en disoluciones de $Ru(NH_3)_6^{3+}$ 0.1 M y KCl 0.1 M (pH~5.4) mediante la realización de curvas de aproximación.

4.- Evaluar las propiedades mecánicas (ensayo de lavado y resistencia al frote) del recubrimiento de $PPy/PW_{12}O_{40}^{3-}$ sobre tejidos de poliéster.

4.1. Para determinar la durabilidad de los recubrimientos de $PPy/PW_{12}O_{40}^{3-}$ frente al desgaste mecánico, se realizan ensayos de resistencia al frote según la norma ISO 105-X12:2001.

4.2. Para determinar la durabilidad de los recubrimientos frente al lavado, se realizan ensayos de resistencia al lavado según la norma ISO 105-C01.

4.3. Después de los ensayos de resistencia al lavado y resistencia al frote, se determinan los valores de degradación del color y de descarga del color según la escala de grises.

4.4. Después de los ensayos de resistencia al frote y al lavado, los tejidos conductores se analizan mediante Microscopía Electrónica de Barrido (SEM) para evaluar la degradación del recubrimiento a escala microscópica.

4.5. Se realizan análisis de Energía Dispersiva de Rayos-X (EDX) para determinar si hay pérdida de contraión después de los ensayos de frote y lavado. Esta técnica es útil sobre todo para analizar las muestras después de los ensayos de frote, donde sí que hay diferencias muy grandes entre las diferentes zonas. En las zonas donde se ha producido una degradación del recubrimiento, la presencia del contraión prácticamente desaparece.

4.6. Se determinan los estados de oxidación de los elementos del recubrimiento (C, O, N, W) después de los ensayos de lavado mediante Espectroscopía Fotoelectrónica de Rayos-X (XPS). Se calcula también el ratio W/N para determinar si hay pérdida de contraión después del ensayo de lavado. El grado de dopaje a partir del ratio (N^+/N) también se calcula para evaluar una posible pérdida de conductividad después de los ensayos de lavado.

4.7. Se realizan medidas de resistividad superficial mediante el método de las 4 puntas y mediante Espectroscopía de Impedancia Electroquímica para medir la pérdida de propiedades eléctricas después de los ensayos de resistencia al frote y al lavado.

5.- Evaluar la estabilidad de los tejidos conductores de PES-PPy/AQSA y PES-PPy/PW$_{12}$O$_{40}$$^{3-}$ en disoluciones con diferente pH y la estabilidad de sus propiedades eléctricas y electroquímicas.

5.1. Se evalúa la estabilidad de los tejidos conductores de PES-PPy/AQSA y PES-PPy/PW$_{12}$O$_{40}$$^{3-}$ en disoluciones con diferentes pH (1-13). Trozos de tejido conductor se ponen en contacto durante 1 h con disoluciones con pH~1, pH~7 y pH~13. Después se lavan las muestras con agua ultrapura y se dejan secar 24 h en un desecador antes de realizar las medidas.

5.2. Se realizan análisis de Energía Dispersiva de Rayos-X (EDX) y Espectroscopía Fotoelectrónica de Rayos-X (XPS) para ver la posible pérdida de parte del contraión. En el caso de los análisis de XPS, a partir de la relación

W/N y S/N como se ha indicado anteriormente. En el caso del tejido de PES-PPy/AQSA se realizan también análisis de FTIR-ATR ya que se observó la variación de la intensidad en una de las bandas atribuidas al AQSA (1670 cm^{-1}) al realizar los diferentes ensayos. En el caso del tejido de PES-PPy/PW$_{12}$O$_{40}$$^{3-}$ no se realizan medidas de FTIR-ATR al coincidir las bandas del PW$_{12}$O$_{40}$$^{3-}$ con las bandas del poliéster y por tanto no ser posible realizar una cuantificación.

5.3. Los estados de oxidación de los elementos del recubrimiento (C, O, N, W, S) se determinan mediante Espectroscopía Fotoelectrónica de Rayos-X (XPS) después de los diferentes tests. Se determina también el grado de dopaje (N$^+$/N) para evaluar variaciones en el estado de oxidación del polipirrol.

5.4. Se mide la resistividad superficial de los tejidos después de los diferentes ensayos mediante Espectroscopía de Impedancia Electroquímica.

5.5. La electroactividad de los recubrimientos después de los diferentes ensayos se determina mediante Microscopía Electroquímica de Barrido (SECM) a partir de las correspondientes curvas de aproximación.

6.- Desarrollar y caracterizar dobles capas de polímeros conductores a partir de la síntesis electroquímica de polipirrol o polianilina sobre tejidos de PES-PPy/AQSA o PES-PPy/PW$_{12}$O$_{40}$$^{3-}$.

6.1. Se realizan recubrimientos de polipirrol sintetizado electroquímicamente sobre tejidos de PES-PPy/PW$_{12}$O$_{40}$$^{3-}$.

6.1.1. Mediante Voltametría Cíclica se determinó el potencial de síntesis adecuado para realizar la síntesis potenciostática.

6.1.2. Se realiza la síntesis de polipirrol mediante síntesis potenciostática al potencial determinado anteriormente.

6.1.3. Se evalúa la morfología del recubrimiento mediante Microscopía Electrónica de Barrido (SEM).

6.1.4. La composición química se determina mediante análisis de Energía Dispersiva de Rayos-X (EDX) y Espectroscopía Fotoelectrónica de Rayos X (XPS).

6.1.5. La electroactividad de las muestras se mide mediante Voltametría Cíclica y Espectroscopía de Impedancia Electroquímica en disoluciones con diferente pH.

6.2. Se realizan recubrimientos de polianilina sobre tejidos de PES-PPy/AQSA mediante síntesis potenciostática y síntesis potenciodinámica.

6.2.1. Mediante Voltametría Cíclica se determina el potencial de síntesis adecuado para realizar la síntesis potenciostática de polianilina sobre tejidos de PES-PPy/AQSA.

6.2.2. Se realiza la síntesis de polianilina sobre tejidos de PES-PPy/AQSA mediante síntesis potenciostática al potencial determinado anteriormente.

6.2.3. Se realiza también la síntesis potenciodinámica a diferentes velocidades de barrido (50, 5 y 1 mV·s^{-1}).

6.2.4. La estructura y composición superficial del recubrimiento se evalúan mediante Espectroscopía de Infrarrojos mediante Transformada de Fourier (FTIR-ATR), Energía Dispersiva de Rayos-X (EDX) y Espectroscopía Fotoelectrónica de Rayos-X (XPS).

6.2.5. Los estados de oxidación de los elementos del recubrimiento (C, O, N, S) se determinan mediante Espectroscopía Fotoelectrónica de Rayos-X (XPS). Se determina también el grado de dopaje de la polianilina (N$^+$/N) que nos da una indicación de la conductividad del polímero.

6.2.6. La electroactividad del recubrimiento se mide mediante Voltametría Cíclica (CV) y Espectroscopía de Impedancia Electroquímica (EIS).

6.2.7. La morfología del recubrimiento de polianilina se evalúa en el apartado 7, al observar la influencia de parámetros como el método de síntesis y la velocidad de barrido en la morfología del recubrimiento obtenido.

7.- Determinar la influencia del método de síntesis (potenciostática o potenciodinámica y sus variables) en la morfología del recubrimiento obtenido. Estudio de la cinética y del mecanismo de crecimiento de la polianilina sobre los tejidos conductores.

7.1. Se realiza la síntesis potenciostática y potenciodinámica de polianilina sobre tejidos de PES-PPy/AQSA.

7.2. En la síntesis potenciodinámica se realizan síntesis a diferentes velocidades de barrido (50, 5 y 1 mV·s^{-1}) para ver la influencia de este

parámetro en la morfología del recubrimiento obtenido y en la forma de los voltagramas obtenidos. La forma de los voltagramas da una idea de la cinética de crecimiento del polímero.

7.3. Se obtienen muestras a diferentes barridos (por ejemplo 1, 2, 3, 5 y 10 barridos) para las diferentes velocidades de barrido con el fin de observar cómo se produce el crecimiento de la polianilina.

7.4. Se evalúa la morfología del recubrimiento y el proceso de crecimiento de la polianilina sobre el tejido de PES-PPy/AQSA mediante Microscopía Electrónica de Barrido (SEM).

8.- Estudiar las propiedades morfológicas, químicas, térmicas, eléctricas y electroquímicas de los polvos no depositados de PPy/PW$_{12}$O$_{40}$$^{3-}$ y PPy/AQSA obtenidos durante la síntesis de los polímeros sobre los tejidos.

8.1. La morfología de los polvos de PPy/PW$_{12}$O$_{40}$$^{3-}$ y PPy/AQSA se observa mediante Microscopía Electrónica de Barrido (SEM).

8.2. Los polvos de PPy/PW$_{12}$O$_{40}$$^{3-}$ y PPy/AQSA se caracterizan químicamente mediante Espectroscopía de Infrarrojos mediante Transformada de Fourier (FTIR-ATR), Energía Dispersiva de Rayos-X (EDX) y Espectroscopía Fotoelectrónica de Rayos-X (XPS).

8.3. Los estados de oxidación de los elementos de los polvos de polipirrol (C, O, N, S, W) se determinan mediante Espectroscopía Fotoelectrónica de Rayos-X (XPS). Se determina también el grado de dopaje del polipirrol (N^{+}/N), que nos da una indicación de la conductividad del polímero.

8.4. La estabilidad térmica de los polvos de PPy/PW$_{12}$O$_{40}$$^{3-}$ y PPy/AQSA se determina mediante Termogravimetría (TG) y Calorimetría Diferencial de Barrido (DSC) en atmósfera de nitrógeno y en atmósfera de aire.

8.5. Los productos de descomposición de los polvos de PPy/PW$_{12}$O$_{40}$$^{3-}$ se determinan mediante Cromatografía de Gases/ Espectrometría de Masas mediante Pirólisis (Py-GC-MS).

8.6. Los polvos de PPy/PW$_{12}$O$_{40}$$^{3-}$ y PPy/AQSA se emplean para obtener pastillas a partir de su compactación en una prensa (10 Toneladas). Se miden sus propiedades eléctricas mediante Voltametría Cíclica y también Espectroscopía de Impedancia Electroquímica a diferentes temperaturas. Se obtiene la energía de activación de las pastillas de PPy/AQSA y PPy/PW$_{12}$O$_{40}$$^{3-}$

mediante la ley de Arrhenius a partir de los datos de impedancia con la temperatura.

8.7. Se determina la electroactividad de las pastillas de PPy/PW$_{12}$O$_{40}^{3-}$ y PPy/AQSA mediante Microscopía Electroquímica de Barrido (SECM) a partir de las curvas de aproximación. Se obtienen también mapas de electroactividad de las pastillas a partir del barrido en dos dimensiones para observar variaciones locales de electroactividad.

6.- DISEÑO EXPERIMENTAL Y MÉTODOS

6.- DISEÑO EXPERIMENTAL Y MÉTODOS

En este capítulo se exponen brevemente los fundamentos teóricos en que se basan las técnicas experimentales empleadas para el desarrollo de la presente investigación, así como la descripción de los dispositivos experimentales utilizados y los procedimientos de trabajo adoptados para aplicar las diferentes técnicas. Las técnicas utilizadas han sido las siguientes: medidas de resistividad superficial, Espectroscopía Infrarroja por Transformada de Fourier por Reflectancia Total Atenuada (FTIR-ATR), Microscopía Electrónica de Barrido (SEM), Energía Dispersiva de Rayos X (EDX), Espectroscopía Fotoelectrónica de Rayos X (XPS), Voltametría Cíclica (CV), Espectroscopía de Impedancia Electroquímica (EIS), Espectroscopía de Impedancia Electroquímica con la Temperatura, Microscopía Electroquímica de Barrido (SECM), Termogravimetría (TG), Calorimetría Diferencial de Barrido (DSC), Pirolisis/Cromotografía de Gases/ Espectrometría de Masas (Py-GC-MS). Además de los ensayos de abrasión y lavado que fueron llevados a cabo para medir la durabilidad de las capas de polipirrol.

6.1. MEDIDAS DE RESISTIVIDAD SUPERFICIAL

La resistividad superficial es un parámetro importante en los tejidos conductores, ya que nos indica la capacidad del tejido de conducir la electricidad a través de la superficie del tejido. En el caso de los polímeros conductores, tenemos un material aislante (poliéster) recubierto de un material conductor (polipirrol). La resistividad superficial nos permite evaluar sólo la superficie, donde se encuentra el polímero conductor. La resistividad volumétrica permitiría evaluar el paso de corriente a través del tejido, en este caso mediríamos las propiedades combinadas del poliéster y el polipirrol.

La resistividad superficial del tejido conductor ($\Omega/\square$) se midió con un resistímetro superficial, modelo SRM-232-2000, con un rango de medida de 0-2000 $\Omega/\square$ (Guardian Manufacturing) (Fig.6.1). El método que se empleó fue el de las cuatro puntas. La célula de medida tiene cuatro puntas. Al presionar las cuatro puntas sobre el tejido, entre dos de las puntas se pasa una corriente de 4.53 mA y se registra la diferencia de potencial que se genera en las otras dos puntas. El resistímetro calcula la

resistividad superficial (Ω/□) según los parámetros de la célula de medida (distancia entre puntas, etc).

Figura 6.1. Resistímetro modelo SRM-232-2000 (Guardian Manufacturing) para medidas de resistividades superficiales 0-2000 Ω/□.

Para resistividades superficiales mayores de 2000 Ω/□, se emplearon medidas de Espectroscopía de Impedancia Electroquímica que permiten un mayor rango de medida, con resistencias mayores de $>10^{12}$. La resistividad superficial se define como:

$$\rho_S = U/L/Is/D$$

Donde:
- ρ_S es la resistividad superficial
- U es la diferencia de potencial
- Is es la corriente superficial
- L es la longitud de la muestra que se mide
- D es la anchura de la muestra que se mide

En el caso de medir un cuadrado L y D son iguales y se anulan, por lo que la resistividad superficial sería la diferencia de potencial partido por la corriente, que es equivalente a la resistencia superficial. En la Fig. 6.2 se muestra un esquema y en la Fig. 6.3 se muestra una imagen del sistema de medida empleado. En las medidas realizadas mediante EIS, realmente se mide la resistencia superficial, pero al medir un cuadrado de muestra de 1.5 x 1.5 cm, la resistencia superficial es igual a la resistividad superficial. La Figura 6.2 muestra el sistema de medida, dos electrodos de cobre se ponen en contacto con el tejido conductor, la longitud de los electrodos en contacto con

el tejido conductor es de 1.5 cm. Los electrodos se encuentran separados 1.5 cm. En los diagramas de impedancia se obtienen diferentes valores de resistencia según la frecuencia, por lo que se calcula un valor medio.
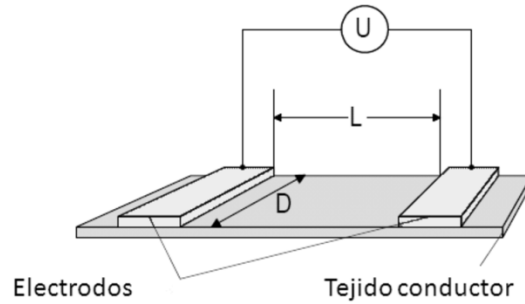

Fig. 6.2. Esquema del sistema de medida empleado en las medidas de resistividad superficial mediante espectroscopía de impedancia electroquímica.

Fig. 6.3. Imagen donde se muestra el sistema de medida de resistividad superficial mediante espectroscopía de impedancia electroquímica.

6.2.- MICROSCOPÍA ELECTRÓNICA DE BARRIDO (SEM)

La microscopía electrónica de barrido, es una técnica basada en el bombardeo de las muestras con un haz de electrones. Como resultado de esta interacción, se obtiene una imagen de la superficie de las muestras, con lo cual es posible estudiar su morfología.

Cuando un haz de electrones choca con la superficie de una muestra, se pueden dar las siguientes interacciones:

a) Dispersión elástica: afectan a las trayectorias de los electrones sin que haya un cambio detectable en la energía del haz de los electrones. La mayoría experimenta numerosas colisiones y como resultado, acaban saliendo de la superficie como electrones retrodispersados.

b) Dispersión inelástica: es cualquier proceso en el que hay una pérdida apreciable en la energía del haz de electrones. Estos procesos son los responsables de que un electrón sea frenado por el sólido. Por ello, casi toda la energía cinética de los electrones termina como calor en la muestra, y una pequeña porción puede escapar como rayos X o como electrones secundarios.

Los electrones secundarios y retrodispersados se han utilizado para la formación de las imágenes en el microscopio electrónico de barrido. Los análisis se han realizado con un Jeol JSM-840 Scanning Microscope (Fig. 6.4). Las muestras para observación mediante SEM, se recubrieron con oro mediante un sputter coater Bal-TEC SCD 005 para conseguir una superficie completamente conductora (Fig. 6.5).

Fig. 6.4. Microscopio electrónico de barrido Jeol JSM-6300.

Fig. 6.5. Recubridor Bal-tec SCD 005 Sputter Coater.

6.3.- ENERGÍA DISPERSIVA DE RAYOS X

Esta técnica se utiliza junto con el SEM y consiste en un microanálisis de la muestra a partir de un espectro de rayos X.

Cuando a consecuencia del bombardeo de la muestra con el haz de electrones, un electrón interno es expulsado fuera del átomo, este se queda en un estado excitado. Los mecanismos que el átomo tiene para relajarse son dos:

a) Emisión característica Auger: la vacante original se ocupa por un electrón más externo con la energía de un tercer electrón que abandona el átomo (Espectroscopía Auger).

b) Emisión característica de rayos X: en este caso, un electrón más externo salta al nivel interno emitiendo una energía que es la diferencia de las energías de los dos niveles y por tanto, es característica de un átomo particular. A partir de esta diferencia de energías, se puede determinar los elementos presentes en cada muestra. Esto constituye la base del microanálisis cualitativo. La medida de la cantidad de rayos X emitidos por segundo nos proporciona el análisis cuantitativo.

Los análisis EDX se han realizado con un microscopio electrónico de barrido Jeol JSM-6300 (Fig. 6.4). Las muestras también se recubrieron mediante un sputter coater para conseguir una superficie completamente conductora. En este caso para evitar la aparición de picos de Au en el espectro EDX, las muestras se recubrieron con C con un sputter coater (Fig. 6.5).

6.4.- ESPECTROSCOPÍA INFRARROJA (FTIR-ATR)

La finalidad principal de la espectroscopía infrarroja es determinar los grupos funcionales que contiene el material objeto de estudio. Como cada grupo funcional absorbe únicamente unas determinadas frecuencias características de la radiación infrarroja, una representación de la intensidad de radiación frente al número de ondas

(espectro de IR), permitirá identificar los grupos químicos reconocibles en la muestra estudiada.

Sin embargo, ningún detector de IR conocido puede monitorizar con precisión suficiente la frecuencia y la intensidad de la radiación de IR de modo simultáneo a una resolución que resulte práctica.

El método de transformada de Fourier presenta una solución que ha encontrado aplicaciones muy amplias. Un espectrómetro por transformada de Fourier sustituye el monocromador convencional por el interferómetro de Michelson. Este interferómetro consta de un divisor de haz, un espejo fijo y un espejo móvil. La ventaja que proporciona es que conserva la información de la frecuencia y de la intensidad simultáneamente. El interferómetro codifica las frecuencias incidentes (tomando físicamente la transformada de Fourier de la radiación) y las convierte en una señal que el detector es capaz de leer en el tiempo. La transformada inversa de Fourier es un método matemático para descodificar la señal y recuperar la frecuencia individual para obtener finalmente el espectro.

La versatilidad y el alcance de la espectrometría IR, como herramienta de análisis cualitativo, ha aumentado sustancialmente por la técnica de la reflectancia total atenuada (ATR). En esta técnica la radiación infrarroja se hace pasar a través de un prisma fabricado con un material que presente un alto índice de refracción, en este caso un prisma de ZnSe, el cual transmite la radiación infrarroja de forma tal que la radiación se refleja una o más veces en las paredes internas del prisma. De este modo, se crea una onda evanescente que penetra en la muestra situada en contacto con la pared externa del prisma, y el haz pierde energía a las longitudes de onda en que el material absorbe. Esta radiación atenuada constituye un espectro de absorción característico del material. Cuando la medida de esta radiación se presenta en función del número de ondas, el resultado es una respuesta similar a la del espectro IR obtenido en el modo de transmisión normal.

En nuestro caso, la muestra se coloca de forma horizontal sobre el prisma. La profundidad aparente a la cual la radiación penetra en la muestra es de sólo unas cuantas micras y es independiente del espesor de la muestra. Como consecuencia, los espectros ATR pueden obtenerse para muchas muestras que no pueden estudiarse con

los métodos de transmisión normales. Así, puede ser usado con muestras intratables por encontrarse en cantidades mínimas; también con materiales sin previa preparación o en estudios de superficie. Tan sólo tiene una limitación: la muestra debe estar en contacto íntimo con el cristal de ATR. Este prisma deberá tener un índice de refracción relativamente alto comparado con el de la muestra.

Los espectros que se presentan en este trabajo han sido realizados con un equipo Nicolet 6700 Spectrometer equipado con un detector DTGS (Fig. 6.6). Un accesorio con control de presión fue empleado para igualar la presión en las diferentes muestras. Se empleó un prisma de ZnSe, los espectros fueron realizados con una resolución de 4 cm^{-1} y 100 espectros fueron promediados para cada muestra.

Fig. 6.6. Espectrómeto FTIR Nicolet 6700 con detector DTGS.

6.5.- ESPECTROSCOPÍA FOTOELECTRÓNICA DE RAYOS X (XPS)

La Espectroscopía Fotoelectrónica de Rayos X es una técnica espectroscópica dedicada a la caracterización de superficies [1]. A través de ella se pueden conocer los elementos químicos que hay presentes en la superficie de la muestra y la naturaleza de los enlaces químicos que existen entre estos elementos. Así mismo, procesando los datos convenientemente, se puede conocer la composición elemental de las especies presentes en la muestra.

La muestra a analizar es irradiada con un haz de rayos X, Fig. 6.7. El fotón incidente posee energía suficiente para expulsar un electrón interno, llamado fotoelectrón, fuera del átomo. La detección de los fotoelectrones, procedentes de diferentes átomos, permite diferenciarlos y determinar su energía de ligadura al núcleo, valor que es característico de cada átomo y del entorno atómico en el que se encuentra.
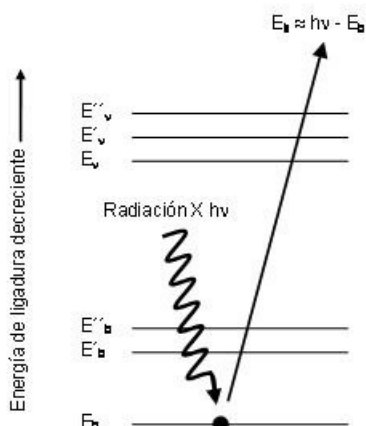

Fig. 6.7. Esquema del proceso XPS. El haz incidente está constituido por fotones de rayos X monoenergéticos. El haz emitido se compone de electrones.

Los análisis han sido realizados con un espectrómetro electrónico VG-Microtech Multilab. Las muestras han sido irradiadas con rayos X procedentes de un ánodo de Mg (emisión Kα 1253.6 eV) empleando el analizador en forma de energía constante con un paso de energía de 50 eV. Durante la emisión de rayos X, la potencia ha sido de 300 W (20 mA, 15kV). La presión en el interior de la cámara de análisis ha sido mantenida a $5 \cdot 10^{-10}$ mbars y a una temperatura de 173 K. Las escalas de las energías de enlace (E_b) han sido calibradas con referencia al C1s a 284.6 eV. La precisión de los valores de E_b es de ± 0.2 eV. Dependiendo de la escala de energía utilizada el rango de resolución espectral oscila de 0.10 a 0.15 eV. Los valores para E_b han sido obtenidos usando el programa Peak-fit incorporado al control del programa informático del espectrómetro.

6.6.- VOLTAMETRÍA CÍCLICA

La voltametría cíclica de barrido [2, 3] es una técnica electroquímica que consiste en la aplicación, sobre un electrodo de trabajo, de una variación de potencial lineal y periódica de acuerdo con el diagrama de la figura 6.8. Partiendo de un valor E_0 (límite inferior), se incrementa el potencial a velocidad constante v hasta un límite superior E_1, a partir del cual vuelve a disminuirse con igual velocidad, completándose cada ciclo o barrido al volver a alcanzarse el potencial de partida E_0.
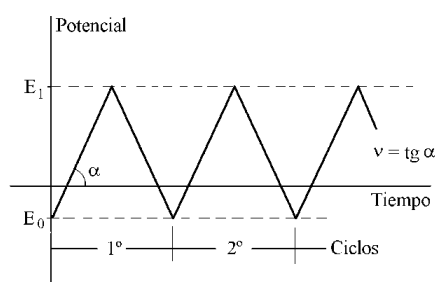

Fig. 6.8. Evolución del potencial aplicado en una típica experiencia de Voltametría Cíclica.

De esta aplicación de potencial se obtiene una corriente que es la respuesta del electrodo a la perturbación a la que es sometido en cada momento del barrido. El resultado de la representación gráfica de la intensidad de corriente obtenida por unidad de área de electrodo, con respecto al potencial aplicado se denomina: voltagrama.

La voltametría cíclica ha demostrado ser una técnica muy potente y flexible que es capaz de proporcionar una información muy variada acerca de los procesos que tienen lugar en la interfase electrodo/disolución. El uso de la voltametría cíclica permite acotar los rangos de potencial en los que aparecen los picos voltamétricos. Estos rangos son característicos de las especies que reaccionan, aunque en ocasiones están condicionadas por el medio electrolítico empleado, por la naturaleza del electrodo y por la estructura superficial del mismo.

La información que proporciona la voltametría cíclica no solamente procede de la forma de cada una de las curvas sino que, dado su carácter cíclico consecutivo, es posible deducir la evolución del comportamiento superficial comparando la evolución de

las curvas entre barridos sucesivos, tanto en su conjunto como en determinados tramos (máximos y mínimos, principalmente).

6.6.1. DISPOSITIVO EXPERIMENTAL

El montaje experimental empleado para llevar a cabo las experiencias voltamétricas consta de una célula de tres o cuatro electrodos conectada a un potenciostato/galvanostato Autolab modelo PGSTAT302 (Fig. 6.9). Los voltagramas se obtienen directamente en el programa informático General Purpose Electrochemical System (GPES) versión 4.9 suministrado por la casa comercial. La Figura 6.10 muestra un diagrama de bloques del sistema voltamétrico.
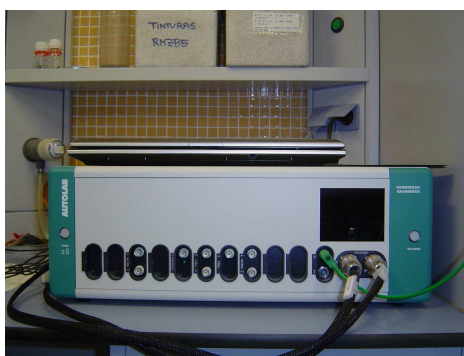

Fig. 6.9. Potenciostato/Galvanostato PGSTAT302 empleado para las medidas de voltametría cíclica y de impedancia electroquímica.
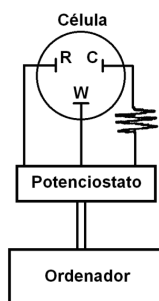

Fig. 6.10. Esquema general de la disposición de equipos y célula en las experiencias voltamétricas.

6.6.2.- CÉLULAS Y ELECTRODOS: DESCRIPCIÓN Y LIMPIEZA

Para llevar a cabo las experiencias voltamétricas se utilizaron células de trabajo de vidrio de la casa comercial Metrohm. Como puede apreciarse en la Fig. 6.11, las células poseen un cuerpo troncocónico y se cierran con un dispositivo de sujeción a presión. El dispositivo de cierre dispone de varios orificios a través de las cuales acceden: el electrodo de trabajo, dos contraelectrodos, electrodo de referencia y el sistema de burbujeo de nitrógeno.

Fig. 6.11. Célula electroquímica y dispositivo de cierre y sujeción en las experiencias voltamétricas.

Teniendo en cuenta que la presencia de pequeñas cantidades de impurezas, especialmente de tipo orgánico, afecta de manera decisiva al comportamiento electroquímico del electrodo de trabajo, fue necesario realizar una limpieza exhaustiva de las células antes de cada experiencia voltamétrica. El procedimiento que se siguió fue el siguiente: Las células, se sumergieron en disolución de $KMnO_4$ en medio básico (NaOH) durante 24 horas. A continuación, se extraen de la disolución oxidante y se lavan con agua oxigenada diluida y levemente acidificada (H_2SO_4). De esta forma se obtienen como productos $O_2\uparrow$ y sales de Mn(II), no perjudiciales para el medio ambiente. Seguidamente las células se enjuagan abundantemente con agua ultrapura obtenida con un sistema Elix 3 Millipore-Milli-Q Advantage A10. La resistividad del agua obtenida mediante este sistema fue 18.2 MΩ cm. Todo el material de vidrio empleado en la presente tesis se limpió mediante el mismo procedimiento de limpieza que el de las células electroquímicas.

En medio acuoso, el electrodo de referencia empleado fue el de Ag/AgCl con electrolito intermedio de KCl 3 M + AgCl. En el caso de la síntesis electroquímica de

polipirrol sobre tejidos conductores y sobre acero inoxidable se emplearon medios orgánicos (acetonitrilo). Así que como electrodo de referencia se empleó un electrodo de Ag/AgCl con electrolito intermedio de LiClO$_4$ 0.1 M en medio acetonitrilo; con el objetivo de disminuir el potencial de unión líquida. Todos los potenciales de las experiencias voltamétricas de este trabajo están referidos al electrodo de Ag/AgCl.

Como contraelectrodos se utilizaron barras cilíndricas (2 contraelectrodos) de acero inoxidable calidad AISI-316 de 4 mm de diámetro sumergidos en la disolución de trabajo.

Los materiales utilizados como electrodos de trabajo han sido acero inoxidable para obtener polímeros conductores sobre los mismos y tejidos conductores de PES-PPy/AQSA o PES-PPy/PW$_{12}$O$_{40}^{3-}$ obtenidos mediante síntesis química. La composición química del acero inoxidable se muestra en la tabla 6.1.

	Acero inoxidable
Fe	70.2-72.5
C	≤ 0.050
Mn	$\leq 2,000$
Si	≤ 0.750
S	0.015
P	0.040
Cr	18-19
Ni	8.5 -9

Tabla 6.1. Composición química media de los aceros usados como electrodos (de trabajo o contraelectrodo) en las experiencias voltamétricas (%, en peso).

Los electrodos de acero inoxidable fueron sometidos en sus extremos a un proceso de limpieza consistente en un pulido mecánico o desbaste mediante una lija mil hojas (tamaño de grano 80), desengrasado con acetona por inmersión en baño con ultrasonidos, pulimentado con polvo de alúmina de 0.05 µm (Buehler), y lavado con agua ultrapura por inmersión en baño de ultrasonidos. Finalmente se secan mediante un

secador por aire pulsado cuando las experiencias voltamétricas se realizan en medio orgánico (acetonitrilo) con el fin de no añadir H_2O al medio de trabajo.

Toda la experimentación voltamétrica fue realizada a la temperatura ambiente del laboratorio y con atmósfera de N_2 (premier X50S).

6.6.3.- CONSIDERACIONES ESPECIALES

A la hora de realizar experiencias voltamétricas con materiales textiles se ha observado que el material presenta unas características especiales que hacen necesario tener algunas consideraciones para obtener los mejores resultados.

Los tejidos conductores mojan la superficie del contacto eléctrico debido a su capilaridad, por lo que para minimizar la influencia de este parámetro se ha utilizado un contacto de Ti que presenta una respuesta mínima y reduce esta aportación. Además, los tejidos conductores presentan una caída óhmica debido a la resistencia que presentan, esta caída óhmica produce un desplazamiento de los potenciales en voltametría cíclica. La caída óhmica se midió mediante el potenciostato y se introdujo en el programa voltamétrico para su compensación.

El material base de los tejidos conductores es poliéster, un material aislante, por lo que la transferencia de carga es más lenta que en un sistema metal/polímero. Por ello se ha observado que velocidades altas de barrido (50 mV s^{-1}) producen una respuesta resistiva en los voltagramas. Menores velocidades de barrido (5 mV s^{-1} y 1 mV s^{-1}) permiten la aparición de los procesos redox.

6.7.- ESPECTROSCOPÍA DE IMPEDANCIA ELECTROQUÍMICA (EIS)

La técnica consiste en la aplicación de un potencial eléctrico de frecuencia variable al material objeto de estudio para medir la respuesta en corriente dentro de una célula electroquímica [4].

La interpretación de los resultados experimentales requiere el uso de una analogía entre el sistema electroquímico en estudio y un circuito eléctrico equivalente. Los resultados pueden ser interpretados mediante los diagramas de Nyquist y los diagramas de Bode. En los diagramas de Nyquist se representa la parte imaginaria de la impedancia frente a la parte real de la misma. En los diagramas de Bode se representa el logaritmo del módulo de la impedancia y la fase frente al logaritmo de la frecuencia. En estos diagramas es posible detectar las regiones que son dominadas por elementos resistivos tales como la resistencia del electrolito, resistencia electrónica del material, resistencia de intercambio electrón-ión e ión-ión, etc., y también los elementos capacitivos como la capacidad de un material dieléctrico y la capacidad de la doble capa electroquímica asociada a las interfases presentes. También se pueden analizar los procesos de difusión de iones mediante la resistencia característica de difusión de Warburg.

6.7.1.- DISPOSITIVO EXPERIMENTAL

Para realizar las medidas de impedancia se ha empleado un potenciostato/galvanostato Autolab modelo PGSTAT302 (Fig. 6.9), como en las experiencias de voltametría cíclica y el programa informático Frequency Response Analyser (FRA) versión 4.9. Las medidas de impedancia fueron realizadas a potencial constante una vez estabilizado el potencial del sistema a circuito abierto. La amplitud del potencial empleado fue de $\pm$ 10 mV y el rango de frecuencias entre 10^5 y 10^{-2} Hz o 10^4-10^{-2} Hz (se realizaron medidas de impedancia en función de la temperatura). Los ajustes mediante circuitos equivalentes de los datos experimentales y las simulaciones fueron realizados mediante el programa informático Zview versión 2.70.

6.7.2.- CÉLULAS Y ELECTRODOS: DESCRIPCIÓN

El estudio de impedancia se dividió en dos partes. La primera parte corresponde al estudio de caracterización de la respuesta de impedancia de los tejidos conductores en disoluciones con diferentes pH. Para ello se empleó una célula como las que se emplea en voltametría (Fig. 6.11). El electrodo de trabajo es el tejido a analizar;

como contraelectrodo se emplea un electrodo de acero inoxidable y un electrodo de referencia Ag/AgCl en medio acuoso.

La segunda parte corresponde al estudio de la impedancia con la temperatura de los tejidos conductores y de las pastillas de PPy/AQSA y PPy/PW$_{12}$O$_{40}$$^{3-}$. Las medidas de espestroscopía de impedancia electroquímica con la temperatura fueron empleadas para obtener la conductividad de las muestras de polipirrol y su comportamiento frente a la temperatura (comportamiento conductor o semiconductor). En las medidas con la temperatura, la interfase Solartron 1286 fue empleada para controlar el potencial y un equipo Solartron 1253 analizador Ganancia-Fase fue empleado para realizar las medidas de EIS en el rango de frecuencia de 10^4-10^{-2} Hz. La amplitud de la señal sinusoidal de potencial empleada para perturbar fue de 10 mV. Cada medida fue realizada a un potencial constante impuesto igual al potencial a circuito abierto al principio del experimento. Para la mayoría de las muestras, las medidas con la temperatura fueron realizadas en el rango de temperaturas 25-70 ºC. Un horno Carbolite CTF 12/65/550 fue empleado para controlar la temperatura con el programa Settemp 3.0. Una célula de temperatura GF-800 fue empleada para realizar las medidas. Para analizar cuantitativamente los resultados experimentales fueron ajustados empleando el programa ZView (versión 2.7).

6.7.2.1. CÉLULA DE MEDIDA PARA MEDIDAS CON LA TEMPERATURA

La célula GF-800 (Fig. 6.12) permite realizar medidas en electrólitos sólidos con temperaturas hasta 800 ºC. Los electrodos donde se inserta la muestra son dos electrodos de Pt activados por muelle (por lo que la presión sobre las muestras es siempre la misma). Los electrodos de Pt son redondos y con un área de 10 mm^2.

Placas y tubos de acero inoxidable especial (inconel$^®$), hilos y electrodos de platino, tubos de aislamiento de aluminio y soportes de cerámica de alúmina mecanizada, son los elementos utilizados para construir la parte de alta temperatura de la célula. Cuatro tubos sujetos por medio de 2 placas intermedias forman la construcción rígida sujeta al cabezal de bronce de la estructura de la célula. El más largo de estos tubos, que atraviesa el cabezal de bronce, sirve como entrada de gas externo; a través del otro se inserta un termopar NiCr-Ni, que llega hasta la zona muy próxima a la

muestra. Un tubo de cuarzo sujeto con una junta tórica permite realizar medidas bajo flujo de gas si se desea. Un apantallado de acero completa la célula para evitar interferencias no deseadas.

Fig. 6.12. Celdas portamuestras GF 800.

En la Fig. 6.13 se muestra el montaje experimental para medir impedancia con la temperatura, donde la célula de medida se introduce en el horno. En la Fig. 6.14 se muestran imágenes del sistema de medida.
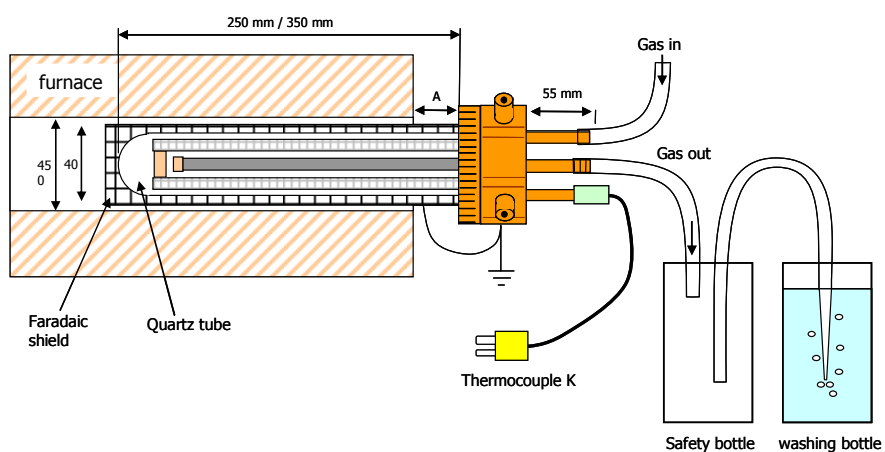

Fig. 6.13. Esquema del montaje de medida impedancia con la temperatura con la célula GF 800 [5].

Fig. 6.14. Imágenes del montaje para realizar medidas de impedancia con la temperatura.

6.8. MICROSCOPÍA ELECTROQUÍMICA DE BARRIDO (SECM) [6-8]

La figura 6.15 muestra un esquema de la instrumentación básica del microscopio electroquímico de barrido (SECM) y en la Fig. 6.16 unas imágenes del equipo empleado para los análisis. Un ultramicroelectrodo (UME) es fijado al posicionador que se puede mover en los tres ejes (x, y, z) que a su vez va conectado a un ordenador que adquiere también los datos. En la Fig. 6.16 se muestra la foto de los UME y una imagen obtenida mediante microscopía óptica de la punta del UME, donde se observa un hilo metálico de Pt dentro del capilar de vidrio. En la presente tesis se ha empleado el modo de altura constante, en ellas el UME siempre se encuentra a una altura constante independientemente del perfil de la muestra. En caso de querer realizar medidas a distancia constante, es decir el UME mantiene siempre la misma distancia de la muestra adaptándose al perfil de ésta, se tendría que usar un posicionador

piezoeléctrico. Un bipotenciostato (de 4 electrodos) controla el potencial del UME y/o el del sustrato frente al electrodo de referencia y mide las corrientes del sustrato y del UME. El SECM suele montarse en una plataforma antivibratoria para evitar vibraciones y dentro de una caja de Faraday para evitar interferencias. Se utiliza un contraelectrodo de Pt. La célula de medida es una microcélula donde se colocan el CE, RE, UME, la muestra y la disolución. Diferentes modos de análisis pueden ser llevados a cabo con la misma configuración como: modo retroalimentación (feedback), generación en el UME/ recogida en el sustrato (TG/SC), generación en el sustrato/ recogida en el UME, modo de penetración y modo retroalimentación con transferencia de iones.

En la presente tesis se ha empleado el método de retroalimentación (feedback) para ver el comportamiento conductor y electroactivo de los tejidos conductores y observar las diferencias después de realizar los tratamientos con disoluciones de diferente pH. También se puede obtener el perfil topográfico de la muestra con el mismo modo de feedback.
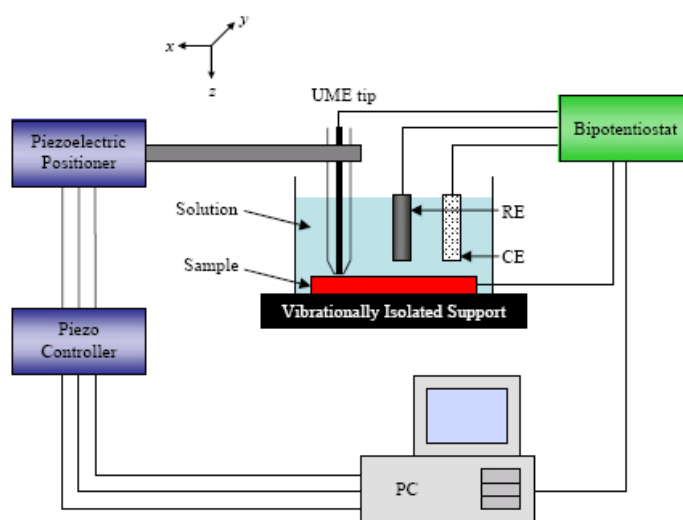

Fig. 6.15. Esquema de la instrumentación básica del microscopio electroquímico de barrido (SECM [9]).
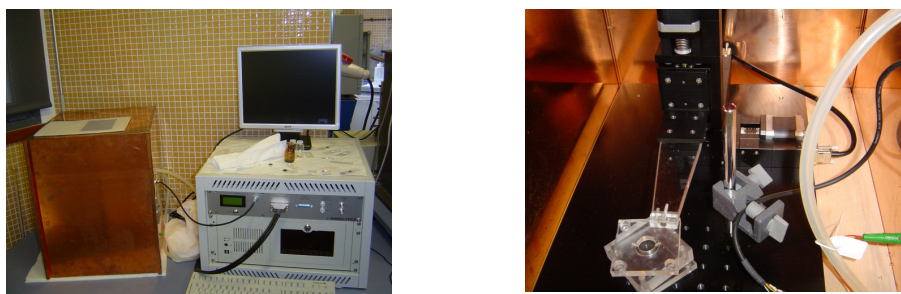
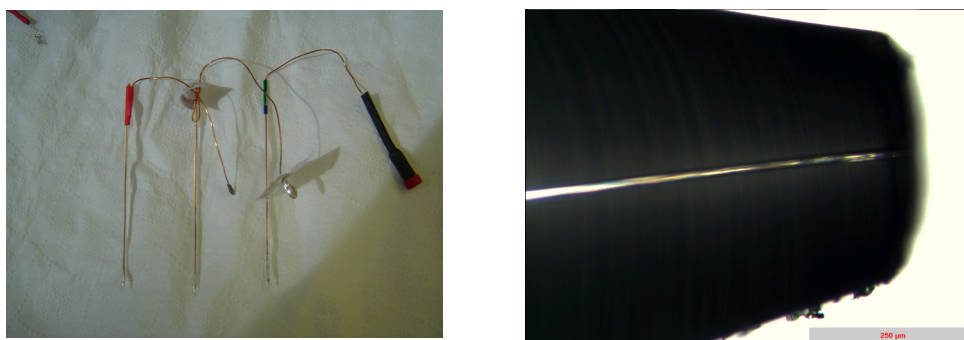*Fig. 6.16. Imagen del equipo de microscopía electroquímica de barrido empleado para el presente trabajo.*

Fig. 6.17. Imagen de los microelectrodos (UME) e imagen obtenida mediante microscopía óptica de la punta del UME.

6.8.1. MODOS DE RETROALIMENTACIÓN

En la Fig. 6.18 se muestran los diferentes modos de feedback de la técnica de SECM. En la disolución se emplea siempre un mediador redox que pueda pasar de estado oxidado (O) a estado reducido (R) y viceversa. En nuestro caso empleamos el mediador $Ru(NH_3)_6^{3+}$ que se reduce en el microelectrodo a $Ru(NH_3)_6^{2+}$, el microelectrodo siempre trabaja a un potencial de reducción, para conseguir la reducción del mediador redox.

La difusión libre se muestra en la Fig. 6.18-A, donde no hay un impedimento para que la especie oxidada llegue al microelectrodo y sea reducida, la corriente que se

alcanza es la corriente límite (i_{lim}); i_{lim}= 4·n·F·D·a·C. Donde n es el número de electrones envueltos en la reacción; F es la constante de Faraday; D es el coeficiente de difusión; a es el radio del ultramicroelectrodo y C es la concentración del reactivo. En el segundo caso (Fig. 6.18-B), tenemos un material conductor como sustrato, por lo que cuando el microelectrodo se acerca a la superficie se produce un aumento de la corriente de reducción ($i>i_{lim}$). El sustrato es capaz de reoxidar el mediador, por lo que el microelectrodo cuando se acerca a la superficie reduce más moléculas de mediador en estado oxidado, por ello se produce un aumento de la corriente normalizada (i/i_{lim}), este caso se denomina feedback positivo. En cambio cuando tenemos un sustrato aislante (Fig. 6.18-C), el mismo no es capaz de reoxidar la forma reducida del mediador. Por ello cuando el microelectrodo se acerca a la superficie se produce un descenso de la corriente de reducción debido a que la difusión de la especie oxidada se encuentra impedida, lo que dificulta la libre difusión ($i<i_{lim}$). Éste último caso es denominado feedback negativo.
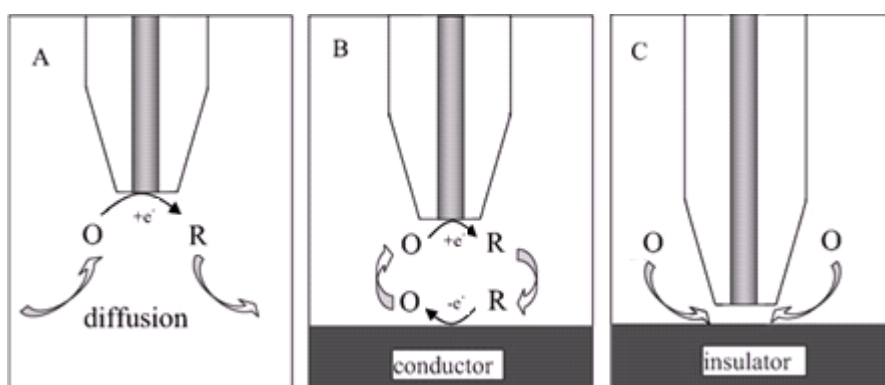

Fig. 6. 18. Esquema donde se presentan las diferentes posibilidades que se pueden dar en el modo de retroalimentación con el sistema Ru(NH$_3$)$_6$$^{3+}$/Ru(NH$_3$)$_6$$^{2+}$, A) difusión libre, B) feedback positivo, C) feedback negativo.

6.8.2. OBTENCIÓN DEL PERFIL TOPOGRÁFICO

El perfil topográfico de las muestras también se puede obtener con la técnica de SECM. Para ello se trabaja también con el modo de retroalimentación (feedback). Se trabaja a una altura (respecto al sustrato) donde no haya difusión libre y al mismo

potencial de reducción que con las curvas de aproximación. Se realiza un barrido de la superficie en el eje x e y, normalmente 1200 μm x 1200 μm y se obtiene el perfil topográfico de las muestras. Aquellas zonas de la muestra que se encuentran más elevadas, producirán un aumento de la corriente de reducción, debido a que el tejido es un material conductor. En las zonas más alejadas, se produce el fenómeno contrario, con lo que se puede obtener un mapa del perfil topográfico de las muestras.

6.9. TERMOGRAVIMETRÍA (TG)

Los análisis termogravimétricos se realizaron con un equipo Mettler-Toledo TGA-SDTA 851e, que permite velocidades de calentamiento de 274 a 473 K min^{-1} hasta una temperatura de 1473 K. Las medidas dinámicas fueron llevadas a cabo desde 303 a 1173 K a una velocidad de calentamiento de 293 K min^{-1}. Las medidas termogravimétricas fueron llevadas a cabo en crisoles de aluminio. Las muestras fueron colocadas sin tratamiento previo en los crisoles y los experimentos fueron llevados a cabo inmediatamente. Las medidas termogravimétricas fueron llevadas a cabo en atmósfera de nitrógeno y aire ambiente empleando un flujo de 200 ml min^{-1}.

Con los análisis termogravimétricos se pretende determinar la estabilidad térmica de los polvos de PPy/AQSA y PPy/$PW_{12}O_{40}^{3-}$ y las pérdidas de masa que tiene lugar a las distintas temperaturas. Los contraiones orgánicos (como el AQSA) se degradan en el mismo rango de temperatura que el polipirrol por lo que es difícil separar los procesos. El empleo de un contraión inorgánico ($PW_{12}O_{40}^{3-}$) que no se degrada en el rango de temperaturas que lo hace el polipirrol permitiría estudiar aisladamente la degradación del polipirrol.

6.10. CALORIMETRÍA DIFERENCIAL DE BARRIDO (DSC)

Los análisis calorimétricos fueron llevados a cabo empleando un Calorímetro Diferencial de Barrido (DSC) Mettler-Toledo 821 (Mettler-Toledo Inc, Schwerzenbach, Switzerland). La masa de las muestras empleadas fue de 8-9 mg.

Mediante calorimetría diferencial de barrido se pretende determinar las posibles transiciones térmicas (procesos exotérmicos o endotérmicos) que puedan tener lugar en las muestras de $PPy/PW_{12}O_{40}^{3-}$.

6.11. PIRÓLISIS/CROMATOGRAFÍA DE GASES/ESPECTROMETRÍA DE MASAS (Py-GC-MS)

Las muestras fueron pirolizadas con un pirolizador (Pyroprobe® 1000 de CDS Analytical, Inc), interconectado con un GC/MS (6890N Agilent Technologies) equipado con un detector selectivo de masas (MSD) (Agilent Technologies España S.L., Madrid, España). Las muestras (1.1-1.2 mg) fueron pirolizadas a 723 K durante 10 s. La columna empleada en el cromatógrafo de gases (GC) fue una columna capilar de 30 m (HP-5 ms), con un espesor de 0.25 mm, fase estacionaria de 0.25 μm. Fue programada desde 313 a 573 K con una velocidad de calentamiento de 283 K min^{-1} y fue mantenida a la temperatura más alta durante 5 min. El gas portador empleado fue He con un ratio de Split de 50:1. El detector selectivo de masas fue programado para detectar masas ente 50 y 650 amu.

Con esta técnica se pretende determinar los posibles compuestos surgidos a partir de la degradación térmica de los polvos de $PPy/PW_{12}O_{40}^{3-}$.

6.12. ENSAYOS DE RESISTENCIA AL FROTE Y LAVADO

Los ensayos de resistencia al frote fueron realizados como se explica en la norma ISO 105-X12:2001 [10]. Cada muestra fue frotada contra un tejido de algodón durante 10 ciclos. La presión aplicada fue de 1 Kg. Se realizaron ensayos en húmedo y en seco. Se utilizó un crockmeter (Atlas Electric Devices Company). Los valores de degradación y descarga del tejido fueron evaluados con la escala de grises. Como ejemplo se muestra en la Figura 6.19-a la muestra original. Tras realizar el ensayo de resistencia al frote, se observa como en la muestra aparece un surco de color más blanquecino (Figura 6.19-b). Esta franja es debida a que el ensayo de fricción ha eliminado parte del recubrimiento de polipirrol. En la Figura 6.19-c se muestra el aspecto del testigo de algodón después de realizar el ensayo de resistencia al frote.
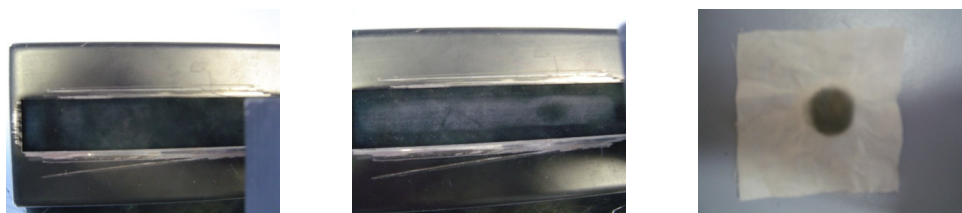
Fig. 6. 19. Imágenes donde se presenta: a) la muestra antes de realizar el ensayo de frote, b) después de realizar el ensayo de frote, c) testigo de algodón después de realizar el ensayo de frote.

Los ensayos de lavado se realizaron según la norma ISO 105-C01 [11]. Para realizar los ensayos se utilizó un Linitest® (Fig. 6.20-a). Los valores de degradación del color y descarga de color fueron obtenidos después de los ensayos mediante la escala de grises.

- Tamaño muestra utilizada 10 x 4 cm.
- Se utiliza un testigo de PES y otro testigo de algodón.
- Se hace un sándwich de PES / PES-PPy/$PW_{12}O_{40}^{3-}$ / Algodón. Se cosen los tres tejidos por uno de los lados cortos (Fig. 6.20-b).
- Masa tela = 1.65 g.
- Relación de baño = 1:50.
- Masa de baño = 82.5g = 82.5 ml.
- Concentración de detergente=5 g/l.
- Se pesan 0.4125g de detergente Solpon OWS.
- Se introducen los tejidos y la disolución con el detergente en un cilindro de acero inoxidable (Fig. 6.20-d).
- Se cierra el cilindro de acero inoxidable y se coloca en el Linitest® (Fig. 6.20-c).
- Se lava a 40 ºC con el Linitest®.
- Se enjuaga dos veces con agua ultrapura.
- Se lava con agua corriente del grifo durante 10 minutos.
- Finalmente se evalúa la degradación en el tejido de PES-PPy/$PW_{12}O_{40}^{3-}$ y la descarga en los dos testigos de PES y de algodón según la escala de grises.
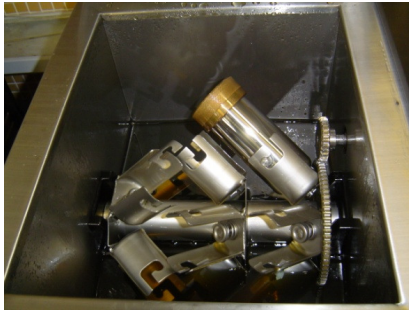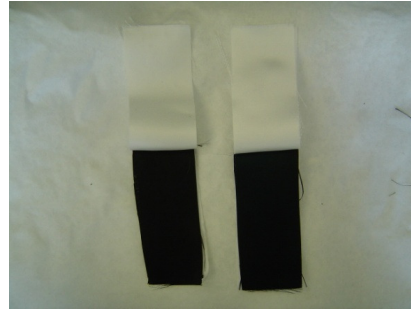
Fig. 6. 20. Imágenes donde se presenta: a) linitest, b) muestras para realizar ensayo de lavado, c) interior del linitest, d) probeta con la muestra y el detergente.

6.13. BIBLIOGRAFÍA

[1] R. Benoit CNRS Orléans, Y. Durand, B. Narjoux, G. Quintana, Y. Georges, X-Ray Photoelectron Spectroscopy Database. La Surface, Thermo Electron Corporation, Thermo Electron France. http:// www.lasurface.com/database/elementxps.php.

[2] A.J. Bard, L.R. Faulkner, "Electrochemical methods Fundamentals and Applications", cap-6, Wiley & Sons, New York, (1980).

[3] Southampton Electrochemistry Group. "Instrumental Methods in Electrochemistry", cap-6, Ellis Horwood, Chichester, (1985).

[4] Princeton Applied. Research Application note AC-1 "Basic Electrochemical Impedance Spectroscopy (EIS)".

[5] http://www.eiccontrol.com/productos/productos/productos%20solartron/GFserie.htm

[6] P. Sun, F.O. Laforge, M.V. Mirkin, Phys. Chem. Chem. Phys. 9 (2007) 802.

[7] M.V. Mirkin, B.R. Horrocks, Anal. Chim. Acta 406 (2000) 119.

[8] A.L. Barker, M. Gonsalves, J.V. Macpherson, C.J. Slevin, P.R. Unwin, Anal. Chim. Acta 385 (1999) 223.

[9] http://www2.warwick.ac.uk/fac/sci/chemistry/research/physicalchemistry/unwin/electrochemistry/research/secm/

[10] Norma UNE-EN ISO 105-X12. Textiles. Ensayos de solidez del color. Parte X12: Solidez del color al frote (ISO 105-X12:2001).

[11] Norma UNE-EN 20105-C01. Textiles. Ensayos de solidez de las tinturas. Parte C01: Solidez de las tinturas al lavado (ISO 105-C01:1989).

7.- ARTÍCULO

CHEMICAL AND ELECTROCHEMICAL POLYMERISATION OF PYRROLE ON POLYESTER TEXTILES IN PRESENCE OF PHOSPHOTUNGSTIC ACID

Chemical and electrochemical polymerisation of pyrrole on polyester textiles in presence of phosphotungstic acid

J. Molina, A.I. del Río, J. Bonastre, F. Cases *

Departamento de Ingeniería Textil y Papelera, EPS de Alcoy, Universidad Politécnica de Valencia, Plaza Ferrándiz y Carbonell s/n, 03801 Alcoy, Spain

Abstract

Polypyrrole (PPy) was chemically synthesised on polyester (PES) textiles to produce conducting textiles. Two different types of counter ion were employed: anthraquinone sulfonic acid (AQSA) and phosphotungstate ($PW_{12}O_{40}^{3-}$). Textiles covered with PPy were characterised by means of FTIR-ATR, SEM, EDX, Cyclic Voltammetry (CV), surface resistivity measurements and Electrochemical Impedance Spectroscopy (EIS). Additionally, friction and washing assays were done to test the resistance of the layer of conducting polymer ($PPy/PW_{12}O_{40}^{3-}$). Electropolymerisation of $PPy/PW_{12}O_{40}^{3-}$ in acetonitrile medium onto chemically synthesised $PES-PPy/PW_{12}O_{40}^{3-}$ showed the improvement of the coating properties.

Keywords: Polypyrrole; phosphotungstate; polymer coating; conducting textiles; electropolymerisation.

_____

* Corresponding author. Fax.: +34 96 652 8438

E-mail address: fjcases@txp.upv.es (Prof. F. Cases)

1. Introduction

The electrical properties of polypyrrole were first reported by Weiss et al. in a complete study [1-3]. In this study polypyrrole was obtained through pyrolysis of tetraiodopyrrole. The first electrochemical polymerisation of pyrrole was reported by Diaz et al. [4-6].

On the other hand, development of textiles with new properties and applications has received great attention during the last years. One of these properties is the electrical conductivity in textiles. Applications of conducting textiles are varied and

numerous; like antistatic applications [7], gas sensors [8], biomechanical sensors [9], electrotherapy [10, 11], heating devices [12-14], microwave attenuation [15], dye removal [16]. Different methods have been used to produce conducting textiles; like employing metallic fibres mixed with non-metallic fibres, chemical metallisation of fibres [17], extrusion of fibres with conductive particles like carbon or the synthesis of conducting polymer films on textiles. The last is the method employed in this paper to produce polypyrrole conducting textiles.

In [18] it can be seen the patent literature evolution on the polymerisation of pyrrole on different textile substrates. Different textile materials have been used to produce polypyrrole conducting textiles obtained by chemical reaction, like polyester [7, 8, 15, 19], nylon [9, 10, 20, 21], cotton [12, 22], silk [22], cellulose derivatives [23-25], polyester-nylon [13] and polyaramide [26]. The methods employed in chemical polymerisation are: in-situ polymerisation [8, 20], two steps polymerisation [9, 10, 12, 13, 19, 21-26] and emulsion polymerisation [7]. When in-situ polymerisation is employed, all the reagents are added at the same time and reaction occurs. Two steps polymerisation has one step of adsorption of certain reagents and the stage of reaction when the rest of reagents are added. Emulsion polymerisation is less employed. Vapour phase polymerisation [22, 23] has been employed as a method available to be automated. The method employed was the two steps process with a previous adsorption of oxidant and counter ion and the subsequent exposure to pyrrole vapours; occurring the polymerisation.

In the polymerisation of pyrrole to form polypyrrole, positive charges are created in the polypyrrole structure. These positive charges need to be neutralised to maintain the electroneutrality; these negative charges are provided by a counter ion. Low size anions like Cl$^-$ have been employed as counter ions, but their stability is low [15]. Typical counter ions employed in textiles covered with polypyrrole are organic molecules with high size; like anthraquinone sulfonic acid (AQSA) [8, 13, 15, 19, 21, 27], dodecylbenzene sulfonic acid (DBSA) [7, 21], p-toluene sulfonic acid (PTSA) [8, 15, 20, 21], naphthalenedisulfonic acid (NDSA) [9, 15, 21], benzenesulfonic acid (BSA) [10, 26], naphthalenesulfonic acid (NSA) [15, 20], anthraquinone disulfonic acid [23, 25]. The higher size of the counter ion, the more difficult the expulsion of the counter ion from the structure is.

Polyoxometalates, POMs, are small oxide clusters whose size and solubility have caused them to be traditionally considered within the framework of molecular chemistry. They are indeed complex molecules with several metallic ions coordinated by shared oxide ions, forming a highly symmetrical metal oxide cluster [28]. They present

the possibility to produce a hybrid material when combined with conducting polymers such as polypyrrole. These polyoxometalates are trapped into the polymeric matrix due to the electroneutrality principle when the synthesis occurs. Therefore, a hybrid material with combined properties (organic-inorganic) is synthesised. The new material has higher density and conductivity than polypyrrole alone [29]. The presence of active ionic species immobilised in the polymeric matrix force the cations instead of the anions present in the medium to diffuse through the polymer structure when an oxidation or a reduction reaction occurs. In addition, polyoxometalates are anions of high volume and charge, so their diffusion coefficient is low, and the exchange with anions present in the solution is prevented. Polyoxometalates have been combined with polypyrrole to produce hybrid materials on Pt [30-32] and carbon steel electrodes [33].

Polyoxometalates have not been employed as counter ions to produce conducting textiles to our knowledge. The aim of this paper is to produce polyester textiles covered with the hybrid material $PPy/PW_{12}O_{40}^{3-}$. Additionally, polyester textiles covered with PPy/AQSA have been produced to compare the results with that obtained with the hybrid material. When the size of the counter ion is high its diffusion is prevented and it remains in the polypyrrole structure [34]. This is the basis for employing $PW_{12}O_{40}^{3-}$ with high molecular size that would difficult the expulsion of the counter ion. The presence of W in the hybrid material with a high atomic weight allows the knowledge of the superficial distribution of the counter ion employing SEM combined with backscattered electrons. Furthermore, $PW_{12}O_{40}^{3-}$ has a high negative charge and catalytic properties that make this hybrid material interesting for catalytic reactions. Electrochemical characterisation with CV and EIS has been employed to characterise the films of conducting polymers on textiles. EIS has not been employed to characterise textiles covered with conducting polymers to our knowledge. Only a few assays of CV have been performed on conducting textiles; in the reference [20] we can see a study of cyclic voltammetry on nylon membranes coated with PPy.

Electropolymerisation of pyrrole has been employed as a method to produce conducting textiles [11, 35]. Bhadani et al. [35] covered a Pt anode with cotton fibre. Electrolysis at 40mA with pyrrole and PTSA was realised. The result was the indirect formation of polypyrrole on cotton fibres. Kim et al. [11] covered nylon/spandex chemically and later electrochemically similarly to [35]. Chemically polypyrrole covered textile was put between stainless steel plates and electropolymerisation occurred. In our study the PES textile covered chemically with polypyrrole is employed as anode material to polymerise electrochemically the hybrid material $PPy/PW_{12}O_{40}^{3-}$.

2. Experimental

2.1. Reagents

Analytical grade pyrrole, sodium sulphate, ferric chloride, anthraquinone sulfonic acid sodium salt (AQSA), sulphuric acid, sodium dihidrogenophosphate, disodium hidrogenophosphate and Lichrosolv. acetonitrile were purchased from Merck. Analytical grade phosphotungstic acid hydrate was supplied by Fluka. Normapur acetone was from Prolabo. Ultrapure water was obtained from an Elix 3 Millipore-Milli-Q RG system with a resistivity near to 18.2 MΩ·cm.

2.2. Chemical synthesis of PPy/$PW_{12}O_{40}{}^{3-}$

Chemical synthesis of polypyrrole on polyester textiles was done as reported by Lin et al. [19]. Size samples were 6 cm x 6 cm approximately. Polyester was degreased with acetone in ultrasound bath previously to reaction. Pyrrole concentrations employed in chemical polymerisations were 0.5, 1 and 2 g/l. The molar relations employed in the chemical synthesis bath were pyrrole: $FeCl_3$: AQSA (1: 2.5: 0.6); when $PW_{12}O_{40}{}^{3-}$ was employed as counter ion the relation was 1: 2.5: 0.2. The molar relation of counter ion is three times lower when $PW_{12}O_{40}{}^{3-}$ is employed than when AQSA is used, due to the fact that $PW_{12}O_{40}{}^{3-}$ has three negative charges; on the other hand AQSA only posses one negative charge. Next stage was the adsorption of pyrrole and counter ion (V = 200 ml) (AQSA or $PW_{12}O_{40}{}^{3-}$) on the textile during 30 minutes at 0 ºC without stirring. Passed this time, $FeCl_3$ solution (50 ml) was added and reaction elapsed during 150 min at 0 ºC without mechanical agitation. Adsorption and reaction elapsed in a precipitates beaker. Polymerised textile was washed with water to remove polypyrrole not joined to fibres. The conducting textile was dried in a desiccator during at least 24 hours before measurements. The weight increase for the textile covered with PPy/$PW_{12}O_{40}{}^{3-}$ was measured obtaining a value between 7-10 % for polymerisations where 2 g/l pyrrole was employed.

2.3. Electrosynthesis and Cyclic Voltammetry

Electrosynthesis and cyclic voltammetry (CV) experiments were performed using an Autolab PGSTAT302 potentiostat/galvanostat. All electrochemical experiments were realised at room temperature and without stirring. Stainless steel counter

electrodes (CE) were employed; the pre-treatment consisted on polishing, degreasing with acetone in ultrasonic bath and washing with water in the ultrasonic bath. In electrochemical synthesis two CE were used to equalise the electrical field around the working electrode (WE) of conducting polymer. Potential measures were referred to Ag/AgCl reference electrode. Oxygen was removed from solution by bubbling nitrogen gas. The pH study was made employing solutions in the range 1-13.

In electrosynthesis and CV experiences the WE were made by cutting a tyre of the material and controlling the area with Teflon®. The conducting textile has an ohmic fall that we need to consider in cyclic voltammetry and electrosynthesis, in a different way the measured potentials will not be real. In these experiments the ohmic fall was measured and entered in the potentiostat/galvanostat. CV measures were done after 1 h of contact of the conducting textile electrode with the measuring solution in N_2 atmosphere to achieve the equilibrium stage; it has been corroborated that contact time had influence in the voltammetric response.

Electrosynthesis was performed in acetonitrile medium with 0.01 M $H_3PW_{12}O_{40}$ and 0.2 M pyrrole in N_2 atmosphere. The conducting textile electrode was soaked with the solution during 10 minutes to allow the diffusion of species to the electrode. The synthesis potential was determined by CV. In this medium the potential was cycled between 2.5 V and -0.8 V. When the slope of the voltammogram rises is a sign that polymerisation is occurring. In our electrochemical system, the determined synthesis potential was 1.5 V. For the potentiostatic synthesis the conducting textile electrode was immersed at open circuit potential and then the potential was risen up to the synthesis potential of 1.5 V, going on the electrosynthesis the necessary time to achieve the desired electrical charge. After synthesis, the electrode was washed with acetonitrile. After that, the electrode was immersed in the measuring solution during 1 h and characterised by means of CV.

2.4. FTIR-ATR Spectroscopy

Fourier Transform Infrared Spectroscopy with horizontal multirebound Attenuated Total Reflection (FTIR-ATR) was performed with a Nicolet Magna 550 Spectrometer equipped with DTGS detector. An accessory with pressure control was employed to equalise pressure in the different solid samples. A prism of ZnSe was employed. Spectra were collected with a resolution of 4 cm^{-1}, and 100 scans were averaged for each sample.

2.5. SEM and EDX

A Jeol JSM-6300 Scanning Electron Microscope was employed to obtain the morphology of the samples and perform EDX analyses. SEM analyses were performed using an acceleration voltage of 20 kV. EDX measures were realised between 0 and 20 kV. Secondary electrons were employed to obtain micrographs and additionally the samples that contained W were also analysed with backscattered electrons.

2.6. Abrasion and washing assays

Abrasion resistance tests of polypyrrole covered textiles were performed as explained in the norm ISO 105-X12:2001. Each sample was abraded against cotton abrasive fabric for 10 cycles. This analysis was performed only for chemically synthesised samples due to the big sample size needed (20 x 18 cm). Washing fastness was determined as related in the norm ISO 105-C01.

Surface resistivity measures were performed employing a surface resistivity meter Model SRM-232-2000, 0-2000 Ω/square (Guardian Manufacturing) that employed the 4-point probe technique. Electrochemical Impedance Spectroscopy (EIS) (Autolab PGSTAT302 potentiostat/galvanostat) was employed to measure surface resistivities higher than 2000 Ω/square and characterise the material with this technique. EIS measures were carried out using two rectangular copper electrodes (0.5 cm x 1.5 cm) separated by 1.5 cm and pressed to the textile sample. The measured area of the textile was a square of 1.5 cm x 1.5 cm, so the measured resistance (Ω) was equal to the surface resistivity (Ω/square).

3. Results and discussion

3.1. FTIR-ATR Spectroscopy

Fig. 1 shows the spectra of PES, PES chemically covered with the hybrid material $PPy/PW_{12}O_{40}^{3-}$ and covered with PPy/AQSA. If we compare the FTIR spectra of PES and PES covered with the hybrid material, it can be distinguished the band centred at 1550 cm^{-1} associated to the pyrrole ring stretching vibration (C=C) [23, 25]. The characteristic bands of the bending vibration of pyrrole can be observed at 775, 1030 and 1160 cm^{-1} [23, 25]. Other bands overlapped with PES bands partially can be observed; like C-C stretching (1450 cm^{-1}) [23, 25] and C-N stretching (1300 cm^{-1}) [23,

25]. The band overlapped with PES band partially at 1075 cm^{-1} (P-O stretching) [36, 37] indicates the presence of the polyoxometalate. This band can be observed more defined in the Fig. 2 for a concentration of pyrrole of 1 g/l or 0.5 g/l. The other bands of $PW_{12}O_{40}^{3-}$ are overlapped with those of PES. EDX analyses were realised to make sure the presence of $PW_{12}O_{40}^{3-}$. FTIR spectrum is not changed substantially when AQSA is employed as counter ion. Additionally to the mentioned bands of polypyrrole, two bands centred at 1670 cm^{-1} and 710 cm^{-1} were observed, attributed to the AQSA structure [38].
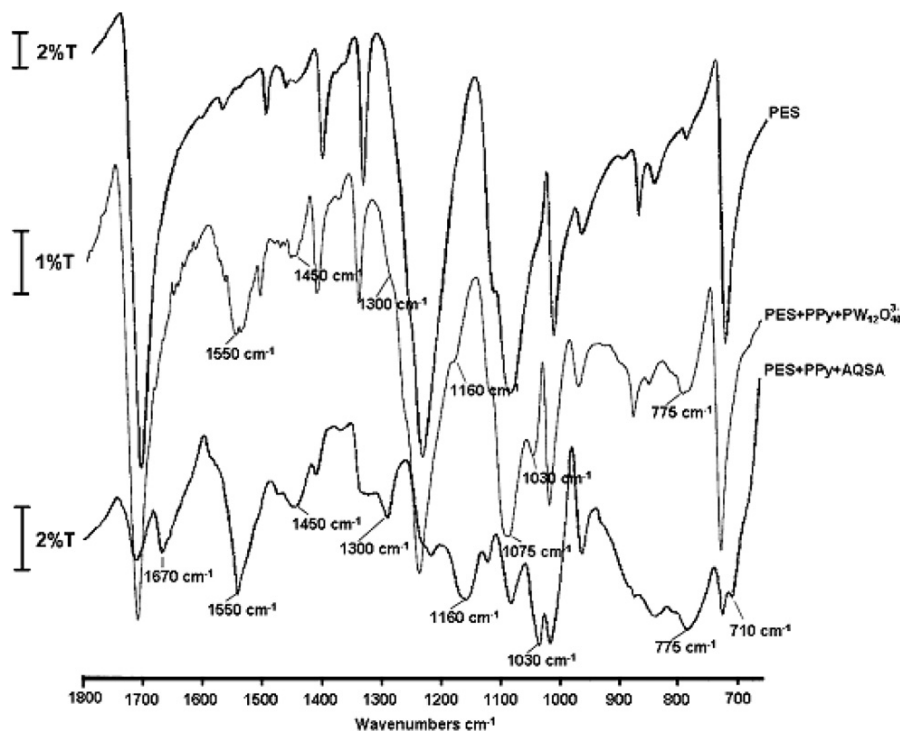

Fig. 1. FTIR-ATR spectrum of PES, PES covered with PPy/PW$_{12}$O$_{40}$$^{3-}$ (2 g/l pyrrole) and PES covered with PPy/AQSA (2 g/l pyrrole). Resolution 4 cm^{-1}, 100 scans.

The effect of pyrrole concentration in the FTIR spectrum can be observed in Fig. 2. It can be seen a general increase of all the bands mentioned previously when the concentration of pyrrole is increased from 0.5 g/l to 1 g/l. When pyrrole concentration is increased from 1 g/l to 2 g/l the tendency is to maintain the band intensity.
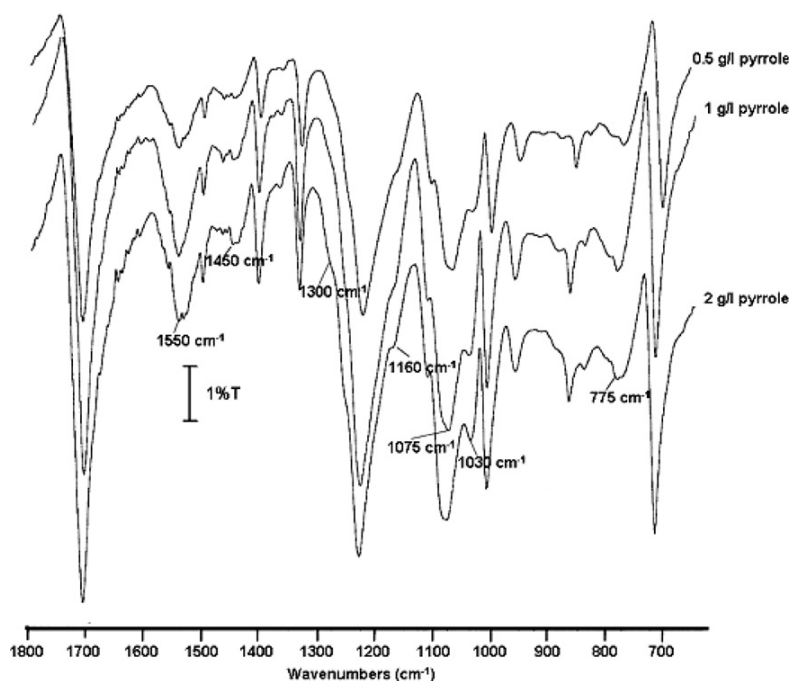
Fig. 2. FTIR-ATR spectrum of PES covered with the hybrid material PPy/PW$_{12}$O$_{40}$$^{3-}$ with pyrrole concentrations of 0.5, 1 and 2 g/l in the synthesis solutions. Resolution 4 cm^{-1}, 100 scans.

3.2. Scanning Electron Microscopy (SEM) and Energy Dispersive X-Ray (EDX)

In this section the PES and PES covered with polypyrrole morphology is analysed by means of SEM obtained by secondary electrons and back-scattered ones. Zonal analysis with EDX was employed to analyse zones of interest by focussing the electron beam in the selected area. The substrate morphology (PES) can be observed in Fig. 3-a. Figs. 3-b, c, d correspond to the coating of PPy/PW$_{12}$O$_{40}$$^{3-}$. Figs. 3-e, f show the PES covered with PPy/AQSA.

PES fibres are covered completely with the hybrid material and the surface has a smooth appearance. The presence of polypyrrole aggregates that were not removed in the washing stage can be seen in Figs. 3-b, d. Elements of high atomic weight (W has an atomic weight of 183.85) backscatter more electrons, so in the micrograph are observed as white colour zones. This fact can be observed in the micrograph 3-c. All the fibres appear white coloured, indicative that PW$_{12}$O$_{40}$$^{3-}$ is distributed homogeneously in the

entire textile surface. Polypyrrole is well distributed consequently, due to the fact that $PW_{12}O_{40}^{3-}$ is the polypyrrole counter ion.
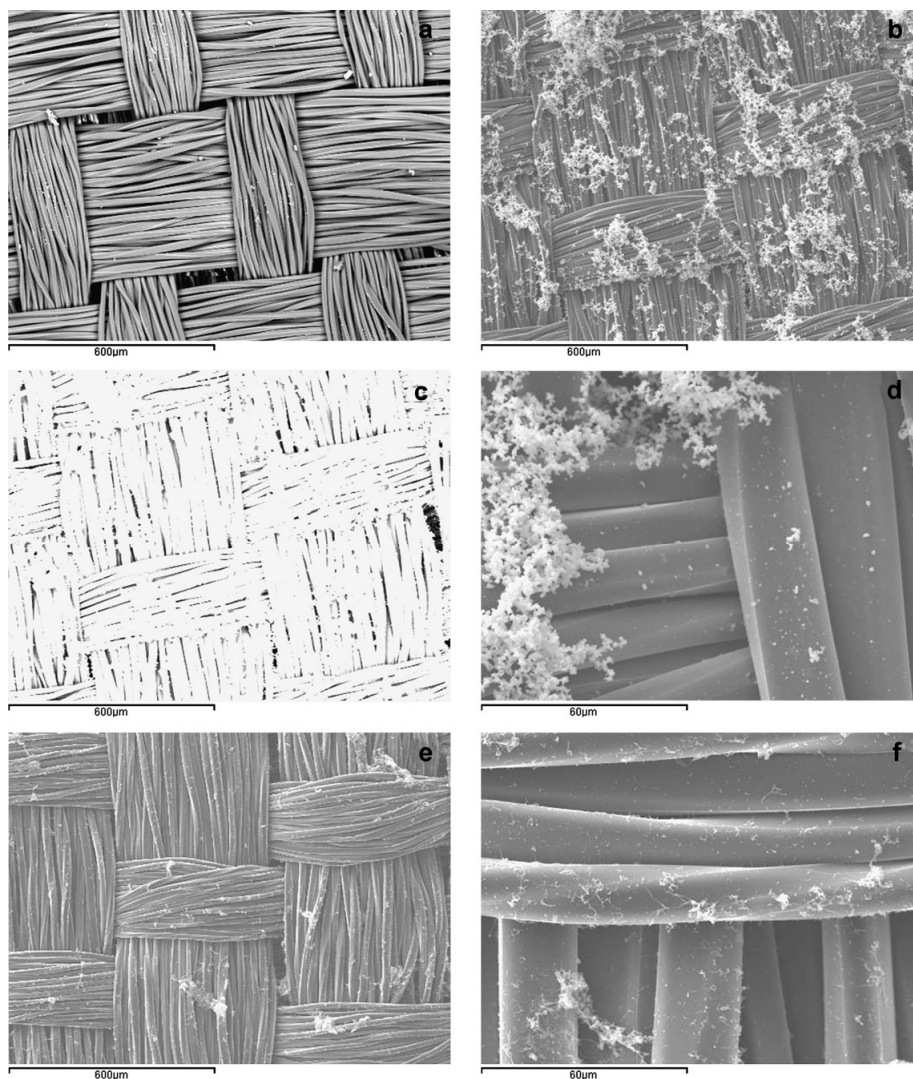

Fig. 3. SEM micrographs of the following samples chemically synthesised (2 g/l pyrrole): (a) PES (x100); (b) PES covered with PPy/ $PW_{12}O_{40}^{3-}$ (x100); (c) PES covered with PPy/$PW_{12}O_{40}^{3-}$ (x100, backscattered electrons); (d) PES covered with PPy/$PW_{12}O_{40}^{3-}$ (x1000); (e) PES covered with PPy/AQSA (x100); (f) PES covered with PPy/AQSA (x1000).

Fig. 3-e shows the morphology when AQSA is employed as counter ion. The presence of aggregates in textile's surface is less than in the case of $PW_{12}O_{40}^{3-}$ use. The coating degree of the fibres is complete too and the surface is smooth. Hakansson et al. [13] demonstrated for PPy/AQSA deposition on PES/Lycra that the reaction at low temperatures (4 ºC) contributed to the development of a smooth surface morphology. Smooth surfaces stabilise the conducting polymer films, due to the inhibition of the oxygen penetration [15]. On the other hand more porous morphology facilities the oxygen diffusion through the film [15] and the subsequent degradation and loss of conductivity. Kuhn et al. [15] demonstrated that the type of counter ion had influence in the morphology, obtaining smoother surfaces with AQSA and more porous surfaces with Cl^-.

So the morphologies obtained with the counter ion AQSA and $PW_{12}O_{40}^{3-}$ facilitate the stability of the conducting polymer films due to the smooth surfaces obtained that hinder the oxygen diffusion.

Figs. 4-a, b, c correspond to EDX analysis performed on textiles covered with $PPy/PW_{12}O_{40}^{3-}$; and in Figs. 4-d, e AQSA was employed as counter ion. Fig. 4-f shows a zonal EDX analysis of PES. In Figs. 4-a, d EDX analysis were performed in the entire area of the micrograph. On the other hand in Figs. 4-b, c, e, f EDX analyses were realised in concrete zones indicated in the adjacent micrograph. The spectrum of Fig. 4-a reveals the presence of W so the molecule $PW_{12}O_{40}^{3-}$ has been incorporated in the polypyrrole structure as counter ion. Fe and Cl also appear in the spectrum and their presence is due to the $FeCl_3$ employed as oxidant. Chlorides could be incorporated as counter ions partially. In the Fig. 4-b an EDX analysis was performed in a zone of the fibre where the presence of aggregates of polypyrrole was not observed. The result obtained was the same, the presence of W that confirmed the presence of $PW_{12}O_{40}^{3-}$. EDX spectrum of the Fig. 4-c was done in a zone with aggregates presence and showed that the aggregate nature was similar to the hybrid material coating on the fibres. Fig. 4-d showed the presence of S that is present in AQSA structure. An analysis performed in a zone without aggregates showed the same result (Fig 4-e). Moreover Ti is present as impurities; that were observed in EDX analysis of the original textile fibres (Fig. 4-f).
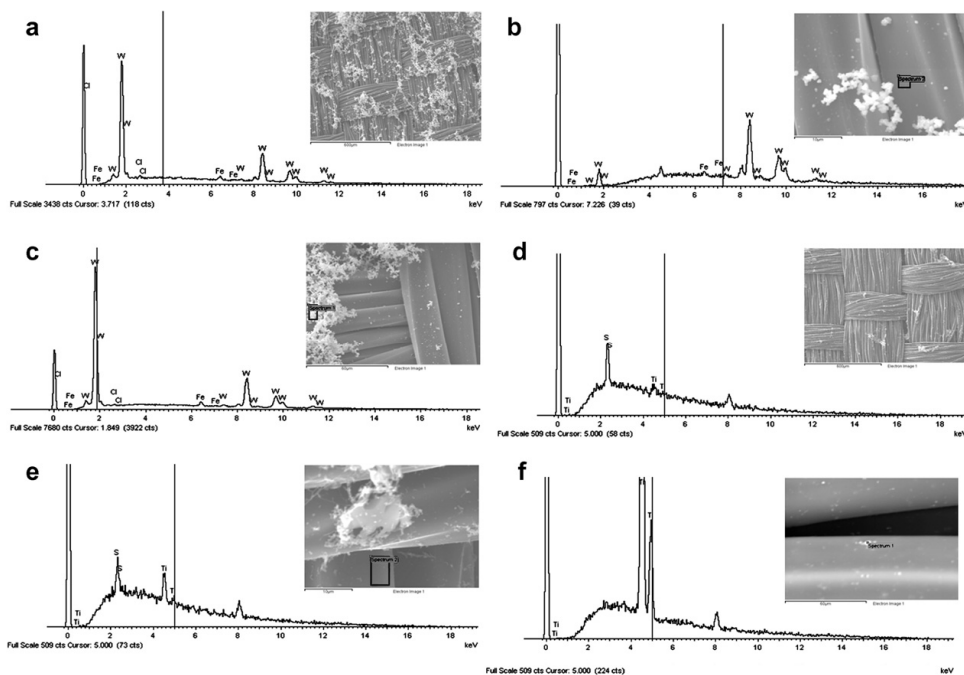
Fig. 4. SEM micrographs and EDX analysis of PES covered with chemically synthesised polypyrrole (2 g/l pyrrole): (a) PPy/PW$_{12}$O$_{40}$$^{3-}$ (x100); (b) PPy/PW$_{12}$O$_{40}$$^{3-}$ (x3500); (c) PPy/PW$_{12}$O$_{40}$$^{3-}$ (x1000); (d) PPy/AQSA (x100); (e) PPy/AQSA (x3500); (f) original PES (x3500).

3.3. Electrochemical synthesis of PPy/PW$_{12}$O$_{40}$$^{3-}$

Electrochemical synthesis was performed in acetonitrile medium with 0.2 M pyrrole and 0.01 M H$_3$PW$_{12}$O$_{40}$ in N$_2$ atmosphere. A potentiodynamic synthesis was employed in order to determine the synthesis potential with our experimental conditions. As can be seen in Fig. 5, around 1.2 V occurs a sudden change of the slop in the voltammetric curve; this fact is indicative that polymerisation begins at this potential. The current density rises with the scan number, indicative that polymerisation is occurring. We selected 1.5 V for the potentiostatic synthesis because it was an adequate potential to assure electropolymerisation and avoid overoxidation. The films were electrosynthesised by potentiostatic techniques on PES substrate chemically covered with PPy/PW$_{12}$O$_{40}$$^{3-}$ previously. The electrode was introduced in the synthesis solution at the open circuit potential and then the potential was fixed at 1.5 V during the necessary time to achieve the desired polymerisation charge. Fig. 6 shows the current transient

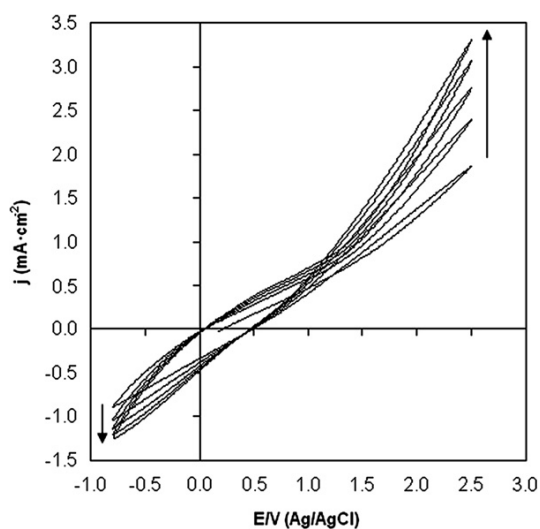curve for potentiostatic synthesis of the hybrid material. The current obtained was around 2.5 mA·cm^{-2}.

Fig. 5. Potentiodynamic synthesis of PPy/PW$_{12}$O$_{40}$$^{3-}$ on a substrate chemically polymerised previously (2 g/l pyrrole) with PPy/PW$_{12}$O$_{40}$$^{3-}$. 0.01 M H$_3PW_{12}O_{40}$ + 0.2 M pyrrole solution in acetonitrile medium. Scan rate 50 mV/s, cycle from -0.8 V to 2.5 V, five scans.
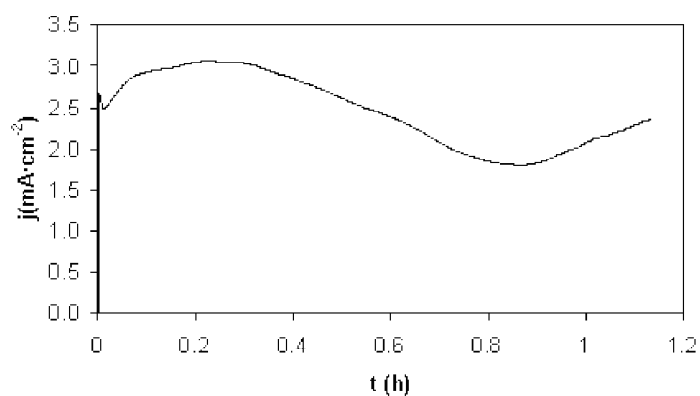

Fig. 6. Current transient curve for potentiostatic synthesis of PPy/PW$_{12}$O$_{40}$$^{3-}$ on a substrate chemically polymerised previously (2 g/l pyrrole) with PPy/PW$_{12}$O$_{40}$$^{3-}$. 0.01 M H$_3PW_{12}O_{40}$ + 0.2M pyrrole solution in acetonitrile medium. Start potential: 0.2 V, synthesis potential: 1.5 V.

The micrograph 7-a (x100) shows the electrochemically $PPy/PW_{12}O_{40}^{3-}$ covered textile for a polymerisation charge of 20.78 C/cm^2. As can be seen in this figure, the textile fibres are not observed and the electrogenerated polymer covers the textile entirely. If we compare the chemically polymerised polymer (Fig 3-b) with the electrochemically generated polymer (Fig 7-a) we can appreciate the great morphology difference. The chemically synthesised polymer produces a smooth surface and the electrochemically synthesised polymer has got a globular structure (Fig 7-b). The polymer grows on the fibres covered with the chemically synthesised $PPy/PW_{12}O_{40}^{3-}$ when the potential of 1.5 V is applied to the conducting textile. Polypyrrole chemically obtained grown predominantly in the plane of the textile (2-D). In the electrochemical polymerisation the growth is in 3-D. The electrochemically generated polymer presents a globular morphology (Fig 7-b) typical of polypyrrole obtained by electrochemical polymerisation and doped with high size dopants [39]. This morphology has been also observed in electrochemically covered conducting textiles [40].

Fig. 7. SEM micrographs of $PPy/PW_{12}O_{40}^{3-}$ electropolymerised on a substrate chemically polymerised previously (2 g/l pyrrole) with $PPy/PW_{12}O_{40}^{3-}$. 0.01 M $H_3PW_{12}O_{40}$ + 0.2 M pyrrole solution in acetonitrile medium. Start potential: 0.2 V, synthesis potential: 1.5 V, polymerisation charge: 20.78 C/cm^2. a) x100, b) x2000.

3.4. Cyclic Voltammetry (CV)

Figs. 8-a, b, c compare the voltammetric response obtained for the textile covered with $PPy/PW_{12}O_{40}^{3-}$ chemically and electrochemically synthesised (polymerisation charge of 2.23 C/cm^2) at different pH solutions (pH 1, pH 7 and pH 13 respectively). In Fig. 8-d the voltammogram of the chemically synthesised textile at pH

13 is extended to observe the different peaks that appear in the voltammogram. The current density obtained for the chemically synthesised textile at different pH varies in this order: pH 7 > pH 1 > pH 13. With a buffer solution of pH 7 the current density doubles that obtained at pH 1. With a basic solution (pH 13) the current density is decreased dramatically due to the deprotonation of oxidised polypyrrole.

Fig. 8. Cyclic Voltammetry of PES covered with chemically synthesised $PPy/PW_{12}O_{40}^{3-}$ (2 g/l pyrrole) (———) and electrochemically (2.23 C/cm^2) (— - —) at different pH: a) pH 1 (0.1 M H_2SO_4), b) pH 7 (phosphates buffer + 0.1 M Na_2SO_4), c) pH 13 (0.1 M NaOH + 0.1 M Na_2SO_4), d) pH 13 (magnified). Scan rate 50 mV/s, cycle from -0.8 to 0.4 V, fifth scan for all samples.

This process happens near pH 10 (pKa 10) and results in polymer conjugation breaking, so the conductivity is decreased [41]. This loss of conductivity is observed in the section 3.6; when the conducting textile is soaked with a basic solution (pH 13) during one hour, the resistivity rises two order of magnitude. The voltammetric response

is also affected, so the current density decreases significantly. The voltammetric characterisation of the electropolymerised polymer shows the increase of the current density compared to the chemically polymerised polymer. This tendency is observed at all pH solution, but at pH 13 the increase is more obvious.

The electropolymerisation produces a more conductive film so the voltammetric reponse is higher than that obtained for the chemical polymer. Only with the chemically synthesised polymer at pH 13 the characteristic voltammetric peaks of polypyrrole are observed clearly. Three main peaks are observed in the Fig. 8-d. The cathodic peak at -0.55 V is attributed to the reduction of polypyrrole and $PW_{12}O_{40}^{3-}$ [42]. The anodic peaks at -0.42 V and -0.16 V are due to the oxidation of the hybrid material [42].

3.5. Abrasion and washing tests

Visual inspection of samples after abrasion tests showed loss of part of the conducting polymer; where it can be distinguished the band that had been submitted to friction. In the table 1 are showed the values of colour degradation for the textile and the values of colour discharge. Dry and wet assays did not show significant differences. Obtained values are small in the scale range (1-5); this implies a significant degradation of the polypyrrole layer.

Wet abrasion fastness	Dry abrasion fastness	Washing fastness
Colour degradation: 1–2	Colour degradation: 1–2	Colour degradation: 4–5
Colour discharge: 1–2	Colour discharge: 1–2	Colour discharge: 4–5

Table 1. Colour degradation and colour discharge values for wet abrasion, dry abrasion and washing assays.

Figs. 9-a and 9-c show the textile micrographs after chemical synthesis, Figs. 9-b, d, e illustrate the effect of dry friction on the layer of polypyrrole that covers polyester fibres and Fig. 9-f shows the sample after the washing assay. The abrasion test degrades the polypyrrole coating of the fibres. The polypyrrole layer in the zone 1 of the textile (Fig. 9-b) is completely degraded (Fig. 9-d). The content of W in the surface fibres of this zone decreased substantially (0.01 % atomic). The PPy layer in the zone 2 of the textile (Fig. 9-b) is only removed from the fibres partially (Fig. 9-e). In this figure it can be

seen that only the upper part of the fibres has lost polypyrrole aggregates and part of the polypyrrole layer that cover the fibres. The presence of W in the fibres of this zone is clear (0.55 % atomic). Fibres in zone 1 are more raised than fibres in zone 2 and friction affects more the fibres of zone 1 due to this fact.

Fig. 9. SEM micrographs of different samples (2 g/l pyrrole): (a) PES+PPy/PW$_{12}$O$_{40}$$^{3-}$ (x100); (b) PES+PPy/PW$_{12}$O$_{40}$$^{3-}$ after abrasion (x100); (c) PES+PPy/PW$_{12}$O$_{40}$$^{3-}$ (x1000); (d) PES+PPy/PW$_{12}$O$_{40}$$^{3-}$ after abrasion in zone 1 (x1000); (e) PES+PPy/PW$_{12}$O$_{40}$$^{3-}$ after abrasion in zone 2 (x1000); (f) PES+PPy/PW$_{12}$O$_{40}$$^{3-}$ after washing assay (x1000).

The washing assay of the textile covered with the hybrid material PPy/PW$_{12}$O$_{40}$$^{3-}$ showed no degradation of polypyrrole coating. The high values of colour degradation and colour discharge in the grey scale (Table 1) imply no significant degradation of the textile covered with PPy. Moreover the aggregates of polypyrrole could not be removed from the textile fibres surface completely (Fig. 9-f). EDX analysis showed that W content in the surface fibre had normal values (0.64 % atomic).
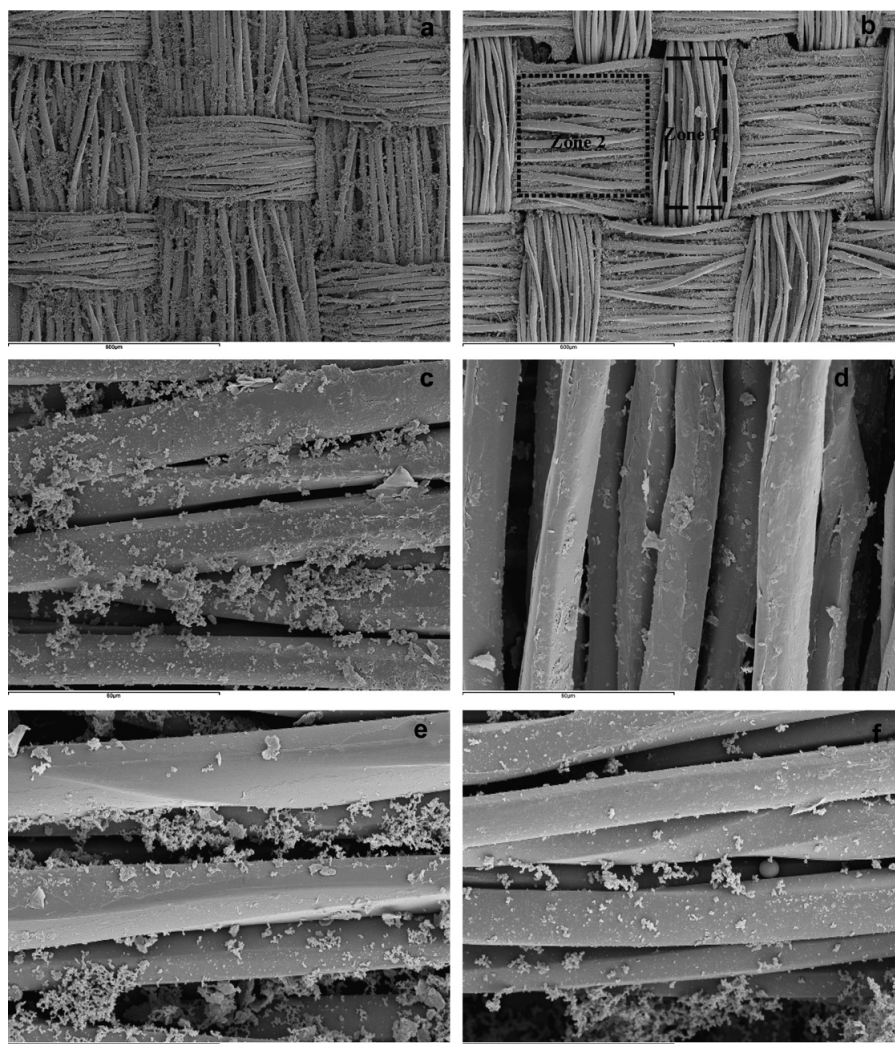
3.6. Measures of surface resistivity and EIS

The surface resistivity obtained for PES covered with the hybrid material measured with the four point probe test was 400-500 Ω/square and 60-70 Ω/square for PPy/AQSA. The counter ion has a significant influence in the polypyrrole conductivity films. The more planar the structure of the counter ion is, the more conductive film is obtained [43]. Anthraquinone sulfonic acid sodium salt has a planar conformation; on the other hand PW$_{12}$O$_{40}$$^{3-}$ is a three dimensional molecule that produces less conductive polymer than AQSA. When the electrochemical synthesis of PPy/PW$_{12}$O$_{40}$$^{3-}$ was performed on the conducting textile, the resistivity obtained was 17-20 Ω/square (20.78 C/cm^2 of polymerisation charge). The electrochemical synthesis produces a more ordered polymer with fewer defects, so the resistivity is lower than the case of chemical synthesis (one order of magnitude).

Surface resistivities of different chemically synthesised samples measured with EIS are showed in the table 2. Samples were soaked with different solutions during 1 hour, dried and measured with EIS. It can be seen that one hour of contact with neutral (phosphates buffer + Na$_2$SO$_4$ 0.1 M) and acid solution (H$_2$SO$_4$ 0.1 M) origins a decrease in textile surface resistivity. On the other hand, contact with basic solutions (NaOH 0.5 M + Na$_2$SO$_4$ 0.1 M) causes a significant increase in the textile surface resistivity, this fact is related with the deprotonation of oxidised polypyrrole [41].

When the textile is submitted to a washing assay the textile resistivity is increased but not excessively. As SEM has proved, the layer morphology is not changed by the washing assay. The friction assay is more abrasive than the washing one and the conductivity loss is higher too. This phenomenon is due to the partial elimination of polypyrrole from the surface fibre that has been proved by SEM. The side that is abraded is affected only partially; only the upper fibres of the textile are degraded. Textiles have a lot of contact points between the fibres. When the layer of conducting polymer in a fibre is damaged with abrasion and has not got conductive areas other contact points

between fibres allow the conduction in the textile. The electricity conduction is more difficult and the resistivity rises up consequently. In conclusion the damage of the polypyrrole layer in the textile submitted to abrasion is obvious but the effect in the electrical resistivity is lower than it could be expected.

Sample	Surface resistivity measured with EIS (KΩ/square)
PES + hybrid material	2.712
1 h contact at pH 1	0.444
1 h contact at pH 7	0.578
1 h contact at pH 13	292.7
After washing assay	4.79
After friction assay	38.8

Table 2. Surface resistivity values for different samples measured with EIS.

In the Fig. 10 it can be seen the Bode diagrams obtained by EIS for PES and PES+hybrid material. As can be seen, the impedance modulus for PES is much higher than the one for PES+hybrid material. Phase angle values around 90º were recorded for PES sample, showing a pure capacitative behaviour. Phase angle data for low frequencies are not showed because noise was observed, due to the very high impedance values obtained (impedance modulus about 10^{10} Ω) for PES sample. PES is an insulating material and acts as a capacitor. The PES+hybrid material showed a phase angle value near to 0º, showing a pure resistive behaviour. Conducting textile acts as a pure resistor.
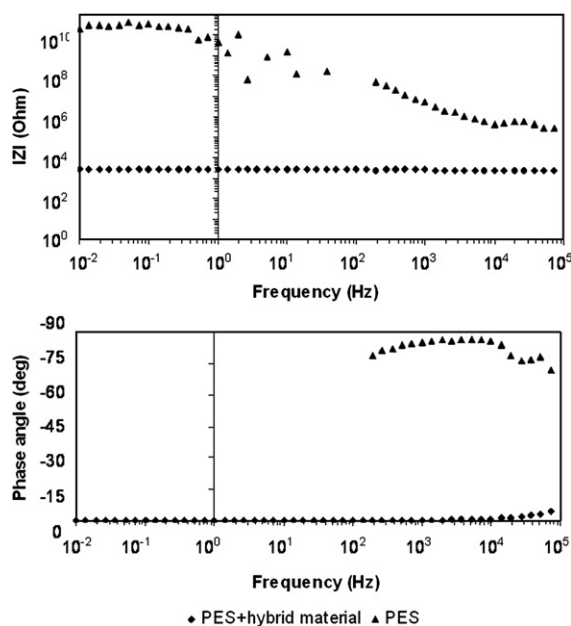
Fig. 10. Bode plots for PES and PES+PPy/PW$_{12}$O$_{40}$$^{3-}$ chemically synthesised (2 g/l pyrrole). Measurements between two copper electrodes above the textile samples. Distance between electrodes 1.5 cm. Textile measured area 1.5 cm x 1.5 cm. Frequency range from 10^{-2} to 10^{5} Hz.

4. Conclusions

The development of PES conducting textiles covered with polypyrrole and the incorporation of PW$_{12}$O$_{40}$$^{3-}$ as counter ion has been achieved. FTIR-ATR spectroscopy showed the presence of bands attributed to polypyrrole but do not showed the bands of PW$_{12}$O$_{40}$$^{3-}$ clearly, so EDX analyses were realised to corroborate the counter ion incorporation.

SEM showed complete coating degree of the fibres with PPy/PW$_{12}$O$_{40}$$^{3-}$ and the presence of aggregates of polypyrrole not removed in the washing stage. EDX analyses demonstrated PW$_{12}$O$_{40}$$^{3-}$ incorporation in the PPy structure and SEM combined with backscattered electrons demonstrated the homogeneous incorporation of PW$_{12}$O$_{40}$$^{3-}$ in the coating. Micrographs of samples submitted to friction showed partial polypyrrole layer degradation. Washing assay showed no degradation of the hybrid material layer.

Cyclic voltammetry (CV) showed that films of PPy/PW$_{12}$O$_{40}^{3-}$ were electroactive. The voltammograms were recorded at different pH to study the influence of the medium. The maximum current density values followed this order: pH 7 > pH 1> pH 13. Only with pH 13 the typical polypyrrole voltammetric peaks were observed. The surface resistivity of PES+PPy/PW$_{12}$O$_{40}^{3-}$ conducting textile measured by the four point probe technique was 400-500 Ω/square. The Bode plots obtained by EIS measurements showed a phase angle value near to 0º for the conducting textile, typical value for a resistor, acting the sample as an electrical resistor. PPy/PW$_{12}$O$_{40}^{3-}$ electropolymerisation on the chemically synthesised polymer has been achieved and showed a current density increase in CV at all pH studied. The surface resistivity measured for this polymer was 17-20 Ω/square (20.78 C/cm^2 of polymerisation charge).

At present we are studying the electrical behaviour by EIS of the conducting textiles in solution to complete the study of these materials.

Acknowledgements

References

[1] McNeill R, Siudak R, Wardlaw JH, Weiss DE. Electronic conduction in polymers. I. The chemical structure of polypyrrole. Aust J Chem 1963;16(6):1056-1075.

[2] Bolto BA, Weiss DE. Electronic conduction in polymers. II. The electrochemical reduction of polypyrrole at controlled potential. Aust J Chem 1963;16(6):1076-1089.

[3] Bolto BA, McNeill R, Weiss DE. Electronic conduction in polymers. III. Electronic properties of polypyrrole. Aust J Chem 1963;16(6):1090-1103.

[4] Diaz AF, Kanazawa KK. Electrochemical polymerization of polypyrrole. JCS Chem Comm 1979(14);635-636.

[5] Kanazawa KK, Diaz AF, Geiss RH, Gill WD, Kwak JF, Logan JA, Rabolt JF, Street GB. 'Organic metals': Polypyrrole, a stable synthetic 'Metallic' polymer. JCS Chem Comm 1979(19);854-855.

[6] Diaz AF, Castillo JI. A polymer electrode with variable conductivity: Polypyrrole. JCS Chem Comm 1980(9);397-398.

[7] Lekpittaya P, Yanumet N, Grady BP, O'Rear EA. Resistivity of conductive polymer-coated fabric. Journal of Applied Polymer Science 2004;92(4):2629-2636.

[8] Kincal D, Kumar A, Child A, Reynolds J. Conductivity switching in polypyrrole-coated textile fabrics as gas sensors. Synthetic Metals 1998;92(1):53-56.

[9] Wu J, Zhou D, Too CO, Wallace GG. Conducting polymer coated lycra. Synthetic Metals 2005;155(3):698-701.

[10] Wha K, Jin H, Hun S. Stretchable conductive fabric for electrotherapy. Journal of Applied Polymer Science 2003;88(5):1225-1229.

[11] Hun S, Wha K, Hyon J. Electrochemically synthesized polypyrrole and Cu-plated nylon/spandex for electrotherapeutic pad electrode. Journal of Applied Polymer Science 2004;91(6):4064.

[12] Bhat NV, Seshadri DT, Nate MN, Gore AV. Development of conductive cotton fabrics for heating devices. Journal of Applied Polymer Science 2006;102(5):4690-4695.

[13] Hakansson E, Kaynak A, Lin T, Nahavandi S, Jones T, Hu E. Characterization of conducting polymer coated synthetic fabrics for heat generation. Synthetic Metals 2004;144(1):21-28.

[14] Boutrois JP, Jolly R, Pétrescu C. Process of polypyrrole deposit on textile. Product characteristics and applications. Synthetic Metals 1997;85(1-3):1405-6.

[15] Kuhn H, Child A, Kimbrell W. Toward real applications of conductive polymers. Synthetic Metals 1995;71(1-3):2139-42.

[16] Lopes A, Martins S, Moraö A, Magrinho M, Gonçalves I. Degradation of a textile dye C.I. Direct Red 80 by electrochemical processes. Portugaliae Electrochimica Acta 2004;22(3):279-294.

[17] Akbarov D, Baymuratov B, Westbroek P, Akbarov R, Declerck K, Kiekens P. Development of electroconductive polyacrylonitrile fibers through chemical metallization and galvanisation. Journal of Applied Electrochemistry 2006;36(4):411-418.

[18] Kuhn HH, Child AD. Electrically conducting textiles. In: Handbook of Conducting Polymers, Skotheim TA, Elsenbaumer RL, Reynolds JR editors. New York; Marcel Dekker, Inc., 1998. p. 993-1013.

[19] Lin T, Wang L, Wang X, Kaynak A. Polymerising pyrrole on polyester textiles and controlling the conductivity through coating thickness. Thin Solid Films 2005;479(1-2):77-82.

[20] SeungLee H and Hong J. Chemical synthesis and characterization of polypyrrole coated on porous membranes and its electrochemical stability. Synthetic Metals 2000;113(1-2):115-119.

[21] Ferrero F, Napoli L, Tonin C, Varesano A. Pyrrole chemical polymerization on textiles: Kinetics and operating conditions. Journal of Applied Polymer Science 2006;102(5):4121-4126.

[22] Hosseini SH, Pairovi A. Preparation of conducting fibres from cellullose and silk by polypyrrole coating. Iranian Polymer Journal 2005;14(11):934-940.

[23] Dall'Acqua L, Tonin C, Varesano A, Canetti M, Porzio W, Catellani M. Vapour phase polymerisation of pyrrole on cellulose-based textile substrates. Synthetic Metals 2006;156(5-6):379-386.

[24] Beneventi D, Alila S, Boufi S, Chaussy D, Nortier P. Polymerization of pyrrole on cellullose fibres using a FeCl3 impregnation- pyrrole polymerization sequence. Cellulose 2006;13(6):725-734.

[25] Dall'Acqua L, Tonin C, Peila R, Ferrero F, Catellani M. Performances and properties of intrinsic conductive cellulose–polypyrrole textiles. Synthetic Metals 2004;146(2):213-221.

[26] Gasana E, Westbroek P, Hakuzimana J, De Clerck K, Priniotakis G, Kiekens P, Tseles D. Electroconductive textile structures through electroless deposition of polypyrrole and copper at polyaramide surfaces. Surface & Coatings Technology 2006;201(6):3547-3551.

[27] Garg S, Hurren C, Kaynak A. Improvement of adhesion of conductive polypyrrole coating on wool and polyester fabrics using atmospheric plasma treatment. Synthetic Metals 2007;157(1):41-7.

[28] Gómez-Romero P. Advanced Materials. Hybrid Organic-Inorganic Materials - In Search of Synergic Activity. 2001;13(3):163-174.

[29] Díaz AF, Bargon J. Electrochemical synthesis of conducting polymers. In: Handbook of Conducting Polymers, Skotheim T, editor. New York; Marcel Dekker, Inc., 1986. Vol. 1, p. 81-115.

[30] Otero TF, Cheng SA, Coronado E, Martínez E, Gómez-García CJ. Functional hybrid materials containing polypyrrole and polyoxometalate clusters: Searching for high conductivities and specificic charges. ChemPhysChem 2002;3(9):808-811.

[31] Cheng SA, Otero TF. Electrogeneration and electrochemical properties of hybrid materials: polypyrrole doped with polyoxometalates PW_{12}-$xMoxO_{40}^{3-}$ (x=0,3,6,12). Synthetic Metals 2002;129(1):53-59.

[32] Gómez-Romero P, Lira-Cantú M. Hybrid organic-inorganic electrodes: The molecular material formed between polypyrrole and the phosphomolybdate anion. Advanced Materials 1997;9(2):144-147.

[33] Bonastre J, Garcés P, Huerta F, Quijada C, Andión LG, Cases F. Electrochemical study of polypyrrole/$PW_{12}O_{40}{}^{3-}$ coatings on carbon steel electrodes as protection against corrosion in chloride aqueous solutions. Corrosion Science 2006;48(5):1122-1136.

[34] Neoh KG, Young TT, Kang ET, Tan KL. Structural and mechanical degradation of polypyrrole films due to the aqueous media and heat treatment and the subsequent redoping characteristics. Journal of Applied Polymer Science 1997;64(3):519-526.

[35] Bhadani SN, Kumari M, Sen Gupta SK, Sahu GC. Preparation of conducting fibres via the electrochemical polymerization of pyrrole. Journal of Applied Polymer Science 1997;64(6):1073-1077.

[36] Su W, Iroh JO. Electropolymerization of pyrrole on steel substrate in the presence of oxalic acid and amines. Electrochimica Acta 1999;44(13):2173-2184

[37] Feng W, Zhang TR, Liu Y, Lu R, Zhao YY. Photochromic behavior of nanocomposite hybrid films of finely dispersed phosphotungstic acid particles into polyacrylamide. Journal of Materials Science 2003;38(5)1045-1048.

[38] Spectral Database for Organic Compounds of the National Institute of Advanced Industrial Science and Technology (AIST). http://riodb01.ibase.aist.go.jp/sdbs/cgi-bin/cre_index.cgi?lang=eng.

[39] Wha K, Jin H, Hun S. Electrical property and stability of electrochemical synthesized polypyrrole films. Journal of Applied Polymer Science 2004;91(6):3659-3666.

[40] Kim MS, Kim HK, Byun SW, Jeong SH, Hong YK, Joo JS, Song KT, Kim JK, Lee CJ, Lee JY. PET fabric/polypyrrole composite with high electrical conductivity for EMI shielding. Synthetic Metals 2002;126(2-3):233-239.

[41] Maksymiuk Krysztof. Chemical reactivity of polypyrrole and its relevance to polypyrrole based electrochemical sensors. Electronalysis 2006;18(16):1537-1551.

[42] Otero TF, Cheng SA, Alonso D, Huerta F. Hybrid materials Polypyrrole/PW12O403. 2. Physical, spectroscopic and electrochemical characterization. J. Phys. Chem. B. 2000;104(45):10528-10533.

[43] Avlyanov JK, Kuhn HH, Josefowicz JY, MacDiarmid AG. In-situ deposited thin films of polypyrrole: Conformational changes induced by variation of dopant and substrate surface. Synthetic Metals 1997;84(1):153-154.

8.- ARTÍCULO

CHEMICAL, ELECTRICAL AND ELECTROCHEMICAL CHARACTERIZATION OF HYBRID ORGANIC/INORGANIC POLYPYRROLE/PW$_{12}$O$_{40}$$^{3-}$ COATING DEPOSITED ON POLYESTER FABRICS

**Chemical, electrical and electrochemical characterization of hybrid
organic/inorganic polypyrrole/PW$_{12}$O$_{40}$$^{3-}$ coating deposited on polyester fabrics.**

J. Molina, J. Fernández, A.I. del Río, J. Bonastre, F. Cases [*]

*Departamento de Ingeniería Textil y Papelera, EPS de Alcoy, Universidad Politécnica de
Valencia, Plaza Ferrándiz y Carbonell s/n, 03801 Alcoy, Spain*

Abstract

A study of the stability of conducting fabrics of polyester (PES) coated with
polypyrrole/PW$_{12}$O$_{40}$$^{3-}$ (organic/inorganic hybrid material) in different pH solutions (1, 7,
13) has been done. Washing tests were also done in views of its possible application in
electronic textiles such as antistatic clothing. X-ray photoelectron spectroscopy (XPS)
studies have been done to quantify the amount of counter ion that remains in the
polymer matrix and determine the doping ratio (=NH^{+}/N) after the different tests.
Scanning electron microscopy (SEM) was also used to observe morphological
differences after the different tests. Surface resistivity changes were measured by means
of electrochemical impedance spectroscopy (EIS). Scanning electrochemical microscopy
(SECM) was employed to measure changes in electroactivity after the different tests.
Higher pHs caused a decrease of the doping ratio (=NH^{+}/N), the loss of part of the
counter ions and the decrease of its conducting and electrocatalytic properties. The
stability in acid, neutral media and after the washing test was good. Only at pH 13 the
loss of the counter ion was widespread and there was a decrease of its conducting and
catalytic properties; although the material continued acting mainly as conducting
material.

Keywords: Polypyrrole, conducting fabric, phosphotungstate, X-ray photoelectron
spectroscopy, scanning electrochemical microscopy.

_____

* Corresponding author. Tel.: +34 966528412; Fax.: +34 96 652 8438

E-mail address: fjcases@txp.upv.es (Prof. F. Cases)

1. Introduction

The development of textiles with new properties and applications has received great attention during the last years; one of these properties is the electrical conductivity. One of the methods that have been employed to produce conducting fabrics is the chemical synthesis of polypyrrole on fabrics [1-9]. Applications of polypyrrole-based conducting fabrics are varied and numerous; like antistatic materials [1], gas sensors [2], biomechanical sensors [3], electrotherapy [4, 5], heating devices [6-8] or microwave attenuation [9].

During the formation of polypyrrole, positive charges are created in its structure (polarons and bipolarons). These positive charges are compensated by anions that act as counter ions to maintain the electroneutrality principle. Low size anions like Cl^- have been employed as counter ions, but their stability is low [9]. If the counter ion is expelled from the structure (dedoping), there is a great loss of its electrical properties. To prevent this phenomenon, bulky anions with a high molecular size have been employed in bibliography. When the size of the counter ion is high, its diffusion is prevented and it remains in the polypyrrole structure [10]. The higher size of the counter ion, the more difficult the expulsion of the counter ion from the structure is. Typical counter ions employed in textiles covered with polypyrrole, are organic molecules with high size; like anthraquinone sulfonic acid (AQSA) [2, 7, 9, 11-14], dodecylbenzene sulfonic acid (DBSA) [1, 12], p-toluene sulfonic acid (PTSA) [2, 9, 12, 15], naphthalenedisulfonic acid (NDSA) [3, 9, 12], benzenesulfonic acid (BSA) [4, 16], naphthalenesulfonic acid (NSA) [9, 15], anthraquinone disulfonic acid [17, 18].

However, very little has been reported about the use of inorganic anions as counter ions when obtaining conducting fabrics. In our previous work [14], we employed an inorganic anion as counter ion ($PW_{12}O_{40}^{3-}$) to produce polypyrrole-based conducting fabrics. A hybrid organic/inorganic layer was obtained ($PPy/PW_{12}O_{40}^{3-}$). $PW_{12}O_{40}^{3-}$ is a polyoxometalate (POM) with high volume and charge [19], so their diffusion coefficient is low, and the exchange with anions present in the solution is prevented. In addition to this, $PW_{12}O_{40}^{3-}$ presents also catalytic properties [20,21].

One of the applications that our group aims to is the employment of conducting fabrics in catalysis, or as a support with high surface area to electrodeposit Pt nanoparticles and enhance its electroactivity [22,23]. For example, conducting polymers have been employed in environmental applications; electrodes modified with conducting polymers have been used in Cr^{6+} (toxic) reduction to Cr^{3+} (not toxic) [24] or nitrites electroreduction [25]. The employment of polypyrrole coated textiles in the

electrochemical removal of the textile dye C. I. Direct Red 80 has also been reported [26]. Polyaniline/MnO_2 catalyst and H_2O_2 as an oxidant have been employed in the degradation of organic dyes such as Direct Red 81, Indigo Carmine and Acid Blue 92 [27, 28]. For this purposes, the study of the stability of the PPy/$PW_{12}O_{40}^{3-}$ layer and its properties in different pH solutions is essential to optimize its operational pH range.

Another application that we are studying at present is its employment in electronic clothing, for instance its antistatic or microwave attenuation properties. For this purpose, the conducting fabrics would have to resist washing tests. X-ray photoelectron spectroscopy (XPS) measurements have been used to quantify the amount of counter ion ($PW_{12}O_{40}^{3-}$) present in the polypyrrole matrix and the doping ratio ($=NH^+$/N) after the different tests. Scanning electron microscopy (SEM) and energy dispersive X-ray (EDX) measurements have been employed for morphology observation and zonal analysis respectively. Surface resistivity ($\Omega/$) changes have been measured by electrochemical impedance spectroscopy (EIS) after the different tests. The electroactivity of the samples after the different tests has been measured by scanning electrochemical microscopy (SECM). SECM is a relatively novel (1989) and powerful technique that is becoming more popular among researchers [29-31]. Its employment in conducting fabrics has not been reported since the most employed substrate in bibliography is Pt.

2. Experimental

2.1. Reagents and materials

Analytical grade pyrrole, ferric chloride, sulphuric acid, sodium dihydrogenophosphate, disodium hydrogenophosphate, sodium sulphate and sodium hydroxide were purchased from Merck. Normapur acetone was from Prolabo. Analytical grade phosphotungstic acid hydrate was supplied by Fluka. Ultrapure water was obtained from an Elix 3 Millipore-Milli-Q Advantage A10 system with a resistivity near to 18.2 MΩ cm. Polyester textile was acquired from Viatex S.A. and their characteristics were: fabric surface density, 140 g m^{-2}; warp threads per cm, 20 (warp linear density, 167 dtex); weft threads per cm, 60 (weft linear density, 500 dtex). These are specific terms used in the field of textile industry and their meaning can be consulted in a textile glossary [32].

2.2. Chemical synthesis of PPy/$PW_{12}O_{40}^{3-}$ on polyester fabrics

Chemical synthesis of PPy on polyester textiles was done as reported in our previous study [14]. The size of the samples was 6 cm x 6 cm approximately. Previously to reaction, polyester was degreased with acetone in ultrasound bath and washed with water. Pyrrole concentration employed was 2 g l^{-1} and the molar relations of reagents employed in the chemical synthesis bath were pyrrole: $FeCl_3$: $H_3PW_{12}O_{40}$ (1: 2.5: 0.2). The next stage was the adsorption of pyrrole and counter ion ($PW_{12}O_{40}^{3-}$) (V=200 ml) on the fabric for 30 min in an ice bath without stirring. At the end of this time, the $FeCl_3$ solution (V=50 ml) was added and oxidation of the monomer took place during 150 min without stirring. Adsorption and reaction were performed in a precipitation beaker. The conducting fabric was washed with water to remove PPy not joined to fibers and dried in a desiccator for at least 24 h before measurements. The weight increase obtained was around 10 %. The thickness of the film obtained on the fibers of the fabric was around 600 nm.

2.3. Stability of $PW_{12}O_{40}^{3-}$ in the conducting textiles of PES-PPy/$PW_{12}O_{40}^{3-}$ in different pH solutions

Different samples of PES-PPy/$PW_{12}O_{40}^{3-}$ (2 cm x 2 cm) were soaked in different pH solutions. The solutions employed were: 0.1 M H_2SO_4 (pH~1), phosphates buffer + 0.1 M Na_2SO_4 (pH~7) and 0.1 M NaOH + 0.1 M Na_2SO_4 (pH~13). After 1 h of contact with the different pH solutions, the samples were rinsed with ultrapure water and dried in a desiccator before measurements. Different samples were obtained equally to perform the different analysis. XPS analyses were done to quantify the amount of counter ion and doping ratio (=NH^+/N). Zonal analyses were performed by means of EDX and morphological changes in the coating were also observed by means of SEM. Surface resistivity and electroactivity changes were measured by EIS and SECM respectively.

2.4. Washing tests

Washing tests were performed to test the stability of the coating and its properties after these tests. The analysis was done as related in the norm ISO 105-C01 at 40º C during 30 min. The different analysis mentioned in section 2.3. were also done for these samples.

2.5. X-ray photoelectron spectroscopy measurements

XPS analyses were conducted at a base pressure of at $5 \cdot 10^{-10}$ mbars and a temperature around 173 K. The XPS spectra were obtained with a VG-Microtech Multilab electron spectrometer by using unmonochromatized Mg Kα (1253.6 eV) radiation from a twin anode source operating at 300 W (20 mA, 15 KV). The binding energy (BE) scale was calibrated with reference to the C1s line at 284.6 eV. The C1s, O1s, N1s, S2p and W4f core levels spectra were analyzed for the sample of PES-PPy/PW$_{12}$O$_{40}$$^{3-}$, and samples of PES-PPy/PW$_{12}$O$_{40}$$^{3-}$ after contact with different pH solutions (1, 7, 13) and after the washing test.

2.6. SEM and EDX characterization

A Jeol JSM-6300 scanning electron microscope was employed to observe the morphology of the samples and perform EDX analyses. SEM micrographs were obtained using an acceleration voltage of 20 kV. EDX measurements were done between 0 and 20 keV.

2.7. Electrochemical impedance spectroscopy measurements

An Autolab PGSTAT302 potentiostat/galvanostat was employed to perform electrochemical impedance spectroscopy (EIS) analyses. EIS measurements were performed in the 10^5-10^{-2} Hz frequency range. The amplitude of the sinusoidal voltage employed was 10 mV. Measurements were carried out using two rectangular copper electrodes (0.5 cm x 1.5 cm) separated by 1.5 cm and pressed to the dry textile sample. The measured area of the textile was a square of 1.5 cm, so when the material acts as a resistor, the measured impedance modulus (Ω) was equal to the surface resistivity (Ω/).

2.8. Scanning electrochemical microscopy measurements

SECM measurements were carried out with a scanning electrochemical microscope of Sensolytics. The three-electrode cell configuration consisted of a 100-μm-diameter Pt ultra-microelectrode (UME) working electrode, a Pt wire auxiliary electrode and an Ag/AgCl (3 M KCl) reference electrode. The solution selected for this study was 0.01 M Ru(NH$_3$)$_6$Cl$_3$ in aqueous 0.1 M KCl supporting electrolyte. All the experiments

were carried out in inert nitrogen atmosphere. Substrates of PES and the samples of PES-PPy/PW$_{12}$O$_{40}$$^{3-}$ after the different pH treatments were chosen as substrates for the SECM measurements. The different samples were glued with epoxy resin on glass microscope slides.

The positioning of the Pt UME tip was achieved by first carefully putting it in contact with the substrate surface and then moving it in z direction (height of the electrode). Once the electrode was at the desired height, the electrode was approached to the substrate surface; the current of the UME was recorded to obtain the approach curves. Approach curves give us an indication of the electroactivity of the surface.

3. Results and discussion

3.1. XPS analysis of PES-PPy/PW$_{12}$O$_{40}$$^{3-}$ treated at different pHs

XPS analyses were done to quantify the amount of counter ion (PW$_{12}$O$_{40}$$^{3-}$) and doping ratio (=NH$^+$/N$_{Total}$) of the fabrics after the different tests. The C1s, O1s, N1s, S2p and W4f core levels spectra were analyzed for the different PES-PPy/PW$_{12}$O$_{40}$$^{3-}$ samples. Table 1 shows chemical composition and doping ratio (=NH$^+$/N$_{Total}$) for polypyrrole/PW$_{12}$O$_{40}$$^{3-}$ (PPy/POM) coated textiles. Samples 2 to 4 were previously treated with different solutions. These hybrid materials should ideally have the formula C$_4$H$_3$N(PW$_{12}$O$_{40}$$^{3-}$)$_x$, where "x" is the fractional doping level obtained by W analysis. XPS analysis showed a systematic carbon excess, which may be due to surface hydrocarbon contamination [33]. The composition analysis showed also an oxygen excess in all specimens. This may be due to PPy ring oxidation attributed to PPy reaction with water as synthesis solvent [34].

Sample code	Sample	Chemical composition	Doping ratio (=NH$^+$/N$_{Total}$)
1	PPy/POM prepared chemically	C$_{5.0}$N(PW$_{12}$O$_{40}$$^{3-}$)$_{0.053}O_{0.60}$	0.196
2	PPy/POM treated at pH 1	C$_{6.8}$N(PW$_{12}$O$_{40}$$^{3-}$)$_{0.051}O_{0.60}$	0.159
3	PPy/POM treated at pH 7	C$_{5.6}$N(PW$_{12}$O$_{40}$$^{3-}$)$_{0.034}O_{0.74}$	0.123
4	PPy/POM treated at pH 13	C$_{6.3}$N(SO$_4$$^{2-}$)$_{0.067}O_{0.63}$	0.046

Table 1. XPS surface compositional data for the selected samples.

Doping ratios divided by 3 (3 negative charges per $PW_{12}O_{40}^{3-}$ molecule) for samples 1 to 3, obtained by nitrogen analysis, were in good agreement with fractional doping level performed by tungsten analysis. POM fractional doping level and doping ratio suffered a significant decrease when samples were treated in more basic solutions. Sample 4 showed a complete POM release and its replacement by SO_4^{2-} anions. These facts will be explained in detail later.

3.1.1. C1s analysis

Fig. 1 shows the deconvoluted high resolution C1s spectrum for an untreated specimen. Three peaks appear at the following binding energies: 284.1, 285.6 and 287.4 eV. The contribution at the lowest binding energy was due to C-C/C-H groups. The peak at 285.6 eV was assigned to C-N groups in the pyrrole rings [35-37]. The binding energy peak at 287.4 eV was ascribed to carbonyl C=O groups [38, 39]. The appearance of C=O groups was mainly due to the presence of pyrrole overoxidation during chemical polymerization in aqueous media, as commented before. It has been proved that polypyrrole is simultaneously degraded during the synthesis in short soluble maleimide molecules. This degradation process may be attributed to the polymer overoxidation which is described as a gradual polymer oxidation by water in the presence of $FeCl_3$. Quantitative measurements confirmed that polymerization presented second-order kinetics with regard to $FeCl_3$, while overoxidation appeared to be only first order [32]. Contamination with particulated PPy might also appear on the surface due to the formation of aggregates and individual particles of colloidal PPy [40]. Fig. 1 shows that C-C/C-H peak area is significant greater than the C-N one. For the pyrrole structure, the atomic ratio (C-C/C-H)/C-N must be equal to 1.0. The higher C-C/C-H contribution is coherent with a maleimide-like structure where C=O groups appear at α positions (C-N groups). This overoxidation might be roughly estimated as the atomic ratio $C=O/C_{Total}$, obtaining a value around 8 %. As surface hydrocarbon contamination may be present, this is a minimum value. This parameter was better estimated taking into account the atomic ratio O/N. Noticing Table 1, for sample 1 and 2, a value of 0.60 was obtained. Four carbons are present for each pyrrole ring (1 nitrogen for each pyrrole ring), therefore the atomic ratio $C_{oxidized}/C_{total}$ will be 0.15 (15 %). From samples 1 to 4, the carbon overoxidation was: 15, 15, 18 and 16 % respectively. Important changes in overoxidation state were not appreciated as a result of treating the PPy/POM samples in different pH solutions.

For samples 1 to 4, Table 2 shows the C1s, O1s, N1s and W4f core level binding energies assignments for PPy/POM untreated and treated with pH 1, 7 and 13 solutions. Noticing in C1s binding energies, there were not important changes in the binding energies obtained for the specimens. The same carbon chemical groups, before commented, appeared for the four samples.
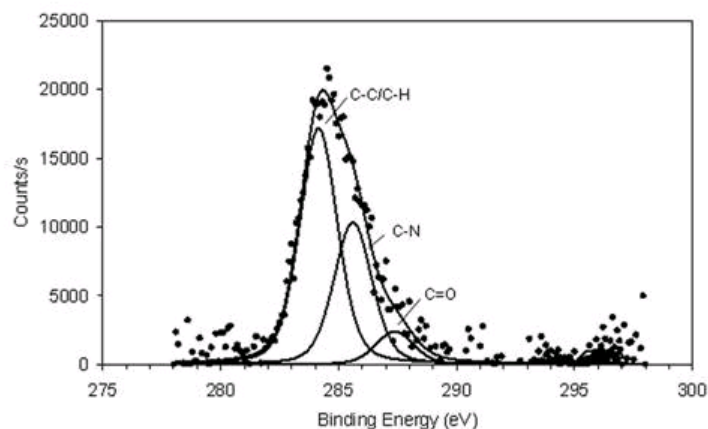

Fig. 1. C1s XPS core level spectrum for untreated PPy/POM sample.

	PPy/POM Sample 1	PPy/POM Sample 2 (pH 1)	PPy/POM Sample 3 (pH 7)	PPy/POM Sample 4 (pH 13)	Assignments
C1s	284.1	284.2	284.2	284.3	C-C/C-H
	285.6	285.6	285.6	285.6	C-N
	287.4	287.8	287.6	287.6	C=O
O1s	530.3	530.3	530.2	—	W-O-W
	531.7	531.7	532.1	—	W=O
	—	—	—	530.9	$C=O; SO_4^{2-}$
	—	—	—	532.6	$C=O\cdots H; HSO_4^-$
N1s	399.7	399.8	399.8	399.7	-NH-
	401.9	402.3	402.0	402.3	N^{2+}
W4f	35.2	35.2	35.1	—	$W^{6+} (W4f_{7/2})$
	37.3	37.3	37.2	—	$W^{6+} (W4f_{5/2})$

Table 2. XPS results for binding energies (eV) of different conducting textiles.

3.1.2. O1s analysis

Fig. 2 shows the high resolution O1s spectrum for the untreated specimen (sample 1). The O1s core level peak was deconvoluted in two contributions centered at 530.3 and 531.7 eV. These contributions were attributed, respectively, to W-O-W groups and W=O groups in the PW$_{12}$O$_{40}$$^{3-}$ counter ion [41]. Seeing Table 2, the binding energy results for sample 1, 2 and 3 are very similar.

The analysis performed for sample 4 shows that the O1s spectrum exhibited two peaks in the sites 530.9 and 532.6 eV. On one hand, the peak at 530.9 eV was caused by C=O group. The peak at 532.6 eV was due to C-OH/C=O--H groups, which indicated that there was a resonant structure of the pyrrole molecule [42]. On the other hand, these binding energies can also be assigned to SO$_4$$^{2-}$ and HSO$_4$$^-$, respectively [43], and are due to incorporated counter ion within the polymer. These functional groups relative to carbonyl and sulfate groups did not appear with different peaks due to their binding energy proximity. The S2p XPS analysis showed only one peak due to a sulfur oxide compound. As a high pH (pH=13) is used for the treatment with Na$_2$SO$_4$ + NaOH solution, the counter ion will be predominantly in the sulfate rather than bisulfate form. Consequently, the peak at 530.9 eV would be representative of SO$_4$$^{2-}$ and C=O groups, and the peak at 532.6 eV would mainly correspond to C-OH/C=O--H group.
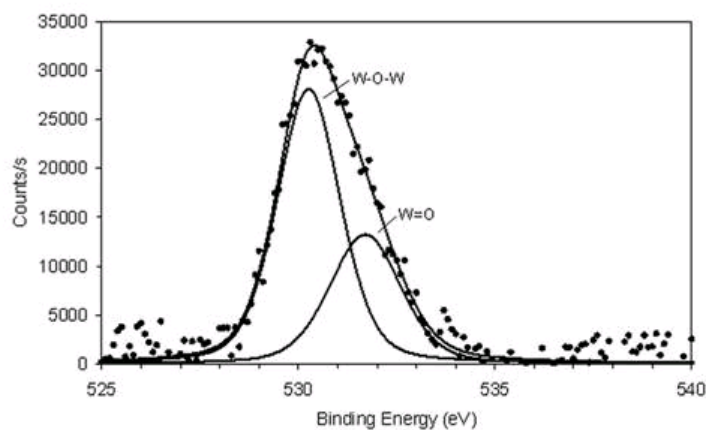

Fig. 2. O1s XPS core level spectrum for untreated PPy/POM sample.

As commented before, all samples presented a similar overoxidation between 15 and 18 %. In samples 1, 2 and 3, it did not appear the contributions for C=O or C=O--H probably due to a high oxygen content from POM molecules, 40 oxygen atoms per

molecule ($PW_{12}O_{40}^{3-}$). In sample 4, the oxygen content from POM counter ion did not interfere because this counter ion had been completely released from the polymer matrix.

3.1.3. N1s analysis

Fig. 3 shows the high resolution N1s spectrum for the untreated specimen (sample 1). The N1s spectrum was deconvoluted into two contributions, centered at 399.7 and 401.9 eV. The peak at 399.7 eV was assigned to the neutral amine-like (–NH–) structure which is characteristic of pyrrolylium nitrogen [35, 38, 44]. The peak at 401.9 eV was attributed to bipolaronic positively charged nitrogen, $=NH^+$ or N^{2+}. The electron-deficient nitrogen species arise from delocalization of electron density from the polypyrrole ring as a result of the formation of electronic defects (bipolarons) [36, 44]. The doping ratio represented by the ($=NH^+/N_{Total}$) ratio was found to be 0.196. As POM presents 3 negative charges per molecule, the POM fractional doping level would be 0.196/3 = 0.065, close to 0.053 obtained by W analysis.
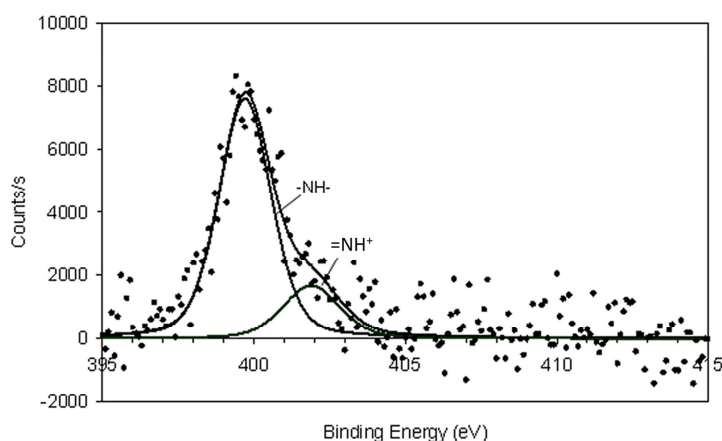

Fig. 3. N1s XPS core level spectrum for untreated PPy/POM sample.

The same nitrogen functional groups appeared when samples were treated at pH 1, 7 and 13. As commented before, these peaks were due to neutral amine-like (–NH–) structure and bipolaronic positively charged nitrogen, $=NH^+$. For the sample treated at pH 13, N1s spectrum presented a significant decrease for $=NH^+$ contribution (compare figure 3 and 4). This fact also confirmed the loss of POM anions, undergoing decomposition (as it will be explained in the W4f analysis) and an anion exchange with

sulfate anions present in the medium (see table 1). The appearance of sulfur in XPS spectrum (not shown) confirmed the anion exchange processes for this sample. The =NH$^+$/N$_{Total}$ ratio was around 0.046. As sulfate ion contains two negative charges per molecule, the SO$_4^{2-}$ fractional doping level would be 0.046/2 = 0.023. The XPS chemical composition in table 1 showed a SO$_4^{2-}$ fractional doping level of 0.067, higher than 0.023. This excess of sulfate could be attributed to covalently bound sulfur [45] since this is accompanied by the loss of the positive nitrogen of bipolarons.
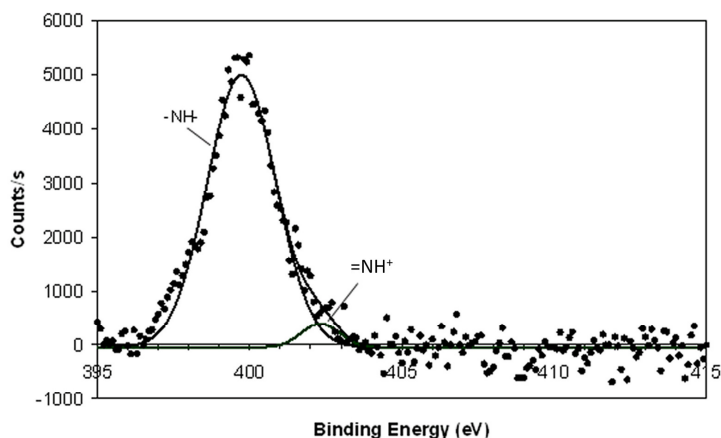

Fig. 4. N1s XPS core level spectrum for PPy/POM sample treated at pH 13.

3.1.4. W4f analysis

Fig. 5 shows the high resolution W4f spectrum for untreated PPy/POM sample. A spin-orbit coupling doublet appeared at 35.2 eV (W4f$_{7/2}$) and 37.3 eV (W4f$_{5/2}$). This doublet is due to W^{6+} that comes from the counter ion, PW$_{12}$O$_{40}$$^{3-}$ [46, 47]. In addition, this doublet with a separation of 2.1 eV is also characteristic of W^{6+} oxidation state [48]. The same binding energies were obtained for samples 2 and 3. When the sample was immersed for 1 hour in pH 13 solution, W4f core level spectrum did not show any peak. W was not present in the polymer; NaOH treatment had caused the removal of the dopant, PW$_{12}$O$_{40}$$^{3-}$. This fact is coherent with data obtained for N1s analysis. Zu et al. corroborated that the PW$_{12}$O$_{40}$$^{3-}$ molecule suffers decomposition into PO$_4^{3-}$ and WO$_4^{2-}$ at pH>8.3 [49], so the treatment at pH 13 caused the total decomposition of the POM dopant and its removal from the polymer matrix. Moreover, an anion exchange took place since sulfate anions were incorporated into the polymer matrix, as commented before.

In addition, the POM fractional doping level can be estimated starting from the P/N atomic ratio. However, P was not detected in the P2p core level spectrum due to its small quantity within the polymer matrix. Therefore, the P/N atomic ratio was calculated dividing the W/N ratio by 12. For sample 1, this value was: 0.64/12=0.053. This datum agrees enough with the $=NH^+/N_{Total}$ doping ratio divided by 3 (3 negative charges per $PW_{12}O_{40}^{3-}$ molecule), 0.196/3 = 0.065. For samples 2 and 3, the data obtained were coherent between the two types of estimation.
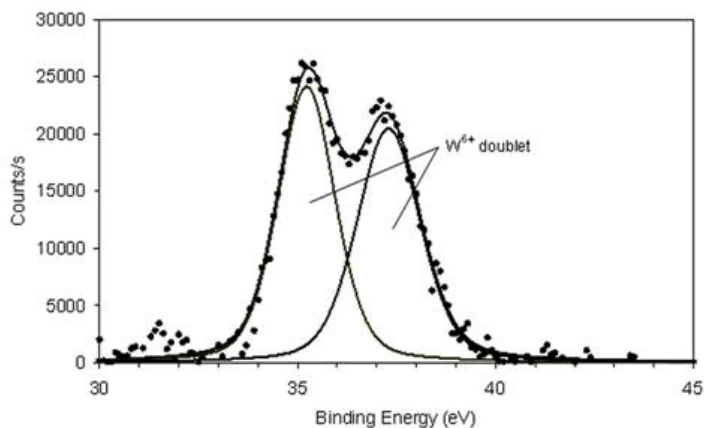

Fig. 5. W4f XPS core level spectrum for untreated PPy/POM sample.

3.2. Washing test of the conducting textile

Sample 1 was submitted to washing test as related in the norm ISO 105-C01. It is important to know the conductivity of the conducting fabric after laundering tests in views of employing in electronic textiles. In that sense, Hurren et al. studied the influence of the detergent and washing temperature on the conductivity of conducting fabrics of polypyrrole/AQSA [50]. This sort of studies has been done in the case of using organic counter ions [50, 51]. The effect of laundering in the case of employing inorganic counter ions has not been reported. In addition to conductivity changes, it is also important to know the doping ratio ($=NH^+/N_{Total}$) and the fractional doping level (counter ion content) after washing tests. If the conducting textile suffers a complete dedoping (release of the counter ion), this textile loses its conducting properties. XPS analysis allows the quantification of the counter ion that remains in the polymer structure, as well as the doping level determination. The chemical composition obtained by XPS analysis was: $C_{7.6}N(PW_{12}O_{40}^{3-})_{0.031}O_{1.96}$. The amount of dopant decreased from 0.053 (table 1) to

0.031 after washing, so the quantity of dopant remaining in the coating was around 60%. This value is high enough taking into account the aggressive test of washing. On the other hand, the oxygen content increased from 0.60 to 1.96 after washing, so an increase of the overoxidation (atomic ratio O/pyrrole ring N) from 15 to 49 % (1.96/4) was obtained. High resolution O1s spectrum (not shown here) showed two binding energy components at 530.7 and 532.5 eV. These contributions were assigned to C=O and C=O···H groups.

3.3. SEM and EDX measurements

EDX analysis can be used as a semi-quantitative analysis to measure the content of W in the conducting fabrics after the different tests. In Fig. 6-a it can be observed the EDX analysis of the sample of PES-PPy/PW$_{12}$O$_{40}^{3-}$ in the area of the micrograph attached. As it can be seen, different W bands are observed. The presence of Fe is due to the use of FeCl$_3$ as oxidant during the synthesis of the polymer. The morphology of the layer of polypyrrole can also be observed in the micrograph. It was observed a hybrid material coating that covered completely the fabric of polyester. The presence of polypyrrole aggregates that could not be removed from the surface of the fabric was also noticeable. The atomic content of W for this sample was 2.48 %. When it was soaked during 1 h in the pH 1 and pH 7 solutions, the content of W was slightly decreased to 2.22 % and 2.17 % respectively (micrographs and analysis not shown). The micrographs did not show any morphological change. In Fig. 6-b it can be observed the EDX analysis and the micrograph for the sample treated at pH 13. It was confirmed the elimination of the counter ion (PW$_{12}$O$_{40}^{3-}$) from the coating since W bands were not observed. Gravimetric measurements showed a significant decrease of the mass of the polymer layer (50 %) for the sample treated in basic media due to the loss of the counter ion. Nevertheless, no apparent morphological changes of the polymer layer were observed with higher magnification. The size of this counter ion is approximately 10 Å [52] and its loss could produce a more porous structure. However the SEM magnification was not sufficient to observe this fact. The sample after the washing test was also analyzed by means of EDX (not shown). A decrease of the W content was also noticed (1.66 % atomic), although no changes in the polypyrrole coating were noticed. The data obtained by EDX analysis was consistent with that obtained by XPS analysis and indicated a gradual loss of the counter ion with the increasing pH and a total loss of the counter ion at pH 13.
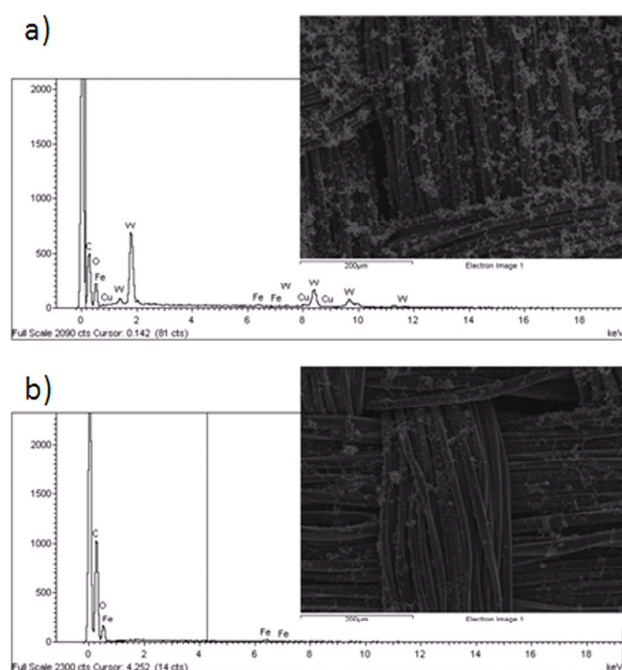
Fig. 6. Micrographs and EDX measurements of PES-PPy/PW$_{12}$O$_{40}$$^{3-}$ (a) and PES-PPy/PW$_{12}$O$_{40}$$^{3-}$ + 1h pH 13 (b).

3.4. Surface resistivity measurements

Surface resistivity measurements were employed to measure variations in the conductivity of the samples due to the different tests performed. In the Fig. 7 the Bode diagrams for different samples of PES/PPy-PW$_{12}$O$_{40}$$^{3-}$ are shown. It is shown the data for the original sample of PES/PPy-PW$_{12}$O$_{40}$$^{3-}$ and the sample after contact with the different pH solutions (1, 7, 13). The Bode plots for the sample after the washing test are also shown.

In the upper diagram it can be seen the impedance modulus (|Z|) at the different frequencies for the different samples. As it was explained previously, the impedance modulus (Ω) is equivalent to the surface resistivity ($\Omega/$) when the material acts as a resistor; as a square of 1.5 cm was measured. In the text it is employed the term impedance modulus but it is equivalent to the surface resistivity. The sample of polyester presents a value of the impedance modulus at low frequencies higher than 10^{11} Ω, typical value of insulating materials. When the sample of polyester was covered with

PPy/PW$_{12}$O$_{40}$$^{3-}$, the value of the impedance modulus lowered more than eight orders of magnitude (a value of approximately 250 Ω was obtained). The contact with the pH 1 solution produced a slight increase of the impedance modulus (315 Ω); this drop of the conductivity may be attributed to the loss of part of the counter ion as XPS analysis revealed (4 %). When the sample was treated in the pH 7 solution the impedance modulus rose to 565 Ω. This result is consistent with a decrease of about 36 % in the doping ratio of PW$_{12}$O$_{40}$$^{3-}$. At pH 13 a large increase of the impedance modulus was observed (9.86·10^5 Ω). The loss of conductivity at pH 13 can be attributed to the deprotonation of polypyrrole that takes place at pH 10 [53] and the reaction of decomposition that PW$_{12}$O$_{40}$$^{3-}$ suffers at pH>8.3 [49]. This loss of conductivity after basic media exposure is consistent with results obtained in bibliography for polypyrrole films [54]. These results corroborate the results obtained by means of XPS and EDX. Nevertheless, the impedance modulus for the sample treated at pH 13 was still lower than that for polyester (5 orders of magnitude for low frequencies). The results for the sample that was submitted to a washing test showed a slight increase of the impedance modulus (698 Ω), slightly higher than the sample treated at pH 7. XPS analysis for the sample after the washing test showed a decrease of about 40 % of the counter ion, this result is consistent with the loss of conductivity observed.

Static charging of the surface of fibers is excluded with surface resistivity below 5 x 10^9 Ω/ [55], so surface resistivity of the conducting textile after the different tests was still adequate for its employment in antistatic applications, including the most adverse conditions that were basic media exposure.

In the second diagram it is shown the data for the phase angle at different frequencies for the same samples of the first diagram. Polyester has a phase angle of nearly 90º, the data at low frequencies is not shown since noise due to the large values of impedance modulus was observed. This value of phase angle is typical of insulating materials that act as a capacitor. All the samples of PES-PPy/PW$_{12}$O$_{40}$$^{3-}$ (except the treated at pH 13) showed values of 0º for the phase angle in the entire frequency range. This indicates that the samples acted as a resistor with different resistances that were indicated previously. The sample treated in basic media showed values of phase angle near to 30º at 10^5 Hz, but it decreased to 0º at 10^3 Hz and was 0º in the rest of frequencies (10^3-10^{-2} Hz). Although the treatment in basic media produced a decrease of the conductivity, the sample continued acting as a resistor.
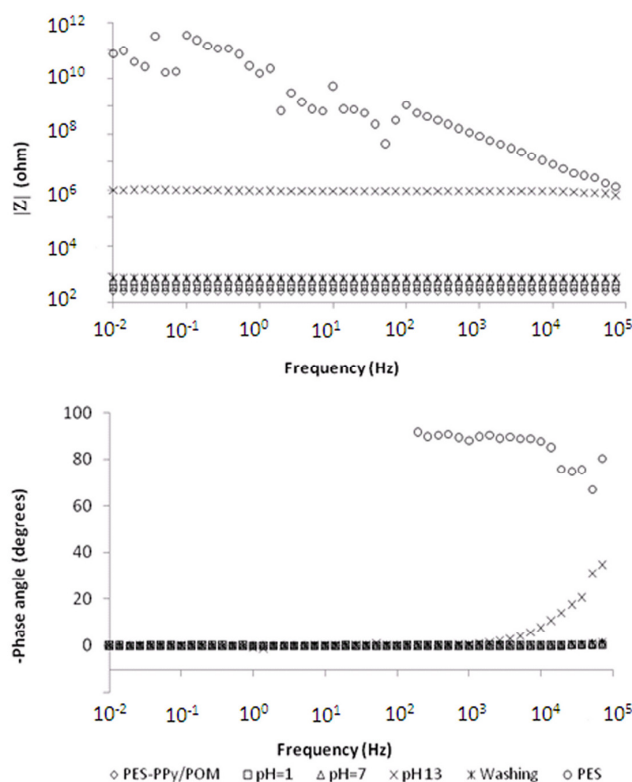
Fig. 7. Bode plots for PES, PES+PPy/PW$_{12}$O$_{40}$$^{3-}$ chemically synthesized, treated during 1 h with pH=1, pH=7 and pH=13 and after the washing test. Measurements between two copper electrodes above the samples. Distance between electrodes 1.5 cm. Textile measured area 1.5 cm x 1.5 cm. Frequency range from 10^5 Hz to 10^{-2} Hz.

3.5. SECM measurements

SECM was used to measure electroactivity variations of the coatings after the different tests. Approach (I$_T$–L) curves were recorded in the feedback mode in a 0.01 M solution of Ru(NH$_3$)$_6$$^{3+}$ in 0.1 M KCl, pH ~5.2, using the 100-µm-diameter Pt tip held at a potential of -0.4 V vs Ag/AgCl (3 M KCl). According to the voltammogram in Fig. 8, this potential was selected to reduce the oxidized form of the mediator, Ru(NH$_3$)$_6$$^{3+}$, at a diffusion-controlled rate.

Approach curves give an indication of the electroactivity of the electrode surface. If the surface is non conductive, when the electrode approaches the surface there is a decrease of the current measured (negative feedback) [29]. On the other hand,

if the electrode is conductive, when the electrode approaches the surface of the substrate the current increases (positive feedback) [29].
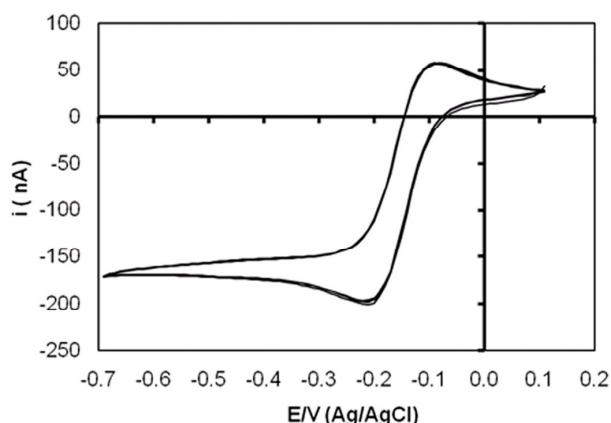

Fig. 8. Cyclic voltammograms for Pt UME 100-µm-diameter tip. The UME potential was scanned from +100 to -700 mV (vs Ag/AgCl) in a 0.01 M Ru(NH$_3$)$_6$$^{3+}$ and 0.1 M KCl at 50 mV s^{-1}.

Figure 9-a, shows a selection of the experimental curves recorded at different points randomly chosen throughout the PES-PPy/PW$_{12}$O$_{40}$$^{3-}$ treated during 1 h in 0.1 M H$_2$SO$_4$ solution. The line scans show different degrees of positive feedback, ranging among 3.8-4.1. The positive feedback indicates an increase of the normalized current (I) when the microelectrode comes close to the surface, according to its conductive nature; (I = i/i$_\infty$ where i$_\infty$ = 4nFDaC in which n is the number of electrons involved in the reaction, F is the Faraday constant, D is the diffusion coefficient, and a is the radius of the UME). On the other hand, for the sample containing only polyester, negative feedback was obtained (I decreases with the normalized distance L = d/a in which d is the distance between UME and surface). Polyester is an insulating material and negative feedback was obtained (Fig. 9-a, or Fig. 9-b). With this technique it is clearly shown the different electrochemical activity and conductivity of the two surfaces analyzed. Samples soaked in the pH 7 solution showed similar values to the sample soaked in the pH 1 solution, values among 3-4.5 were obtained (figure not shown).

In Fig. 9-b, it is shown the electrochemical activity of PES-PPy/PW$_{12}$O$_{40}$$^{3-}$ after 1 h of contact with the pH 13 solution. It can be seen a significant decrease of the degree of positive feedback; after the treatment with the pH 13 solution the values obtained were among 0.9-1.4. There has been a decrease of the material electroactivity due to the

deprotonation of polypyrrole that takes place at pH 10 [53] and the elimination of the counter ion from the coating. However the conducting fabric continued showing some degree of positive feedback, it can be appreciated the difference with the results for the PES sample. These results are consistent with EIS measurements that showed a loss of its conducting properties, but the material continued acting as a conductor.
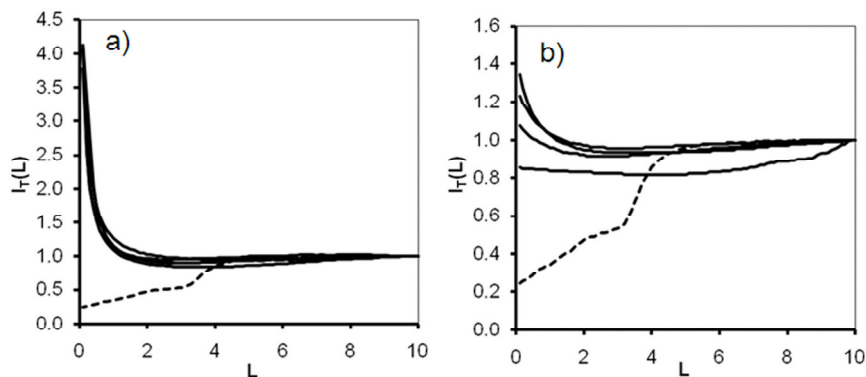

Fig. 9. Approaching curves for: a) PES (---), PES-PPy/AQSA + 1 h pH 1 (—) and b) PES-PPy/AQSA + 1 h pH 13 (—); obtained with a 100 μm diameter Pt tip in 0.01 M Ru(NH₃)₆³⁺ and 0.1 M KCl. The tip potential was -400 mV (vs Ag/AgCl) and the approach rate was 10 μm s⁻¹.

4. Conclusions

Conductive fabrics of PES-PPy/$PW_{12}O_{40}{}^{3-}$ are stable in acid media and neutral media. Higher pHs cause a decrease of the doping ratio (=NH^+/N_{Total}) as well as the expulsion of part of the counter ions from the polymer matrix. The direct effect was the increase in the surface resistivity of the conducting fabric. The increase of the surface resistivity in acid and neutral media was small, as well as after the washing test. On the other hand, in basic media medium a large increase of the surface resistivity was observed, more than three orders. At pHs>8.4, the decomposition reaction of the counter ion is another factor that influences the loss of conductivity. The different tests produced a loss of conductivity but its conducting nature was not modified; the samples continued acting mainly as a resistor, without capacitive behavior. The sample treated in basic medium merits special mention because it continued acting as a resistor (except at high frequencies) regardless the noticeable loss of conductivity. The surface resistivity of the

conducting textile after the different tests was still adequate (below 5 x 10^9 Ω/) for its employment in antistatic applications.

SECM measurements showed that the coatings of PPy/PW$_{12}$O$_{40}$$^{3-}$ were electroactive after the tests in acid and neutral media. The treatment in the pH 13 solution caused a significant decrease of its electroactivity, this decrease is related to the deprotonation of polypyrrole and the loss of the counter ion from the polymer matrix. Zonal EDX analysis showed similar results to that obtained by XPS measurements. SEM micrographs did not show morphological changes in the fibers surface. The loss of the counter ion would produce a more porous structure, however the small size of the counter ion (10 Å approximately) and SEM resolution was not sufficient to observe this effect.

Acknowledgements

References

[1] P. Lekpittaya, N. Yanumet, B.P. Grady, E.A. O'Rear, Resistivity of conductive polymer-coated fabric, J. Appl. Polym. Sci. 92 (2004) 2629-2636.

[2] D. Kincal, A. Kumar, A. Child, J. Reynolds, Conductivity switching in polypyrrole-coated textile fabrics as gas sensors, Synth. Met. 92 (1998) 53-56.

[3] J. Wu, D. Zhou, C.O. Too, G.G. Wallace, Conducting polymer coated lycra, Synth. Met. 155 (2005) 698-701.

[4] K.W. Oh, H.J. Park, S.H. Kim, Stretchable conductive fabric for electrotherapy, J. Appl. Polym. Sci. 88 (2003) 1225-1229.

[5] S.H. Kim, K.W. Oh, J.H. Bahk, Electrochemically synthesized polypyrrole and Cu-plated nylon/spandex for electrotherapeutic pad electrode, J. Appl. Polym. Sci. 91 (2004) 4064-4071.

[6] N.V. Bhat, D.T. Seshadri, M.N. Nate, A.V. Gore, Development of conductive cotton fabrics for heating devices, J. Appl. Polym. Sci. 102 (2006) 4690-4695.

[7] E. Hakansson, A. Kaynak, T. Lin, S. Nahavandi, T. Jones, E. Hu, Characterization of conducting polymer coated synthetic fabrics for heat generation, Synth. Met. 144 (2004) 21-28.

[8] J.P. Boutrois, R. Jolly, C. Pétrescu, Process of polypyrrole deposit on textile. Product characteristics and applications, Synth. Met. 85 (1997) 1405-1406.

[9] H. Kuhn, A. Child, W. Kimbrell, Toward real applications of conductive polymers, Synth. Met. 71 (1995) 2139-2142.

[10] K.G. Neoh, T.T. Young, E.T. Kang, K.L. Tan, Structural and mechanical degradation of polypyrrole films due to aqueous media and heat treatment and the subsequent redoping characteristics, J. Appl. Polym. Sci. 64 (1997) 519-526.

[11] T. Lin, L. Wang, X. Wang, A. Kaynak, Polymerising pyrrole on polyester textiles and controlling the conductivity through coating thickness, Thin Solid Films 479 (2005) 77-82.

[12] F. Ferrero, L. Napoli, C. Tonin, A. Varesano, Pyrrole chemical polymerization on textiles: Kinetics and operating conditions, J. Appl. Polym. Sci. 102 (2006) 4121-4126.

[13] S. Garg, C. Hurren, A. Kaynak, Improvement of adhesion of conductive polypyrrole coating on wool and polyester fabrics using atmospheric plasma treatment, Synth. Met. 157 (2007) 41-47.

[14] J. Molina, A.I. del Río, J. Bonastre, F. Cases, Chemical and electrochemical polymerisation of pyrrole on polyester textiles in presence of phosphotungstic acid. Eur. Poly. J. 44 (2008) 2087-2098.

[15] H.S. Lee, J. Hong, Chemical synthesis and characterization of polypyrrole coated on porous membranes and its electrochemical stability, Synth. Met. 113 (2000) 115-119.

[16] E. Gasana, P. Westbroek, J. Hakuzimana, K. De Clerck, G. Priniotakis, P. Kiekens, D. Tseles, Electroconductive textile structures through electroless deposition of polypyrrole and copper at polyaramide surfaces, Surf. Coat. Technol. 201 (2006) 3547-3551.

[17] L. Dall'Acqua, C. Tonin, A. Varesano, M. Canetti, W. Porzio, M. Catellani, Vapour phase polymerisation of pyrrole on cellulose-based textile substrates, Synth. Met. 156 (2006) 379-386.

[18] L. Dall'Acqua, C. Tonin, R. Peila, F. Ferrero, M. Catellani, Performances and properties of intrinsic conductive cellulose–polypyrrole textiles, Synth. Met. 146 (2004) 213-221.

[19] P. Gómez-Romero, Hybrid Organic-Inorganic Materials - In Search of Synergic Activity, Adv. Mater. 13 (2001) 163-174.

[20] P. Kormali, T. Triantis, D. Dimotikali, A. Hiskia, E. Papaconstantinou, On the photooxidative behavior of TiO$_2$ and PW$_{12}$O$_{40}$$^{3-}$: OH radicals versus holes, Appl. Catal. B-Environ. 68 (2006) 139-146.

[21] B.M. Devassy, F. Lefebvre, S.B. Halligudi, Zirconia-supported 12-tungstophosphoric acid as a solid catalyst for the synthesis of linear alkyl benzenes, J. Catal. 231 (2005) 1-10.

[22] K. Bouzek, K.-M. Mangold, K. Jüttner, Electrocatalytic activity of platinum modified polypyrrole films for the methanol oxidation reaction, J. Appl. Electrochem. 31 (2001) 501-507.

[23] L. Li, Y. Zhang, J.-F. Drillet, R. Dittmeyer, K.-M. Jüttner, Preparation and characterization of Pt direct deposition on polypyrrole modified Nafion composite membranes for direct methanol fuel cell applications, Chem. Eng. J. 133 (2007) 113-119.

[24] F.J. Rodríguez, S. Gutiérrez, J.S. Ibanez, J.L. Bravo, N. Batina, The efficiency of toxic chromate reduction by a conducting polymer (polypyrrole): influence of electropolymerization conditions, Environ. Sci. Technol. 34 (2000) 2018-2023.

[25] Y. Tian, J. Wang, Z. Wang, S. Wang, Electroreduction of nitrite at an electrode modified with polypyrrole nanowires, Synth. Met. 143 (2004) 309-313.

[26] A. Lopes, S. Martins, A. Moraö, M. Magrinho, I. Gonçalves, Degradation of a textile dye C. I. Direct Red 80 by electrochemical processes, Port. Electrochim. Acta 22 (2004) 279-294.

[27] A.H. Gemeay, R.G. El-Sharkawy, I.A. Mansour, A.B. Zaki, Catalytic activity of polyaniline/MnO$_2$ composites towards the oxidative decolorization of organic dyes, Appl. Catal. B-Environ. 80 (2008) 106-115.

[28] A.H. Gemeay, R.G. El-Sharkawy, I.A. Mansour, A.B. Zaki, Preparation and characterization of polyaniline/manganese dioxide composites and their catalytic activity, J. Colloid Interf. Sci. 308 (2007) 385-394.

[29] P. Sun, F.O. Laforge, M.V. Mirkin, Scanning electrochemical microscopy in the 21st century, Phys. Chem. Chem. Phys. 9 (2007) 802-823.

[30] M.V. Mirkin, B.R. Horrocks, Electroanalytical measurements using the scanning electrochemical microscope, Anal. Chim. Acta 406 (2000) 119-146.

[31] A.L. Barker, M. Gonsalves, J.V. Macpherson, C.J. Slevin, P.R. Unwin, Scanning electrochemical microscopy: beyond the solid/liquid interface, Anal. Chim. Acta 385 (1999) 223-240.

[32] Complete textile glossary, Available from: http://www.celaneseacetate.com/textile_glossary_filament_acetate.pdf, 2001. Last accessed 17th May 2010.

[33] J.M. Ribo, A. Dicko, J.M. Tura, D. Bloor, Chemical structure of polypyrrole: X-ray photoelectron spectroscopy of polypyrrole with 5-yliden-3-pyrrolin-2-one end groups, Polymer 32 (1991) 728-732.

[34] J.C. Thiéblemont, J.L. Gabelle, M.F. Planche, Polypyrrole overoxidation during its chemical synthesis, Synth. Met. 66 (1994) 243-247.

[35] R. Rajagopalan, J.O. Iroh, Characterization of polyaniline-polypyrrole composite coatings on low carbon steel: a XPS and infrared spectroscopy study, Appl. Surf. Sci. 218 (2003) 58-69.

[36] W. Prissanaroon-Ouajai, P.J. Pigram, R. Jones, A. Sirivat, A novel pH sensor based on hydroquinone monosulfonate-doped conducting polypyrrole, Sensor. Actuat. B-Chem. 135 (2008) 366-374.

[37] L.G. Paterno, S. Manolache, F. Denes, Synthesis of polyaniline-type thin layer structures under low-pressure RF-plasma conditions, Synth. Met. 130 (2002) 85-97.

[38] L. Sabbatini, C. Malitesta, E. De Giglio, I. Losito, L. Torsi, P.G. Zambonin, Electrosynthesised thin polymer films: the role of XPS in the design of application oriented innovative materials, J. Electron. Spectrosc. Relat. Phenom. 100 (1999) 35-53.

[39] J. Starck, P. Burg, S. Muller, J. Bimer, G. Furdin, P. Fioux, C.V. Guterl, D. Begin, P. Faure, B. Azambre, The influence of demineralisation and ammoxidation on the adsorption properties of an activated carbon prepared from a Polish lignite, Carbon 44 (2006) 2549-2557.

[40] C.G.J. Koopal, M.C. Feiters, R.J.M. Nolte, B. de Ruiter, R.B.M. Schasfoort, R. Czajka, H. Van Kempen, Polypyrrole microtubules and their use in the construction of a third generation biosensor, Synth. Met. 51 (1992) 397-405.

[41] L. Pesaresi, D.R. Brown, A.F. Lee, J.M. Montero, H. Williams, K. Wilson, Structural study of compartmental complexes of europium and copper, Appl. Catal. A-Gen. 360 (2009) 50-58.

[42] Z. Zude, Z. Xiong, Z. Tao, Y. Huaming, L. Qingliang, Structural study of compartmental complexes of europium and copper, J. Mol. Struct. 478 (1999) 23-27.

[43] M. Wahlqvist, A. Shchukarev, XPS spectra and electronic structure of Group IA sulfates, J. Electron. Spectrosc. Relat. Phenom. 156–158 (2007) 310-314.

[44] S. Carquigny, O. Segut, B. Lakard, F. Lallemand, P. Fievet, Effect of electrolyte solvent on the morphology of polypyrrole films: Application to the use of polypyrrole in pH sensors, Synth. Met. 158 (2008) 453-461.

[45] M. Makhlouki, J.C. Bernède, M. Morsli, A. Bonnet, A. Conan, S. Lefrant, XPS study of conducting polypyrrole-poly(vinyl alcohol) composites, Synth. Met. 62 (1994) 101-106.

[46] B. Dong, J. Peng, P. Zhang, A. Tian, J. Chen, B. Xue, Hydrothermal synthesis and crystal structure of a novel Keggin polyoxoanion-templated multichain coordination polymer with a flexible bis(imidazole) ligand, Inorg. Chem. Commun. 10 (2007) 839-842.

[47] P.A. Jalil, M. Faiz, N. Tabet, N.M. Hamdan, Z. Hussain, A study of the stability of tungstophosphoric acid, H$_3$PW$_{12}$O$_{40}$, using synchrotron XPS, XANES, hexane cracking, XRD, and IR spectroscopy, J. Catal. 217 (2003) 292-297.

[48] C.D. Wagner, A.V. Naumkin, A. Kraut-Vass, J.W. Allison, C.J. Powell, J.R. Rumble Jr., X-Ray Photoelectron Spectroscopy Database, The National Institute of Standards and Technology, U.S. Secretary of Commerce, Available from: http://srdata.nist.gov/xps, 2007. Last accessed 17th May 2010.

[49] Z. Zu, R. Tain, C. Rhodes, A study of the decomposition behaviour of 12-tungstophosphate heteropolyacid in solution, Can. J. Chem. 81 (2003) 1044-1050.

[50] C. Hurren, A. Kaynak, X. Wang, Effects of laundering on conductivity of polypyrrole-coated textiles, Res. J. Text. Appar. 11 (2007) 11-17.

[51] A. Varesano, L. Dall'Acqua, C. Tonin, A study on the electrical conductivity decay of polypyrrole coated wool textiles, Polym. Degrad. Stabil. 89 (2005) 125-132.

[52] E. López-Salinas, J.G. Hernández-Cortéz, M.A. Cortés-Jácome, J. Navarrete, M.E. Llanos, A. Vázquez, H. Armendáriz, T. López, Skeletal isomerization of 1-butene on 12-tungstophosphoric acid supported on zirconia, Appl. Catal. A-Gen. 175 (1998) 43-53.

[53] M. Krzysztof, Chemical reactivity of polypyrrole and its relevance to polypyrrole based electrochemical sensors, Electroanal. 18 (2006) 1537-1551.

[54] Y. Li, J. Ouyang, J. Yang, Two doping structures and structural anisotropy revealed by the mass loss and shrinkage of polypyrrole films on alkali treatment, Synth. Met. 74 (1995) 49-53.

[55] T. Textor, B. Mahltig, A sol–gel based surface treatment for preparation of water repellent antistatic textiles, Appl. Surf. Sci. 256 (2010) 1668–1674.

9.- ARTÍCULO

STABILITY OF CONDUCTING FABRICS OF PES-PPy/AQSA IN DIFFERENT pH SOLUTIONS. CHEMICAL AND ELECTROCHEMICAL CHARACTERIZATION.
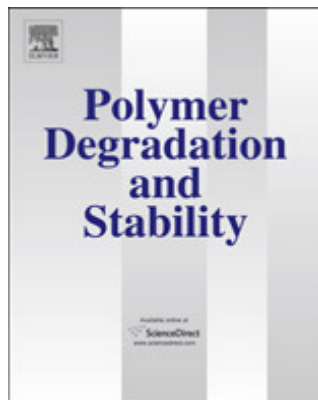
Stability of conducting fabrics of PES-PPy/AQSA in different pH solutions. Chemical and electrochemical characterization.

J. Molina[a], J. Fernández[a], A.I. del Río[a], R. Lapuente[b], J. Bonastre[a], F. Cases[a] [*]

[a]*Departamento de Ingeniería Textil y Papelera, EPS de Alcoy, Universidad Politécnica de Valencia, Plaza Ferrándiz y Carbonell s/n, 03801 Alcoy, Spain*
[b]*Departamento de Ingeniería de la Construcción, OP, Inf. Urbana, Universidad de Alicante, Apdo. 99, 03080 Alicante, Spain*

Abstract

The stability of conducting fabrics of polyester (PES) covered with polypyrrole/ anthraquinone sulfonic acid (AQSA) has been tested in different pH solutions (1, 7, 13) and after washing tests. It is important to determine the stability of the counter ion in the polymer matrix; since its loss causes the decrease of the conducting properties of the fabrics. X-ray photoelectron spectroscopy (XPS) studies were done to quantify the amount of counter ion in the polymer matrix and obtain the doping level ($N^{\delta+}/N$). Surface resistivity changes after the different tests were measured by means of electrochemical impedance spectroscopy (EIS). An increase in the pH solution, caused a decrease of the doping level ($N^{\delta+}/N$), the release of part of the counter ions and an increase in the surface resistivity. Cyclic voltammetry (CV) measurements showed a gradual loss of electroactivity as pH increased. It has been also demonstrated the influence of the scan rate on the characterization of conducting fabrics by CV. Lower scan rates produce a more characteristic response than higher ones. Scanning electrochemical microscopy (SECM) measurements showed a loss of electroactivity when the sample was tested in the pH 13 solution, although the material continued being electroactive.

Keywords: Conducting fabrics, polypyrrole, anthraquinone sulfonic acid, X-ray photoelectron spectroscopy, scanning electrochemical microscopy.

---

* Corresponding author. Fax.: +34 96 652 8438

E-mail address: fjcases@txp.upv.es (Prof. F. Cases)

1. **Introduction**

The development of textiles with new properties and applications has received great attention during the last years; one of these properties is the electrical conductivity. Different methods have been employed to produce conducting textiles, like the synthesis of conducting polymers on the fabrics [1-9], the chemical metallization of fibres [10], etc. The first one is the method that has been employed in this paper to produce conducting fabrics. Applications of conducting textiles are varied and numerous; like antistatic materials [1], gas sensors [2], biomechanical sensors [3], electrotherapy [4, 5], heating devices [6-8] or microwave attenuation [9].

During the formation of polypyrrole (PPy), positive charges are created in the polypyrrole structure. Negative charges provided by a counter ion compensate the positive charges to maintain the electroneutrality principle. If the counter ion is expelled from the structure (dedoping), there is a great loss of its electrical properties. Low size anions like Cl^- have been employed as counter ions, but their stability is low [9]. To prevent this phenomenon, bulky anions with high molecular size have been employed in bibliography. Typical counter ions employed in the production of polypyrrole covered textiles are organic molecules with high size; like anthraquinone sulfonic acid (AQSA) [2, 7, 9, 11-14], dodecylbenzene sulfonic acid (DBSA) [1, 12], p-toluene sulfonic acid (PTSA) [2, 9, 12, 15], naphthalenedisulfonic acid (NDSA) [3, 9, 12], benzenesulfonic acid (BSA) [4, 16], naphthalenesulfonic acid (NSA) [9, 15] or anthraquinone disulfonic acid (AQDSA) [17, 18]. If the size of the counter ion is high, its diffusion is prevented and it remains in the polypyrrole structure [19]. This is the basis for employing AQSA; its high molecular size would difficult its expulsion from the polymer matrix.

One of the applications that our group is investigating, is the employment of conducting fabrics in catalysis; or as a support with high surface area to electrodeposit Pt nanoparticles and enhance its electroactivity [20,21]. The employment of conducting polymers in environmental purposes has been reported [22-26]. For instance, electrodes modified with conducting polymers have been used in Cr^{6+} (toxic) reduction to Cr^{3+} (not toxic) [22] or nitrites electroreduction [23]. Polypyrrole coated fabrics have been employed in the electrochemical removal of the textile dye C. I. Direct Red 80 [24]. Polyaniline/MnO_2 catalyst has been employed in the degradation of organic dyes such as Direct Red 81, Indigo Carmine and Acid Blue 92 [25, 26]. For this purpose, the study of the stability of the PPy/AQSA coating and its electrical and electrochemical properties in different pH solutions is essential to optimize its operational pH range. Another application that we are studying at present is its employment in electronic clothing, for

example we are studying its electromagnetic interference shielding properties. For these applications, the conducting fabrics would have to resist washing tests. In that sense, Varesano et al. performed washing tests to polypyrrole coated wool textiles [27]. In addition to the conductivity changes, it is also important to know the doping level ($N^{\delta+}/N$) and counter ion content in the conducting fabrics after the different tests (these data have been obtained by X-ray photoelectron spectroscopy measurements (XPS)). If the conducting textile suffers dedoping (release of the counter ion), the conducting fabric loses part of its conducting properties. Energy dispersive X-ray (EDX) measurements were done to perform local analyses. Fourier transform infrared spectroscopy with attenuated total reflection (FTIR-ATR) analyses were also performed after the different tests. Surface resistivity changes of the conducting fabric after the different tests were measured by means of electrochemical impedance spectroscopy (EIS). The electroactivity of the conducting fabrics in the different pH solutions was also measured by means of cyclic voltammetry (CV). Very little has been reported about conducting textiles characterization by CV [15, 28]. In this paper we report the influence of the scan rate in the characterization of conducting fabrics. Scanning electrochemical microscopy (SECM) has been also employed to measure the electroactivity of the conducting fabrics after being in contact with the different pH solutions. SECM is a relatively novel (1989) and powerful technique that is becoming more popular among researchers [29-31]. SECM has not been used in bibliography to characterize conducting fabrics to our knowledge.

2. Experimental

2.1. Reagents and materials

Analytical grade pyrrole, ferric chloride, anthraquinone sulphonic acid sodium salt (AQSA), sulphuric acid, sodium sulphate, sodium hydroxide, sodium dihydrogenophosphate and disodium hydrogenophosphate were purchased from Merck. Normapur acetone was from Prolabo. Hexaammineruthenium (III) choride ($Ru(NH_3)_6Cl_3$) and potassium chloride were used as received from Acros Organics and Scharlau respectively. When needed, solutions were deoxygenated by bubbling nitrogen (N_2 premier X50S). Ultrapure water was obtained from an Elix 3 Millipore-Milli-Q Advantage A10 system with a resistivity near to 18.2 MΩ cm.

Polyester textile was acquired from Viatex S A and their characteristics were: fabric surface density, 140 g m^{-2}; warp threads per cm, 20 (warp linear density, 167 dtex); weft threads per cm, 60 (weft linear density, 500 dtex). These are specific terms used in the field of textile industry and their meaning can be consulted in a textile glossary [32].

2.2. Chemical synthesis of PPy/AQSA on polyester fabrics

Chemical synthesis of PPy on polyester (PES) textiles was done as reported in our previous study [14]. The size of the samples was 6 cm x 6 cm approximately. Previously to reaction, polyester was degreased with acetone in ultrasound bath and washed with water. Pyrrole concentration employed was 2 g L^{-1} and the molar relations of reagents employed in the chemical synthesis bath were pyrrole: $FeCl_3$: AQSA (1: 2.5: 0.6). The next stage was the adsorption of pyrrole and counter ion (AQSA) (V=200 ml) on the fabric for 30 min in an ice bath without stirring. At the end of this time, the $FeCl_3$ solution (V=50 ml) was added and oxidation of the monomer took place during 150 min without stirring. Adsorption and reaction were performed in a precipitation beaker. The conducting fabric was washed with water to remove PPy not joined to fibers. The conducting textile was dried in a desiccator for at least 24 h before measurements. The weight increase was measured obtaining a value near to 6 %.

2.3. Stability of AQSA in the conducting fabrics of PES-PPy/AQSA in different pH solutions

Different samples of PES-PPy/AQSA (2 cm x 2 cm) were soaked in different pH solutions. The solutions employed were: 0.1 M H_2SO_4 (pH~1), NaH_2PO_4-NaH_2PO_4 buffer + 0.1 M Na_2SO_4 (pH~7) and 0.1 M NaOH + 0.1 M Na_2SO_4 (pH~13). After 1 h of contact with the different pH solutions, the samples were rinsed with ultrapure water, dried in a desiccator and analyzed by means of XPS. Other samples obtained equally, were used to perform EDX and SECM measurements; their morphology was also observed by means of SEM. The surface resistivity of the conducting fabric was also measured before and after contact with the different pH solutions.

2.4. Washing test

A washing test was performed to determine the loss of conductivity after this test. The analysis was done as related in the norm ISO 105-C01 at 40 ºC during 30 min. The surface resistivity was measured before and after the washing test. XPS and EDX analyses were also done to quantify the dopant before and after the washing test.

2.5. X-Ray photoelectron spectroscopy

XPS analyses were conducted at a base pressure of $5 \cdot 10^{-10}$ mbars and a temperature around -100 ºC. XPS spectra were obtained with a VG-Microtech Multilab electron spectrometer by using unmonochromatized Mg Kα (1253.6 eV) radiation from a twin anode source operating at 300 W (20 mA, 15 kV). The binding energy (BE) scale was calibrated with reference to the C_{1s} line at 284.6 eV. The N1s and S2p levels spectra were analyzed for the different samples of PES-PPy/AQSA.

2.6. Scanning electron microscopy and energy dispersive X-ray characterization

A Jeol JSM-6300 scanning electron microscope was employed to observe the morphology of the samples and perform EDX analyses. Scanning electron microscopy (SEM) analyses were performed using an acceleration voltage of 20 kV. EDX measurements were done between 0 and 20 keV.

2.7. Surface resistivity measurements

An Autolab PGSTAT302 potentiostat/galvanostat was employed to perform electrochemical impedance spectroscopy (EIS) analyses. EIS measurements were performed in the 10^5-10^{-2} Hz frequency range. The amplitude of the sinusoidal voltage was 10 mV. Measurements were carried out in a two-electrode arrangement; using two rectangular copper electrodes (0.5 cm x 1.5 cm) separated by 1.5 cm and pressed to the dry textile sample. The measured area of the textile was a square of 1.5 cm, so the measured impedance modulus (Ω) was equal to the surface resistivity ($\Omega/\square$).

2.8. FTIR-ATR measurements

Fourier transform infrared spectroscopy with horizontal multirebound attenuated total reflection (FTIR-ATR) was performed with a Nicolet 6700 Spectrometer equipped with DTGS detector. An accessory with pressure control was employed to equalize the pressure in the different solid samples. A prism of ZnSe was employed. Spectra were collected with a resolution of 4 cm^{-1} and 100 scans were averaged for each sample.

2.9. Cyclic voltammetry measurements

An Autolab PGSTAT302 potentiostat/galvanostat was employed to perform CV measurements in the different pH solutions: pH~1 (0.1 M H_2SO_4), pH~7 (NaH_2PO_4-NaH_2PO_4 buffer and Na_2SO_4 0.1 M) and pH~13 (0.1 M NaOH and 0.1 M Na_2SO_4). The conducting fabric sample was located between two Ti plates to perform the measurements. The measurements were performed in a three electrodes arrangement. The counter electrode employed was made of stainless steel; the pre-treatment consisted on polishing, degreasing with acetone in an ultrasonic bath and washing with water in the ultrasonic bath. The working electrode was made by cutting a strip of the conducting fabric of PPy. Potential measurements were referred to Ag/AgCl (3 M KCl) reference electrode. Oxygen was removed from solution by bubbling nitrogen gas for 10 min and then a N_2 atmosphere was maintained during the measurements. The ohmic potential drop was measured and introduced in the Autolab software (GPES). The measurements were done between -0.4 V and +0.4 V. The characterization by means of CV has been done at different scan rates as it has been corroborated the influence of this parameter on the electrochemical response obtained. The scan rates employed were 50 mV s^{-1}, 5 mV s^{-1} and 1 mV s^{-1}.

2.10. Scanning electrochemical microscopy measurements

SECM measurements were carried out with a scanning electrochemical microscope of Sensolytics. The three-electrode cell configuration consisted of a 100 μm diameter Pt ultra-microelectrode (UME) working electrode, a Pt wire auxiliary electrode and an Ag/AgCl (3 M KCl) reference electrode. The solution selected for this study was 0.01 M $Ru(NH_3)_6Cl_3$ in aqueous 0.1 M KCl supporting electrolyte. All the experiments were carried out in inert nitrogen atmosphere. Substrates of PES and PES-PPy/AQSA were chosen as substrates for the SECM measurements. Different samples of PES-

PPy/AQSA were treated during 1 h with pH 1 and pH 13 solutions and dried in a desiccator before obtaining approach curves. The substrates were glued with epoxy resin on glass microscope slides.

The positioning of the Pt UME tip was achieved by first carefully putting it in contact with the substrate surface and then moving it in z direction (height of the electrode). Once the electrode was at the desired height, the electrode was approached to the substrate surface; the current of the UME was recorded to obtain the approach curves. Approach curves give us an indication of the electroactivity of the surface.

The surfaces were also scanned at their open circuit potential (OCP), scanning the surface of the fabrics, a topographic profile of the sample was obtained. The scanning was done at 100 µm height from the substrate. The potential of the substrate was controlled indirectly by the redox couple concentration.

3. Results and discussion

3.1. XPS analysis of PES-PPy/AQSA treated at different pHs and after the washing test

Different samples of PES-PPy/AQSA were treated during 1 h in different pH solutions (pH 1, 7 and 13). Some samples were also submitted to washing tests as related in the norm ISO 105-C01. The N1s and S2p core levels spectra were analyzed for the different samples. Table 1 shows the core level binding energies and the assignments for the samples analyzed. The doping level ($N^{\delta+}$/N) and counter ion content (S/N) after these tests was also obtained (Table 2).

3.1.1. N1s analysis

Fig. 1-a shows the high resolution N1s spectrum for the untreated sample of PES-PPy/AQSA specimen. The N1s spectrum was deconvoluted into two contributions, centered at 399.5 and 401.1 eV. The peak at 399.5 eV was assigned to the neutral amine-like (–NH–) structure which is characteristic of pyrrolylium nitrogen [33-35]. The peak at 401.1 eV was attributed to positively charged nitrogen species ($N^{\delta+}$) [35-37]. The electron-deficient nitrogen species arise from delocalization of electron density from the polypyrrole ring as a result of the formation of electronic defects (polarons or bipolarons). The doping ratio represented by the ($N^{\delta+}/N_{Total}$) ratio was found to be 0.16.

	PPy/AQSA	PPy/AQSA +pH1	PPy/AQSA +pH7	PPy/AQSA +pH13	PPy/AQSA +Washing	Assignments
N1s	399.5	399.5	399.5	399.7	399.6	$-NH-$
	401.1	401.4	400.9	401.1	401.7	$N^{\delta+}$
S2p	167.3	167.2	167.2	167.5	167.4	$-SO_3-$
	169.0	168.8	168.5	169.1	169.1	

Table 1. XPS results for binding energies (eV) and assignments for the samples analyzed.

Table 1 shows that the N1s binding energies were similar for all the samples. The same nitrogen functional groups appeared when samples were treated at pH 1, 7, 13 and after the washing test. As commented before, these peaks were due to neutral amine-like (-NH-) structure and positively charged nitrogen species ($N^{\delta+}$).
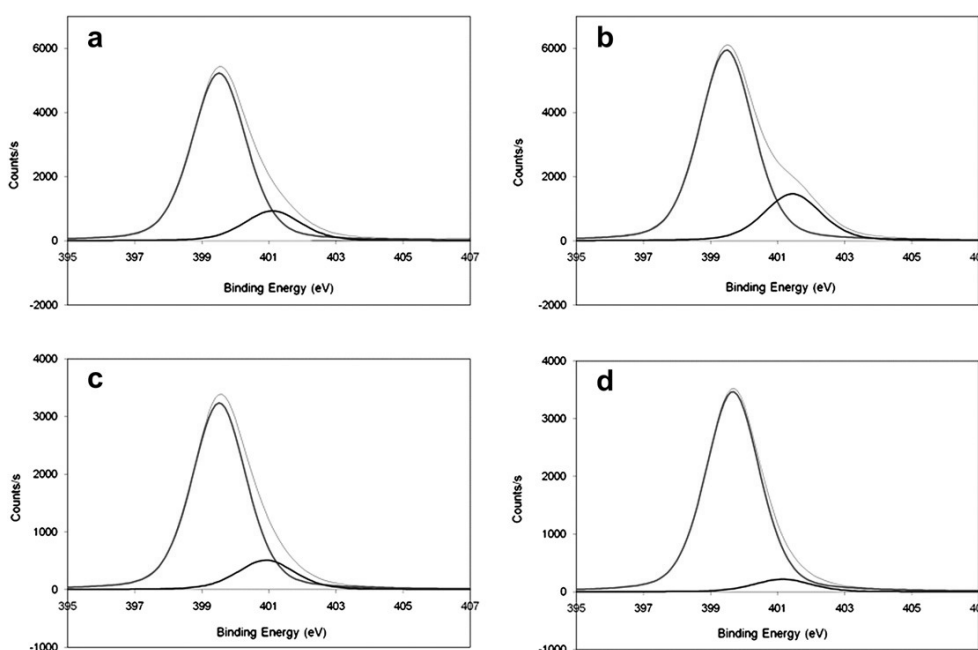

Fig. 1. XPS high resolution spectra for N1s for the different samples of PES/PPy-AQSA: a) original sample, b) + 1 h pH 1, c) + 1 h pH 7, d) + 1 h pH 13.

The sample treated during 1 h in the pH 1 solution showed a slight increase of the doping level (0.21) (Fig. 1-b). This is due to the protonation of polypyrrole that takes place at pH~3 [38]. The sample treated at pH 7 showed similar values of doping level to

the untreated sample (0.14) (Fig. 1-c). For the sample treated at pH 13, N1s spectrum presents a significant decrease for $N^{\delta+}$ contribution and the doping level obtained was 0.06 (Fig. 1-d). This decrease in the doping level is due to the deprotonation of polypyrrole which takes place at pH 10 [38]. For the sample submitted to a washing test, the doping level obtained was 0.16 (figure not shown), value equal to the original sample of PES-PPy/AQSA. The washing test does not produce a decrease of the doping level since the pH of the solution employed for the washing test was around 7 and the deprotonation of polypyrrole takes place at pH 10 [38]. Only the more basic solution treatment produced a significant decrease of the doping level due to the deprotonation of the polypyrrole chains as mentioned previously.

3.1.2. S2p analysis

Fig. 2 shows the high resolution S2p spectrum for the untreated sample of PES-PPy/AQSA specimen. The S2p core level signal was deconvoluted into two contributions attributed to the covalently bonded sulfonate anion ($-SO_3^-$) [39] arising from the counter ion. The two peaks were attributed to a spin-orbit doublet S2p3/2 and S2p1/2 at 167.3 and 169 eV respectively [39]. The AQSA molecule presents an S atom in its structure, so the ratio S/N could also be used as an indication of the doping ratio (counter ion content) of the different samples. As it can be seen in Table 2, there is a difference between the S/N and the $N^{\delta+}$/N ratio. The AQSA content (represented by S/N ratio) is greater than the positively charged nitrogen content ($N^{\delta+}$/N), this indicates an excess of AQSA at the PPy/AQSA surface. This happens for all the samples analyzed. Similar results were observed by Prissanaroon-Ouajai et al. in films of PPy/HQS [36] and by Neoh et al. in films of PPy/PSSA [40]. The excess of counter ions could be associated with H^+ [40]. At pH 1, the increase of the doping level ($N^{\delta+}$/N) is accompanied by an increase of the S/N ratio, maybe due to the incorporation of SO_4^{2-}/HSO_4^-, arising from the sulphuric media employed (0.1 M H_2SO_4). At pH 7 there was a slight decrease of the S/N ratio, so part of the counter ions were removed from the polymer surface. When the sample was soaked with the pH 13 solution, there was a significant decrease of the S/N ratio (0.24). Part of the counter ions had been removed from the polypyrrole structure due to the polypyrrole deprotonation (around the 38 % of AQSA counter ions were removed). The washing test showed similar results to the treatment in the pH 13 solution, a loss of the 38 % of the AQSA counter ions was also obtained. However, in the case of the washing test, the $N^{\delta+}$/N ratio was not modified. There was a loss of part of the counter ion that did not

affect the $N^{\delta+}/N$ ratio and the S/N ratio was still higher than the $N^{\delta+}/N$ ratio. This loss of counter ion could be associated to protonated anthraquinone sulphonate groups which are incorporated in the polymeric matrix as no-charged species when carrying out the synthesis. In this case, these no-charged species have not influence on the polymer doping level. The washing tests produces a higher loss of counter ions maybe due to the vigorous agitation and the use of detergents that produce a decrease of the surface tension and consequently the removal of the counter ions less joined to the polypyrrole structure.

Sample	S/N	$N^{\delta+}/N$
PES-PPy/AQSA	0.39	0.16
PES-PPy/AQSA + 1 h pH 1	0.41	0.21
PES-PPy/AQSA + 1 h pH 7	0.37	0.14
PES-PPy/AQSA + 1 h pH 13	0.24	0.06
PES-PPy/AQSA + washing	0.24	0.16

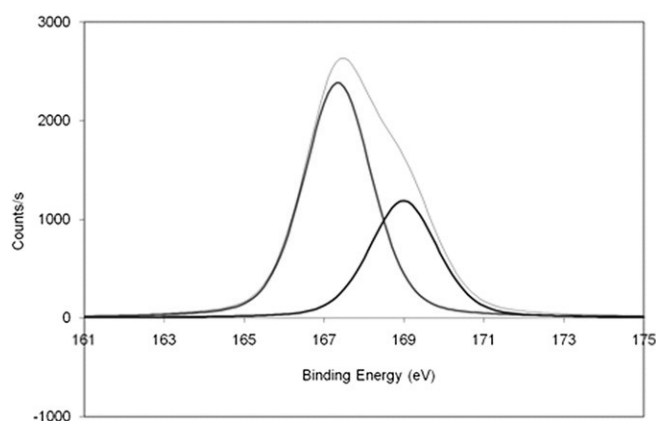Table 2. S/N and $N^{\delta+}/N$ ratios for the different samples of PES-PPy/AQSA.

Fig. 2. XPS high resolution spectra for S2p for the original sample of PES/PPy-AQSA.

3.2. Scanning electron microscopy and energy dispersive X-ray characterization

EDX analysis can be used as a semi-quantitative analysis to calculate the content of the counter ion in the polymer matrix. The presence of S was employed as an indication of the presence of the counter ion (AQSA) since S is present in its structure. The analyses were performed after the different treatments. In Fig. 3-a it can be

observed the EDX analysis of the original sample of PES-PPy/AQSA in the area of the micrograph attached. As it can be seen, a band attributed to S appears around 2 keV. In the micrograph it could be seen that the layer of polypyrrole covered completely the fabric of polyester. The presence of polypyrrole aggregates that could not be removed from the surface of the fabric during the washing stage of the synthesis process was also noticeable. The atomic content of S for this sample was 0.84 %.
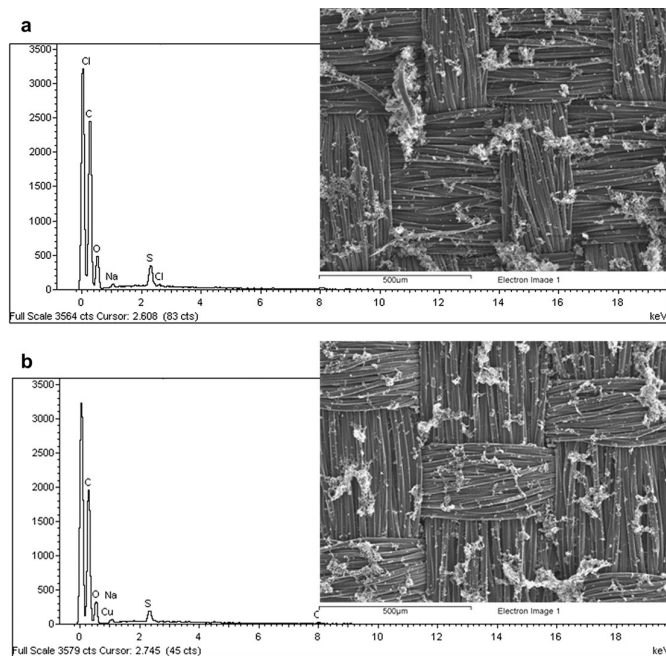

Fig. 3. Micrographs and EDX measurements of PES-PPy/AQSA (a) and PES-PPy/AQSA + 1 h pH 13 (b).

When it was soaked during 1 h in the pH 1 and pH 7 solutions, the content of S was not substantially modified (micrographs and analysis not shown). The micrographs did not show any morphological change. Polypyrrole deprotonation takes place at pH 10 [38], so after the treatment with the basic solution it could be expected a deprotonation of polypyrrole and the subsequent release of part of the counter ion to maintain the electroneutrality principle. In Fig. 3-b it can be observed the EDX analysis and the micrograph for the sample treated at pH 13. The presence of S in the EDX spectrum was obvious and the atomic content obtained was 0.59 %. Approximately, the 30 % of the

counter ion (AQSA), was released from the polypyrrole structure. The sample submitted to a washing test showed a value of 0.45 % of S, there was a loss of part of the counter ion (46 %). AQSA is a bulky molecule, so part of the counter ion remains in the polypyrrole matrix and is not expelled. EDX results were consistent with that obtained by XPS, taking into account that EDX technique provides a semi-quantitative analysis.

3.3. Surface resistivity measurements

In the Fig. 4 the Bode diagrams for different samples of PES/PPy-AQSA are shown. It is shown the data for the original sample of PES/PPy-AQSA and the sample after contact with the different pH solutions (1, 7, 13). The Bode plots for the sample after the washing test are also shown.

In the Fig. 4-a it can be seen the impedance modulus ($|Z|$) at the different frequencies for the different samples. As it was explained previously, the impedance modulus (Ω) is equivalent to the surface resistivity (Ω/square), as a square of 1.5 cm was measured. In the text it is employed the term impedance modulus but it is equivalent to the surface resistivity. The sample of polyester presents a value of the impedance modulus at low frequencies higher than 10^{11} Ω, typical value of insulating materials. When the sample of polyester was covered with PPy/AQSA, the value of the impedance modulus lowered more than nine orders of magnitude (a value of approximately 45 Ω was obtained). The contact with the pH 1 solution produced a slight decrease of the impedance modulus (41 Ω); this variation of the conductivity may be assigned to the protonation of polypyrrole [38] and is consistent with the higher $N^{\delta+}/N$ ratio obtained in the XPS analysis. When the sample was treated in the pH 7 solution the impedance modulus rose to 61 Ω. XPS analysis showed a slight decrease of the $N^{\delta+}/N$ and the loss of part of the AQSA counter ions. At pH 13 a large increase of the impedance modulus was observed (1662 Ω). The loss of conductivity at pH 13 can be attributed to the deprotonation of polypyrrole that takes place at pH 10 [38]. XPS analyses showed an important decrease of the $N^{\delta+}/N$ ratio (0.06) and also the loss of part of the counter ions (38 %). These two factors contribute to the higher impedance modulus obtained. This loss of conductivity after basic media exposure is consistent with results obtained in bibliography for polypyrrole films [41]. Nevertheless, the impedance modulus for the sample treated at pH 13 was still lower than that for polyester (7-8 orders of magnitude for low frequencies) as it can be seen in Fig. 4.
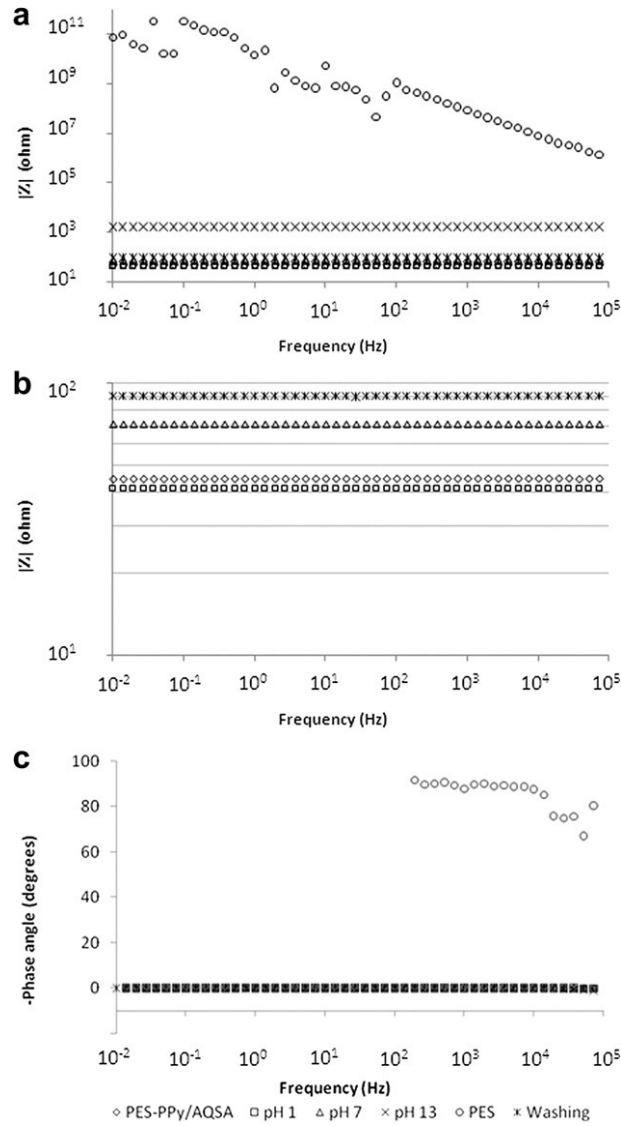
Fig. 4. Bode plots for PES, PES-PPy/AQSA chemically synthesized, treated during 1 h with pH 1, pH 7 and pH 13 and after the washing assay. Measurements between two copper electrodes above the samples. Distance between electrodes 1.5 cm. Textile measured area 1.5 cm x 1.5 cm. Frequency range from 10^5 Hz to 10^{-2} Hz.

The results for the sample that was submitted to a washing test, showed a slight increase of the impedance modulus (90 Ω), slightly higher than the sample treated at pH

7. XPS analysis for the sample after the washing test showed a decrease of about 38 % of the counter ion content (S/N ratio), although the $N^{\delta+}/N$ ratio was not modified. This result is consistent with a small increase in the impedance modulus due to the loss of part of the counter ions. In Fig. 4-b, part of the graphics have been magnified for better observation.

In Fig. 4-c, it is shown the data for the phase angle at different frequencies for the same samples of the first diagram. Polyester has a phase angle of nearly 90º, the data at low frequencies is not shown since noise due to the large values of impedance modulus was observed. This value of phase angle is typical of insulating materials that act as a capacitor. All the samples of PES-PPy/AQSA showed values of 0º for the phase angle in the entire frequency range. This indicates that the samples acted as a resistor with different resistances that were indicated previously. Although the treatment in basic media produced a decrease of the conductivity, the sample continued acting as a resistor.

3.4. FTIR-ATR measurements

Fig. 5 shows the spectra of the different samples of PES-PPy/AQSA: a) original sample, b) + 1 h pH 1, c) + 1 h pH 7, d) + 1 h pH 13, e) + washing test. In the different spectra, bands from the polyester substrate can be observed. The bands have been obtained from a spectrum of polyester [14]; the most representative bands are: 700, 960, 1014, 1090, 1236 and 1714 cm^{-1} (the PES bands have not been marked in the spectrum). Different bands associated with the polypyrrole layer have been observed:

- 1540 cm^{-1}, associated to the pyrrole ring stretching vibration (C=C) [17, 18].
- 1450 cm^{-1}, C-C stretching (1450 cm^{-1}) [17, 18].
- 1300 cm^{-1}, C-N stretching (1300 cm^{-1}) [17, 18].
- 775, 1030 (partially overlapped with a PES band) and 1160 cm^{-1}, associated with bending vibration of pyrrole [17, 18].
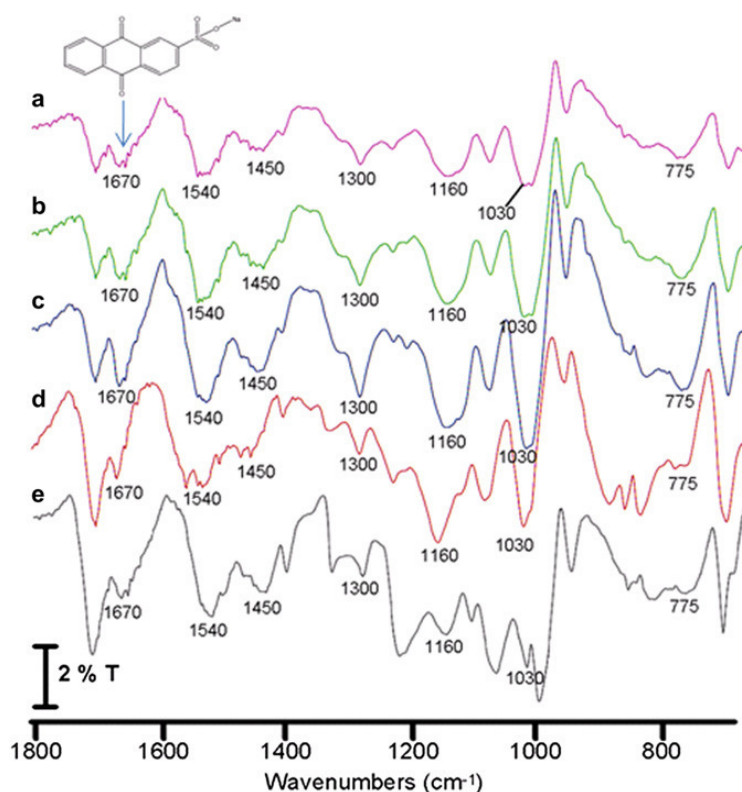
Fig. 5. FTIR-ATR spectra of samples of PES-PPy/AQSA: a) original sample, b) + 1 h pH 1, c) + 1 h pH 7, d) + 1 h pH 13, e) + washing test. Resolution 4 cm^{-1}, 100 scans.

A band at 1670 cm^{-1} indicates the presence of the counter ion (AQSA) [42]. This band is attributed to the stretching of C=O in quinones [43]. For the original sample (Fig. 5-a), if the intensity of the AQSA band is compared with the intensity of the PES band at 1714 cm^{-1}, it can be seen that the relative intensity of the bands is approximately the same. When the sample was treated with the pH 1 (Fig. 5-b) and pH 7 (Fig. 5-c) solutions, the relative intensity of these bands was not substantially modified. XPS analysis showed the same results, the S/N ratio was not substantially varied and hence the AQSA content did not vary noticeably, as commented before. The treatment with the pH 13 solution (Fig. 5-d) caused a decrease of the AQSA band in relation to the PES band. This is due to the removal of part of the AQSA counter ions, as it was explained in the XPS analysis. The sample submitted to a washing test (Fig. 5-e), showed the same

results; a decrease of the AQSA band due to the expulsion of part of the AQSA counter ions.

3.5. Cyclic voltammetry measurements

Cyclic voltammetry measurements for the samples of PES-PPy/AQSA were performed in different pH solutions to test the electroactivity of the conducting fabrics. The measurements were also made at different scan rates to see the influence of this parameter on the electrochemical response. To compare the electrochemical response, in all the figures it is shown the second scan.

In Fig. 6 it is compared the voltammograms obtained for the sample of PES-PPy/AQSA in 0.1 M H_2SO_4 at the different scan rates (50, 5 and 1 mV s^{-1}). It can be seen that with the higher scan rate, a resistive response was obtained and no redox peaks were observed in the voltammogram. A decrease in the scan rate to 5 mV s^{-1} caused a decrease of the current density, although an oxidation peak could be observed at 0.28 V. With the lowest scan rate (1 mV s^{-1}) an oxidation peak located at 0.14 V was observed. The form of the voltammogram obtained was similar to that obtained in bibliography for polypyrrole-based conducting fabrics [44]. Analyzing the results, it is evident that the scan rate influences the electrochemical response of conducting fabrics obtained by cyclic voltammetry. Higher scan rates (like 50 mV s^{-1}) do not allow the observation of redox processes. On the other hand, lower scan rates (1 or 5 mV s^{-1}) permit the apparition of those processes. The explanation for these facts is that the substrate (polyester) is an insulating material, so the charge transference has to be produced along polypyrrole chains. The charge transfer begins from the zone below the electric contact and extends to the other parts of the electrode. If the scan rate is too fast, there is not enough time to allow the polymer transformation and that is why a resistive response was obtained in the voltammograms. When lower scan rates are employed, there is more time to allow the transformation of the polymer so the redox processes can be observed; this is clearly observed with the lowest scan rate (1 mV s^{-1}). Cyclic voltammetry studies of conducting polymers have been made on metallic substrates mainly, where the charge transfer is produced between the metal-polymer interface instantaneously. Studies on metallic substrates employing different scan rates have demonstrated that the form of the voltammogram is not changed by the scan rate, only the peak current of the redox processes is affected [45]. If insulating substrates are employed, the charge transfer is not produced instantaneously, so the scan rate in this case is an important parameter.
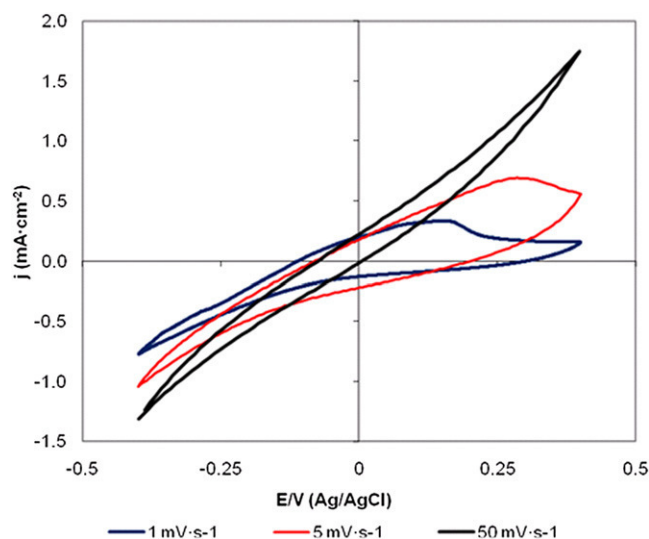
Fig. 6. Cyclic voltammograms of PES-PPy/AQSA, second scan for all measurements: a) 0.1 M H₂SO₄, 50, 5 and 1 mV s⁻¹.

In Fig. 7 it can be observed the voltammograms employing the lowest san rate (1 mV s^{-1}) in the different pH solutions. It has been employed the lowest scan rate because it produced the best electrochemical response. It can be seen that the highest electroactivity was obtained in 0.1 M H_2SO_4, protonation influences the electrochemical response of conducting polymers [38]. As it was commented previously an oxidation peak appeared at 0.14 V. In the pH 7 solution, the electroactivity of polypyrrole film was reduced and no redox peaks were observed in the voltammogram. In the pH 13 solutions it was found a greater lost of electroactivity, attributed to the deprotonation of polypyrrole that takes place at pH 10 [38]. As the pH of the solution increases, the electroactivity of the conducting textile decreases.
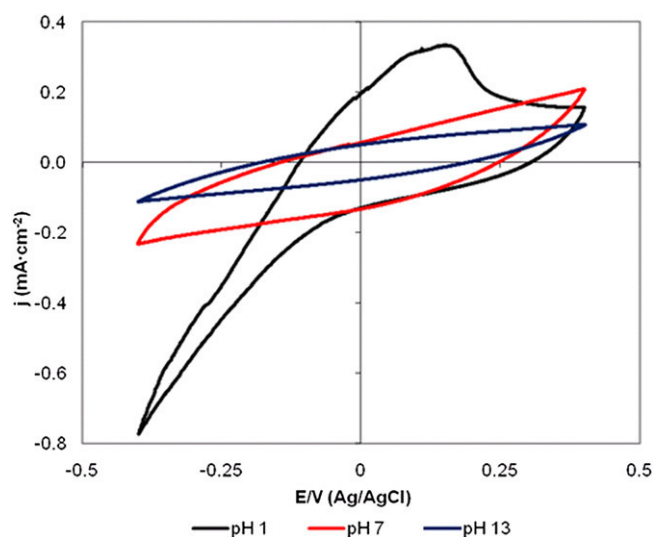
Fig. 7. Cyclic voltammograms of PES-PPy/AQSA, second scan for all measurements: 1 mV s^{-1}; pH 1, pH 7, pH 13.

3.6. Scanning electrochemical microscopy measurements

Approach (I_T–L) curves were recorded in the feedback mode in a 0.01 M solution of $Ru(NH_3)_6^{3+}$ in 0.1 M KCl, pH ~5.2, using the 100 µm diameter Pt tip held at a potential of -0.4 V vs Ag/AgCl (3 M KCl). According to the voltammogram in Fig. 8, this potential was selected to reduce the oxidized form of the mediator, $Ru(NH_3)_6^{3+}$, at a diffusion-controlled rate.

Approach curves give an indication of the electroactivity of the electrode surface. If the surface is non conductive, when the electrode approaches the surface there is a decrease of the current measured (negative feedback) [29]. On the other hand, if the electrode is conductive, when the electrode approaches the surface of the substrate the current increases (positive feedback) [29]. The samples selected for the SECM measurements were the sample after pH 1 treatment (lower surface resistivity and higher $N^{\delta+}/N$ and S/N ratios) and the sample after the basic treatment (higher surface resistivity and lower $N^{\delta+}/N$ and S/N ratios). PES samples were also measured to obtain the response of the substrate material without the conducting polymer layer.
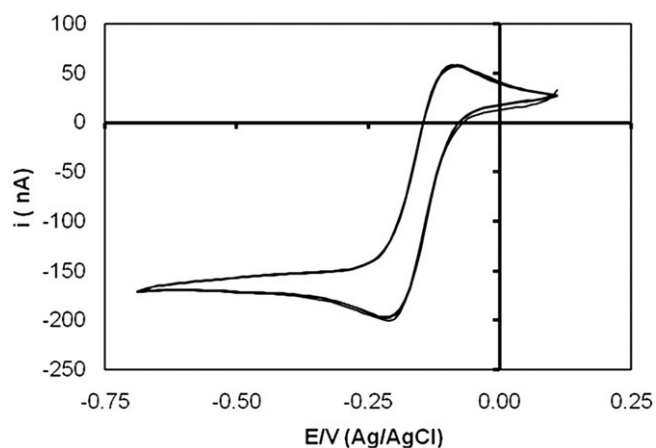
Fig. 8. Cyclic voltammograms for Pt UME 100 µm diameter tip. The UME potential was scanned from +100 to -700 mV (vs Ag/AgCl) in a 0.01 M Ru(NH$_3$)$_6^{3+}$ and 0.1 M KCl at 50 mV s^{-1}.

Figure 9-a shows a selection of the experimental curves recorded at different points randomly chosen throughout the PES-PPy/AQSA treated during 1 h in 0.1 M H$_2$SO$_4$ solution. The line scans show different degrees of positive feedback, ranging among 3-5. The positive feedback indicates an increase of the normalized current (I) when the microelectrode comes close to the surface, according to its conductive nature; (I=i/i$_\infty$ where i$_\infty$=4nFDaC in which n is the number of electrons involved in the reaction, F is the Faraday constant, D is the diffusion coefficient, and a is the radius of the UME). On the other hand, for the sample containing only polyester, negative feedback was obtained (I decreases with the normalized distance L=d/a in which d is the distance between UME and surface). Polyester is an insulating material and negative feedback was obtained. With this technique it is clearly shown the different electrochemical activity and conductivity of the two surfaces analyzed.

In Fig. 9-b, it is shown the electrochemical activity of PES-PPy/AQSA after 1 h of contact with the pH 13 solution. It can be seen a slight decrease of the degree of positive feedback; after the treatment with the pH 13 solution the values obtained were among 1.5-3. There has been a decrease of the material electroactivity due to the deprotonation of polypyrrole that takes place at pH 10 [38]. However the conducting fabric continues acting as a conducting material. These results are consistent with EIS measurements that showed that the material continued acting as a conductor.
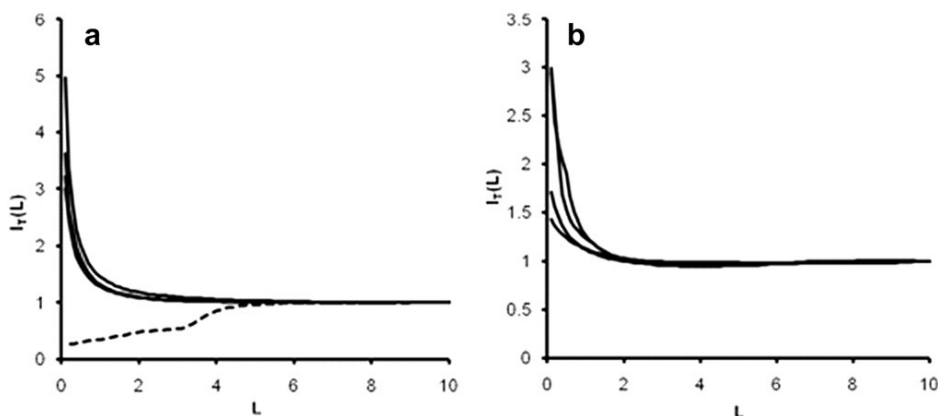
Fig. 9. Approaching curves for: a) PES (---), PES-PPy/AQSA + 1 h pH 1 (—) and b) PES-PPy/AQSA + 1 h pH 13 (—); obtained with a 100 μm diameter Pt tip in 0.01 M Ru(NH$_3$)$_6^{3+}$ and 0.1 M KCl. The tip potential was -400 mV (vs Ag/AgCl) and the approach rate was 10 μm s^{-1}.

One main application of the SECM microscopy is the scanning of a surface to obtain 2D and 3D images of the electrochemical activity or topographical information [29]. In this work, the experiments were done at constant height, so the information of electroactivity and morphology cannot be separated. The PES fabric topography presents significant differences (zones more elevated than others) and the polypyrrole coating obtained on the fabric was uniform, so topographical features of the fabric have more influence on the electrochemical response obtained than local differences of electroactivity. As example of this application, the 2D and 3D images of a PES-PPy/AQSA substrate are shown. In Fig. 10, it is shown the 2D and 3D images of a conductive PES-PPy/AQSA substrate taken at a constant height of 100 μm.

In the 2D image, a SEM micrograph of the substrate surface has been superposed to illustrate the topographical influence on the response obtained. The more raised parts of the textile produce a higher increase of the current than the lower ones. The 3D image exemplifies better the influence of the textile topography on the electrochemical response obtained. The holes represent an increase of the current due to a major proximity of the substrate surface to the UME.
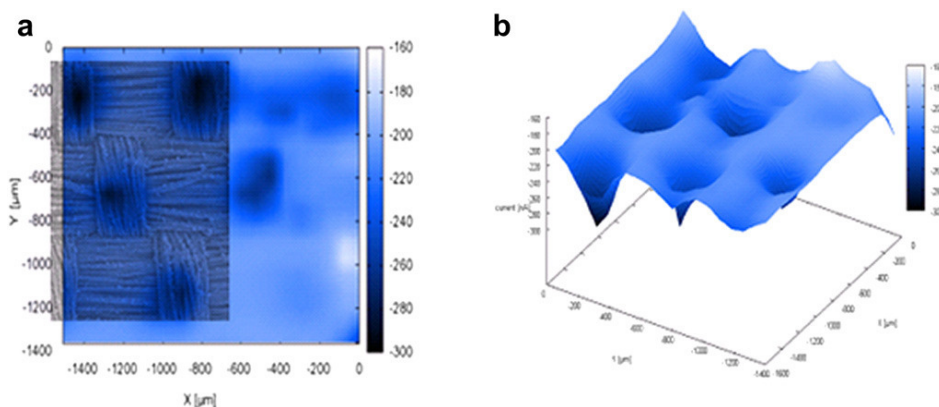
Fig. 10. 2D (SEM micrograph superposed) and 3D constant height SECM images of a PES-PPy/AQSA, 0.25 cm^2 geometrical area. These images were taken with a 100 μm diameter Pt tip, in 0.01 M Ru(NH$_3$)$_6$$^{3+}$ and 0.1 M KCl at a constant height of 100 μm. The scan rate was 200 μm s^{-1} in comb mode; lengths of x and y lines were 1600 x 1400 μm with increments of 75 μm.

4. Conclusions

The stability of conducting fabrics of PES-PPy/AQSA has been tested in a wide range of pH (1, 7, 13) and after washing tests. The treatment with higher pHs causes a decrease of the doping level (N$^{\delta+}$/N) as well as the release of part of the counter ions from the polymer matrix (the ratio S/N was measured as an indication of the counter ion content). Both phenomena cause an increase in the surface resistivity of the fabric. The polymer layer was stable in acid and neutral solutions since significant changes in doping level, counter ion content and surface resistivity were not observed. The less favorable conditions were basic media, where a 40 % of the counter ion was lost due to the drop in the doping level. In spite of an increase of two orders in the surface resistivity, the conducting fabric continued acting as a resistor (conducting material). The sample after the washing test, showed the same doping level (N$^{\delta+}$/N) than the original sample and the loss of part of the counter ions; although the surface resistivity was not substantially changed.

CV measurements showed the influence of the scan rate in the characterization of conducting fabrics. Lower scan rates produced the appearance of the redox processes. A gradual loss of electroactivity in the different measuring solutions was also obtained when the pH was increased. Approach curves obtained by SECM showed that PPy/AQSA conducting fabrics were electroactive. Only the treatment with the pH 13

solution produced a slight decrease of the electroactivity. That loss of electroactivity can be related to the lower doping level ($N^{\delta+}$/N) and the loss of part of the counter ions that were measured by XPS analysis after exposure to the pH 13 solution. More work is in progress to evaluate the electroactivity of these coatings towards organic molecules degradation.

Acknowledgements

References

[1] Lekpittaya P, Yanumet N, Grady BP, O'Rear EA. Resistivity of conductive polymer-coated fabric. J Appl Polym Sci 2004;92(4):2629-2636.

[2] Kincal D, Kumar A, Child A, Reynolds J. Conductivity switching in polypyrrole-coated textile fabrics as gas sensors. Synth Met 1998;92(1):53-56.

[3] Wu J, Zhou D, Too CO, Wallace GG. Conducting polymer coated lycra. Synth Met 2005;155(3):698-701.

[4] Wha K, Jin H, Hun S. Stretchable conductive fabric for electrotherapy. J Appl Polym Sci 2003;88(5):1225-1229.

[5] Hun S, Wha K, Hyon J. Electrochemically synthesized polypyrrole and Cu-plated nylon/spandex for electrotherapeutic pad electrode. J Appl Polym Sci 2004;91(6):4064-4071.

[6] Bhat NV, Seshadri DT, Nate MN, Gore AV. Development of conductive cotton fabrics for heating devices. J Appl Polym Sci 2006;102(5):4690-4695.

[7] Hakansson E, Kaynak A, Lin T, Nahavandi S, Jones T, Hu E. Characterization of conducting polymer coated synthetic fabrics for heat generation. Synth Met 2004;144(1):21-28.

[8] Boutrois JP, Jolly R, Pétrescu C. Process of polypyrrole deposit on textile. Product characteristics and applications. Synth Met 1997;85(1-3):1405-1406.

[9] Kuhn H, Child A, Kimbrell W. Toward real applications of conductive polymers. Synth Met 1995;71(1-3):2139-2142.

[10] Akbarov D, Baymuratov B, Westbroek P, Akbarov R, Declerck K, Kiekens P. Development of electroconductive polyacrylonitrile fibers through chemical metallization and galvanisation. J Appl Electrochem 2006;36(4):411-418.

[11] Lin T, Wang L, Wang X, Kaynak A. Polymerising pyrrole on polyester textiles and controlling the conductivity through coating thickness. Thin Solid Films 2005;479(1-2):77-82.

[12] Ferrero F, Napoli L, Tonin C, Varesano A. Pyrrole chemical polymerization on textiles: Kinetics and operating conditions. J Appl Polym Sci 2006;102(5):4121-4126.

[13] Garg S, Hurren C, Kaynak A. Improvement of adhesion of conductive polypyrrole coating on wool and polyester fabrics using atmospheric plasma treatment. Synth Met 2007;157(1):41-47.

[14] Molina J, del Río AI, Bonastre J, Cases F. Chemical and electrochemical polymerization of pyrrole on polyester textiles in presence of phosphotungstic acid. Eur Polym J 2008;44(7):2087-2098.

[15] Lee HS, Hong J. Chemical synthesis and characterization of polypyrrole coated on porous membranes and its electrochemical stability. Synth Met 2000;113(1-2):115-119.

[16] Gasana E, Westbroek P, Hakuzimana J, De Clerck K, Priniotakis G, Kiekens P, Tseles D. Electroconductive textile structures through electroless deposition of polypyrrole and copper at polyaramide surfaces. Surf Coat Tech 2006;201(6):3547-3551.

[17] Dall'Acqua L, Tonin C, Varesano A, Canetti M, Porzio W, Catellani M. Vapour phase polymerisation of pyrrole on cellulose-based textile substrates. Synth Met 2006;156(5-6):379-386.

[18] Dall'Acqua L, Tonin C, Peila R, Ferrero F, Catellani M. Performances and properties of intrinsic conductive cellulose–polypyrrole textiles. Synth Met 2004;146(2):213-221.

[19] Neoh KG, Young TT, Kang ET, Tan KL. Structural and mechanical degradation of polypyrrole films due to the aqueous media and heat treatment and the subsequent redoping characteristics. J Appl Polym Sci 1997;64(3):519-526.

[20] Bouzek K, Mangold K-M, Jüttner K. Electrocatalytic activity of platinum modified polypyrrole films for the methanol oxidation reaction. J Appl Electrochem 2001;31(5):501-507.

[21] Li L, Zhang Y, Drillet J-F, Dittmeyer R, Jüttner K-M. Preparation and characterization of Pt direct deposition on polypyrrole modified Nafion composite membranes for direct methanol fuel cell applications. Chem Eng J 2007;133(1-3):113-119.

[22] Rodríguez FJ, Gutiérrez S, Ibanez JS, Bravo JL, Batina N. The efficiency of toxic chromate reduction by a conducting polymer (polypyrrole): influence of electropolymerization conditions. Environ Sci Technol 2000;34(10):2018-2023.

[23] Tian Y, Wang J, Wang Z, Wang S. Electroreduction of nitrite at an electrode modified with polypyrrole nanowires. Synth Met 2004;143(3):309-313.

[24] Lopes A, Martins S, Moraö A, Magrinho M, Gonçalves I. Degradation of a textile dye C. I. Direct Red 80 by electrochemical processes. Port Electrochim Acta 2004;22(3):279-294.

[25] Gemeay AH, El-Sharkawy RG, Mansour IA, Zaki AB. Catalytic activity of polyaniline/MnO$_2$ composites towards the oxidative decoloriaztion of organic dyes. Appl Catal B-Environ 2008;80(1-2):106-115.

[26] Gemeay AH, El-Sharkawy RG, Mansour IA, Zaki AB. Preparation and characterization of polyaniline/manganese dioxide composites and their catalytic activity. J Colloid Interf Sci 2007;308(2):385-394.

[27] Varesano A, Dall'Acqua L, Tonin C. A study on the electrical conductivity decay of polypyrrole coated wool textiles. Polym Degrad Stabil 2005;89(1):125-132.

[28] Wu J, Zhou D, Looney MG, Waters PJ, Wallace GG, Too CO. A molecular template approach to integration of polyaniline into textiles. Synth Met 2009;159(12):1135-1140.

[29] Sun P, Laforge FO, Mirkin MV. Scanning electrochemical microscopy in the 21st century. Phys Chem Chem Phys 2007;9(7):802-823.

[30] Mirkin MV, Horrocks BR. Electroanalytical measurements using the scanning electrochemical microscope. Anal Chim Acta 2000;406(2):119-146.

[31] Barker AL, Gonsalves M, Macpherson JV, Slevin CJ, Unwin PR. Scanning electrochemical microscopy: beyond the solid/liquid interface. Anal Chim Acta 1999;385(1-3):223-240.

[32] Complete textile glossary, available from: http://www.celaneseacetate.com/textile_glossary_filament_acetate.pdf, 2001. Last accessed 15th June 2010.

[33] Rajagopalan R, Iroh JO. Characterization of polyaniline-polypyrrole composite coatings on low carbon steel: a XPS and infrared spectroscopy study. Appl Surf Sci 2003;218(1-4):58-69.

[34] Sabbatini L, Malitesta C, De Giglio E, Losito I, Torsi L, Zambonin PG. Electrosynthesised thin polymer films: the role of XPS in the design of application oriented innovative materials. J Electron Spectrosc Relat Phenom 1999;100(1-3):35-53.

[35] Carquigny S, Segut O, Lakard B, Lallemand F, Fievet P. Effect of electrolyte solvent on the morphology of polypyrrole films: Application to the use of polypyrrole in pH sensors. Synth Met 2008;158(11):453-461.

[36] Prissanaroon-Ouajai W, Pigram PJ, Jones R, Sirivat A. A novel pH sensor based on hydroquinone monosulfonate-doped conducting polypyrrole. Sensor Actuat B-Chem 2008;135(1):366-374.

[37] Neoh KG, Young TT, Looi NT, Kang ET, Tan KL. Oxidation-Reduction interactions between electroactive polymer thin films and Au(III) ions in acid solutions. Chem Mater 1997;9(12):2906-2912.

[38] Krzysztof M. Chemical reactivity of polypyrrole and its relevance to polypyrrole based electrochemical sensors. Electroanal 2006;18(16):1537-1551.

[39] Jousseaume V, Morsli M, Bonnet A. XPS Study of Aged Polyaniline Films. J Appl Polym Sci 2003;90(13):3730–3736.

[40] Neoh KG, Lau KKS, Wong VVT, Kang ET. Structure and degradation behavior of polypyrrole doped with sulfonate anions of different sizes subjected to undoping-redoping cycles. Chem Mater 1996;8(1):167-172.

[41] Li Y, Ouyang J, Yang J. Two doping structures and structural anisotropy revealed by the mass loss and shrinkage of polypyrrole films on alkali treatment. Synth Met 1995;74(1):49-53.

[42] Spectral database for organic compounds of the National Institute of Advanced Industrial Science and Technology (AIST). Available from: http://riodb01.ibase.aist.go.jp/sdbs/cgi-bin/cre_index.cgi?lang=eng, 2001. Last accessed 15th June 2010.

[43] Higo M, Miake T, Mitsushio M, Yoshidome T, Ozono Y. Adsorption state and morphology of anthraquinone-2-carboxylic acid deposited from solution onto the atomically-smooth native oxide surface of Al(111) films studied by infrared reflection absorption spectroscopy, X-ray photoelectron spectroscopy, and atomic force microscopy. Anal Sci 2008:24(3):313-320.

[44] Babu KF, Senthilkumar R, Noel M, Kulandainathan MA. Polypyrrole microstructure deposited by chemical and electrochemical methods on cotton fabrics. Synth Met 2009;159(13):1353-1358.

[45] Bhadani SN, Gupta MK, Sen Gupta SK. Cyclic voltammetry and conductivity investigations of polyaniline. J Appl Polym Sci 1993;49(3):397-403.

10.- ARTÍCULO

MONITORING THE POLYMERIZATION PROCESS OF POLYPYRROLE BY THERMOGRAVIMETRIC AND X-RAY ANALYSIS
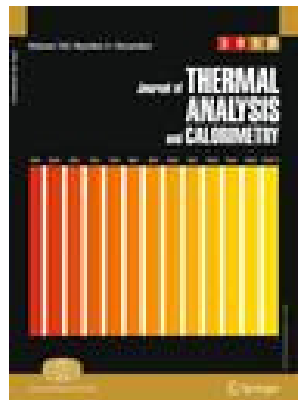
Monitoring the polymerization process of polypyrrole films by thermogravimetric and X-ray analysis

J. López[1], F. Parres[1], I. Rico[1], J. Molina[2], J. Bonastre[2], F. Cases[2]

[1]*Instituto de Tecnología de Materiales, Universidad Politécnica de Valencia, Plaza Ferrándiz y Carbonell s/n, 03801 Alcoy, Alicante, Spain*

[2]*Departamento de Ingeniería Textil y Papelera, Universidad Politécnica de Valencia, Plaza Ferrandiz y Carbonell s/n, 03801 Alcoy, Alicante, Spain*

Abstract

The thermal behavior of different synthesized polypyrrole (Ppy) composites was studied in order to obtain quantitative information about the synthesis process and qualitative information about thermal stability of composites. An inorganic anion has been used as dopant ($PW_{12}O_{40}^{3-}$), and this has allowed obtaining a complete analysis of Ppy degradation process, since this anion does not degrade in the range of temperature used. In order to validate the quantitative information obtained by thermogravimetric analysis (TG), the work was completed with X-ray photoelectron spectroscopy (XPS) study, since the use of the N^+/N or W/N ratios are useful to measure the doping level reached by the synthesis process. Also pyrolysis/gas chromatography/mass spectrometry (py-GC-MS) and differential scanning calorimetry (DSC) were used to obtain information of the products generated as a conse- quence of the degradation process. FTIR-ATR has been used to characterize Ppy powders.

Keywords: Polypyrrole, Thermal stability, XPS, Pyrolysis, GC-MS

---

* Corresponding author. E-mail address: jlopezm@mcm.upv.es (Prof. J. López)

Introduction

Among the wide variety of electroconductive polymers, polypyrrole (Ppy) and its derivatives show a relevant interest due to their good electrical properties. It is feasible to obtain films and powders by means of several synthesis routes, thus obtaining invariably a black material which solubility is limited depending on the dopant and solvent employed. In the synthesis process, a cross-linking occurs so that the synthesized material becomes a thermoset and this fact makes processing difficult. The introduction of bulky anions reduces molecular interactions between polymer chains, and facilities Ppy solubility [1].

In addition to this, one of the main problems that present the use of conductive polymers in technical applications is their thermal stability which is related to their thermal conductivity. It has been reported the influence of the thermal degradation of Ppy on its electrical conductivity [2-4]; the thermal treatments conducted in inert or air atmosphere can produce a decrease in its conductivity. So the improvement of thermal stability will have a positive effect on the long-term stability of conductivity.

Thermal methods of analysis, mainly thermogravimetry (TG), are probably the most widely used to investigate thermal degradation and polymer composition. The information available consists of the number of stages of degradation and a quantitative measurement of the mass loss for each stage. The major weakness of TG as a tool for studying polymer degradation is that it provides no information about the degradation products, thus making necessary the use of alternatives-complementary techniques. In the case of Ppy, little published studies can be found. Some studies have focused on the use of this technique for Ppy characterization [5-7]. These studies indicate that the thermal decomposition of Ppy occurs in several steps, but their definition highly depends on the test conditions and the nature of the dopant. During the synthesis of Ppy, some positive charges are generated in the structure; these positive charges must be compensated by a counter ion (also named dopant) to maintain the principle of electroneutrality. These negative charges are supplied by an anion. Organic dopants have been traditionally used, as reported in bibliography, but they present some disadvantages because their degradation can interfere with Ppy signal [8], thus difficult the interpretation of results. In this study it has been used a dopant with inorganic nature ($PW_{12}O_{40}^{3-}$) that does not decompose in the range of Ppy degradation, and this allows the analysis of Ppy without interferences of the dopant degradation.

In order to validate the quantitative information obtained by thermogravimetry (TG) additional study with X-ray photoelectron spectroscopy (XPS) has been carried out,

since the N^+/N or W/N ratios are directly related to the doping level reached in the synthesis process. Also pyrolysis-gas chromatography-mass spectrometry (py-GC-MS) techniques and differential scanning calorimetry (DSC) have been used to obtain information about the species generated in the degradation process. FTIR has been used to characterize the material obtained in the chemical synthesis.

Experimental

Reagents

Analytical grade pyrrole, ferric chloride, anthraquinone sulfonic acid (AQSA) sodium salt were purchased from Merck. Analytical grade phosphotungstic acid hydrate was supplied by Fluka. Ultrapure water was obtained from an Elix 3 Millipore-Milli-Q RG system with a resistivity near to 18.2 MΩ cm.

Chemical synthesis of Ppy/$PW_{12}O_{40}^{3-}$ and Ppy/AQSA

Pyrrole concentrations employed in chemical polymerizations were 0.5 or 2 g l^{-1}. The molar relations used in the chemical synthesis bath were pyrrole:$FeCl_3$:AQSA (1:2.5:0.6); when $PW_{12}O_{40}^{3-}$ was employed as counter ion the relation was 1:2.5:0.2. The molar relation of counter ion is three times lower when $PW_{12}O_{40}^{3-}$ is employed than when AQSA is used, due to the fact that $PW_{12}O_{40}^{3-}$ has three negative charges; on the other hand AQSA only posses one negative charge. Pyrrole and counter ion are mixed in a solution. When $FeCl_3$ is added the oxidation of pyrrole to Ppy occurs and AQSA or $PW_{12}O_{40}^{3-}$ are incorporated in the Ppy structure as counter ions. Reaction elapsed during 150 min without stirring in a precipitates beaker. In the synthesis two parameters were varied; reaction temperature and pyrrole concentration. In some experiments there was an ice bath to lower the reaction temperature and the other experiments were done at 293-296 K. Two different concentrations of pyrrole were employed (0.5 and 2 g l^{-1}). Experimental conditions for the different samples can be observed in the Table 1. After the reaction, Ppy powders were filtered and dried in a desiccator during at least 24 h before measurements. Polymerization yield has been calculated, taking into account the average doping level obtained by the different techniques (0.2). Table 1 shows experimental conditions for the synthesis of different samples of Ppy.

Experiment	Dopant	Temperature/K	Pyrrole/g l^{-1}	Polymerization yield/%
P1	AQSA	273	2	–
P2	$PW_{12}O_{40}^{3-}$	273	2	90
P3	$PW_{12}O_{40}^{3-}$	273	0.5	64
P4	$PW_{12}O_{40}^{3-}$	293–296	2	82

Table 1. Experimental conditions for the synthesis of different samples of polypyrrole.

Thermal degradation characterization

Thermogravimetric measurements were performed using a Mettler-Toledo TGA-SDTA 851e instrument, which allows heating rates from 274 to 473 K min^{-1} up to a temperature of 1473 K. Dynamic tests were run from 303 to 1173 K at 293 K min^{-1} heating rate. TG tests were performed in alumina crucibles where samples were placed without any previous treatment and experiments were run immediately. TG tests were carried out in nitrogen and air environment using a flow rate 200 mL min^{-1}.

The calorimetric analysis was carried out using a DSC Mettler-Toledo 821 (Mettler-Toledo Inc, Schwerzenbach, Switzerland). Samples of mass between 8 and 9 mg were used.

All samples were pyrolyzed with the use of a pyrolyzator (Pyroprobe® 1000 by CDS Analytical, Inc), interconnected with a GC/MS (6890N Agilent Technologies) equipped with a 5973N mass selective detector (MSD) (Agilent Technologies España S.L., Madrid, Spain). A 30 m long capillary column (HP-5 ms) 0.25 mm thickness, with a 0.25 µm stationary phase, which was programmed from 313 to 573 K at 283 K min^{-1} and was subsequently maintained at the highest temperature for 5 min. The gas used was Helium with a 50:1 split ratio. The MSD was programmed to detect masses between 50 and 650 amu. Samples (around 1.2-1.1 mg) were pyrolyzed at 723 K for 10 s.

Spectroscopic characterization

Fourier transform infrared spectroscopy with horizontal multirebound attenuated total reflection (FTIR-ATR) was performed with a Nicolet Magna 550 Spectrometer equipped with DTGS detector. An accessory with pressure control was employed to equalize pressure in the different solid samples. A prism of ZnSe was employed. Spectra were collected with a resolution of 4 cm^{-1}, and 100 scans were averaged for each sample.

X-ray photoelectron spectroscopy analyses were conducted at a base pressure of at $5 \cdot 10^{-10}$ mbars and a temperature at around 173 K. The XPS spectra were obtained with a VG-Microtech Multilab electron spectrometer by using unmonochromatized Mg Kα (1253.6 eV) radiation from a twin anode source operated at 300 W (20 mA, 15 kV). The binding energy (BE) scale was calibrated with reference to the C1s line at 284.6 eV.

Results and discussion

FTIR-ATR analysis

Figure 1 shows the spectra of Ppy/AQSA and Ppy/$PW_{12}O_{40}^{3-}$ powders. It can be observed that different bands attributed to Ppy in both spectrums. One band centered at 1550 cm^{-1} associated to the pyrrole ring stretching vibration (C=C), C-C stretching (1450 cm^{-1}) [6, 7], and C-N stretching (1300 cm^{-1}) [9, 10]. The characteristic bands of the bending vibration of pyrrole can be observed at 1160, 1030, and 775 cm^{-1} [11, 12]. Additionally, other bands can be observed, like C-H in plane vibration (1090 cm^{-1}), C-H bending vibrations (960 cm^{-1}) [13], and =C-H out of phase vibration (890 cm^{-1}); the last band is not clearly observed in Ppy/AQSA spectrum.
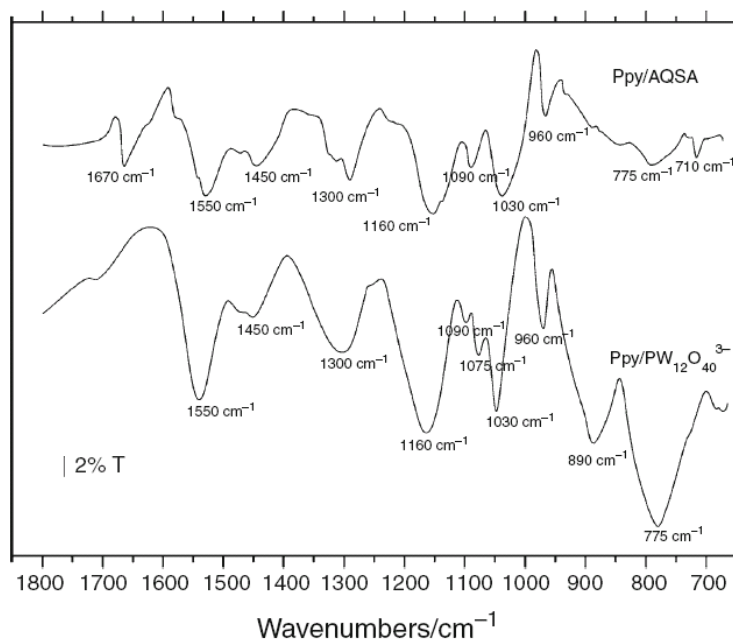

Fig. 1. Spectra of Ppy/AQSA and Ppy/$PW_{12}O_{40}^{3-}$ powders.

Additionally to these bands it can be observed that the bands attributed to the counter ion. The band in the spectrum of Ppy/PW$_{12}$O$_{40}$$^{3-}$ at 1075 cm^{-1} (P-O stretching) [14,15] indicates the presence of the PW$_{12}$O$_{40}$$^{3-}$. The other bands of PW$_{12}O_{40}$$^{3-}$ are overlapped with those of Ppy. In the spectrum of Ppy/AQSA two bands centered at 1670 and 710 cm^{-1} were observed, attributed to the AQSA structure (Fig. 1).

Quantitative analysis

TG analysis

We have combined thermogravimetric (TG) and differential thermal analysis (DTG) to determine the thermal stability of the polymer. For a correct analysis, it is necessary to consider the influence of dopant used in the synthesis process. Its nature can interfere with the interpretation of the results; if the dopant is organic, generally the mass loss will overlap the mass loss of Ppy, making difficult the analysis of results due to the two overlapped processes. The insertion of inorganic dopants in the structure of Ppy allows a more complete analysis by determining the mass loss ranges and degradation kinetic parameters [16]. In order to avoid this problem we have worked with an inorganic dopant (PW$_{12}$O$_{40}$$^{3-}$), since this compound shows higher thermal stability; this fact allows obtaining both qualitative and quantitative information about the degradation process.

In oxidizing atmosphere as well as in inert atmosphere, the PW$_{12}$O$_{40}$$^{3-}$ shows a great range of thermal stability up to 1173 K; we can only observe a mass loss at about 473 K which represents a 3 wt% loss; this is probably due to the loss of hydration water of polyoxometalate (Fig. 2a). This behavior cannot be expected when using an organic dopant, as it is observed in the Fig. 2b AQSA degrades in the same temperature range that most polymers (Table 2).

This wide range of thermal stability allows a quantitative determination of Ppy and to obtain the main decomposition kinetic parameters of samples in different atmospheres. Independently of the atmosphere employed, the degradation passes in two steps. The first step begins at the 473-573 K range (Fig. 3), and it represents a small proportion of the total polymer mass loss when using an inert atmosphere. In this type of atmosphere the principal mass loss starts at about 773 K. In an oxidizing atmosphere the situation is inverted, so that the first jump acquires major relevance, though it begins at similar temperatures.
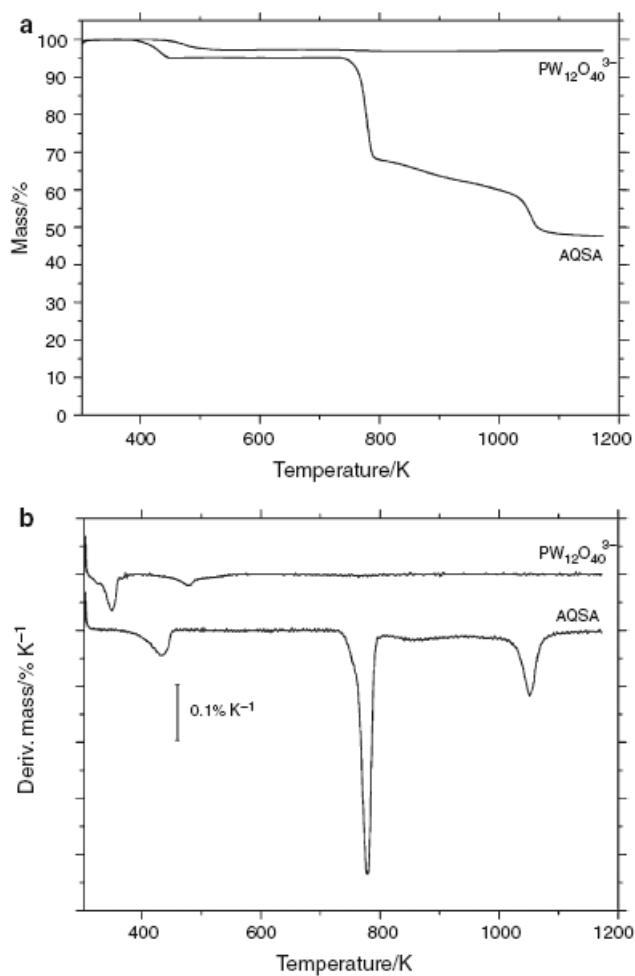
Fig. 2. Thermogravimetric analysis of $PW_{12}O_{40}^{3-}$ and AQSA. Relative mass loss derivate (N_2 atmosphere).

Sample	N$_2$ atmosphere				Air atmosphere			
	Mass loss/%				Mass loss/%			
	573–773 K	773–1173 K	Total	Doping level	573–773 K	773–1173 K	Total	Doping level
P2	2.8	29.3	32.1	0.218	15.2	14.2	29.4	0.238
P3	3.4	29.7	33.1	0.211	17.4	16.19	33.6	0.208
P4	2.0	28.2	30.2	0.231	18.8	13.94	32.7	0.214
Average			31.8	0.220			31.9	0.220

Table 2. Values of weight loss and doping level for the different samples.

Quantitatively, the sum of mass loss for both jumps is identical in both atmospheres and the differences between different samples are very small; in addition to this, changes in the synthesis conditions do not seem to alter the content of Ppy in a significant way.
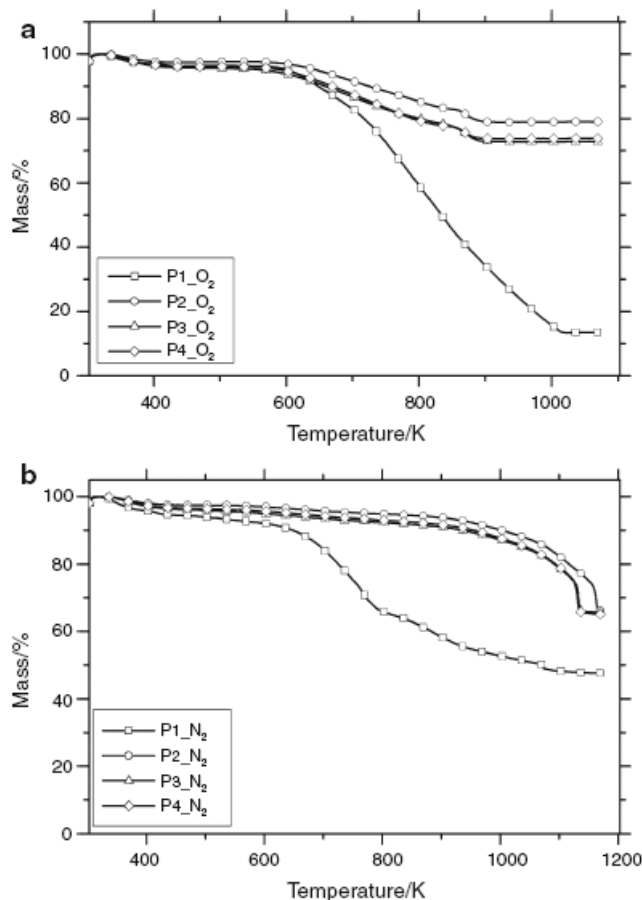

Fig. 3. Comparative curves of polypyrrole doped with $PW_{12}O_{40}^{3-}$ in air and N^2 atmosphere.

In general we can observe that the beginning of the decomposition is in good agreement with other studies described previously [17], but in this case due to the inorganic nature of the dopant we do not have interferences and we can ensure that the observed mass loss is due to polymeric film, and not the dopant.

From the mass percentage of Ppy obtained experimentally by TG and using the molecular mass of the pyrrole (65.09) (considering that in the polymerization process 2 H^+ are removed) and $PW_{12}O_{40}^{3-}$ (2877.17), it is possible to calculate the number of

positive charges per pyrrole molecule (doping level). The average value of the doping level obtained by means of TG is close to 0.22. The result does not depend on the atmosphere employed (air or N_2 atmosphere).

XPS analysis

To verify the validity of TG techniques, the obtained results of doping level have been contrasted with that obtained by means of XPS. It is possible to obtain some ratios from the information obtained about the powders surface composition. By using the atomic ratio W/N it is possible to determine the doping level. Using this ratio, obtained by XPS, the doping level is about 0.16, which is a bit lower than the value obtained by means of TG; this is probably due to the XPS experimental error. It is not possible to calculate the atomic ratio P/N, since the limit of detection of this technique does not allow detecting the presence of P in the sample, since it appears in a small concentration.

In Fig. 4 it is possible to observe the high resolution XPS spectrum of N1s, which can be easily deconvoluted in two peaks. The peak located at 399.7 eV corresponds to amine (-NH)-type groups in the film [18] while the peak located at 401.7 eV can be assigned to protonated amines (N^+) [19]. So it is possible to calculate the percentage of pyrrole rings with positive charges and the total pyrrole rings thus obtaining the N^+/N ratio, which has a value of 0.19. This value is in more agreement with the value obtained by means of TG.

In Fig. 5 it is possible to observe the high resolution XPS spectrum of W4f. The BEs of 35.1 and 37.2 eV correspond to the atomic environment of the W4f, consisting in a coupling spin-orbit doublet (W4f7/2 and W4f5/2). The lowest BE corresponds to the contribution W4f7/2, and the highest is related to the contribution W4f5/2. Both contributions are due to an oxidation state W^{+6} [21,22].

The obtained results confirm that it is possible to use thermogravimetry as a quantitative technique; on the one hand the results are coincident independently of the experimental conditions used and on the other hand are similar to those obtained with XPS techniques. A summary of the results can be observed in the Table 3. The average doping level calculated by different techniques is 0.20, which indicates that of every five pyrrole molecules, one is positively charged.
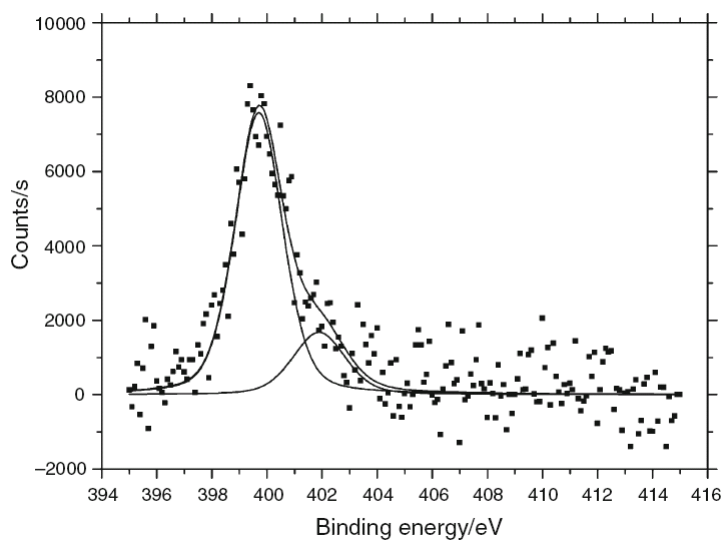
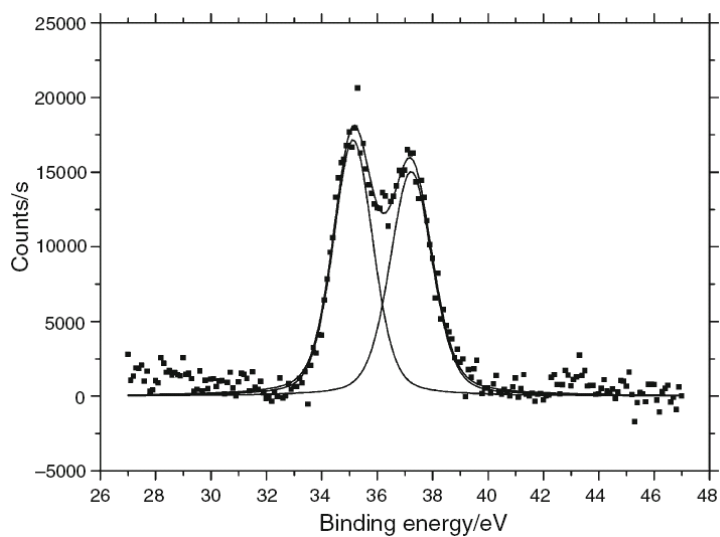*Fig. 4. High resolution XPS spectrum for N1s.*

Fig. 5. High resolution XPS spectrum for W4f.

Technique	Conditions	Doping level
Thermogravimetry	N_2 atmosphere	0.22
Thermogravimetry	Air	0.22
XPS	W/N	0.16
XPS	N^+/N	0.19
Average		0.20

Table 3. Values of doping level obtained with different methods.

Qualitative analysis

The total amount of Ppy does not depend on the testing method. When inert atmosphere is used, the degradation below 873 K concerns only a very small percentage of polymer, whereas in air atmosphere the degradation concerns the totality of the polymer. This fact is clearly observed when using DTG and DSC (Fig. 6), where the signal below 873 K is very low in nitrogen atmosphere, but very significant in air atmosphere. When using inert atmosphere, the first jump would concern some Ppy chains poorly cross-linked to the three-dimensional network that forms the material.
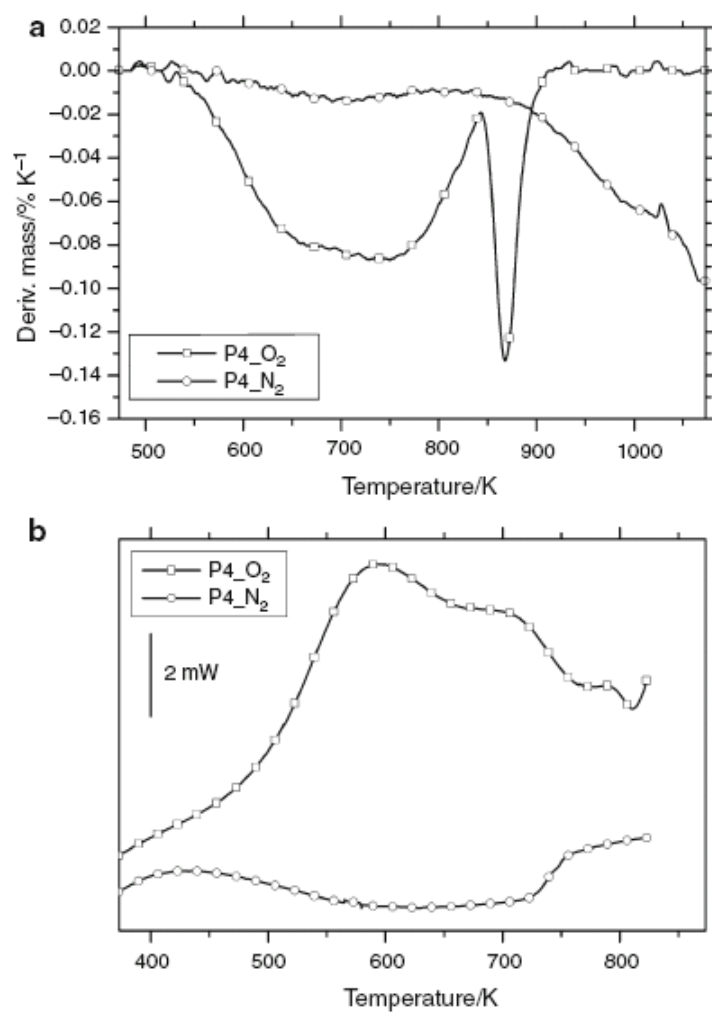
Fig. 6 DTG and DSC comparative of the sample 4 in N_2 and air atmosphere.

The Py-GMC analysis by means of direct insertion in atmosphere produces a very weak signal at 873 K (Fig. 7) where only the presence of the monomer is detected, $m/z = 67$, and the dimer and trimer have no significant presence in the totality of the analyzed samples (Fig. 7). This can be due to the fact that part of the monomer has not been oxidized by the $FeCl_3$ and has been retained inside the structure of the polymer.
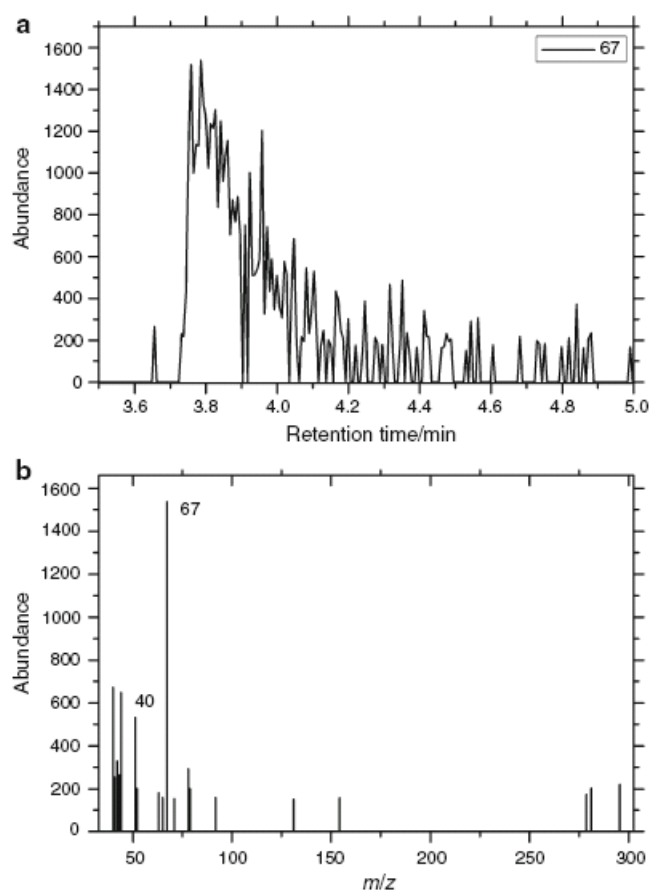
Fig. 7. Py-GC-MS spectrum of sample 4.

When heating the material by TG, the evaporation of the pyrrole takes place, and therefore, it is removed from the structure. The m/z ratio is 67, so this peak corresponds to the pyrrole ring that has not lost both protons in the polymerization reaction; consequently they are monomer units that have not reacted in the synthesis process. Furthermore, the use of an inorganic dopant avoids the formation of some species related to dopant-Ppy interactions [20, 21].If we compare samples when the synthesis temperature is varied (P2 and P4), we can observe that the sample synthesized at lower temperature (P2) is more stable than that synthesized at high temperature (P4) (Fig. 8). As the synthesis temperature increases, the reactions occur more quickly and some non-polymerized pyrrole molecules can remain as monomer in

the polymer structure. Regarding the synthesis method for P2, the loss of volatiles does not begin until 523 K, whereas in sample P4 the degradation begins at about 473 K.
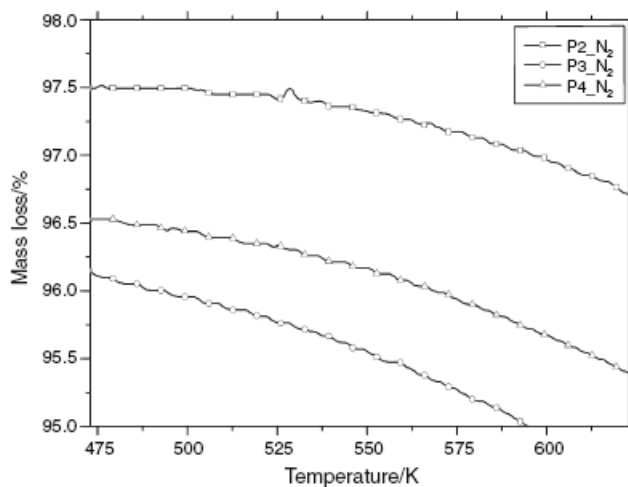

Fig. 8. Magnified comparative curves of polypyrrole doped with $PW_{12}O_{40}^{3-}$ in N_2 atmosphere in the zone 473-623 K.

If we compare samples at pyrrole concentrations (P2 and P3) we can observe that samples with higher pyrrole concentration (P2, 2 g l^{-1}) are more stable than that with lower pyrrole concentration (P3, 0.5 g l^{-1}) (Fig. 8). This can be explained if we take into account that low reactive concentrations lead to a slow a reaction since the diffusion is difficult. Pyrrole monomer oxidation is more difficult since some of these monomers could be trapped by the Ppy structure.

So we can conclude that to obtain the most stable material, the synthesis process must be carried out in an ice bath and high pyrrole concentration (2 g l^{-1}). The polymerization yield of the synthesis reaction follows similar trend (Table 1). Low temperatures and high pyrrole con- centration lead to high polymerization yield and then the probability of incorporation of non-oxidized pyrrole molecules decrease. This is in agreement with the obtained results with TG analysis. Polymers showing higher polymerization yield are more stable in the temperature range 473-523 K since they posses lower amounts of non-polymerized pyrrole.

Conclusions

The use of an inorganic anion $PW_{12}O_{40}^{3-}$ as dopant in the synthesis of Ppy has allowed us to obtain qualitative and quantitative information about the thermal behavior of the synthesized polymer. From a quantitative point of view we can determine the doping level by means of TG with identical results for both inert and oxidizing atmosphere. The comparison with other techniques such as XPS is satisfactory, and indicates that the doping level of the synthesized polymers is near to 0.2.

Qualitatively, the analysis in inert atmosphere indicates that Ppy degradation of Ppy starts at relatively low temperatures (473-523 K), concerning a small percentage of the synthesized material, being the pyrrole monomer the only significant degradation product. Lower temperature during polymer synthesis (273 K) and higher pyrrole concentrations (2 g l^{-1}) lead a higher stable polymer (the degradation of the polymer starts at 523 K) in comparison to synthesis process carried out at room temperature or low pyrrole concentration (0.5 g l^{-1}) (polymer degradation starts at 473 K).

References

1. Lee JY, Kim DY, Kim CY. Synthesis of soluble polypyrrole of the doped state in organic-solvents. Synth Met. 1995;74:103-6.

2. Chehimi MM, Abdeljalil E. A study of the degradation and stability of polypyrrole by inverse gas chromatography, X-ray photoelectron spectroscopy, and conductivity measurements. Synth Met. 2004;145:15-22.

3. Migahed MD, Fahmy T, Ishra M, Barakat A. Preparation, characterization, and electrical conductivity of polypyrrole composite films. Polym Test. 2004;23:361-5.

4. Papathanassiou AN, Sakellis I, Grammatikakis J, Vitoratos E, Sakkopoulos S, Dalas E. Low frequency a.c. conductivity of fresh and thermally aged polypyrrole-polyaniline conductive blends. Synth Met. 2004;142:81-4.

5. Abthagir PS, Saraswathi R. Thermal stability of polypyrrole prepared from a ternary eutectic melt. Mater Chem Phys. 2005;92:21-6.

6. Jakab E, Meszaros E, Omastova M. Thermal decomposition of polypyrroles. J Therm Anal Calorim. 2007;88:515-21.

7. Varesano A, Tonin C, Ferrero F, Stringhetta M. Thermal stability and flame resistance of polypyrrole-coated PET fibres. J Therm Anal Calorim. 2008;94:559-65.

8. Shen YQ, Wan MX. Soluble conducting polypyrrole doped with DBSA-CSA mixed acid. J Appl Polym Sci. 1998;68:1277-84.

9. Dall'Acqua L, Tonin C, Peila R, Ferrero F, Catellani M. Per- formances and properties of intrinsic conductive cellulose-polypyrrole textiles. Synth Met. 2004;146:213-21.

10. Dall'Acqua L, Tonin C, Varesano A, Canetti M, Porzio W, Catellani M. Vapour phase polymerisation of pyrrole on cellulose-based textile substrates. Synth Met. 2006;156:379-86.

11. Bhat NV, Seshadri DT, Nate MM, Gore AV. Development of conductive cotton fabrics for heating devices. J Appl Polym Sci. 2006;102:4690-5.

12. Davidson RG, Turner TG. An IR spectroscopic study of the electrochemical reduction of polypyrrole doped with dodecylsulfate anion. Synth Met. 1995;72:121-8.

13. Vishnuvardhan TK, Kulkarni VR, Basavaraja C, Raghavendra SC. Synthesis, characterization and a.c. conductivity of polypyrrole/Y_2O_3 composites. Bull Mater Sci. 2006;29:77-83.

14. Feng W, Zhang TR, Liu Y, Lu R, Zhao YY. Photochromic behavior of nanocomposite hybrid films of finely dispersed phosphotungstic acid particles into polyacrylamide. J Mater Sci. 2003;38:1045-8.

15. Su WC, Iroh JO. Electropolymerization of pyrrole on steel substrate in the presence of oxalic acid and amines. Electrochim Acta. 1999;44:2173-84.

16. Bissessur R, Liu PKY. Direct insertion of polypyrrole into molybdenum disulfide. Solid State Ionics. 2006;177:191-6.

17. Cakmak G, Kucukyavuz Z, Kucukyavuz S. Conductive copolymers of polyaniline, polypyrrole and poly (dimethylsiloxane). Synth Met. 2005;151:10-8.

18. Suzer S, Birer O, Sevil UA, Guven O. XPS investigations on conducting polymers. Turk J Chem. 1998;22:59-65.

19. Rajagopalan R, Iroh JO. Characterization of polyaniline-polypyrrole composite coatings on low carbon steel: a XPS and infrared spectroscopy study. Appl Surf Sci. 2003;218:58-69.

20. Uyar T, Toppare L, Hacaloglu J. Characterization of electrochemically synthesized p-toluene sulfonic acid doped polypyrrole by direct insertion probe pyrolysis mass spectrometry. J Anal Appl Pyrol. 2002;64:1-13.

21. Ozdilek C, Toppare L, Yagci Y, Hacaloglu J. Characterization of polypyrrole/polytetrahydrofuran graft copolymers by direct pyrolysis mass spectrometry. J Anal Appl Pyrol. 2002;64:363-78.

11.- ARTÍCULO

ELECTROCHEMICAL CHARACTERIZATION AND INFLUENCE OF THE TEMPERATURE IN THE ELECTRICAL PROPERTIES OF POLYPYRROLE DISCS DOPED WITH ORGANIC AND INORGANIC COUNTER IONS

Electrochemical characterization and influence of the temperature in the electrical properties of polypyrrole discs doped with organic and inorganic counter ions

J. Molina[a], J. C. Galván[b], J. Fernández[a], J. Bonastre[a], F. Cases[a,*]

[a]*Departamento de Ingeniería Textil y Papelera, EPS de Alcoy, Universidad Politécnica de Valencia, Plaza Ferrándiz y Carbonell s/n, 03801 Alcoy, Spain*

[b]*Centro Nacional de Investigaciones Metalúrgicas, CSIC, Avda. Gregorio del Amo 8, 28040 Madrid, Spain*

Abstract

Discs of polypyrrole doped with organic (AQSA) and inorganic ($PW_{12}O_{40}^{3-}$) counter ions have been obtained and their electrical and electrochemical properties have been compared. The electrical properties were studied by means of electrochemical impedance spectroscopy with temperature (EIS). EIS measurements showed in general an increase of conductivity with temperature, typical behavior of semiconductors. Scanning electrochemical microscopy (SECM) measurements were also performed to measure their electroactivity. Positive feedback was obtained for both counter ions, indicating its electroactivity. PPy/AQSA showed more conductivity and electroactivity than $PPy/PW_{12}O_{40}^{3-}$ due to the planar conformation of AQSA that allows a more ordered polymer with better properties.

Keywords: Polypyrrole, polyoxometallate, electrical properties, thermal properties, electrochemical impedance spectroscopy, scanning electrochemical microscopy.

_____

* Corresponding author. Fax.: +34 966528438; telephone: +34 966528812.

E-mail address: fjcases@txp.upv.es (Prof. F. Cases).

1. Introduction

During the formation of conducting polymers like polypyrrole (PPy), positive charges which are responsible for its electronic conduction (polarons and bipolarons) are created in its structure. These charges are compensated by counter ions to maintain the electroneutrality principle and the counter ions can be either organic or inorganic [1].

Polyoxometallates (POMs) are small oxide clusters with several metallic ions coordinated by shared oxide ions, forming a highly symmetrical metal oxide cluster [2]. They present the possibility to produce a hybrid material when combined with conducting polymers such as polypyrrole [2,3]. Polyoxometallates do not degrade in the same temperature range than polypyrrole, so its use allowed us the study of the thermal decomposition of polypyrrole without the interference of the degradation of organic counter ions like AQSA [1]. In a further step, in the present work we have employed phosphotungstate ($PW_{12}O_{40}^{3-}$) and AQSA as counter ions and we have compared their electrical and electrochemical properties. The electrical properties have been measured by means electrochemical impedance spectroscopy with temperature (EIS). The electroactivity has been measured employing scanning electrochemical microscopy (SECM).

2. Experimental

2.1. Reagents and methods

All reagents employed were of analytical grade. Pyrrole, $FeCl_3$ and AQSA were purchased from Merck. $H_3PW_{12}O_{40}$ was supplied by Fluka. $Ru(NH_3)_6Cl_3$ and KCl were supplied by Acros Organics and Scharlau respectively. Ultrapure water was obtained from an Elix 3 Millipore-Milli-Q RG system with a resistivity near to 18.2 MΩ·cm.

Chemical synthesis of PPy/AQSA and $PPy/PW_{12}O_{40}^{3-}$ was carried out similarly to López et al. [1]. Polypyrrole powders were pressed (10 tons) to obtain discs that were employed to carry out the electrical and electrochemical measurements.

2.2. Electrochemical impedance spectroscopy characterization with temperature

An electrochemical interface Solartron 1286 was employed to control the potential and a Solartron 1253 gain-phase analyzer was employed to perform EIS measurements in the 10^4 to 10^{-2} Hz frequency range. The amplitude of the sinusoidal

voltage employed was ± 10 mV. Measurements were carried out in a temperature cell (GF-1000) at different temperatures (25-70 ºC) employing a Carbolite CTF 12/65/550 furnace to control the temperature with the Settemp 3.0 software. The results were fitted employing the ZView software (2.7 version).

2.3. Scanning electrochemical microscopy

A scanning electrochemical microscope (Sensolytics) was employed to perform SECM measurements in a three-electrode cell configuration; consisting of a 25 μm diameter Pt ultra-microelectrode (UME) working electrode, a Pt wire auxiliary electrode and an Ag/AgCl (3 M KCl) reference electrode. The surfaces were tested at their open circuit potential (OCP). Approach (I_T–L) curves were recorded in the feedback mode in a 0.01 M solution of $Ru(NH_3)_6^{3+}$ in 0.1 M KCl using the 25 μm diameter Pt tip held at a potential of -0.4 V (potential selected to reduce the oxidized form of the mediator, $Ru(NH_3)_6^{3+}$, at a diffusion-controlled rate). All the experiments were carried out in inert nitrogen atmosphere (N_2 Premier X50S). Discs of PPy/AQSA and $PPy/PW_{12}O_{40}^{3-}$ glued with epoxy resin on glass microscope slides were employed as substrates.

3. Results and discussion

3.1. Electrochemical impedance spectroscopy characterization with temperature

In Fig. 1, the Bode plots measured at different temperatures (25-70 ºC) for the PPy/AQSA disc are shown as example. In the upper diagram it can be seen the impedance modulus (|Z|) at the different frequencies. The impedance modulus gives the resistance of the polypyrrole disc at the different frequencies employed. It can be seen that as the temperature increases, the impedance modulus lowers until it stabilizes at 50 ºC. The equivalent circuit employed to adjust the data was a single resistance (R). The values of R obtained were employed to obtain the electrical conductivity (S·cm^{-1}). The conductivity at 25 ºC of the PPy/AQSA sample is approximately six times higher than the $PPy/PW_{12}O_{40}^{3-}$ sample (0.16 S·cm^{-1} vs. 0.026 S·cm^{-1}). Anions with planar structures have been reported to produce more conductive polymers in polypyrrole-based conducting fabrics [4]. Therefore the employment of the $PW_{12}O_{40}^{3-}$ (3D) produces a polymer with less conductivity than with the AQSA molecule (2D).

Fig. 1-b shows the data for the phase angle at different frequencies of the PPy/AQSA sample. 0º of phase angle were mainly obtained at all the temperatures

employed, indicating that the material acts as a resistor. The sample of PPy-PW$_{12}$O$_{40}$$^{3-}$ showed the same conductive behavior with 0º of phase angle (figure not shown).
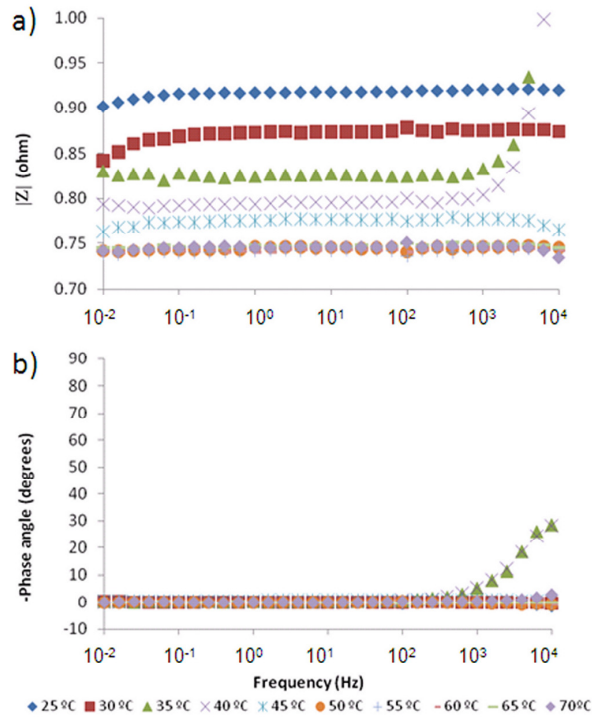

Fig. 1. Bode plots for the disc of PPy/AQSA at different temperatures (25-70 ºC).

3.1.1. Adjustment to the Arrhenius model

In general, the electrical conductivity of conducting polymers increases with the increase of temperature (semiconducting nature), as thermal excitation is needed to move charge carriers [5]. The opposite behavior (metallic conduction) only has been reported in ordered polyaniline [6]. The electrical conductivity behavior with temperature can be explained for example by the Arrhenius model (1) [7,8]:

$$\sigma = \sigma_0 \exp\left[-\frac{E_a}{kT}\right] (1)$$

Where σ is the conductivity (S·cm^{-1}) at each temperature, σ$_0$ is the conductivity at room temperature, E$_a$ (eV) is the carrier activation energy and k is the Boltzmann constant (8.61734·10^5 eV·K^{-1}). The plots of Ln(σ) vs 1000/T are shown in Fig. 2. The

slope of the adjustment is equal to $E_a/1000 \cdot k$, so the activation energy can be calculated from the value of the slope obtained by the linear adjustment. For the sample of PPy/AQSA, from 25 ºC to 50 ºC the conductivity increased with the increase of the temperature and the activation energy obtained was 68 meV. Similar values have been obtained in blibliography for polypyrrole [7,8]. From 50 to 70 ºC the conductivity stabilized with temperature.

For the sample of PPy/PW$_{12}$O$_{40}$$^{3-}$ there was a variability of the data that did not allow the adjustment to the Arrhenius model (Fig. 2-b). Several measurements were performed and the same result was obtained.
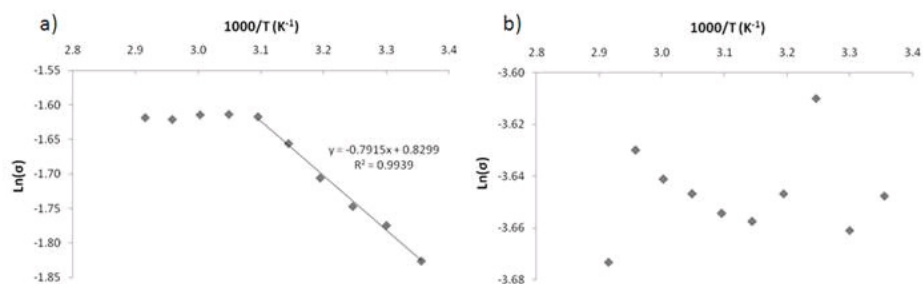

Fig. 2. Plot of Ln(σ) vs. 1000/T for the discs of: a) PPy/AQSA, b) PPy/PW$_{12}$O$_{40}$$^{3-}$.

3.2. SECM measurements

Approach curves give an indication of the electroactivity of the electrode surface. If the surface is non conductive, when the electrode approaches the surface there is a decrease of the current measured (negative feedback). Conversely, if the electrode is conductive, the current increases when the electrode approaches the surface of the substrate (positive feedback) [9].

The normalized currents are defined as: $I_T(L)=i/i_\infty$; where $i_\infty=4 \cdot n \cdot F \cdot D \cdot a \cdot C$ in which n is the number of electrons involved in the reaction, F is the Faraday constant, D is the diffusion coefficient, a is the radius of the ultra-microelectrode (UME) and C is the concentration of the reactant. The normalized currents depend on RG (RG=Rg/a, where Rg is the radius of the insulating glass surrounding the Pt tip of radius "a") and the normalized distance L where L=d/a (d is the UME-substrate separation). The RG of our UME tip is RG≥20. According to Rajendran el al. [10], Pade's approximation gives a close and simple equation with less relative error for all distances and valid for RG>10.

The approximate expression of the steady-state normalized current assuming positive feedback for finite insulator thickness is:

$$I_T{}^C = \left[\frac{1 + 1.5647/L + 1.316855/L^2 + 0.4919707/L^3}{1 + 1.1234/L + 0.626395/L^2} \right] \quad (2)$$

The election of the expression for the normalized tip current assuming negative feedback was based on the equation for a RG=20 and L range 0.4-20 [11]:

$$I_T{}^{INS} = \left[\frac{1}{0.3554 + 2.0259/L + 0.62832 \times \exp\left(-2.55622/L\right)} \right] \quad (3)$$

Fig. 3 shows a selection of the experimental curves recorded at different points randomly chosen throughout the PPy/AQSA and PPy/PW$_{12}$O$_{40}$$^{3-}$ discs surfaces. The approach curves predicted for pure positive and negative feedback calculated from equations 2 and 3 have been also included. Fig. 3-a shows different approach curves to the PPy/AQSA surface. Positive feedback was obtained and all the measurements almost followed the theoretical curve for positive feedback, indicating that the surface presents homogeneous conducting areas, with fast heterogeneous kinetics at -0.4 V.

In Fig. 3-b, approach curves for the disc of PPy/PW$_{12}$O$_{40}$$^{3-}$ are shown. The same behaviour than in the AQSA discs was observed. In this case, the adjustment was worse than in PPy/AQSA and more variability was also observed, indicating less uniformity of the distribution of the conducting areas or a variation of its conductivity. The discs of PPy/PW$_{12}$O$_{40}$$^{3-}$ are a bit less electroactive than PPy/AQSA ones.
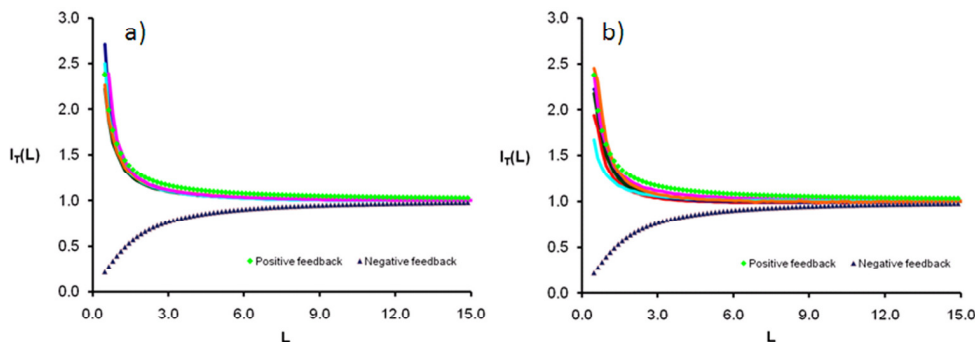

Fig. 3. Approach (I$_T$–L) curves for: a) PPy/AQSA and b) PPy/PW$_{12}$O$_{40}$$^{3-}$ (continuous lines). Theoretical positive and negative feedback models represented as dashed lines.

4. Conclusions

PPy/AQSA discs showed higher conductivity than PPy/PW$_{12}$O$_{40}$$^{3-}$ ones. Counter ions with planar structures (AQSA) produce more conductive polymers than 3D molecules (PW$_{12}$O$_{40}$$^{3-}$) (0.177 S·cm^{-1} vs. 0.023 S·cm^{-1} respectively) due to the obtention of polypyrrole with a more ordered structure. EIS measurements with temperature of PPy/AQSA sample showed an increase of the conductivity with temperature (25 ºC to 50 ºC), this behavior is typical of semiconductors. The activation energy obtained by the Arrhenius model was of 68 meV. From 50 ºC to 70 ºC the conductivity stabilized. The sample of PPy/PW$_{12}$O$_{40}$$^{3-}$ did not adjust properly to the Arrhenius model due to a variability of the values.

Approach curves in SECM measurements showed positive feedback indicating that PPy/PW$_{12}$O$_{40}$$^{3-}$ and PPy/AQSA discs behaved like a conducting material. PPy/AQSA samples were a bit more electroactive than PPy/PW$_{12}$O$_{40}$$^{3-}$ ones.

Acknowledgements

References

[1] López J, Parres F, Rico I, Molina J, Bonastre J, Cases F. Monitoring the polymerization process of polypyrrole by thermogravimetric and X-ray analysis. J Therm Anal Calorim 2010;102:695-701.

[2] Gómez-Romero P. Hybrid organic-inorganic materials. In search of synergic activity. Adv Mater 2001;13:163-74.

[3] Cuia Y, Wu Q, Mao J. Preparation and conductivity of polypyrrole molybdotungstovanadogermanic heteropoly acid hybrid material. Mater Lett 2004;58:2354-6.

[4] Avlyanov JK, Kuhn HH, Josefowicz JY, MacDiarmid AG. In-situ deposited thin films of polypyrrole: conformational changes induced by variation of dopant and substrate surface. Synth Met 1997;84:153-4.

[5] Friend R. Materials science: Polymers show they're metal. Nature 2006;441:37.

[6] Lee K, Cho S, Park SH, Heeger AJ, Lee C-W, Lee S-H. Metallic transport in polyaniline. Nature 2006;441:65-8.

[7] Shaktawat V, Jain N, Saxena R, Saxena NS, Sharma K, Sharma TP. Temperature dependence of electrical conduction in pure and doped polypyrrole. Polym Bull 2006;57:535-43.

[8] Taunk M, Kapil A, Chand S. Chemical synthesis and low temperature electrical transport in polypyrrole doped with sodium bis(2-ethylhexyl) sulfosuccinate. J Mater Sci: Mater Electron 2010; doi:10.1007/s10854-010-0102-2.

[9] Sun P, Laforge FO, Mirkin MV. Scanning electrochemical microscopy in the 21st century. Phys Chem Chem Phys 2007;9:802-23.

[10] Rajendran L, Ananthi SP. Analysis of positive feedback currents at the scanning electrochemical microscope. J. Electroanal. Chem. 2004;561:113-8.

[11] Bard AJ, Mirkin MV. Scanning electrochemical microscopy, New York: Marcel Dekker Inc; 2001, p. 145-60.

12.- ARTÍCULO

ELECTROCHEMICAL POLYMERISATION OF ANILINE ON CONDUCTING TEXTILES OF POLYESTER COVERED WITH POLYPYRROLE/AQSA

Electrochemical polymerisation of aniline on conducting textiles of polyester covered with polypyrrole/AQSA

J. Molina, A.I. del Río, J. Bonastre, F. Cases *

Departamento de Ingeniería Textil y Papelera, EPS de Alcoy, Universidad Politécnica de Valencia, Plaza Ferrándiz y Carbonell s/n, 03801 Alcoy, Spain

Abstract

Polyaniline (Pani) has been electrochemically polymerised on conducting textiles of polyester covered with polypyrrole (Ppy)/anthraquinone sulphonic acid (AQSA), obtaining a double conducting polymer layer. Electrochemical syntheses have been performed by means of cyclic voltammetry (CV) and potentiostatic methods. Pani morphology varies with the method of synthesis as it has been corroborated by scanning electron microscopy. EDX analyses have been performed to study zonal composition of the samples. Surface resistivity measurements have been carried out with a 4-point probe equipment. Electrochemical impedance spectroscopy (EIS) and CV have been employed to characterise the electroactivity of the samples in solutions with different pH values. X-Ray photoelectron spectroscopy (XPS) was employed in order to determine the doping level of polyaniline films and the oxidation state of the sample. With the potentiodynamic synthesis the doping level was higher than that obtained with potentiostatic synthesis, however polymer overoxidation appeared.

Keywords: Polyaniline; polypyrrole; polymer coating; conducting textiles; electropolymerisation; polyester.

_____

* Corresponding author. Fax.: +34 96 652 8438

E-mail address: fjcases@txp.upv.es (Prof. F. Cases)

1. Introduction

Polyaniline is one of the most widely employed conducting polymers, and between the years 1993-2002 it was at the top of the number of research papers in the field of conducting polymers [1]. The synthesis of polyaniline was first reported by Letheby [2]; aniline was oxidised on a Pt-sheet in acidic media. Polyaniline layers have been used as gas sensors [3-4], electrode material for redox supercapacitor [5], shield material for electromagnetic interference control [6], corrosion control [7], etc. Besides conducting polymers are promising materials in the field of catalysis; such catalytic properties have been reviewed [8]. Conducting polymers have been employed in environmental applications; electrodes modified with conducting polymers have been used in Cr^{6+} (toxic) reduction to Cr^{3+} (not toxic) [9] or nitrites electroreduction [10]. The employment of polypyrrole coated textiles in the electrochemical removal of the textile dye C. I. Direct Red 80 has been reported [11]. Polyaniline/MnO_2 catalyst and H_2O_2 as an oxidant have been employed in the degradation of organic dyes such as Direct Red 81, Indigo Carmine and Acid Blue 92 [12,13]. Polypyrrole and polyaniline powders; membranes, fabrics and reticulated vitreous carbon electrodes coated with both polymers were employed for silver recovery from solution [14]. Silver recovery is selective since the higher redox potential of the couple $Ag+/Ag^0$ (+0.80 V) compared with other metal couples, makes Ag^+ reduction process the most probable reaction [14].

The production of textiles with new properties such as conductivity is a new field being investigated. Conducting polymers can be deposited on textile surfaces chemically [15,16] or electrochemically [17]. The electrochemical deposition is an indirect process since the substrate is not a conducting material. Polyaniline was deposited on poly(ethylene terephthalate) fabrics through an indirect electrochemical deposition, Pani was formed on the anode and was adsorbed onto the fabric [17]. In the present paper polyaniline has been synthesised directly on conducting textiles of PES-Ppy/AQSA by potentiostatic and potentiodynamic syntheses obtaining a double conducting polymer layer. Polyester has been used as a base material because it has been extensively used in bibliography [18-23]. The polymerisation of pyrrole is quite independent of the substrate. Only the polarity of the surface may have an effect on the adhesion of the conducting polymer. The adhesion is worse with fibres without polar groups (polyethylene for example) [24]. Moreover, the electrochemical synthesis of polyaniline takes place in acidic medium, so the selected substrate should not be damaged by acids. For this purpose, the employment of natural fibres like cotton should be avoided, because acids damage this sort of fibres.

Polypyrrole has a wider pH-range of electroactivity than polyaniline. With the double conducting polymer layer, one advantage is that the electroactivity in acidic medium is enhanced due to the presence of both polymers. On the other hand, in basic medium polyaniline is not electroactive, but the presence of the polypyrrole layer gives electroactivity to this material. So it is obtained a material with better electrochemical properties than the original material that only was covered with a single layer of polypyrrole.

More work is in progress in order to evaluate the electrocatalytic behaviour of these materials with the purpose to use them as electrodes in the electrochemical degradation of organic dyes.

2. Experimental

2.1. Reagents

Analytical grade aniline, pyrrole, sodium sulphate, ferric chloride, anthraquinone sulfonic acid sodium salt (AQSA), sulphuric acid, sodium hydroxide, sodium dihydrogenophosphate and disodium hydrogenophosphate were purchased from Merck. Normapur acetone was from Prolabo. Ultrapure water was obtained from an Elix 3 Millipore-Milli-Q RG system with a resistivity near to 18.2 MΩ cm.

Aniline was purified by distillation before use. The distillation was performed at reduced pressure in order to avoid thermal degradation of the monomer. After distillation aniline was stored in the dark at 0 ºC.

Polyester textile was acquired from Viatex S.A. and their characteristics were: fabric surface density, 140 g·m^{-2}; warp threads per cm, 20 (warp linear density, 167 dtex); weft threads per cm, 60 (weft linear density, 500 dtex).

2.2. Chemical synthesis of Ppy/AQSA covered fabrics

Chemical synthesis of polypyrrole on polyester textiles was done as reported in our previous study [25]. The size of the samples was 6 cm x 6 cm approximately. Previously to reaction, polyester was degreased with acetone in ultrasound bath and washed with water. Pyrrole concentration employed was 2 g/l and molar relations of reagents employed in the chemical synthesis bath were pyrrole:FeCl$_3$:AQSA (1:2.5:0.6). Next stage was the adsorption of pyrrole and counter ion (AQSA) (V = 200 ml) into textile

for 30 min at 0 ºC without stirring. At the end of this time, FeCl$_3$ solution (V = 50 ml) was added and oxidation of the monomer took place during 150 min at 0 ºC without stirring. Adsorption and reaction were performed in a precipitation beaker. Polymerised textile was washed with water to remove polypyrrole not joined to fibres. The conducting textile was dried in a desiccator for at least 24 h before measurements. The weight increase was measured obtaining a value between 4-6 %.

2.3. Electrochemical synthesis of Pani films on conducting fabrics.

Electrosyntheses were performed using an Autolab PGSTAT302 potentiostat/galvanostat. All electrochemical experiments were carried out at room temperature and without stirring. The counter electrodes (CE) employed were made of stainless steel; the pre-treatment consisted on polishing, degreasing with acetone in ultrasonic bath and washing with water in an ultrasonic bath. In electrochemical synthesis two CE were used to equalise the electrical field around the working electrode (WE) of conducting textile. The WE were made by cutting a strip of the conducting textile PES-Ppy/AQSA and controlling the area with Teflon®. Potential measurements were referred to Ag/AgCl (3 M KCl) reference electrode. Oxygen was removed from solution by bubbling nitrogen gas.

The conducting textile has an ohmic potential drop that it needs to be considered, otherwise the measured potentials will not be real. Therefore, in these experiments the ohmic potential drop was measured and entered in the potentiostat/galvanostat.

Electrosyntheses were performed in aqueous media with 0.5 M H$_2$SO$_4$ and 0.5 M aniline in N$_2$ atmosphere. The electrode of conducting textile was soaked with the solution for 10 minutes to allow the diffusion of the monomer to the textile electrode. Two different methods of electrosynthesis were employed: cyclic voltammetry (CV) and potentiostatic synthesis. The potential for the potentiostatic synthesis was determined with the results of CV. In potentiostatic synthesis the potential was risen up from the open circuit potential (ocp) of the electrode to 1 V. The electrosynthesis went on during the necessary time to achieve the desired electrical charge (C cm^{-2}).

2.4. FTIR-ATR spectroscopy

Fourier transform infrared spectroscopy with horizontal multirebound attenuated total reflection (FTIR-ATR) was performed with a Nicolet Magna 550 Spectrometer

equipped with DTGS detector. An accessory with pressure control was employed to equalise the pressure in the different solid samples. A prism of ZnSe was employed. Spectra were collected with a resolution of 4 cm^{-1}, and 100 scans were averaged for each sample.

2.5. Electrochemical characterisation by cyclic voltammetry

Cyclic voltammetry and electrochemical impedance spectroscopy (EIS) measurements were performed with an Autolab PGSTAT302 potentiostat/galvanostat (Ecochemie) in different pH aqueous solutions. The solutions employed were pH 0 (0.5 M H_2SO_4), pH 0.7 (0.1 M H_2SO_4), pH 7 (NaH_2PO_4-Na_2HPO_4 buffer and 0.1 M Na_2SO_4), pH 13 (0.5 M NaOH and 0.1 M Na_2SO_4).

Measurements were done at room temperature and without stirring. The CE employed was made of stainless steel with the same pre-treatment as in the section 2.3. The WE was made by cutting a strip of the conducting textile of polypyrrole or the conducting textile covered with polyaniline. The area was controlled with Teflon®. Potential measurements were referred to Ag/AgCl (3 M KCl) reference electrode. Oxygen was removed from solution by bubbling nitrogen gas for 30 min and then a N_2 atmosphere was maintained during the measurements. The textile electrode ohmic potential drop was measured and introduced in the potentiostat/galvanostat. CV measurements were done in the range -0.2 V to 0.7 V for the textile covered with Pani and -0.4 to 0.4 V for the sample not covered with Pani; the scan rate employed in both cases was 50 mV s^{-1}.

2.6. Electrochemical characterisation by electrochemical impedance spectroscopy

The electrochemical impedance spectroscopy (EIS) measurements were performed in the 10^4-10^{-2} Hz frequency range. The amplitude of the sinusoidal voltage was 10 mV. Each measurement was carried out at a constant imposed potential equal to the stabilised ocp at the beginning of the experiment.

To analyse quantitatively the behaviour of the films, the experimental results were fitted using a non-linear least squares fitting minimisation method by ZView software (version 2.7).

The electronic resistance of dry polymers was measured locating the polymeric film between two metal tweezers, in a two-electrode configuration. The electrolyte resistance was measured in a four-electrode arrangement with two Ag/AgCl reference electrodes and two platinum wires. A standard three-electrode design was employed for the ordinary impedance measurements of the polymers immersed in the electrolyte solutions, in the same way as the cyclic voltammetry experiments.

2.7. SEM and EDX

A Jeol JSM-6300 scanning electron microscope was employed to obtain the morphology of the samples and perform EDX analyses. SEM analyses were done using an acceleration voltage of 20 kV.

2.8. Surface resistivity measurements

Surface resistivity measurements were performed employing a surface resistivity meter Model SRM-232-2000, 0-2000 Ω/square (Guardian Manufacturing) using the 4-point probe technique.

2.9. X-Ray photoelectron spectroscopy

XPS analyses were conducted at a base pressure of at $5 \cdot 10^{-10}$ mbars and a temperature around 173 K. The XPS spectra were obtained with a VG-Microtech Multilab electron spectrometer by using unmonochromatized Mg Kα (1253.6 eV) radiation from a twin anode source operating at 300 W (20 mA, 15 KV). The binding energy (BE) scale was calibrated with reference to the C_{1s} line at 284.6 eV.

3. Results and discussion

3.1. Electrochemical synthesis by a potentiodynamic technique

Electrochemical synthesis of polyaniline on conducting textiles of PES-Ppy/AQSA was performed in 0.5 M H_2SO_4 aqueous medium, aniline concentration was 0.5 M. The textile electrode was soaked in the synthesis solution for 10 min and then the electrode was introduced at -0.2 V and cycled from this potential to 1.1 V for 70 scans. Fig. 1 shows the voltammograms obtained in the potentiodynamic synthesis of

polyaniline. In the first scans the current density did not grow significantly, the oxidation and reduction processes of polypyrrole were not observed and the sample presented a resistive behaviour. The current density grew slowly from the 1st to the 20th scan. In the 30th scan it could be observed an important increase in the current density and the tendency in the next scans was a constant increase in the current density.

In the 70th scan a maximum anodic current density of nearly 22 mA cm^{-2} was reached. In the Fig. 2 the anodic and cathodic charge are represented vs the number of scans. The first 20th scans showed the same behaviour as in Fig. 1, the charges were very low and it was from the 30th scan that it could be noticed an important increase in the charges.
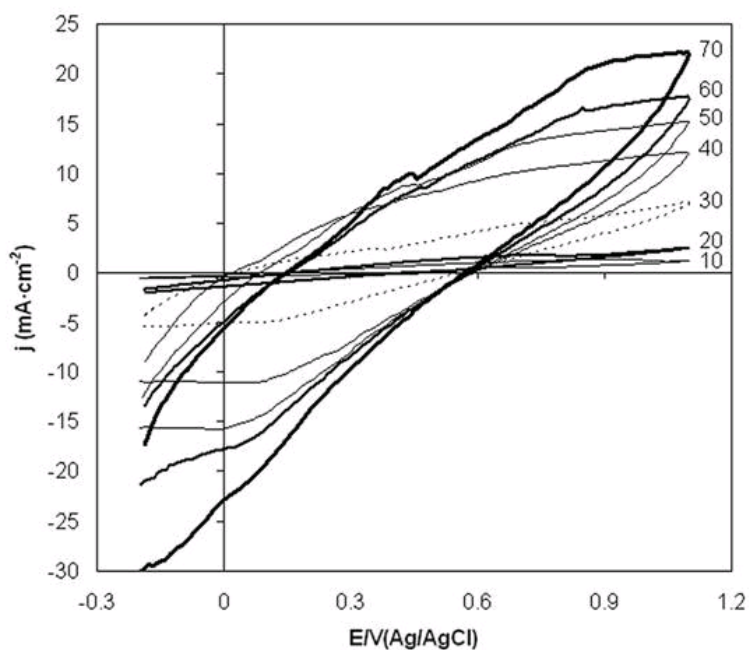

Fig. 1. Potentiodynamic synthesis of polyaniline on PES/Ppy-AQSA. Conditions: 0.5 M H$_2$SO$_4$, 0.5 M aniline, start potential -0.2 V, range -0.2 V to 1.1 V, 50 mV s^{-1}, 70 scans.

The electrochemical formation of polyaniline has an induction period that varies depending on different factors. This behaviour has been observed for the potentiodynamic synthesis of polyaniline on Pt [26] and glassy carbon electrodes [27]. The influence of the acid solution in the kinetics has been studied and the highest charge increases are obtained when H$_2$SO$_4$ is employed [26,27]. From the 30th to the 70th scan

an increase of the charges was obtained. In Fig. 1 it can be seen that with the increasing number of scan a wider form of the voltammogram was obtained, although oxidation and reduction peaks were not observed clearly. The polymerisation of aniline by means of cyclic voltammetry on conducting textiles of polyester covered with Ppy/AQSA was obvious from the continuous increase in the current density and the charge with the increasing number of scan. At the end of the experiment the sample was washed with water and dried in a desiccator. The sample was green coloured, so polyaniline was obtained in its emeraldine form.

From this experiment, 1 V was selected as an adequate potential for the potentiostatic synthesis of polyaniline. As it can be seen in the 40th and following scans in Fig. 1, at this potential the current density reached a plateau, so this potential was selected as an appropriate potential for the potentiostatic synthesis. Besides polyaniline overoxidation was avoided.
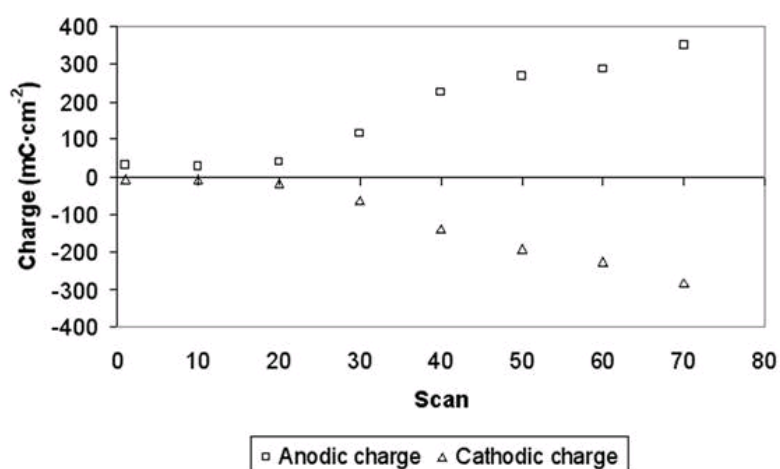

Fig. 2. Values of anodic and cathodic charge vs number of scan for the potentiodynamic synthesis of polyaniline.

3.2. SEM characterisation of polyaniline synthesised by a potentiodynamic technique

The samples synthesised by the potentiodynamic technique were obtained as explained in section 3.1 employing 0.5 M aniline and 0.5 M H_2SO_4 medium.
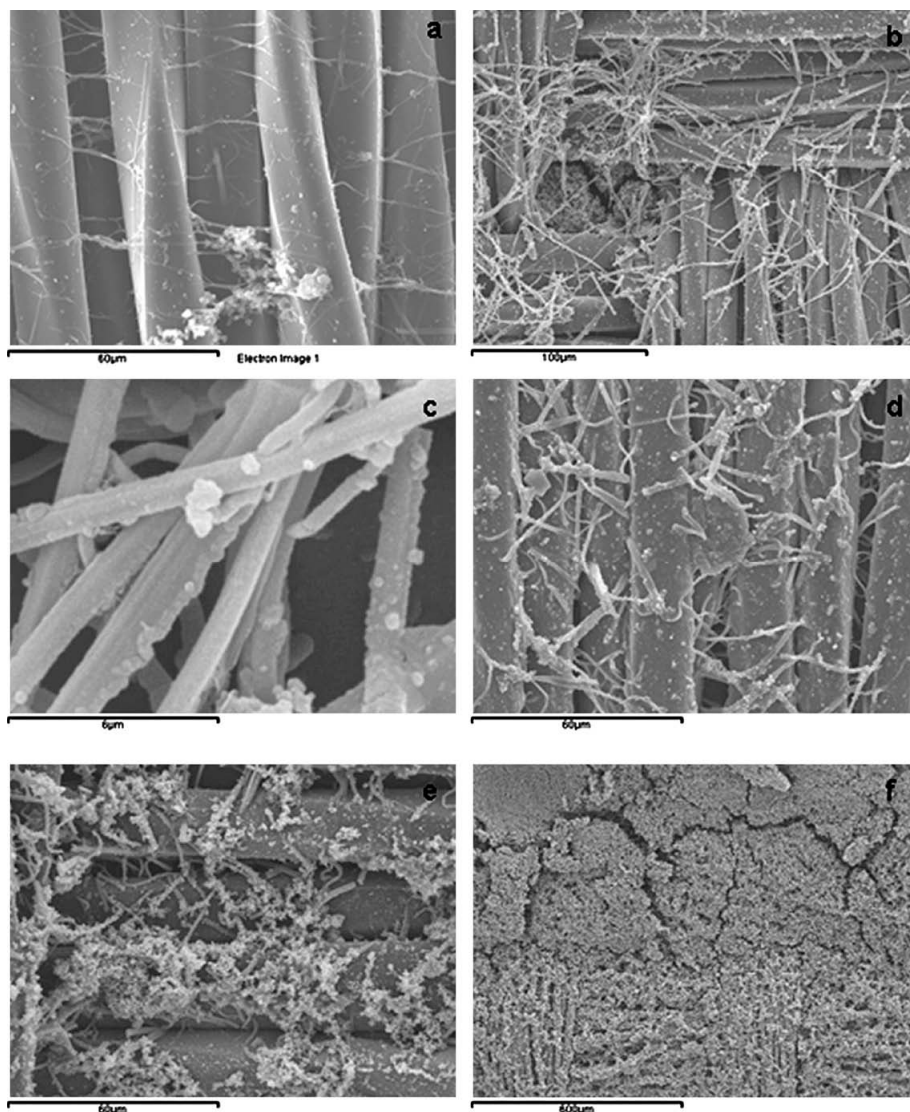
Fig. 3. Micrographs of PES/Ppy-AQSA covered with polyaniline synthesised by cyclic voltammetry. Synthesis conditions: 0.5 M H_2SO_4, 0.5 M aniline, start potential -0.2 V, range -0.2 V to 1.1 V, 50 mV s^{-1}, 70 scans. Micrographs of the electrode taken at different distances from the electric contact: a (x1000), b (x500), c (x10000), d (x1000), e (x1000), f (x100).

During the synthesis, the formation of polyaniline was greater in the zones near to the electric contact. The resistance of the electrode becomes greater as the distance from the electric contact increases. In the further zones of the electrode the

polymerisation was slower, so at the end of the synthesis it could be observed the polymerisation in a more initial stage. The micrographs of the electrode after the synthesis have been taken at different distances from the electric contact. The formation of polyaniline micro-fibres has been observed at different distances from the electric contact (Fig. 3a-e). It seems that the first step in the potentiodynamic synthesis of polyaniline was the formation of polyaniline micro-fibres. Representation of charge vs number of scan (Fig. 2) indicated that in the first 20 scans the charge of the voltammograms was not significantly increased, the nucleation sites were limited during these scans.

So it seems that during these scans the formation of Pani micro-fibres occurred. In Fig. 3a it can be seen the formation of polyaniline micro-fibres between polyester fibres (in the furthest zones of the electrode from the electric contact). In this micrograph, the formation of polyaniline on the surface of the fabric fibres was not observed. Fig. 3b shows Pani micro-fibres with a greater electrochemical growth, the form of the fibres is observed clearly. A magnified micrograph of the micro-fibres is showed in Fig. 3c. Polyaniline fibres have an average diameter of 1-2 µm and their length varies between 10-50 µm.

Polyaniline fibres length obtained by electrochemical synthesis in bibliography were of several microns [28] and their diameter ranged from 80 to 100 nm [28] and 30-60 nm [5]. When chemical synthesis was performed 30-50 nm diameter and 500 nm to several microns length fibres were obtained [4]. In this work fibres of higher diameter and length are obtained. In the nearer zones to the electric contact, the polymerisation of polyaniline on the fabric fibres occurred.

Fig. 3d shows the presence of Pani fibres and the growth of Pani with globular morphology on the surface of the fabric fibres. The nucleation sites for the Pani growth rose with the number of scan. The anodic charge increased as a result (Fig. 2), occurring the polymerisation in the fibres of the fabric. In Fig. 3e it can be seen the formation of globular polyaniline on polyaniline micro-fibres formed previously and on the surface of the textile fibres. In Fig. 3f it can be observed that the textile was covered with globular polyaniline and Pani micro-fibres were not observed at this magnification (x100). In this zone, the micro-fibres of polyaniline could be observed under the globular Pani with more magnification (figure not showed).

3.3. Electrochemical synthesis by a potentiostatic technique

Potentiostatic synthesis of Pani on the conducting textile was performed in the same medium employed in the potentiodynamic synthesis. The textile electrode was soaked in the synthesis solution for 10 min. The electrode was introduced at open circuit potential (ocp) and then the potential was risen to the synthesis potential of 1 V. The electrosynthesis elapsed during the necessary time to achieve the desired electrical charge.

Fig. 4 gives the current density transient curve for the potentiostatic synthesis of Pani, in this synthesis 20 C cm^{-2} of electrical charge were achieved. As soon as the electrode potential was risen from ocp to 1 V, an increase of current density happened. In the first part of the synthesis the current density decreased during the first eight min, this fact is characteristic of nucleus growth kinetics and it is related to the charging of the double electric layer. Similar behaviour has been observed for the electrochemical grafting of polyaniline onto cotton, silk and wool fibres [29]. Up to this time the current density increased constantly, a sign that the electropolymerisation of aniline took place and the electroactive area of the electrode increased with the synthesis time. The maximum current density value achieved in the polymerisation before it was stopped was 9.7 mA cm^{-2}.
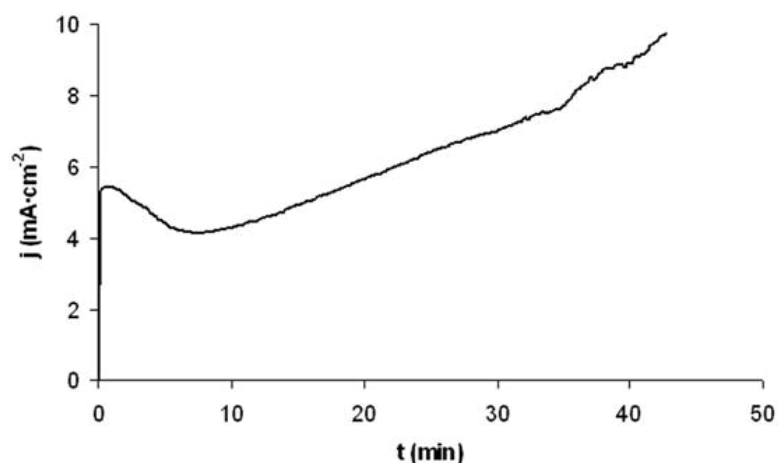

Fig. 4. Current density transient curve for the potentiostatic synthesis of Pani. Conditions: 0.5 M H$_2$SO$_4$, 0.5 M aniline, ocp -0.38 V, synthesis potential 1 V.

Mass increment of the electrode was measured after potentiostatic synthesis obtaining a value of 14.3 mg. With the charge value (28.95 C) and mass change, a value of polymer mass per charge unit of 508 µg/C was obtained. This value is close to that shown by other authors when the synthesis was performed on metallic materials. In [30] polyaniline was electropolymerised on gold films at 0.8 V in 0.5 M H_2SO_4 and 0.03 M aniline and a charge of 60 mC was achieved. The value of polymer mass per unit charge was 600 µg/C approximately, value a bit higher than that obtained for this work.

3.4. SEM characterisation of polyaniline synthesised by a potentiostatic technique

In Fig. 5a,b it can be seen the morphology of the PES fabric covered with Ppy/AQSA. A continuous layer of polypyrrole covered the fibres homogeneously, as we confirmed in a previous work by EDX analysis [25]. Additionally, it could be observed the presence of polypyrrole aggregates formed in the chemical polymerisation that were not removed during the sample washing. In Fig. 5c,d it can be observed the morphology of the conducting textile after the potentiostatic synthesis of polyaniline (20 C cm^{-2}). The entire surface of the fibres was covered by a continuous layer of polyaniline.

The morphology of the Pani film was globular, similar morphology has been obtained when polyaniline was deposited by potentiostatic method on Al-Pt electrode [31]. Polyaniline fibrilar morphology has been also observed in potentiostatic synthesis [28]. Polyaniline morphology depends on various factors such as polymerisation conditions, synthesis technique, acid employed as electrolyte, etc [27,30]. Fig. 5e,f shows the fabric micrographs after an electrical polymerisation charge of 80 C cm^{-2}. As it is observed in Fig. 5e, the fibres of the fabric were not observed, they had been covered entirely by polyaniline. When the polymerisation charge was 20 C cm^{-2}, the growth of the polymer happened on the fibres as it can be seen in Fig. 5d. When the polymerisation charge increased the growth occurred in the 3-D, the spaces between fibres were completely covered with the polymer so they could not be seen. In Fig. 5f it can be observed the globular morphology obtained.
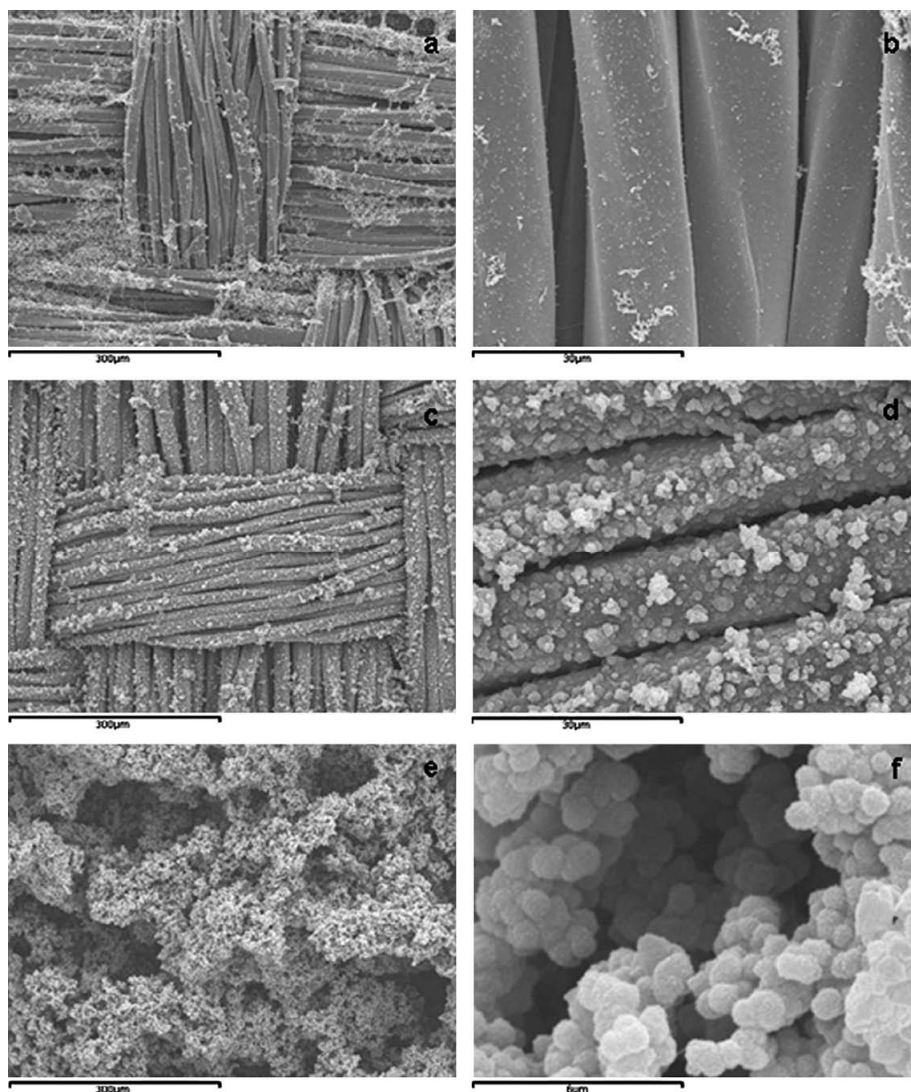
Fig. 5. Micrographs of: PES/Ppy-AQSA, a (x100), b (x1000); PES/Ppy-AQSA + Pani (20 C cm^{-2}), c (x100), d (x1000); PES/Ppy-AQSA + Pani (80 C cm^{-2}), e (x100), f (x10000).

3.5. Energy dispersive X-ray (EDX)

In Fig. 6a it can be seen the EDX analysis performed on the fibres of polyaniline formed during the cyclic voltammetric synthesis of polyaniline. In Fig. 6b the EDX analysis were made on the surface of the textile after the potentiostatic synthesis of

polyaniline. The result obtained was the same, the presence of S in both polymers, due to the presence of HSO_4^- that acts as counter ion of polyaniline. This analysis is qualitative, so the doping level cannot be evaluated by means of EDX; for this purpose XPS has been employed (section 3.10).
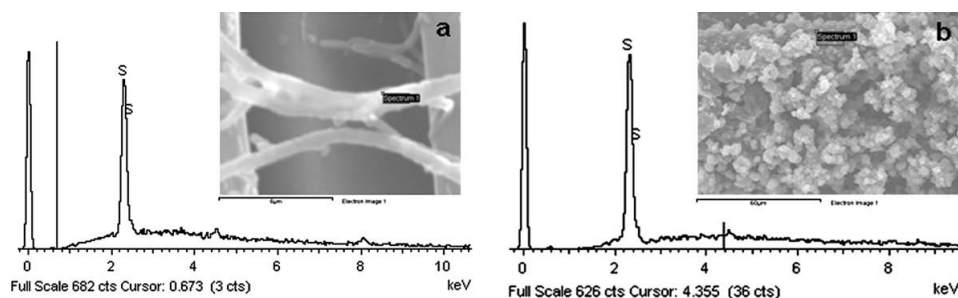

Fig. 6. EDX spectrum of: a) Pani fibre obtained by CV, b) Pani obtained by potentiostatic synthesis.

3.6. FTIR-ATR

Fig. 7 shows the spectra of PES/Ppy-AQSA, polyaniline powders obtained from the textile surface after potentiostatic synthesis and PES/Ppy-AQSA covered with Pani obtained by potentiostatic synthesis. PES/Ppy-AQSA spectrum shows characteristic bands of polypyrrole like C=C stretching (1550 cm^{-1}) [32,33], C-C stretching (1450 cm^{-1}) [32,33], C-N stretching (1300 cm^{-1}) [32,33], pyrrole bending (1160, 1030, 775 cm^{-1}) [32,33]. Characteristic bands of the counter ion (AQSA) can be observed at 1670 and 710 cm^{-1} [34].

The rest of the bands are due to the polyester substrate (1700, 1400, 1240, 1075, 1010, 960, 730 cm^{-1}). When the electrochemical synthesis of Pani was carried out on the textile of PES/Ppy-AQSA, the bands of PES and AQSA vanished. This detail can be appreciated clearly with the PES band at 1700 cm^{-1} and the bands attributed to AQSA (1670 and 710 cm^{-1}). This fact indicates that the layer of polyaniline formed during the electrochemical synthesis was thick enough to avoid IR radiation penetration down to the substrate, so the characteristic bands of PES/Ppy-AQSA were not observed.
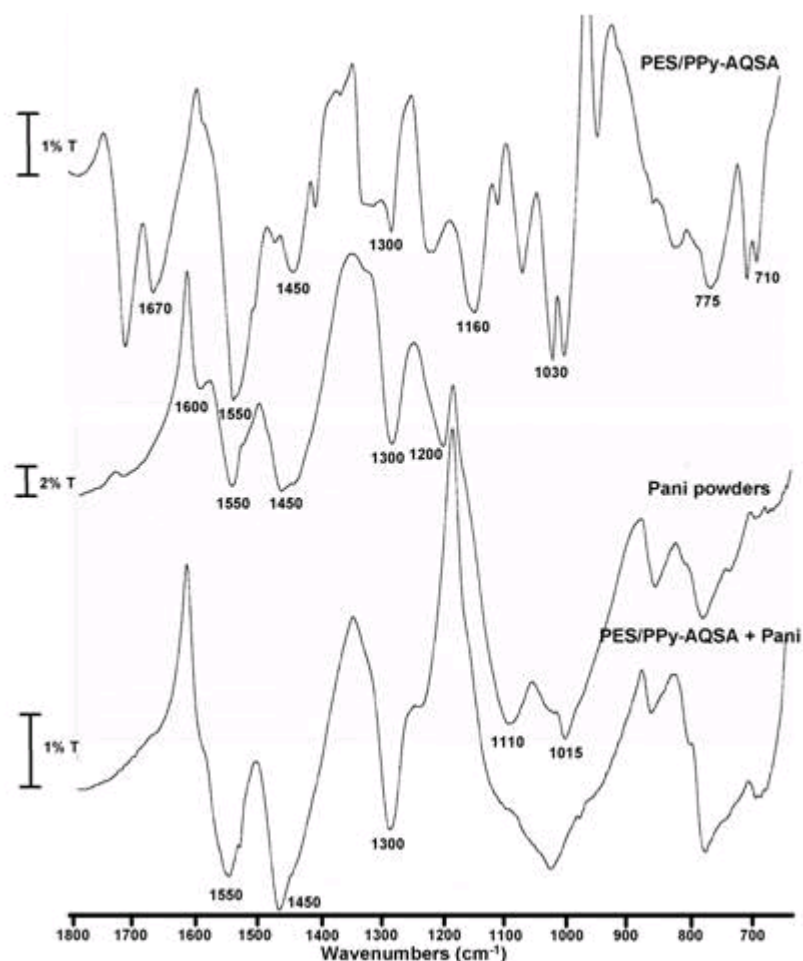
Fig. 7. FTIR-ATR spectrum of PES/Ppy-AQSA, Pani powders and PES/Ppy-AQSA covered with
polyaniline obtained by potentiostatic synthesis (30 C cm^{-2}). Resolution 4 cm^{-1}, 100 scans.

The spectrum of Pani powders obtained from the textile surface was obtained in
order to compare the spectrum of the textile covered with polyaniline and the Pani
powders. Some of the bands obtained for Pani coincide with that of polypyrrole: C=C
stretching (1550 cm^{-1}), C-C stretching (1450 cm^{-1}) and C-N stretching band (1300 cm^{-1}).
The last band is magnified when Pani is synthesised, this fact is due to C-N bonds
stretching vibration of the secondary amines probably related to the leucoemeraldine
component [35]. Other bands attributed to Pani appears in the spectra; one band at 1600
cm^{-1} was due to C=C stretching vibrations in quinoid rings [36-40]. The band at 1200 cm^{-}

[1] that appears in Pani powders is due to C-N stretching vibrations [41]. The bands at 1110 and 1015 cm^{-1} are due to the C-H in-plane bending of 1,4-ring [42].

3.7. Cyclic voltammetry

Cyclic voltammetry in different pH solutions for the samples of PES/Ppy-AQSA and PES/Ppy-AQSA covered with polyaniline synthesised potentiostatically (20 C cm^{-2}) can be observed in Fig. 8.
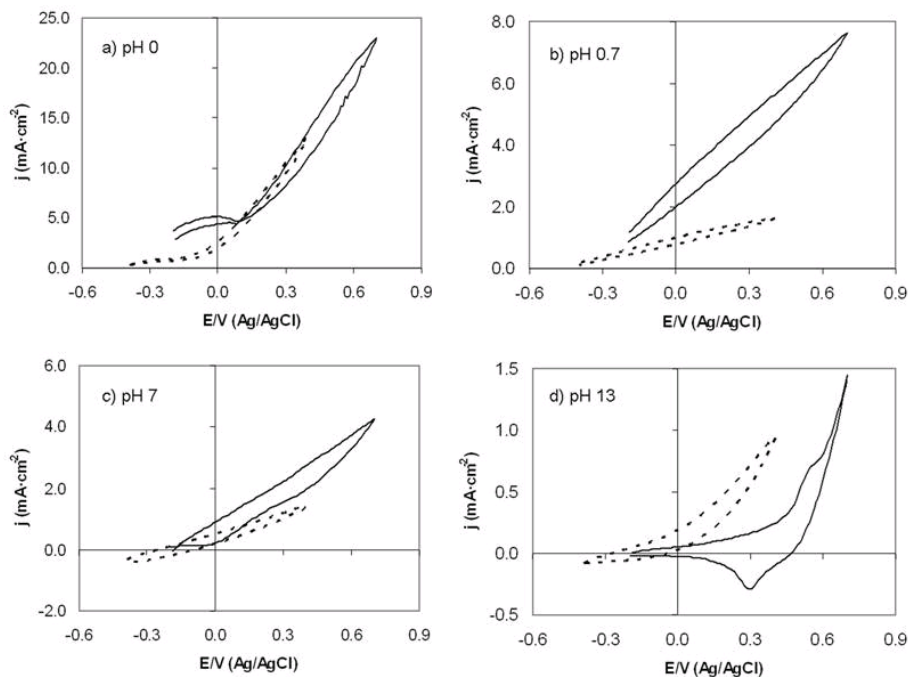
Fig. 8. Cyclic voltammetry of PES/Ppy-AQSA (---) and PES/Ppy-AQSA covered with Pani (20 C cm^{-2}) (—) in different pH: (a) pH 0 (0.5 M H_2SO_4), (b) pH 0.7 (0.1 M H_2SO_4), (c) pH 7 (phosphates buffer + 0.1 M Na_2SO_4), (d) pH 13 (0.1 M NaOH + 0.1 M Na_2SO_4). Scan rate 50 mV/s, second scan for all samples.

Oxidation and reduction processes were not observed in the voltammograms and a resistive response was obtained. As pH solution rose, the current density in the different voltammograms decreased since the conductivity and electroactivity of polyaniline and polypyrrole depends on the protonation level.

At pH 0 the voltammograms are almost coincident for both samples. At pH 0.7 and pH 7, the voltammograms of the sample containing Pani had higher slope (less resistance) than that for the sample of PES/Ppy-AQSA. At pH 13 close values of maximum current density were obtained for both samples.

3.8. Surface resistivity measurements

Surface resistivity was measured before and after the electrochemical polymerisation of aniline with the four point probe test. The surface resistivity of the PES-Ppy/AQSA sample was 60-70 $\Omega/\square$; after polyaniline deposition measurements were below 20 $\Omega/\square$. Surface resistivity was slightly improved with the polyaniline coating. Polyaniline and polypyrrole had close values of conductivity.

3.9. Electrochemical impedance spectroscopy

3.9.1. PES/Ppy-AQSA

For an electroactive conducting polymer (deposited on PES that is an electrical insulating material) in solution it can be expected the following contributions to its impedance:

– An ohmic contact between the Ppy film and the metal tweezer.
– Charge transport within the conducting polymer film: electrons, anions, cations and holes.
– The oxidation/reduction of polypyrrole involving a charge transfer reaction (Faraday reaction) and diffusion of reactants.
– The electrochemical double layer at the polymer film.

A Randless equivalent circuit (Fig. 9) was employed to model the a-c response of the system with charge transfer and diffusion of the electroactive species. The

Faraday reaction can be represented by an ionic charge transfer resistance (R_{ifs}) and a Warburg impedance (W_d) to model the ion diffusion from the conducting polymer. The double layer at the polypyrrole/solution interface can be represented by a capacitance (C_{ifs}). The high frequency limit of the impedance (R_e) is the sum of the ohmic resistances

of the polymer film, of the electrical contact between the polymer film and the metal tweezer and of the electrolyte between working and reference electrode [43].

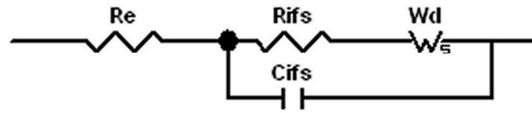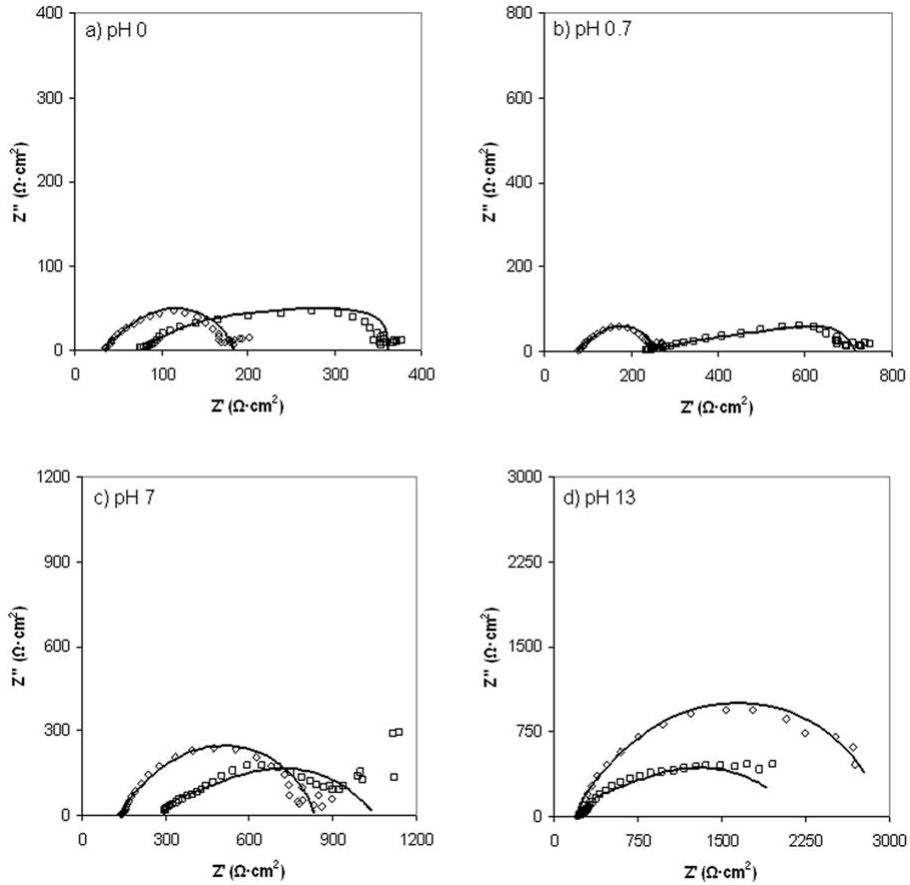*Fig. 9. Equivalent circuit model used for the polymer/electrolyte system.*

Fig. 10. Nyquist plots of PES/Ppy-AQSA (□), PES/Ppy-AQSA+Pani (◊) and simulated Nyquist plots (—) in different pH: a) pH 0 (0.5 M H_2SO_4), b) pH 0.7 (0.1 M H_2SO_4), c) pH 7 (phosphates buffer + 0.1 M Na_2SO_4), d) pH 13 (0.1 M NaOH + 0.1 M Na_2SO_4).

Firstly, EIS measurements were carried out in a two-electrode configuration on a dry sample of PES/Ppy-AQSA. The electrical resistance of the polymer film and the electrical contacts were measured locating the PES/Ppy-AQSA polymer between two metal tweezers, obtaining a value around 210 Ω cm^2.

The electrolyte resistance of the pH 13 solution (0.5 M NaOH + 0.1 M Na$_2$SO$_4$) was measured in a four-electrode arrangement, obtaining a value of 12 Ω. For the system polymer/electrolyte, the ohmic resistance of samples of PES/Ppy-AQSA in the pH 13 solution was around 247 Ω cm^2 (see Table 1). This value was approximately the sum of the electronic resistance of the polymer including the electrical contact of the tweezer and the electrolyte resistance obtained by the separated experiments mentioned previously.

Nyquist plots of PES/Ppy-AQSA and the simulated plots in different pH solutions are shown in Fig. 10.

The Warburg impedance is a finite-length diffusion with transmissive boundary. This Warburg impedance is defined by a diffusion resistance W_d-R, W_d-T = l^2/D; l: length of the diffusion layer, D: diffusion coefficient and W_d-P: Warburg exponent. Fig. 11 represents the Nyquist plot for an ideal finite-length Warburg impedance with transmissive boundary conditions.
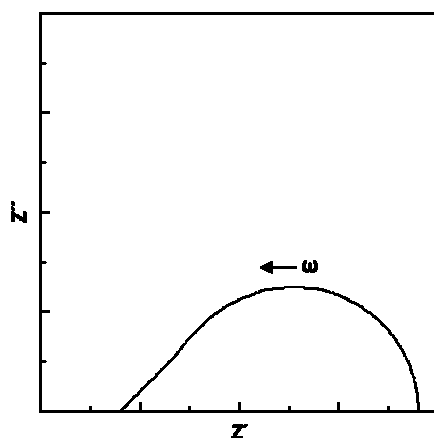

Fig. 11. Nyquist plot for an ideal finite-length Warburg impedance with transmissive boundary conditions.

The impedance for this Warburg element is [44]:

$$Z(j\omega) = \frac{dE}{dc}\frac{1}{zF}\frac{\tanh l\sqrt{(j\omega/D)}}{\sqrt{(j\omega/D)}}$$

where dE/dc represents the change in the electrode potential with concentration, l is the length of the diffusion layer, D the diffusion coefficient (cm^2 s^{-1}) and the value l^2/D is a factor related to the diffusion coefficient of the electroactive species. For a non uniform diffusion (NUD) in a finite-length region, a heuristically expression is:

$$Z_{NUD} = R_0\tanh[A_0R_0(j\omega)^\psi]/[A_0R_0(j\omega)^\psi]$$

where R_0, which might be high frequency resistance for bulk behaviour. For ψ = 0.5, this expression reduces to the above mentioned when one takes $A_0 = l/R_0D^{0.5}$. This expression is useful for $0 < \psi < 0.6$. We obtained Warburg exponents between 0.3 and 0.5, wherein the above interval commented and near the ideal value of 0.5. A pure Warburg regime (W_d-P = 0.5) must be excluded. However, if we fit the low frequency arc to a CPE element, CPE coefficients about 0.5 and 0.6 were obtained, showing Warburg diffusion behaviour.

The numeric fitting values of the model are shown in Table 1. At pH 0, a considerably increase of the electronic conductivity of the film (decrease of R_e) was observed. When pH decreases, a slight decrease of the ionic charge transfer resistance (R_{ifs}) occurs. In addition, diffusion of the ionic species (W_d) is faster, probably due to the fact that at pH 0 and pH 0.7 the exchanged species are H^+ and this ion presents a high ionic mobility. Additionally, protonated polymers in acidic media present higher conductivity [45]. From pH 7 to pH 0, an increase of the capacitance of the polymer/electrolyte interface happens. This fact could be attributed to a greater conductivity of the polymer due to a higher number of electroactive sites in its structure (polarons, bipolarons and counter ions), so it exists a higher charge distribution in the interface. In the case of pH 13 solution, it could exist polymer degradation due to hydroxyl attack [46]. The polymer/electrolyte interface capacitance is high, probably due to OH^- incorporation to the polymer backbone, the conjugation is reduced and the conductivity as a result decreases.

pH 0	pH 0.7	pH 7	pH 13
$R_e = 78\ \Omega\,cm^2$	$R_e = 237\ \Omega\,cm^2$	$R_e = 294\ \Omega\,cm^2$	$R_e = 247\ \Omega cm^2$
$R_{ifs} = 2\ \Omega\,cm^2$	$R_{ifs} = 5\ \Omega\,cm^2$	$R_{ifs} = 11\ \Omega\,cm^2$	$R_{ifs} = 19\ \Omega\,cm^2$
$C_{ifs} = 5.8 \times 10^{-6}\ F\,cm^{-2}$	$C_{ifs} = 3.0 \times 10^{-6}\ F\,cm^{-2}$	$C_{ifs} = 2.3 \times 10^{-6}\ F\,cm^{-2}$	$C_{ife} = 3.9 \times 10^{-5}\ F\,cm^{-2}$
$W_d{-}R = 281\ \Omega\,cm^2$	$W_d{-}R = 472\ \Omega\,cm^2$	$W_d{-}R = 745\ \Omega\,cm^2$	$W_d{-}R = 1895\ \Omega\,cm^2$
$W_d{-}T = 0.03\ s$	$W_d{-}T = 0.05\ s$	$W_d{-}T = 0.3\ s$	$W_d{-}T = 8.2\ s$
$W_d{-}P = 0.5$	$W_d{-}P = 0.4$	$W_d{-}P = 0.3$	$W_d{-}P = 0.3$

Table 1. Fitted parameters for EIS measurements obtained in the samples of PES/Ppy-AQSA in different pH: pH 0 (0.5 M H_2SO_4), pH 0.7 (0.1 M H_2SO_4), pH 7 (phosphates buffer + 0.1 M Na_2SO_4), pH 13 (0.1 M NaOH + 0.1 M Na_2SO_4). W_d-T = l^2/D; l: length of the diffusion layer, D: diffusion coefficient. W_d-P: Warburg exponent.

3.9.2. PES/ Ppy-AQSA + Pani

Nyquist plots of PES/Ppy-AQSA + Pani and the simulated plots in different pH solutions are shown in Fig. 10. The numeric fitting values are shown in Table 2. When pH decreases, the electronic conductivity of the polymer is higher (lower R_e) and the ion-ion charge transfer is faster (lower R_{ifs}). As it has been pointed out, this is attributed to a higher protonation level of the polymer. The protonation level has a great influence in Pani conductivity [47]. The ion diffusion rate increases (lower W_d) when pH decreases, due to the high ion mobility of protons. At pH 13 it can be observed a high capacitance of the interface polymer/electrolyte, probably due to the hydroxyl attack in the polymer structure.

pH 0	pH 0.7	pH 7	pH 13
$R_e = 36\ \Omega\,cm^2$	$R_e = 80\ \Omega\,cm^2$	$R_e = 146\ \Omega\,cm^2$	$R_e = 218\ \Omega\,cm^2$
$R_{ifs} = 1\ \Omega\,cm^2$	$R_{ifs} = 2\ \Omega\,cm^2$	$R_{ifs} = 5\ \Omega\,cm^2$	$R_{ifs} = 16\ \Omega\,cm^2$
$C_{ifs} = 1.9 \times 10^{-5}\ F\,cm^{-2}$	$C_{ifs} = 3.5 \times 10^{-5}\ F\,cm^{-2}$	$C_{ifs} = 2.8 \times 10^{-5}\ F\,cm^{-2}$	$C_{ife} = 2.3 \times 10^{-4}\ F\,cm^{-2}$
$W_d{-}R = 147\ \Omega\,cm^2$	$W_d{-}R = 177\ \Omega\,cm^2$	$W_d{-}R = 683\ \Omega\,cm^2$	$W_d{-}R = 2709\ \Omega\,cm^2$
$W_d{-}T = 0.06\ s$	$W_d{-}T = 0.13\ s$	$W_d{-}T = 0.2\ s$	$W_d{-}T = 5.0\ s$
$W_d{-}P = 0.4$	$W_d{-}P = 0.4$	$W_d{-}P = 0.4$	$W_d{-}P = 0.4$

Table 2. Fitted parameters for EIS measurements obtained in the samples of PES/Ppy-AQSA + Pani in different pH: pH 0 (0.5 M H_2SO_4), pH 0.7 (0.1 M H_2SO_4), pH 7 (phosphates buffer + 0.1 M Na_2SO_4), pH 13 (0.1 M NaOH + 0.1 M Na_2SO_4). W_d-T = l^2/D; l: length of the diffusion layer, D: diffusion coefficient. W_d-P: Warburg exponent.

3.9.3. PES/Ppy-AQSA and PES/Ppy-AQSA + Pani comparison

In both cases, when pH diminishes from pH 7 to pH 0, the electronic conductivity increases and the ionic charge transfer resistance decreases. For each pH,

the diffusion rate is higher in samples that contain Pani, except when pH 13 is employed that occurs the inverse situation. At pH 13 the sample of PES/Ppy-AQSA could be more degraded, so the diffusion is easier. The capacitance of the interface polymer/electrolyte is one order of magnitude higher when Pani is electrosynthesised on the samples of PES/Ppy-AQSA. The samples that contain Pani could present a high charge distribution with a higher number of electroactive sites in the polymer structure. The sample with the best electrical conductive properties is the one that contains Pani in a pH 0 solution.

3.10. X-Ray photoelectron spectroscopy analysis

Fig. 12a,c,e (N_{1s}) and Fig. 12b,d,f (C_{1s}) show the high resolution spectra for PES/Ppy-AQSA (Fig. 12a,b), PES/Ppy-AQSA covered with polyaniline synthesised by potentiostatic synthesis (Fig. 12c,d) and PES/Ppy-AQSA covered with polyaniline synthesised by potentiodynamic synthesis (Fig. 12e,f). Two main peaks are observed in the N_{1s} spectra; one peak around 399-399.3 eV attributed to (-NH-) and another peak with binding energy > 400 eV assigned to positively charged nitrogen atoms (N^+) [42]. Additionally to these peaks, in the sample of PES/Ppy-AQSA and the sample covered with Pani synthesised potentiostatically another peak around 410 eV was observed (not showed). This peak is assigned to an enhanced shake-up satellite of N_{1s} in conjugate systems and appears 10 eV higher than the main peak [48]. The doping level of the polymer can be calculated from the ratio N^+/N. The doping level value obtained for the fabric covered with Ppy/AQSA was 0.31. When the potentiostatic synthesis of polyaniline was carried out, the doping level obtained was 0.22. With the potentiodynamic synthesis a doping level of 0.34 was reached. This fact indicates that with the potentiodynamic method of synthesis, a polymer with higher oxidation state was obtained.

In the C_{1s} spectra two peaks appear for each sample. One peak appears around 284.1-284.4 eV that is assigned to C-C and C-H [49,50]. The other peak that appears in the samples that contain polyaniline at 285.6 eV is attributed to C-N [50]. The second peak in the sample of PES/Ppy-AQSA appears at 286 eV and is also attributed to C-N [51]. Additionally in the C_{1s} spectrum of the sample polymerised potentiodinamically, one peak appeared around 288.3 eV, this peak is assigned to C=O [49,52], and its presence is due to overoxidation. This peak did not appear in the XPS spectrum of the sample synthesised by potentiostatic synthesis. The potential reached in the potentiodynamic synthesis was higher than that employed for the potentiostatic synthesis (1.1 V vs 1 V), so it seems that the sample synthesised by cyclic voltammetry was slightly overoxydised (7.6 %). These results indicate that the potential selected for

the potentiostatic synthesis was an adequate potential due to the fact that overoxidation was avoided; on the other hand the doping level reached was lower than the one obtained for the potentiodynamic synthesis.
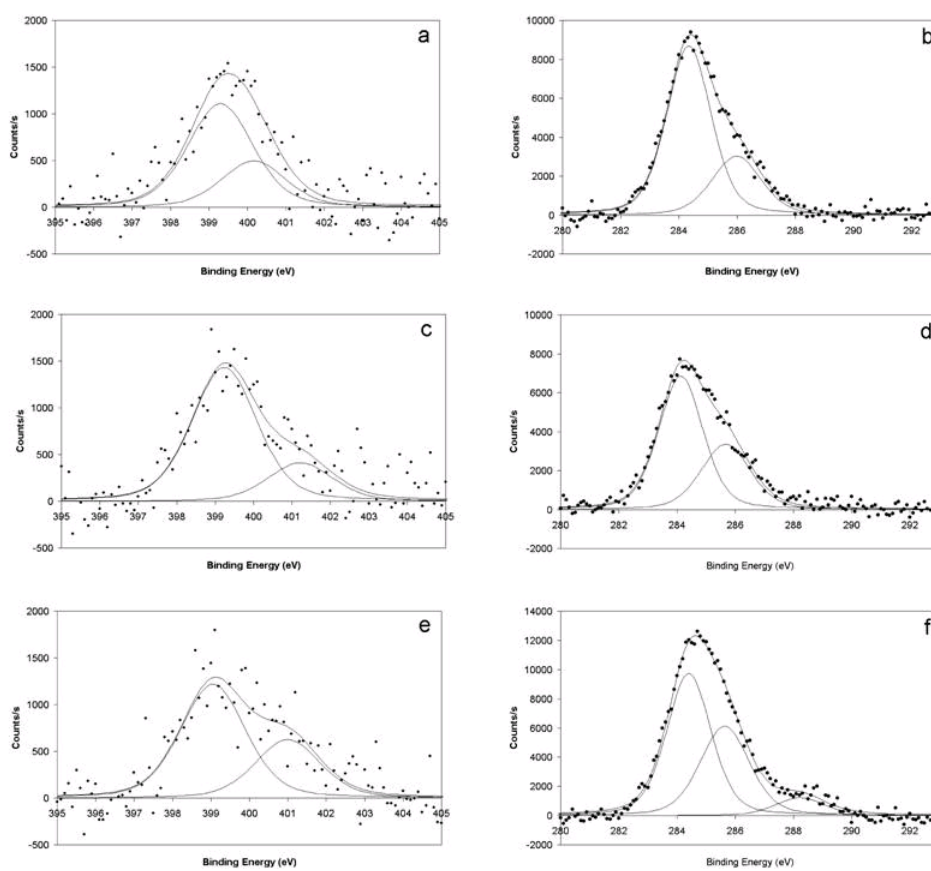

Fig. 12. XPS high resolution spectra for N_{1s} and C_{1s}: PES/Ppy-AQSA, a) N_{1s}, b) C_{1s}; PES/Ppy-AQSA + Pani potentiostatically synthesised, c) N_{1s}, d) C_{1s}; PES/Ppy-AQSA + Pani pontentiodinamically synthesised, e) N_{1s}, f) C_{1s}.

4. Conclusions

Potentiodynamic and potentiostatic synthesis of polyaniline on conducting fabrics of PES-Ppy/AQSA has been achieved. In the potentiodynamic synthesis two different stages could be observed. In a first stage, it seems that the formation of polyaniline fibres took place since the nucleation sites were limited. Fibres length was 10-50 μm and an average diameter of 1-2 μm was obtained. As the nucleation sites increased, the current density grew and polyaniline with globular morphology was obtained.

When potentiostatic synthesis was employed, globular morphology was obtained with a 2-D growth at the beginning of the synthesis. A mass variation value of 508 μg/C was obtained. Surface resistivity of the textile after the electrochemical deposition of polyaniline was around 20 Ω/□ for both methods of synthesis. Electrochemical impedance measurements confirmed that Pani films electrosynthesised on PES/Ppy-AQSA improved the electronic conductivity of the samples. Cyclic voltammetry and impedance measurements showed that the electroactivity of the conducting polymers studied was also enhanced when they were treated in lower pH solutions.

With the potentyodinamic synthesis the doping level (N^+/N) was higher than with the potentiostatic synthesis, however the sample potentiodinamically synthesised was slightly overoxidised (as XPS has corroborated) since an higher synthesis potential was reached.

References

[1] Trojanowicz M. Application of conducting polymers in chemical analysis. Microchim Acta 2003;143(2-3):75-91.

[2] Letheby H. On the production of a blue substance by the electrolysis of sulphate of aniline. J Chem Soc 1862;15:161-163.

[3] Nicolas-Debarnot D, Poncin-Epaillard F. Polyaniline as a new sensitive layer for gas sensors. Anal Chim Acta 2003;475(1-2):1-15.

[4] Huang J, Virji S, Weiller BH, Kaner RB. Polyaniline nanofibers: facile synthesis and chemical sensors. J Am Chem Soc 2003;125(2):314-315.

[5] Gupta V, Miura N. Electrochemically deposited polyaniline nanowire's network. A high-performance electrode material for redox supercapacitor. Electrochem Solid-State Lett 2005;8(12):A630-A632.

[6] Dhawan SK, Singh N, Venkatachalam S. Shielding efectiveness of conducting polyaniline coated fabrics at 101 GHz. Synth Met 2002;125(3):389-393.

[7] Sazou D, Kourouzidou M, Pavlidou E. Potentiodynamic and potentiostatic deposition of polyaniline on stainless steel: Electrochemical and structural studies for a potential application to corrosion control. Electrochim Acta 2007;52(13):4385-4397.

[8] Malinauskas A. Electrocatalysis at conducting polymers. Synth Met 1999;107(2):75-83.

[9] Rodríguez FJ, Gutiérrez S, Ibanez JS, Bravo JL, Batina N. The efficiency of toxic chromate reduction by a conducting polymer (polypyrrole): Influence of electropolymerization conditions. Environ Sci Technol 2000;34(10):2018-2023.

[10] Tian Y, Wang J, Wang Z, Wang S. Electroreduction of nitrite at an electrode modified with polypyrrole nanowires. Synth Met 2004;143(3):309-313.

[11] Lopes A, Martins S, Moraö A, Magrinho M, Gonçalves I. Degradation of a textile dye C. I. Direct Red 80 by electrochemical processes. Portugaliae Electrochim Acta 2004;22(3):279-294.

[12] Gemeay AH, El-Sharkawy RG, Mansour IA, Zaki AB. Catalytic activity of polyaniline/MnO_2 composites towards the oxidative decolorization of organic dyes. Appl Catal B 2008;80(1-2):106-115.

[13] Gemeay AH, El-Sharkawy RG, Mansour IA, Zaki AB. Preparation and characterization of polyaniline/manganese dioxide composites and their catalytic activity. J Colloid Interface Sci 2007;308(2):385-394.

[14] Dimeska R, Murray PS, Ralph SF, Wallace GG. Electroless recovery of silver by inherently conducting polymer powders, membranes and composite materials. Polymer 2006;47(13):4520-4530.

[15] Oh KW, Kim SH, Kim EA. Improved surface characteristics and the conductivity of polyaniline-nylon 6 fabrics by plasma treatment. J Appl Polym Sci 2001;81(3):684-694.

[16] Fryczkowsky R, Rom M, Fryczkowska B. Polyester fibres finished with polyaniline. Fibres Text East Eur 2005;13(5):141-143.

[17] Hirase R, Hasegawa M, Shirai M. Conductive fibers based on poly(ethylene terephthalate)-polyaniline composites manufactured by electrochemical polymerization. J Appl Polym Sci 2003;87(7):1073-1078.

[18] Lekpittaya P, Yanumet N, Grady BP, O'Rear EA. Resistivity of conductive polymer-coated fabric. J Appl Polym Sci 2004;92(4):2629-2636.

[19] Kincal D, Kumar A, Child A, Reynolds J. Conductivity switching in polypyrrole-coated textile fabrics as gas sensors. Synth Met 1998;92(1):53-56.

[20] Kuhn H, Child A, Kimbrell W. Toward real applications of conductive polymers. Synth Met 1995;71(1-3):2139-2142.

[21] Lin T, Wang L, Wang X, Kaynak A. Polymerising pyrrole on polyester textiles and controlling the conductivity through coating thickness. Thin Solid Films 2005;479(1-2):77-82.

[22] Kaynak A, Håkansson E. Short-term heating tests on doped polypyrrole-coated polyester fabrics. Synth Met 2008;158(8-9):350-354.

[23] Håkansson E, Amiet A, Kaynak A. Electromagnetic shielding properties of polypyrrole/polyester composites in the 1-18 GHz frequency range. Synth Met 2006;156(14-15):917-925.

[24] Kuhn HH, Child AD. Electrically conducting textiles. In: Handbook of Conducting Polymers, Skotheim TA, Elsenbaumer RL, Reynolds JR editors. New York; Marcel Dekker, Inc., 1998. p. 993-1013.

[25] Molina J, del Río AI, Bonastre J, Cases F. Chemical and electrochemical polymerisation of pyrrole on polyester textiles in presence of phosphotungstic acid. Eur Poly J 2008;44(7):2087-2098.

[26] Duić LJ, Mandić Z, Kovačiček F. The effect of supporting electrolyte on the electrochemical synthesis, morphology, and conductivity of polyaniline. J Polym Sci Part A: Polym Chem 1994;32(1):105-111.

[27] Desilvestro J, Schelfele W. Morphology of electrochemically prepared polyaniline. J Mater Chem 1993;3(3):263-272.

[28] Guo Y, Zhou Y. Polyaniline nanofibers fabricated by electrochemical polymerization: a mechanistic study. Eur Polym J 2007;43(6):2292-2297.

[29] Bhadani SN, Sen Gupta SK, Sahu GC, Kumari M. Electrochemical formation of some conducting fibers. J Appl Polym Sci 1996;61(2):207-212.

[30] Choi SJ, Park SM. Electrochemistry of conductive polymers. XXVI. Effects of electrolytes and growth methods on polyaniline morphology. J Electrochem Soc 2002;149(2):E26-E34.

[31] Pournaghi-Azar MH, Habibi B. Electropolymerization of aniline in acid media on the bare and chemically pre-treated aluminium electrodes. A comparative characterization of the polyaniline deposited electrodes. Electrochim Acta 2007;52(12):4222-4230.

[32] Dall'Acqua L, Tonin C, Varesano A, Canetti M, Porzio W, Catellani M. Vapour phase polymerisation of pyrrole on cellulose-based textile substrates. Synth Met 2006;156(5-6):379-386.

[33] Dall'Acqua L, Tonin C, Peila R, Ferrero F, Catellani M. Performances and properties of intrinsic conductive cellulose–polypyrrole textiles. Synth Met 2004;146(2):213-221.

[34] Spectral Database for Organic Compounds of the National Institute of Advanced Industrial Science and Technology (AIST). Available from: http://riodb01.ibase.aist.go.jp/sdbs/cgi-bin/cre_index.cgi?lang=eng.

[35] Jiang, L, Cui, Z. One-step synthesis of oriented polyaniline nanorods through electrochemical deposition. Polym Bull 2006;56(6):529-537.

[36] Osaka T, Ohnuki Y, Oyama N. IR absorption spectroscopic identification of electroactive and electroinactive polyaniline films prepared by the electrochemical polymerization of aniline. J Electroanal Chem 1984;161(2):399-405.

[37] Camalet JL, Lacroix JC, Nguyen TD, Aeiyach S, Pham MC, Petitjean J, Lacaze, PC. Aniline electropolymerization on platinum and mild steel from neutral aqueous media. J Electroanal Chem 2000;485(1):13-20.

[38] Hirase R, Shikata T, Shirai M. Selective formation of polyaniline on wool by chemical polymerization, using potassium iodate. Synth Met 2004;146(1):73-77

[39] Wen L, Kocherginsky NM. Doping-dependent ion selectivity of polyaniline membranas. Synth Met 1999;106(1):19-27.

[40] Rodrigues PC, Cantão MP, Janissek P, Scarpa PCN, Mathias AL, Ramos LP, Gomes AB. Polyaniline/lignin blends: FTIR, MEV and electrochemical characterization. Eur Polym J 2002;38(11):2213-2217.

[41] Sócrates G editor. Infrared characteristic group frequencies: tables and charts. Chichester: John Wiley & Sons; 1997.

[42] Kang ET, Neoh KG, Tan KL. Polyaniline: A polymer with many interesting intrinsic redox states. Prog Polym Sci 1998;23(2):277-324.

[43] Roßberg K, Paasch G, Dunsch L, Ludwig S. The influence of porosity and the nature of the charge storage capacitance on the impedance behaviour of electropolymerized polyaniline films. J Electroanal Chem 1998;443(1):49-62.

[44] Macdonald JR, editor. Impedance spectroscopy. Emphasizing solid materials and systems. (Ch. 2 and 3). New York: Wiley, 1987. p. 27-190.

[45] Hwang JH, Pyo M. pH induced mass and volume changes of perchlorate doped polypyrrole. Synth Met 2007;157(2-3):155-159.

[46] Münstedt H. Properties of polypyrrole treated with base and acids. Polymer 1986;27(6):899-904.

[47] MacDiarmid AG. Synthetic metals: a novel role for organic polymers. Synth Met 2002;125(1):11-22.

[48] Bater C, Sanders M, Craig Jr JH, Pannell KH, Wang PW. Observation of an enhanced N1s shake-up satellite on nitrided Si(100) and correlation with N bonding geometry. Appl Surf Sci 2000;161(3-4):328-332.

[49] R. Benoit CNRS Orléans, Y. Durand, B. Narjoux, G. Quintana, Y. Georges, X-Ray Photoelectron Spectroscopy Database. La Surface, Thermo Electron Corporation, Thermo Electron France. Available from:

http:// www.lasurface.com/database/elementxps.php.

[50] Rajagopalan R, Iroh JO. Characterization of polyaniline-polypyrrole composite coatings on low carbon steel: a XPS and infrared spectroscopy study. Appl Surf Sci 2003;218(1-4):58-69.

[51] Paterno LG, Manolache S, Denes F. Synthesis of polyaniline-type thin layer structures under low-pressure RF-plasma conditions. Synth Met 2002;130(1):85-97.

[52] Yu D, Cheng J, Yang Z. Performance of polyaniline-coated short carbon fibers in electromagnetic shielding coating. J Mater Sci Technol 2007;23(4):529-534.

13.- ARTÍCULO

INFLUENCE OF THE SCAN RATE ON THE MORPHOLOGY OF POLYANILINE GROWN ON CONDUCTING FABRICS. CENTIPEDE-LIKE MORPHOLOGY

Influence of the scan rate on the morphology of polyaniline grown on conducting fabrics. Centipede-like morphology

J. Molina, A.I. del Río, J. Bonastre, F. Cases [*]

Departamento de Ingeniería Textil y Papelera, EPS de Alcoy, Universidad Politécnica de Valencia, Plaza Ferrándiz y Carbonell s/n, 03801 Alcoy, Spain

Abstract

We report the apparition of different polyaniline (PANI) morphologies when different scan rates were employed in the electrochemical deposition of PANI on conducting fabrics. The most impressive structure obtained was the centipede-like morphology. PANI was deposited on conducting textiles of polyester covered with polypyrrole (PPy)/anthraquinone sulphonic acid (AQSA) by means of cyclic voltammetry. With the scan rates of 50 mV s^{-1} and 5 mV s^{-1} PANI with centipede-like morphology was obtained in the first scans. Globular PANI gained importance for higher number of scans due to the formation of new nucleation sites. When a scan rate of 1 mV s^{-1} was employed a variety of different morphologies were observed, such as: fibrillar, stalagmite-like, coral-like and plain irregular forms. Such variety of morphologies is due to the slow growth that allowed different types of morphologies.

Keywords: Polyaniline; electropolymerization; conducting fabrics; morphology; centipede-like morphology.

_____

* Corresponding author. Fax.: +34 96 652 8438

E-mail address: fjcases@txp.upv.es (Prof. F. Cases)

1. Introduction

Polyaniline (PANI) is one of the most widely employed conducting polymers and, between the years 1993-2002 it was at the top of the number of research papers in the field of conducting polymers [1]. PANI layers have been used as gas sensors [2,3] electrode material for redox supercapacitor [4], shield material for electromagnetic interference control [5], corrosion control [6], etc. It has been reviewed that conducting polymers are promising materials in the field of catalysis [7]. During the last years; the development of polymer nanostructures has been an important item in the field of conducting polymers. For instance, PANI nanofibers have demonstrated to have higher sensitivity and lower time response than traditional films when used as gas sensors [3]. Different 1-D nanostructures have been reported for PANI obtained by chemical oxidation synthesis: plate-like structures [8], leaf-like structures [9], nanoflakes [10], nanofibers [10-16], nanotubular [17,18], nanospheres [9,14,19] and nanostructured covered rectangular shapes [20]. The aggregation or growth of different microstructures can cause the apparition of 3-D structures. Flower-like structures [8,12], mushroom-like morphology [18], 3-D box-like structures composed of nanofibers [11] and micromats of nanofibers have been reported [13]. Zhou et al. reported also the apparition of nanosheet, nanorod based microspheres and nanorod based microrods in alkaline solution synthesis [9].

Electrochemical methods are appropriate for the synthesis of conducting polymers. The synthesis can be easily controlled and the polymer is obtained in its oxidized form. The morphology obtained by means of electrochemical synthesis is less varied than with chemical oxidation methods. The most observed morphology in bibliography is PANI nanofibers [4,21-25] that in some cases form nano-wires networks as 3-D structures. Also coral-like structures have been reported [25].

The production of textiles with new properties, such as conductivity, is a new field being investigated. Conducting polymers can be deposited on textile surfaces chemically [26,27] or by indirect electrochemical deposition [28]. The chemical deposition produces a smooth layer of polymer on the fibers of the fabric. The electrochemical polymerization is a suitable method for obtaining microstructured PANI on conducting textiles. In this work PANI has been deposited potentiodinamically on the surface of conducting fabrics (polyester covered with PPy/AQSA). Since the substratum is conductive, a direct electrochemical deposition can be performed. Different scan rates were employed to obtain different growth velocities. It has been demonstrated that the scan rate has influence on the morphology of PANI. Different morphologies have been

obtained, but the most surprising is the centipede-like morphology obtained at 50 mV s^{-1} and 5 mV s^{-1}. PANI branched structures have been obtained by chemical oxidation methods [29,30]. However, their structure was less ordered than the centipede-like structure obtained in this paper.

2. Experimental

2.1. Reagents and materials

Analytical grade aniline, pyrrole, ferric chloride, anthraquinone-2-sulfonic acid sodium salt (AQSA) and sulphuric acid were purchased from Merck. Normapur acetone was from Prolabo. Ultrapure water was obtained from an Elix 3 Millipore-Milli-Q RG system with a resistivity near to 18.2 MΩ cm.

Aniline was purified by distillation before use. The distillation was performed at reduced pressure in order to avoid thermal degradation of the monomer. After distillation aniline was stored in the dark at 0 ºC.

Polyester textile was acquired from Viatex S.A. and their characteristics were: fabric surface density, 140 g m^{-2}; warp threads per cm, 20 (warp linear density, 167 dtex); weft threads per cm, 60 (weft linear density, 500 dtex). These are specific terms used in the field of textile industry and their meaning can be consulted in a textile glossary [31].

2.2. Chemical synthesis of PPy/AQSA on polyester fabrics

Chemical synthesis of PPy on polyester textiles was done as reported in our previous study [32]. The size of the samples was 6 cm x 6 cm approximately. Previously to reaction, polyester was degreased with acetone in ultrasound bath and washed with water. Pyrrole concentration employed was 2 g/l and molar relations of reagents employed in the chemical synthesis bath were pyrrole:FeCl$_3$:AQSA (1:2.5:0.6). The next stage was the adsorption of pyrrole and counter ion (AQSA) (V=200 ml) on the fabric for 30 min at 0 ºC without stirring. At the end of this time, the FeCl$_3$ solution (V=50 ml) was added and oxidation of the monomer took place during 150 min at 0 ºC without stirring. Adsorption and reaction were performed in a precipitation beaker. The conducting fabric was washed with water to remove PPy not joined to fibers. The conducting textile was

dried in a desiccator for at least 24 h before measurements. The weight increase was measured obtaining a value between 4-6 %.

2.3. Electrochemical synthesis of PANI films on conducting fabrics.

Electrosyntheses were performed by cyclic voltammetry using an Autolab PGSTAT302 potentiostat/galvanostat. All electrochemical experiments were carried out at room temperature and without stirring. The counter electrodes (CE) employed were made of stainless steel; the pre-treatment consisted on polishing, degreasing with acetone in ultrasonic bath and washing with water in an ultrasonic bath. In electrochemical synthesis two CE were used to equalize the electrical field around the working electrode (WE) of conducting textile. The WEs were made by cutting a strip of the conducting fabric of PES-PPy/AQSA (0.5 cm wide x 2.5 cm length). The electric contact was made by means of two Ti plates, the sample was located between them. Potential measurements were referred to Ag/AgCl (3 M KCl) reference electrode. Oxygen was removed from solution by bubbling nitrogen gas.

The conducting textile has an ohmic potential drop that it needs to be considered; otherwise the measured potentials will not be real. Therefore, the ohmic potential drop was measured and entered in the potentiostat/galvanostat.

Potentiodynamic syntheses were performed in aqueous medium with 0.5 M H_2SO_4 and 0.5 M aniline in N_2 atmosphere. The electrode of conducting textile was soaked with the solution for 10 minutes to allow the diffusion of the monomer to the textile electrode. Then, the potential was cycled between -0.2 V and 1.1 V. The upper potential limit of 1.1 V it would be excessive for the synthesis of PANI on metals like Pt since overoxidation would be expected. But it is an adequate potential to synthesize polyaniline on our conducting fabrics. The conducting fabric has an ohmic drop that varies with the applied potential since the electroactivity of conducting polymers varies with the potential. This phenomenon causes the displacement of the redox processes and aniline oxidation appears at higher potentials than it could be expected. Previous XPS analyses did not show important overoxidation at this potential [33].

Different samples were obtained at different scan rates for observing the influence of this parameter on the morphology of the PANI obtained. The scan rates employed were; 50 mV s^{-1}, 5 mV s^{-1} and 1 mV s^{-1}. With these values it has been covered a large range of synthesis velocities. Several samples were obtained at different number of scans for each scan rate to see the evolution of the conducting polymer growth.

2.4. SEM characterization

A Jeol JSM-6300 scanning electron microscope was employed to observe the morphology of the samples. SEM analyses were done using an acceleration voltage of 10 kV.

2.5. FTIR-ATR spectroscopy

Fourier transform infrared spectroscopy with horizontal multirebound attenuated total reflection (FTIR-ATR) was performed with a Nicolet Magna 550 Spectrometer equipped with DTGS detector. An accessory with pressure control was employed to equalize the pressure in the different solid samples. A prism of ZnSe was employed. Spectra were collected with a resolution of 4 cm^{-1}, and 100 scans were averaged for each sample.

2.6. Surface resisitivity measurements

Surface resistivity measurements were performed using a surface resistivity meter Model SRM-232-2000, 0-2000 Ω/square (Guardian Manufacturing) using the 4-point probe technique.

2.7. Electrochemical characterization by cyclic voltammetry

An Autolab PGSTAT302 potentiostat/galvanostat was employed to carry out the voltammetric measurements. The voltammetric measurements were carried out similarly to the electrochemical synthesis of PANI films on conducting fabrics. Only the medium employed (0.5 M H$_2$SO$_4$), the scan rate (1 mV s^{-1}) and the potential range (-0.2 V, +0.7 V) were varied. The sample of PES/PPy-AQSA and samples of PES/PPy-AQSA covered with PANI synthesized at 50 mV s^{-1}, 5 mV s^{-1} and 1 mV s^{-1} were measured. Five scans were used to obtain each PANI sample.

3. Results and discussion

3.1. Synthesis at 50 mV s^{-1}.

In Fig. 1-a it can be seen the voltammograms obtained during the potentiodynamic synthesis of PANI at 50 mV s^{-1}. During the five first scans it was not noticed an important increase in the current density. There were not oxidation or reduction characteristic peaks and a resistive response was obtained. In our previous study, it was found that only from the 20th scan the polymerization was obvious and an increase in the current density of the voltammograms was obtained [33]. The scan rate of 50 mV s^{-1} has been widely used in bibliography for the synthesis of conducting polymers on metals [24,25]. However, this scan rate seems to be inadequate for a substratum with a limited conductivity since the charge transfer is slower than in metals.
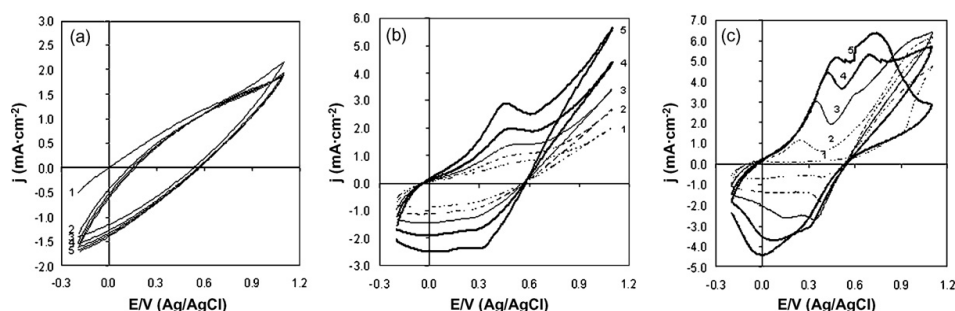

Fig. 1. PANI synthesis voltammograms on PES/PPy-AQSA at different scan rates. Synthesis conditions: 0.5 M H$_2$SO$_4$, 0.5 M aniline, start potential -0.2 V; range, -0.2 V, +1.1 V. a) 50 mV s^{-1}, b) 5 mV s^{-1}, c) 1 mV s^{-1}.

3.2. Synthesis at 50 mV s^{-1}: morphology

The fabric after the chemical polymerization was covered with a uniform and smooth layer of polypyrrole. No microstructures were observed; only the presence of aggregates of polypyrrole not joined to the fibers was outstanding [32]. The PANI synthesized after one scan showed the development of some polymer structures. However, more scans were needed to observe the polymer structures better. Samples after 5 and 10 scans were synthesized and analyzed. In Fig. 2-a it is showed the sample after 5 scans, the development of PANI with different morphologies is obvious. The most interesting structure present in the micrograph is the centipede-like morphology. Different PANI structures with centipede-like morphology can be observed in this micrograph. These structures have a central fiber and from this fiber, branched fibers are present at each side of the central fiber forming two rows of branched nanofibers. The angle

between the rows of branched nanofibers is approximately 180º, forming the centipede-like morphology. In this micrograph the length of the structures obtained was below 30 μm, but longer structures have been obtained. As this morphology has also been observed at 5 mV s^{-1}, the formation mechanism will be explained later. The concept of centipede-like molecular architecture can be found in bibliography [34-35]. Comb-g-comb centipedes have been reported in step-by-step synthesis [36]. Similar structures to that obtained in this paper have also been reported in inorganic films such as; boron nitride phosphide films [37] or CdTe films [38]. Nevertheless, the centipede-like morphology has not been reported in bibliography for conducting polymers to our knowledge. Only Hsieh et al. mentioned the apparition of PANI with centipede-like morphology [17]. However the morphology obtained by Hsieh et al. was like an accumulation of PANI nanofibers. Branched PANI nanofibers have been obtained by template-free synthesis, but the structure obtained was like a treelike superstructure [39]. The structure was not as ordered as the centipede-like morphology obtained in this paper. Another similar structure that has been mentioned for polymers in bibliography is the shish-kebab structure. This morphology has been obtained for high density polyethylene [40] or carbon nanotubes [41].

In Fig. 2-a it can also be seen the coexistence of Pani fibrils and Pani with stalagmite-like morphology. In Fig. 2-b an area with centipede and stalagmite-like morphology is magnified. The structures with stalagmite-like morphology grow with different orientations and their length is lower than 10 μm. This type of morphology has not been observed for PANI in bibliography. A substrate where the stalagmites can grow is needed to obtain the stalagmite-like morphology. The most similar morphology observed in bibliography is the needle-like morphology obtained by chemical oxidation [42]. Globular morphology has not been observed during the first scans, this fact demonstrates that the nucleation sites are limited during these scans. The posterior growth goes through the nucleation sites formed previously. This allows the formation of stalagmite-like, fibril or centipede-like forms. In Fig. 2-c an isolated centipede-like structure can be observed. The structure has been magnified for better observation in the inset figure. The average diameter of the branched nanofibers is around 200 nm and their length is between 1-3 μm approximately. In Fig. 2-d it is showed a micrograph of a sample after 10 scans. A lot of centipede-like structures can be observed as well as PANI fibers. With higher number of scans the globular morphology gains importance due to the formation of a lot of nucleation sites (figure not showed) [33]. The morphology of PANI synthesized on conducting fabrics depends on the electrochemical method of

synthesis too. Although the potentiostatic synthesis is a method which can control easily the amount of consumed electricity (Q), lots of nucleation sites were produced during the synthesis and only globular PANI was obtained [33]. We observed that with the potentiodynamic technique microfibers were obtained [33]. This is why cyclic voltammetry and different scan rates were selected as an alternative method to produce PANI nanostructures on conducting fabrics.
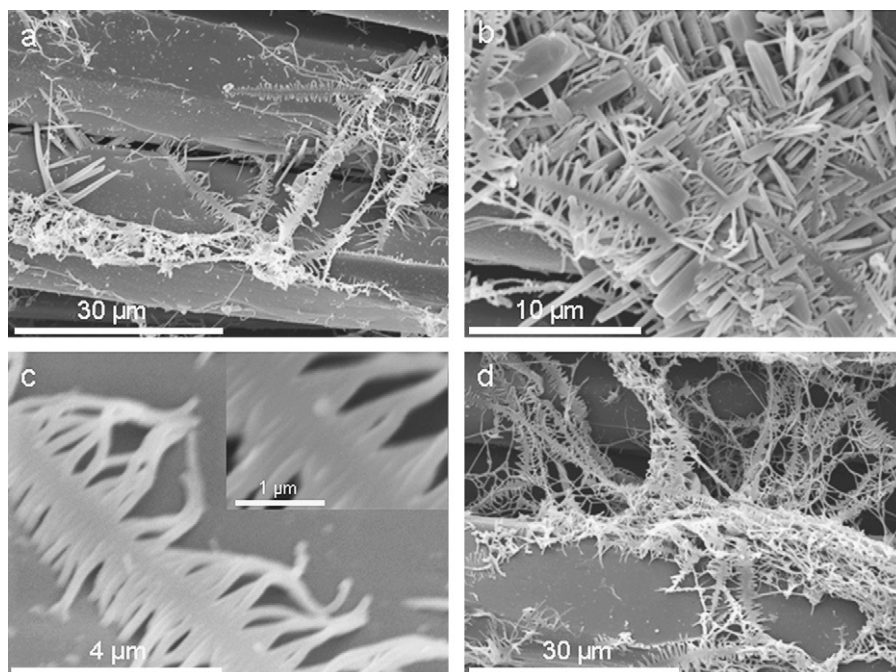
Fig. 2. Micrographs of PANI synthesized by cyclic voltammetry on PES/PPy-AQSA. Synthesis conditions: 0.5 M H$_2$SO$_4$; 0.5 M aniline; start potential, -0.2 V; range, -0.2 V, +1.1 V; scan rate, 50 mV s^{-1}. a) 5 scans (2000x), b) 5 scans (5000x), c) 5 scans (15000x); inset (35000x), d) 10 scans (2000x).

3.3. Synthesis at 5 mV s^{-1}

In Fig. 1-b it can be seen the voltammograms obtained during the potentiodynamic synthesis of PANI at 5 mV s^{-1}. Only from the third scan it could be noticed the appearance of one oxidation and one reduction peaks. Besides, the peak maximum position changed with the number of scan. In the fifth scan the maximum of the oxidation peak was located at 0.49 V and the maximum of the reduction peak at 0.30

V. The current density increased with the number of scans, fact that demonstrates that electropolymerization was taking place. At 50 mV s^{-1} no redox peaks were observed, so the scan rate has influence on PANI formation and apparition of oxidation and reduction peaks in the voltammograms. The substratum has an ohmic drop that difficulties the charge transfer and the electrochemical processes. PPy is the polymer originally deposited on the surface of the fabric to produce conducting fabrics. When the electrochemical measurements are carried out, the charge transfer begins from the zone below the electric contact and extends to the other parts of the electrode. This transformation requires time; the charge transfer goes through PPy and Pani when it is formed, since polyester is an insulating material. Then, oxidation and reduction processes can only be observed if the process is so slow to allow the polymer transformation. With lower scan rates (5 mV s^{-1} and 1 mV s^{-1}) the oxidation and reduction processes can be observed due to the slow scan velocity that allows the development of these processes. That is why a resistive response was obtained at 50 mV s^{-1}, there was no sufficient time to allow the polymer transformation and the oxidation and reduction peaks of polyaniline were not observed. So it can be concluded that the scan rate affects the synthesis of PANI by potentiodynamic methods.

3.4. Synthesis at 5 mV s^{-1}: morphology

The micrographs of the sample after one scan did not show a general polymerization of aniline on the surface of the fabric. Only in some areas the growth of PANI with fibrillar morphology was observed, as it can be seen in Fig. 3-a. If this micrograph is analyzed in more detail, it can be seen that the actual morphology in some parts of the micrograph is a centipede-like morphology, as it was obtained for 50 mV s^{-1}. The centipede-like morphology can be clearly appreciated in Fig. 3-b since the structure is more developed than in Fig. 3-a. In Fig. 3-b two centipede-like structures can be observed. The length of the branched nanofibers is not regular, since there are fibers more developed than others as it can be noted in Fig. 3-b. The amount of consumed electricity (Q) is another important factor in the synthesis and is directly related to the scan rate employed. With higher scan rates, the Q is lower than with lower scan rates. At 50 mV s^{-1} and 5 mV s^{-1}, during the first polymerization stage the nucleation centers were limited due to the low Q and only few PANI microfibers were formed. According to the classical nucleation theory, the nanofibers formed previously can serve as nucleation sites for new nanofibers [29,30,39]. It seems that the secondary growth is easier if it is

produced on the preformed microfibers than when it is produced on the surface of the conducting fabric. The new nucleation sites are predominantly formed on the surface of the preformed microfibers. So it seems that the first step is the formation of PANI fibers on the surface of the fabric. Later new nucleation sites are generated on the microfibers of PANI generated previously. This nucleation sites generate new fibers that begin to grow regularly at both sides of this central fiber. The mechanism of formation for this type of morphology has been represented in Fig. 4.
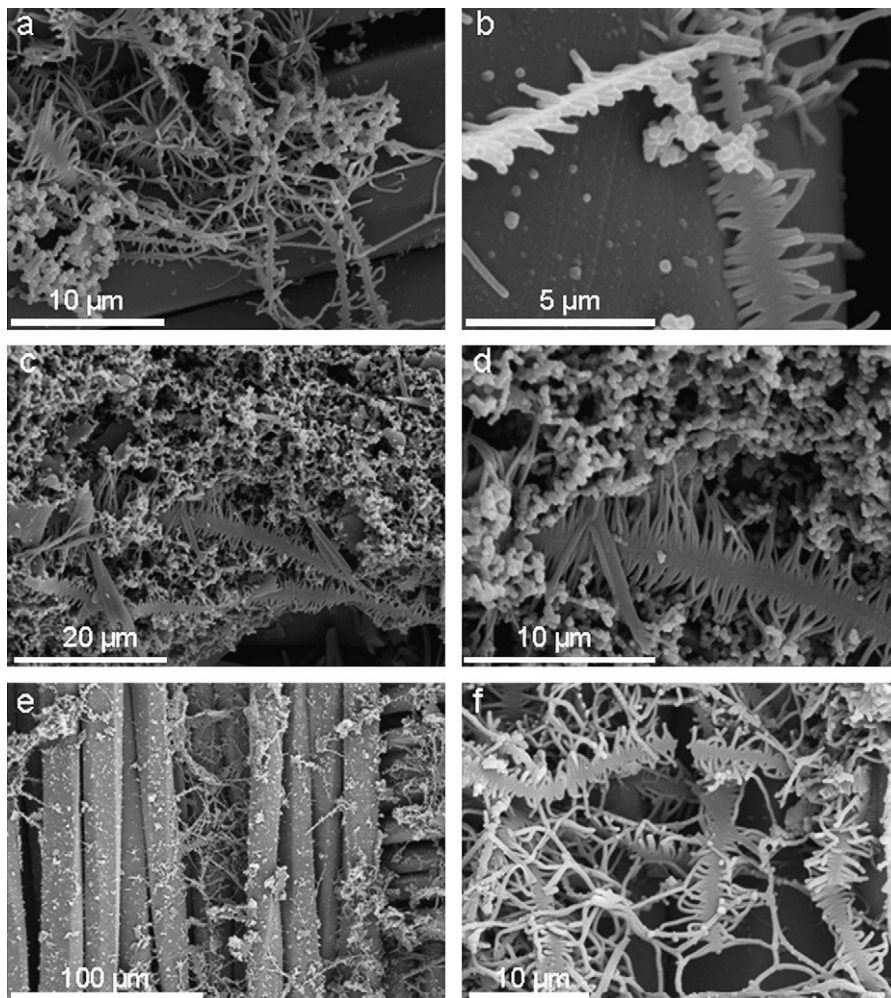

Fig. 3. Micrographs of PANI synthesized by cyclic voltammetry on PES/PPy-AQSA. Synthesis conditions: 0.5 M H_2SO_4; 0.5 M aniline; start potential, -0.2 V; range, -0.2 V, +1.1 V; scan rate, 5 mV s^{-1}. a) 1 scan (4000x), b) 1 scan (10000x), c) 2 scans (2000x), d) 2 scans (5000x), e) 3 scans (500x), f) 3 scans (3000x).

Branched structures have been obtained with chemical oxidation methods [29,30], but their growth was not as ordered as that obtained in this paper. In this paper it has been achieved the regular growth of PANI nanofibers at both sides of the fibers generated previously. In the case of 50 mV s^{-1} the growth of centipede-like structures was more extended than with a scan rate of 5 mV s^{-1}.
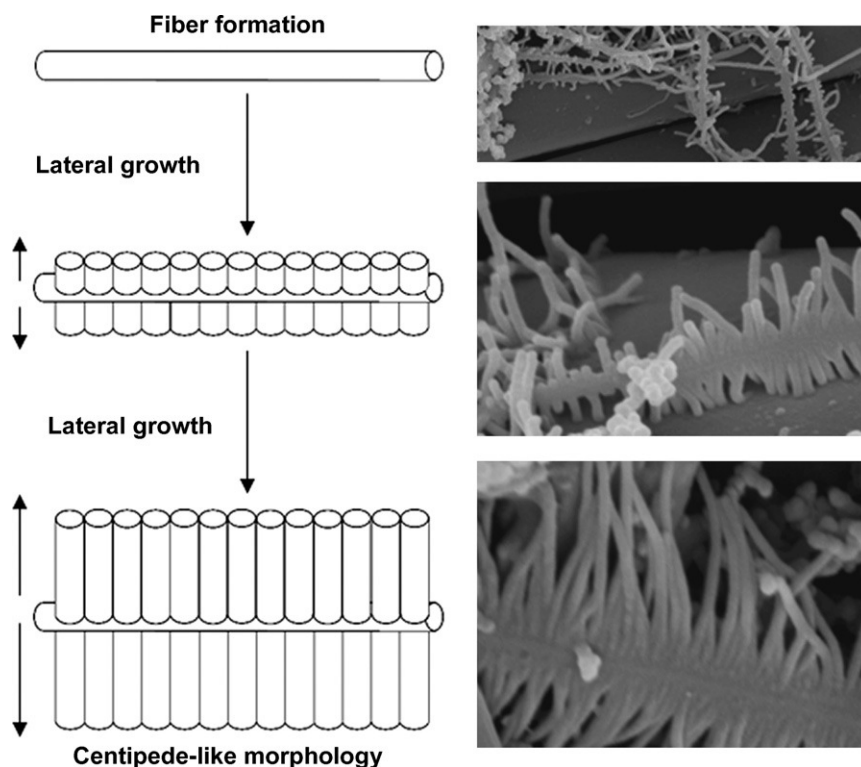
Fig. 4. Formation process for centipede-like morphology.

With a scan rate of 5 mV s^{-1} it was employed more Q than with a scan rate of 50 mV s^{-1}; this implied the formation of more nucleation sites. This is the reason why globular morphology was observed for low number of scans at 5 mV s^{-1} but not at 50 mV s^{-1}. In Fig. 3-c it can be seen the micrograph of a sample after two scans. In this figure, it can be seen that the two centipede-like structures present in this micrograph are longer than 60 µm. One of these structures has been magnified in Fig. 3-d. The scan rate did not affect the diameter of the branched nanofibers, the diameter was the same that for

50 mV·s^{-1}, 200 nm approximately. So each of the structures in Fig. 3-c had nearly 600 branched microfibers (300 on each side of the central fiber). The length of the branched nanofibers was approximately 3 µm. As it was mentioned previously, PANI with globular morphology has also been observed in all figures. This fact is due to the development of new nucleation sites as the number of scan and Q increase. Fig. 3-e,f show the morphology of the sample after three scans. In Fig. 3-e it can be seen that some centipede-like structures are present. The magnified micrograph (Fig. 3-f) shows this fact. In this micrograph several centipede-like structures and several isolated fibers can be observed. After seven scans (figure not showed), the surface of the sample was covered by PANI with globular and fibrillar morphology. The centipede-like morphology can be hardly observed since it has been covered by PANI with globular and fibrillar morphology. The original fibers of the fabric can still be observed as the fabric has not been entirely covered by PANI.

3.5. Synthesis at 1 mV s^{-1}

In Fig. 1-c it can be seen the voltammograms obtained during the potentiodynamic synthesis of PANI at 1 mV s^{-1}. From the first scan it could be noticed the appearance of oxidation and reduction peaks. In the second scan it appeared an oxidation peak at 0.26 V and a reduction peak at 0.38 V. In the following scans it could be noted a displacement of both, the oxidation and reduction peaks. The oxidation peaks were displaced to more positive potentials and the reduction peaks were displaced towards less positive potentials. The current density grew with the number of scans, indicating PANI deposition. As it was pointed out, the scan rate has influence on the cyclic voltammetry measurements. With a scan rate of 1 mV s^{-1} more oxidation and reduction peaks than at 5 mV s^{-1} were observed.

3.6. Synthesis at 1 mV s^{-1}: morphology

In Fig. 5-a it is showed the micrograph of the conducting textile after one scan. As it can be seen, all the surface of the fabric has been covered with PANI. A network of PANI has grown on the surface of the fabric but the original fibers of the fabric can still be observed. It can be noticed that the scan rate (and consequently Q) has a great influence on the velocity of deposition of PANI. In the first scan; with a scan rate of 50 mV s^{-1}; PANI deposition was almost negligible; with 5 mV s^{-1} the growth was small and with 1 mV s^{-1} the growth was widespread and the whole surface of the fabric was almost

covered with PANI. The morphology of the deposit in Fig. 5 is variable and different types of morphology have been observed. Fibrillar morphology and globular morphology are the most observed PANI forms. As it has been observed, it seems that the first polymerization step is the formation of PANI microfibers. The lack of new nucleation sites during the first stage of the polymerization can be the reason. During the secondary growth, a lot of new nucleation sites are generated on the preformed microfibers and PANI with globular morphology is developed. Huang et al. [43] observed the same process in the chemical polymerization of aniline. To obtain only fibrillar PANI and suppress the secondary growth, they employed interfacial polymerization. During the secondary growth, the apparition of new nucleation sites is higher at 1 mV s^{-1} than at 50 mV s^{-1} and 5 mV s^{-1}. This is due to the fact that the Q employed is higher at 1 mV s^{-1} than at these scan rates. This does not allow the formation of centipede-like structures. In some areas of the fabric PANI microfibers can be clearly observed as it is showed in Fig. 5-b. The growth of the fibers in this area was not straight and the fibers were twisted. The appearance of the fibers is like an octopus tentacle since there are globular particles distributed uniformly along the surface of the fibers. This can be the origin of the subsequent globular growth that has been observed. In other areas, the secondary globular growth hinders the observation of the microfibers. The fibrillar and globular morphology are the predominant PANI forms at this scan rate, however other types of morphology have also been observed in the sample synthesized with only one scan. These types of morphology have not been observed with higher number of scans, since the widespread growth of PANI with globular morphology hindered their observation. It has been observed the coexistence of PANI with plain and irregular structure and PANI with stalagmite-like morphology. In Fig. 5-c the area with stalagmite-like morphology has been magnified for better observation. The growth of stalagmite-like PANI is straight but there is no predominant orientation for the growth. It has been observed the development of PANI structures in all directions. Their average length is lower than 10 μm and their average width is lower than 1 μm. In Fig. 5-d it can be appreciated the development of PANI forms with irregular and plain structure. The different irregular forms have a plain structure on its main planes. However their sides are not regular and have not a predominant shape. The size of the longest side of these irregular forms is not higher than 10 μm. Similar morphology was obtained by Zhu et al. [11]. However, they obtained 3-D box-like structures composed of assembled 1-D nanofibers. In our samples, higher magnification showed that the structures were compact and no

substructures could be observed. The explanation for these morphologies could be the slower velocity of growth in some areas of the fabric due to a higher electrical resistance. After two scans the fabric was entirely covered with fibrillar and globular PANI and the textile substratum could be hardly observed. A network that covered the whole surface of the fabric was formed.

Fig. 5. Micrographs of PANI synthesized by cyclic voltammetry on PES/PPy-AQSA. Synthesis conditions: 0.5 M H_2SO_4; 0.5 M aniline; start potential, -0.2 V; range, -0.2 V, +1.1 V; scan rate, 1 mV s^{-1}; 1 scan for all the samples. a) (100x), b) (5000x), c) (6000x), d) (1000x).

In Fig. 6-a it can be observed an area of the fabric that was not covered with globular PANI. It can be observed PANI with fibrillar and irregular forms as it happened with only one scan. The development of PANI with globular morphology is general on the fabric surface. PANI with coral-like morphology has also been observed as it can be seen in Fig. 6-b. This morphology has also been observed for the potentiodynamic synthesis of PANI on glassy carbon electrodes [44]. The fibers of the fabric cannot be observed after three scans as it can be seen in Fig. 6-c. PANI with globular morphology

(Fig. 6-d) has covered all the surface of the fabric. Higher number of scans does not produce any changes in the samples and only globular morphology is observed.
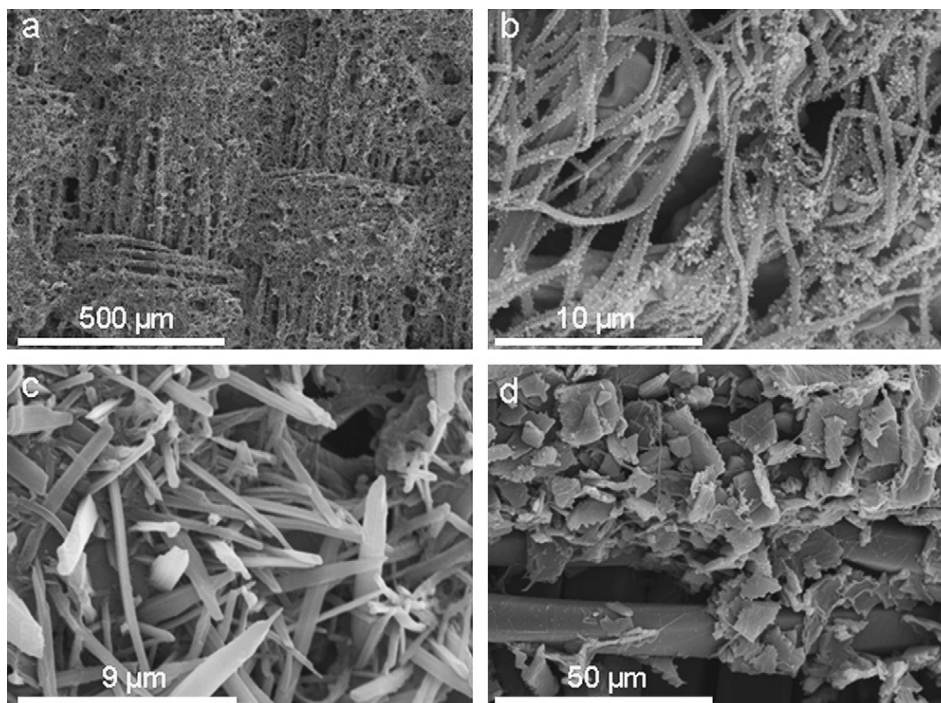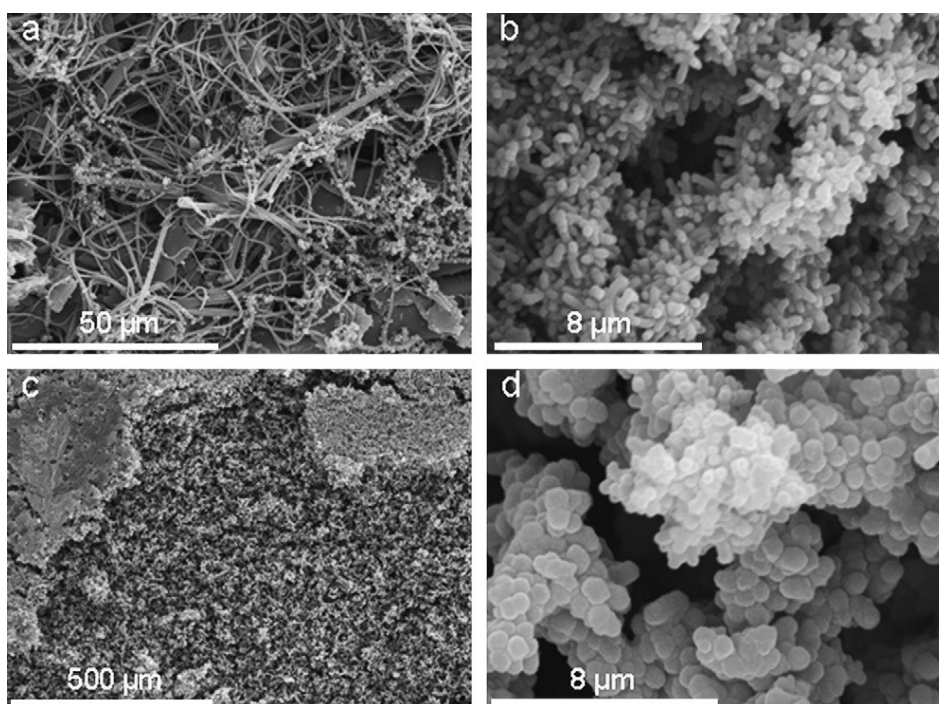

Fig. 6. Micrographs of PANI synthesized by cyclic voltammetry on PES/PPy-AQSA. Synthesis conditions: 0.5 M H$_2$SO$_4$; 0.5 M aniline; start potential, -0.2 V; range, -0.2 V, +1.1 V; scan rate, 1 mV s^{-1}. a) scan 2 (1000x), b) scan 2 (x5000), c) scan 3 (100x), d) scan 3 (7000x).

3.7. FTIR-ATR spectroscopy

Fig. 7 shows the spectra of PES/PPy-AQSA and PES/PPy-AQSA covered with PANI after five scans at different scan rates (50 mV s^{-1}, 5 mV s^{-1} and 1 mV s^{-1}). The spectrum of PES/PPy-AQSA shows characteristic bands of PPy like: C=C stretching (1550 cm^{-1}) [45,46], C-C stretching (1450 cm^{-1}) [45,46], C-N stretching (1300 cm^{-1}) [45,46], PPy bending (1160, 1030, 775 cm^{-1}) [45,46]. One band attributed to the counter ion (AQSA) can be observed around 1670 cm^{-1} [47]. The bands at 1700, 1080, 960 and 705 cm^{-1} are due to the polyester substrate.

Fig. 7. FTIR-ATR spectrum of PES/PPy-AQSA and PANI synthesized on PES/PPy-AQSA potentiodinamically at 50 mV s⁻¹, 5 mV s⁻¹ and 1 mV s⁻¹. Sample area, 2 cm²; resolution; 4 cm⁻¹,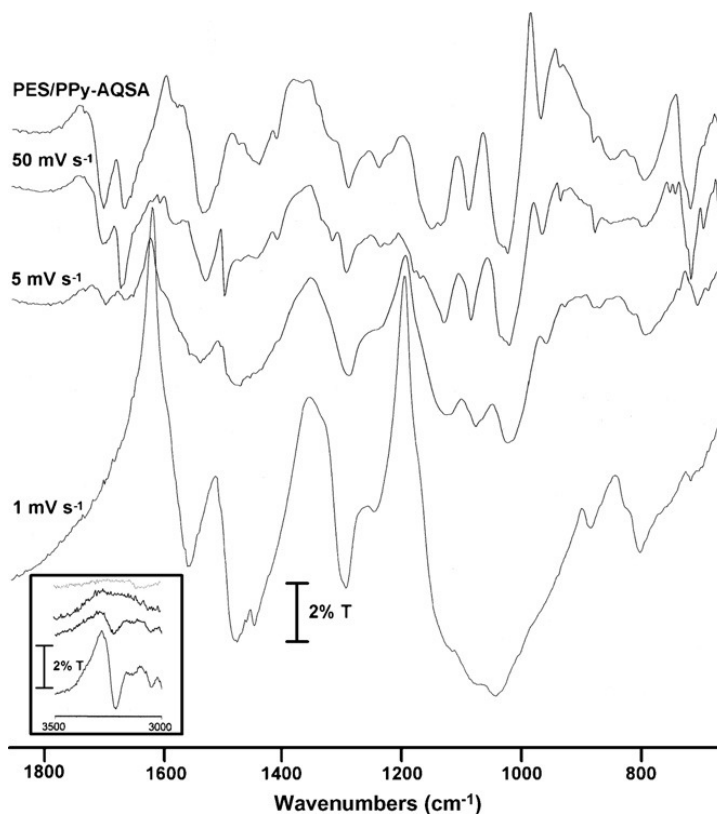 100 scans. Synthesis conditions: 0.5 M H₂SO₄; 0.5 M aniline; start potential, -0.2 V; range, -0.2 V, +1.1 V; five scans for all the samples.

With the synthesis at 50 mV s⁻¹, the spectrum is slightly modified; only the apparition of a band around 1490 cm⁻¹ is remarkable. The PANI deposit after five scans at 50 mV s⁻¹ was not extended as it was corroborated by means of SEM. With a scan rate of 5 mV s⁻¹ it can be noticed the diminution of the different bands attributed to polyester and AQSA. This fact is due to the thick layer of PANI formed at 5 mV s⁻¹ that difficulties the infrared radiation penetration to the substrate. One band attributed to the stretching vibrations of benzenoid rings of PANI can be observed around 1470 cm⁻¹ [48]. It can also be noticed the increase in the intensity of the band at 1300 cm⁻¹ (C-N stretching). This band is present in PPy and PANI but the increase in its intensity indicates that the amount of PANI has increased. With a scan rate of 1 mV s⁻¹, the bands

of PES and AQSA have disappeared since PANI film is thick enough to avoid their observation. The bands at 1470 and 1300 cm^{-1} also increased their intensity. In the inset figure it is showed the zone between 3500 and 3000 cm^{-1}. It can be seen that a band around 3220 cm^{-1} increases its intensity as the scan rate of synthesis decreases. This band is attributed to the N-H stretching that presents PANI structure [48,49], so its intensity is directly related to the amount of PANI present in the sample. With lower scan rates, the consumed electricity (Q) is higher than with lower scan rates and consequently the amount of polymer formed is higher.

3.8. Cyclic voltammetry

Fig. 8 shows the characterization voltammograms of PES/PPy-AQSA and PES/PPy-AQSA covered with PANI synthesized at different scan rates (50 mV s^{-1}, 5 mV s^{-1} and 1 mV s^{-1}). Five scans were employed to synthesize the samples covered with PANI. In the figure it is shown the fifth scan for all the samples. It has been corroborated that the scan rate has influence on the synthesis of PANI on conducting fabrics as we explained previously. The same problem appears in the electrochemical characterization by cyclic voltammetry. To minimize this problem and obtain the best electrochemical response, it has been used the lowest scan rate to characterize the samples (1 mV s^{-1}). The original sample of PES/PPy-AQSA only showed oxidation current densities values around 0.5 mA cm^{-2}. The surface resistivity measured for this sample was 40 Ω/□. When PANI was synthesized at 50 mV s^{-1} the characterization voltammogram did not change significantly; the same occurred with the surface resistivity. The characterization of the sample synthesized at 5 mV s^{-1} showed an important increase in the current density; current density values of nearly 3 mA cm^{-2} were reached. This voltammogram has been magnified for better observation of the peaks (Fig. 8, inset figure). One oxidation peak appeared located around 0.41 V and two reduction peaks at 0.37 V and 0.11 V were observed. The surface resistivity obtained was around 19 Ω/□. When the synthesis scan rate synthesis was decreased to 1 mV s^{-1}, the current density in the voltammogram of characterization increased to more than 9 mA cm^{-2}. Two redox peaks could be clearly distinguished; one oxidation peak at 0.58 V and one reduction peak at 0.2 V. The surface resistivity decreased to a value of 3 Ω/□. The synthesis of PANI on conducting fabrics increases the electroactivity of the samples. The lower the scan rate during the synthesis, the higher polymer deposition rate and the higher the electrochemical response was found.
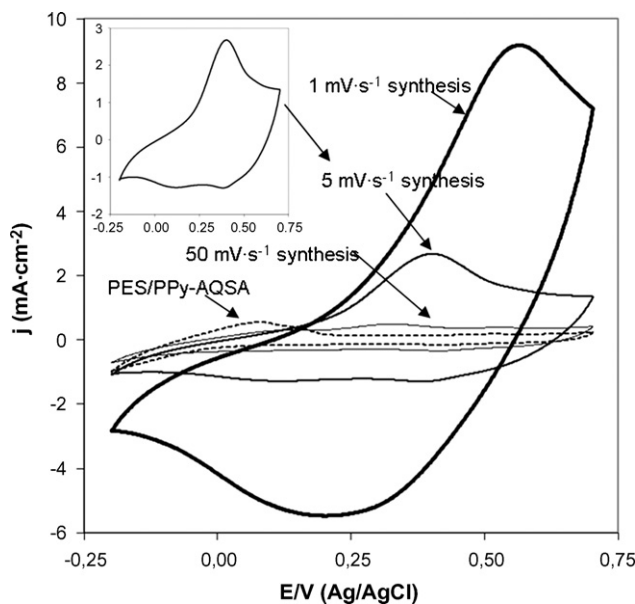
Fig. 8. Cyclic voltammograms of characterization at 1 mV s⁻¹ of different samples (PES/PPy-AQSA and PANI synthesized on PES/PPy-AQSA potentiodinamically at 50 mV s⁻¹, 5 mV s⁻¹ and 1 mV s⁻¹). Characterization conditions: 0.5 M H₂SO₄ aqueous medium; start potential, -0.2 V; range, -0.2 V, +0.7 V; scan rate, 1 mV s⁻¹; fifth scan for all the samples. Inset figure: 5 mV s⁻¹ magnified.

4. Conclusions

Electrochemical methods are suitable methods to obtain nanostructured materials as it has been reported in this article. It has been demonstrated that the scan rate has influence on the morphology and the formation of PANI deposited on conducting fabrics by means of cyclic voltammetry. The higher the scan rate, the lower the polymer formation rate was obtained. This is due to the fact that less amount of electricity (Q) is consumed with higher scan rates. At 50 mV s⁻¹, the polymer formation was very slow and no oxidation or reduction peaks were observed in the voltammograms of synthesis. A decrease in the scan rate produced the apparition of oxidation and reduction peaks in the voltammograms. The polymer rate deposition was also increased as the scan rate decreased. These facts can be explained as follows: the charge transfer is produced through the layer of conducting polymer since the substrate (polyester) is an insulating material. If the scan rate is too fast, there is not enough time to allow the polymer

transformation. The charge transfer is more difficult, the polymer deposition is slower and the redox processes are not observed.

At 50 mV s^{-1} and 5 mV s^{-1} it has been observed the formation of PANI with centipede-like morphology that has not been reported for conducting polymers in bibliography to our knowledge. It seems that the first step was the formation of PANI microfibers. During the secondary growth, branched nanofibers began to grow regularly on both sides of the preformed fibers. Centipede-like structures with a length of 60 μm have been obtained. The width of the branched nanofibers was 200 nm approximately, so structures with nearly 600 branched nanofibers have been obtained. With higher number of scans, globular and fibrillar forms of PANI gain significance due to the generation of new nucleation sites.

With a scan rate of 1 mV s^{-1}, the most widespread form was the fibrillar morphology. As the number of scans increased, the globular morphology gained importance. Stalagmite-like morphology, coral-like morphology and plain and irregular structures have also been observed. Zones with higher electrical resistance and the slow velocity of formation could be the reason for the formation of these types of morphologies.

FTIR-ATR spectroscopy demonstrated the presence of different bands attributed to PANI. The lower the scan rate, the higher the amount of PANI deposited on the fabric. This is due to the higher consumption of electricity (Q). Cyclic voltammetry measurements showed the same tendency. With lower scan rates the electrochemical response was higher due to the presence of more PANI on the sample.

References

[1] M. Trojanowicz, Microchim. Acta 143 (2003) 75.

[2] D. Nicolas-Debarnot, F. Poncin-Epaillard, Anal. Chim. Acta 475 (2003) 1.

[3] J. Huang, S. Virji, B.H. Weiller, R.B. Kaner, J. Am. Chem. Soc. 125 (2003) 314.

[4] V. Gupta, N. Miura, Electrochem, Solid-State Lett. 8 (2005) A630.

[5] S.K. Dhawan, N. Singh, S. Venkatachalam, Synth. Met. 125 (2002) 389.

[6] D. Sazou, M. Kourouzidou, E. Pavlidou, Electrochim. Acta 52 (2007) 4385.

[7] A. Malinauskas, Synth. Met. 107 (1999) 75.

[8] C. Zhou, J. Han, R. Guo, Macromolecules 41 (2008) 6473.

[9] C. Zhou, J. Han, G. Song, R. Guo, Eur. Polym. J. 44 (2008) 2850.

[10] C.A. Amarnath, J. Kim, K. Kim, J. Choi, D. Sohn, Polymer 49 (2008) 432.

[11] Y. Zhu, J. Li, M. Wan, L. Jiang, Polymer 49 (2008) 3419.

[12] Z. Zhang, J. Deng, L. Yu, M. Wan, Synth. Met. 158 (2008) 712.

[13] C. Zhou, J. Han, G. Song, R. Guo, Macromolecules 40 (2007) 7075.

[14] P. Anilkumar, M. Jayakannan, Macromolecules 40 (2007) 7311.

[15] S.P. Surwade, N. Manohar, S.K. Manohar, Macromolecules 42 (2009) 1792.

[16] G. Li, L. Jiang, H. Peng, Macromolecules 40 (2007) 7890.

[17] B.-Z. Hsieh, H.-Y. Chuang, L. Chao, Y.-J. Li, Y.-J. Huang, P.-H. Tseng, T.-H. Hsieh, K.-S. Ho, Polymer 49 (2008) 4218.

[18] Q. Sun, Y. Deng, Mater. Lett. 62 (2008) 1831.

[19] Y. He, J. Lu, React. Funct. Polym. 67 (2007) 476.

[20] C. Zhou, J. Han, R. Guo, Macromolecules 42 (2009) 1252.

[21] Y. Guo, Y. Zhou, Eur. Polym. J. 43 (2007) 2292.

[22] H. Zhang, J. Wang, Z. Wang, Z. Zhang, S. Wang, Synth. Met. 159 (2009) 277.

[23] H.H. Zhou, S.Q. Jiao, J.H. Chen, W.Z. Wei, Y.F. Kuang, Thin Solid Films 450 (2004) 233.

[24] S.J. Choi, S.M. Park, J. Electrochem. Soc. 149 (2002) E26.

[25] L.J. Duić, Z. Mandić, F. Kovačiček, J. Polym. Sci. Part A: Polym. Chem. 32 (1994) 105.

[26] K.W. Oh, S.H. Kim, E.A. Kim, J. Appl. Polym. Sci. 81 (2001) 684.

[27] R. Fryczkowsky, M. Rom, B. Fryczkowska, Fibres Text. East. Eur. 13 (2005) 141.

[28] R. Hirase, M. Hasegawa, M. Shirai, J. Appl. Polym. Sci. 87 (2003) 1073.

[29] N.-R. Chiou, A.J. Epstein, Synth. Met. 153 (2005) 69.

[30] N.-R. Chiou, A.J. Epstein, Adv. Mater. 17 (2005) 1679.

[31] Complete textile glossary, available from:

http://www.celaneseacetate.com/textile_glossary_filament_acetate.pdf

[32] J. Molina, A.I. del Río, J. Bonastre, F. Cases, Eur. Polym. J. 44 (2008) 2087.

[33] J. Molina, A.I. del Río, J. Bonastre, F. Cases, Eur. Polym. J. 45 (2009) 1302.

[34] J. Mijovi, M. Sun, S. Pejanovi, J.W. Mays, Macromolecules 36 (2003) 7640.

[35] L. Gu, Z. Shen, S. Zhang, G. Lu, X. Zhang, X. Huang, Macromolecules 40 (2007) 4486.

[36] M. Schappacher, A. Deffieux, Macromolecules 38 (2005) 7209.

[37] X.W. Zhang, S.Y. Xu, G.R. Han, Phys. Status Solidi A 201 (2004) 2922.

[38] Y. Wang, Z. Tang, X. Liang, L.-M. Liz-Marzán, N.A. Koto, Nano Lett. 4 (2004) 225.

[39] X.-S. Du, C.-F. Zhou, G.-T. Wang, Y.-W. Mai, Chem. Mater. 20 (2008) 3806.

[40] G.-Q. Zheng, L. Huang, W. Yang, B. Yang, M.-B. Yang, Q. Li, C.-S. Shen, Polymer 48 (2007) 5486.

[41] L. Li, Y.C. Li, C. Ni, J. Am. Chem. Soc. 128 (2006) 1692.

[42] W.-H. Jung, Y.M. Lee, S.P. McCarthy, J. Vinyl Add. Tech. 13 (2007) 76.

[43] J. Huang, R.B. Kaner, Angew. Chem. Int. Ed. 43 (2004) 5817.

[44] J. Desilvestro, W. Schelfele, J. Mater. Chem. 3 (1993) 263.

[45] L. Dall'Acqua, C. Tonin, A. Varesano, M. Canetti, W. Porzio, M. Catellani, Synth. Met. 156 (2006) 379.

[46] L. Dall'Acqua, C. Tonin, R. Peila, F. Ferrero, M. Catellani, Synth. Met. 146 (2004) 213.

[47] Spectral Database for Organic Compounds of the National Institute of Advanced Industrial Science and Technology (AIST). Available from: http://riodb01.ibase.aist.go.jp/sdbs/cgi-bin/cre_index.cgi?lang=eng.

[48] E.T. Kang, K.G. Neoh, K.L. Tan, Prog. Polym. Sci. 23 (1998) 277.

[49] P.C. Rodrigues, M.P. Cantão, P. Janissek, P.C.N. Scarpa, A.L. Mathias, L.P. Ramos, M.A.B. Gomes, Eur. Polym. J. 38 (2002) 2213.

14.- RESUMEN DE RESULTADOS

14.- RESUMEN DE RESULTADOS

En la presente tesis se ha conseguido obtener tejidos conductores de la electricidad basados en el recubrimiento químico de tejidos de poliéster con polipirrol. Dado que durante la síntesis del polipirrol, se generan cargas positivas en la estructura (al presentar un dopado tipo p), se tienen que emplear aniones como contraiones para neutralizar las cargas positivas y mantener el principio de electroneutralidad en el material. En el presente trabajo se han empleado un contraión orgánico (AQSA) y uno inorgánico ($PW_{12}O_{40}^{3-}$). El contraión orgánico sí que había sido empleado en bibliografía, pero el inorgánico es la primera vez que ha sido empleado para obtener tejidos conductores. El uso de ambos contraiones permite comparar sus propiedades morfológicas, químicas, eléctricas y electroquímicas.

El poliéster es un material aislante y presenta una resistividad superficial mayor de 10^{11} $\Omega/\square$. Cuando se realizó la síntesis in-situ de los polímeros conductores la resistividad superficial bajó más de ocho órdenes de magnitud; hasta valores de 40 $\Omega/\square$ para el PES-PPy/AQSA y 250 $\Omega/\square$ para el caso del PES-PPy/$PW_{12}O_{40}^{3-}$. La resistividad superficial cuando se emplea el anión orgánico es menor debido a su estructura plana. La estructura plana del AQSA permite un mayor ordenamiento de las cadenas de polipirrol, lo que permite obtener recubrimientos más conductores pues los polímeros conductores presentan estructuras también planas. El $PW_{12}O_{40}^{3-}$ presenta una estructura tridimensional, por lo que produce polímeros menos conductores. Los análisis de Espectroscopía de Impedancia Electroquímica (EIS) demostraron que el poliéster actúa como un material aislante, comportándose como un condensador (dieléctrico) con valores de 90º de fase. Los tejidos conductores de PES-PPy/AQSA y PES-PPy/$PW_{12}O_{40}^{3-}$ mostraron 0º de fase, lo que indica que ambos presentan un comportamiento resistivo y conductor. Por lo tanto, al depositar la capa de polipirrol el comportamiento eléctrico cambia completamente.

Los análisis de Microscopía Electrónica de Barrido demostraron la formación de una capa uniforme y plana de polipirrol sobre toda la superficie del tejido. El espesor del recubrimiento se estimó en unos 400 nm a partir de la observación del espesor en zonas de rotura del recubrimiento. Los análisis de Energía Dispersiva de Rayos-X demostraron la incorporación de los contraiones en la estructura del polipirrol. En el caso del AQSA la presencia del S indica su incorporación en la estructura. El W y el O indican la

incorporación del contraión en el caso del $PW_{12}O_{40}^{3-}$. La presencia de elementos con un alto peso atómico como el W, permite también obtener micrografías con electrones retrodispersados que muestran la distribución del contraión sobre el tejido. Se observaron también agregados globulares de polipirrol que no fueron eliminados durante la fase del lavado después de la síntesis. Los análisis de FTIR-ATR demostraron la presencia de diferentes bandas atribuidas al polipirrol (1550, 1450, 1300, 1160, 775 y 1030 cm^{-1}) y también a los contraiones (1075 en el caso del $PW_{12}O_{40}^{3-}$ y 1670 y 710 cm^{-1} en el caso del AQSA). Los análisis de Espectroscopía Fotoelectrónica de Rayos-X (XPS) permitieron también cuantificar el contenido del contraión en la estructura del polímero. Otro parámetro importante que se puede obtener mediante los análisis de XPS es el grado de dopaje del polímero, que se define como la relación de los nitrógenos cargados positivamente respecto del contenido total de nitrógeno (N^+/N). Un mayor grado de dopaje implica un polímero con un mayor grado de oxidación y por tanto más conductor. Los análisis de Microscopía Electroquímica de Barrido (SECM) demostraron la electroactividad de los tejidos conductores de PES-PPy/AQSA y PES-PPy/$PW_{12}O_{40}^{3-}$. Para ambos tejidos conductores se obtuvo feedback positivo, lo que indica que el sustrato es electroactivo. En cambio para el poliéster se obtuvo feedback negativo, indicando que el sustrato no es electroactivo.

Los ensayos de lavado realizados sobre las muestras de PES-PPy/AQSA y PES-PPy/$PW_{12}O_{40}^{3-}$ mostraron que el polímero es resistente al lavado, no se produjo una degradación y descarga de color apreciable. Los análisis de Microscopía Electrónica de Barrido no mostraron una degradación apreciable del recubrimiento. En ambos casos, el grado de dopaje (N^+/N) no se modificó sustancialmente; sin embargo se observó la pérdida de parte de los contraiones, traduciéndose en un ligero aumento de la resistividad superficial.

Los ensayos de resistencia al desgaste en seco y en húmedo de las muestras de PES-PPy/$PW_{12}O_{40}^{3-}$ produjeron una pérdida parcial del recubrimiento debido a la abrasión que tiene lugar en la zona de los tomos, como se observó a partir de las micrografías. La zona de los dejos no se ve afectada por el desgaste debido a su menor elevación. Es por ello que la resistividad superficial aumenta debido a la degradación en la zona de los tomos, los valores que se obtuvieron después del ensayo de resistencia al frote fueron de 40 kΩ/□.

Se realizaron también ensayos de estabilidad en disoluciones con diferentes pH con el fin de optimizar el rango operacional de pH donde los tejidos de PES-PPy/AQSA y PES-PPy/PW$_{12}$O$_{40}$$^{3-}$ mantienen unas propiedades eléctricas y electroquímicas aceptables.

Los tejidos conductores de PPy/AQSA son estables en disoluciones con diferentes pH (1-13). A pH ácido (~1) se produce un aumento del grado de dopaje (N^{+}/N), lo que se traduce en una disminución de la resistividad superficial. A pH neutro (~7) las propiedades del recubrimiento no varían apreciablemente. A pH básico (~13) se produce una pérdida de parte del contraión (AQSA) debido a la desprotonación del polipirrol que tiene lugar a pH>10 y por tanto una disminución muy grande del grado de dopaje. La resistividad superficial aumenta menos de dos órdenes de magnitud, lo que es un valor aceptable para el pH básico. Las medidas de SECM mostraron una bajada de la electroactividad a pH básico (valores de I$_T$(L) entre 1.5 y 3); mientras que las muestras tratadas con pH 1 mostraron valores de I$_T$(L) entre 3 y 5.

Los ensayos de estabilidad de los tejidos PES-PPy/PW$_{12}$O$_{40}$$^{3-}$ demostraron su estabilidad a pH ácido y neutro. Sin embargo, a pH 13 se observó la descomposición del PW$_{12}$O$_{40}$$^{3-}$ en PO$_4$$^{3-}$ y WO$_4$$^{2-}$. En este caso sí que se observó un aumento muy grande de la resistividad superficial. A pesar de ello los valores de resistividad superficial continúan siendo 5 órdenes de magnitud menor que los del poliéster, lo que permitiría su empleo en tejidos antiestáticos, donde la resistividad superficial debe ser menor de 5·10^9 Ω/□. Se observó también una pérdida importante de la electroactividad después del tratamiento a pH 13 a partir de las medidas de SECM.

Las medidas de voltametría cíclica mostraron una pérdida de electroactividad con el pH para ambos tejidos conductores (PES-PPy/AQSA y PES-PPy/PW$_{12}$O$_{40}$$^{3-}$), dado que la protonación del polipirrol es un parámetro determinante en la electroactividad del polímero. La protonación y desprotonación del polipirrol tienen lugar a pH 2 y pH 10 respectivamente. Además se ha demostrado que la velocidad de barrido es un parámetro importante que influye en la caracterización mediante Voltametría Cíclica de los tejidos conductores. Velocidades de barrido altas no permiten observar los procesos redox que tienen lugar en los polímeros conductores. En cambio, las velocidades de barrido bajas sí que permiten observar los procesos de oxidación y reducción de los polímeros conductores. En los tejidos conductores el material base es

aislante (poliéster), debido a ello, la transferencia electrónica debe producirse a través del polímero conductor. La transferencia electrónica empieza desde el contacto metálico y se va extendiendo a las partes más alejadas del tejido conductor. La cinética de éste proceso es lenta y por ello sólo las velocidades de barrido bajas permiten observar los procesos redox. Los sustratos más ampliamente empleados para depositar polímeros conductores son los metales, donde la transferencia de carga es instantánea y la cinética es rápida; por lo que éste fenómeno no ha sido descrito.

Los polvos de $PPy/PW_{12}O_{40}^{3-}$ no depositados sobre los tejidos han permitido caracterizar la descomposición térmica del polipirrol mediante termogravimetría. Los contraiones orgánicos se descomponen en el mismo rango de temperaturas que el polipirrol, por lo que con este tipo de contraiones no se podían separar los procesos de degradación del polipirrol y del contraión. En el caso del $PPy/PW_{12}O_{40}^{3-}$, donde se separan los procesos de degradación (el $PW_{12}O_{40}^{3-}$ es estable hasta una temperatura mayor de 1000 ºC). Esta técnica puede ser empleada también para calcular el porcentaje de contraión ($PW_{12}O_{40}^{3-}$), los porcentajes de contraión obtenidos tanto en atmósfera de N_2 como con atmósfera de aire fueron similares a los obtenidos mediante las medidas de XPS. Los análisis de Py-GC-MS mostraron la presencia en los polvos de $PPy/PW_{12}O_{40}^{3-}$ de monómeros de pirrol que no habían sido oxidados durante la síntesis química.

Se obtuvieron también pastillas de $PPy/PW_{12}O_{40}^{3-}$ y PPy/AQSA a partir de la compactación de los correspondientes polvos no depositados sobre los tejidos. Los análisis de Espectroscopía de Impedancia Electroquímica con la temperatura permitieron obtener las energías de activación de los polvos de $PPy/PW_{12}O_{40}^{3-}$ y PPy/AQSA en forma de pastilla. El comportamiento obtenido fue el típico de un material semiconductor, en el que la conductividad aumenta con la temperatura. La conductividad obtenida para las pastillas de PPy/AQSA y $PPy/PW_{12}O_{40}^{3-}$ fue de 0.177 $S \cdot cm^{-1}$ y 0.023 $S \cdot cm^{-1}$ respectivamente (siendo menor en el caso del contraión orgánico debido a que el AQSA presenta una estructura más plana que el $PW_{12}O_{40}^{3-}$). Los análisis de SECM mostraron feedback positivo para ambos polímeros (son electroactivos), obteniéndose también una mayor electroactividad en el caso del PPy/AQSA.

Una vez caracterizados los tejidos conductores, se procedió a realizar la síntesis electroquímica de polímeros conductores sobre los tejidos. La síntesis electroquímica es interesante ya que produce polímeros más ordenados y por tanto más conductores y electroactivos. Por lo que respecta a la síntesis electroquímica de $PPy/PW_{12}O_{40}^{3-}$ sobre tejidos conductores de $PES-PPy/PW_{12}O_{40}^{3-}$, se determinó el potencial al cual tiene lugar la oxidación del monómero para formar el polímero mediante voltametría cíclica. Así pues, se determinó un potencial de síntesis de 1.5 V como el más adecuado para realizar la síntesis electroquímica de polipirrol. El potencial de síntesis en este caso es mayor que en el caso de síntesis sobre metales debido a la caída óhmica que presenta el tejido conductor. Una vez determinado el potencial de síntesis mediante síntesis potenciodinámica se realizó la síntesis potenciostática a este potencial (1.5 V). La síntesis potenciostática produjo un depósito con morfología globular, típica del polipirrol sintetizado electroquímicamente.

Se obtuvieron también dobles capas de polímeros conductores al realizar la síntesis electroquímica de polianilina sobre tejidos de PES-PPy/AQSA. Se ha demostrado la influencia del método de síntesis en la morfología del recubrimiento obtenido para la síntesis de polianilina sobre PES-PPy/AQSA. La síntesis potenciostática produce un recubrimiento de polianilina con morfología globular, primero se recubren superficialmente las fibras y posteriormente se recubren las zonas interfibrilares, recubriéndose el tejido totalmente. La síntesis potenciodinámica a 50 $mV·s^{-1}$ produce la formación de fibras de polianilina durante las primeras fases de síntesis, debido a que durante los primeros barridos el número de sitios de nucleación está limitado. Posteriormente la morfología globular predomina debido a la formación de un mayor número de sitios de nucleación cuando la síntesis avanza. Los análisis de FTIR-ATR demostraron la presencia de diferentes bandas debidas a la polianilina.

La velocidad de barrido es también un parámetro muy importante en la síntesis potenciodinámica de la polianilina. Se ha demostrado la influencia de éste parámetro en la forma de los voltagramas de síntesis, al igual que ocurría con la caracterización de los tejidos conductores mediante esta técnica. Además se ha demostrado que la morfología del recubrimiento también depende de la velocidad de barrido empleada. Para velocidades de barrido altas (50 $mV·s^{-1}$ y 5 $mV·s^{-1}$) se ha demostrado la formación de polianilina con morfología de ciempiés que no ha sido obtenida en bibliografía para los polímeros conductores. Éste crecimiento se produce durante los primeros barridos,

cuando los sitios de nucleación están limitados debido a la alta velocidad de barrido. Primero se produce un crecimiento de fibras de polianilina y sobre estas fibras empiezan a crecer las fibras secundarias, formando la morfología de ciempiés. A mayor número de barridos de síntesis, predomina el crecimiento globular, debido a que se producen un mayor número de sitios de nucleación. Para la velocidad de barrido baja (1 mV·s^{-1}) no se observa la formación de este tipo de morfología debido a que se forman un mayor número de sitios de nucleación desde el principio debido a la baja velocidad de síntesis.

Los recubrimientos electroquímicos de polipirrol y polianilina sobre los tejidos conductores producen en general electrodos con mejores propiedades eléctricas y electroquímicas según han demostrado las medidas de resistividad superficial, Voltametría Cíclica y Espectroscopía de Impedancia Electroquímica. La electroactividad aumenta debido probablemente a la obtención de un polímero con mayor número de conjugaciones dobles y también a una mayor área superficial del recubrimiento.

15.- CONCLUSIONES

15.- CONCLUSIONES

A continuación se exponen las principales conclusiones que se han obtenido a partir de los experimentos realizados:

1.- Se pueden obtener tejidos conductores de poliéster recubierto con polipirrol y con un contraión inorgánico ($PW_{12}O_{40}^{3-}$) con el mismo procedimiento que se emplea en bibliografía cuando se emplean contraiones orgánicos (AQSA). El empleo de un contraión inorgánico no influye en el proceso, obteniéndose un recubrimiento de características morfológicas similares a los obtenidos cuando se emplea un contraión orgánico como el ácido antraquinona sulfónico (AQSA).

2.- La resistividad superficial que se obtiene con el contraión inorgánico es mayor que en el caso de emplear un contraión orgánico (AQSA). Esto es debido a que el $PW_{12}O_{40}^{3-}$ presenta una estructura tridimensional, lo que produce polímeros menos conductores. La estructura plana del AQSA permite un mayor ordenamiento de las cadenas de polipirrol, lo que permite obtener recubrimientos más conductores.

3.- El empleo de un contraión ($PW_{12}O_{40}^{3-}$) que contiene en su estructura un elemento con alto peso atómico (W) permite obtener micrografías mediante electrones retrodispersados y observar la distribución del contraión en la superficie del tejido. A partir de las micrografías se ha observado una distribución homogénea del contraión sobre toda la superficie del tejido, lo que indica un recubrimiento de polipirrol uniforme.

4.- El recubrimiento de $PPy/PW_{12}O_{40}^{3-}$ es resistente al ensayo de lavado, produciéndose sólo un aumento ligero de la resistividad superficial sin pérdida aparente de polímero. Los ensayos de resistencia al frote sí que producen una pérdida del recubrimiento en la zona de los tomos debido a la fricción en las zonas más elevadas del tejido. En la zona de los dejos no se produce degradación del recubrimiento. Ello se traduce en un aumento de la resistividad superficial, aunque menor de lo que cabría esperar a la vista de la degradación sufrida en la zona de los tomos.

5.- Los tejidos de $PES-PPy/PW_{12}O_{40}^{3-}$ son estables en disoluciones de pH 1 y pH 7 y a los ensayos de lavado. Sin embargo no son estables en disoluciones básicas

(pH 13), debido a la descomposición del contraión que provoca una pérdida notable de propiedades eléctricas y electroquímicas. A pesar de la notable pérdida de propiedades eléctricas, podrían ser empleados en tejidos antiestáticos donde la resistividad superficial necesaria debe ser menor de $5 \cdot 10^9$ $\Omega/\square$.

6.- Los tejidos de PES-PPy/AQSA son estables en disoluciones con diferentes pH (1, 7, 13) y a los ensayos de lavado, sin producirse una pérdida notable de la conductividad y electroactividad del recubrimiento. El contraión (AQSA) queda retenido en la estructura, sólo perdiéndose parte del AQSA que estaba en exceso en la estructura del polímero como han demostrado los análisis de XPS.

7.- El potencial para conseguir la síntesis electroquímica de polipirrol sobre el tejido conductor de PES-PPy/PW$_{12}$O$_{40}$$^{3-}$ es de 1.5 V. Este desplazamiento respecto del potencial normal de síntesis sobre un electrodo metálico (0.86 V vs. Ag/AgCl para el acero inoxidable por ejemplo) indica una caída óhmica del material debido a su conductividad limitada.

8.- El recubrimiento electroquímico de PPy/PW$_{12}$O$_{40}$$^{3-}$ mejora las propiedades eléctricas y electroquímicas del tejido conductor debido a la formación de una estructura del polipirrol más ordenada que con la síntesis química.

9.- En la síntesis de polianilina sobre tejidos conductores de PES-PPy/AQSA se observa también un desplazamiento del potencial de síntesis debido a la caída óhmica del material.

10.- El método de síntesis (potenciostático o potenciodinámico) determina la morfología del recubrimiento de polianilina sobre tejidos de PES-PPy/AQSA. La síntesis potenciodinámica produce microfibras de polianilina durante los primeros barridos voltamétricos; posteriormente se produce un crecimiento globular. La síntesis potenciostática produce un recubrimiento con morfología globular desde el principio de la síntesis.

11.- La velocidad de barrido también es un parámetro determinante en la síntesis potenciodinámica de polianilina sobre tejidos de PES-PPy/AQSA. A mayores velocidades de barrido se obtiene polianilina con morfología de ciempiés durante las

primeras fases de crecimiento. Menores velocidades de barrido producen un mayor número de sitios de nucleación y se obtiene polianilina con morfología fibrilar y globular.

12.- El recubrimiento de polianilina mejora las propiedades eléctricas y electroquímicas del tejido original de PES-PPy/AQSA.

13.- Sólo las velocidades de barrido bajas permiten observar los procesos redox que tiene lugar en la caracterización voltamétrica de los tejidos conductores debido a que la transferencia de carga es un proceso lento en este tipo de materiales.

14.- El uso de un contraión inorgánico ($PW_{12}O_{40}^{3-}$) permite obtener información cualitativa y cuantitativa sobre la degradación del polipirrol mediante métodos térmicos, al no degradarse el contraión en el rango de temperaturas estudiado.

15.- Los análisis de termogravimetría son válidos para obtener el grado de dopaje del polímero (contenido del contraión), ya que el contraión ($PW_{12}O_{40}^{3-}$) no se degrada en el rango de temperaturas estudiado. Los resultados obtenidos son similares a los obtenidos mediante otras técnicas como Espectroscopía Fotoelectrónica de Rayos-X (XPS).

16.- EXPERIENCIAS FUTURAS Y NUEVAS LÍNEAS DE TRABAJO

16.- EXPERIENCIAS FUTURAS Y NUEVAS LÍNEAS DE TRABAJO

1. Los recubrimientos de material híbrido polipirrol/$PW_{12}O_{40}^{3-}$ y polipirrol/AQSA han sido sintetizados sobre tejidos de poliéster obteniendo tejidos conductores de la electricidad. Sin embargo el tamaño del tejido que se puede obtener es pequeño debido a la limitación del proceso de síntesis. Para ello se propone continuar la investigación con el recubrimiento de hilos de poliéster para obtener hilos conductores. Posteriormente mediante un proceso de tejeduría se podrían obtener tejidos conductores de la electricidad de mayor tamaño. Este trabajo está siendo desarrollado en el grupo de investigación por el doctorando Eduardo Romero Senabre. Parte del trabajo ya ha sido llevado a cabo en su proyecto final de Máster, "Elaboración de prototipos textiles capaces de conducir la electricidad a través de la síntesis química de polipirrol sobre sustratos textiles", el cual codirigimos el profesor Francisco Cases y yo mismo.

2. Si el proceso de tejido de los hilos conductores de PES-PPy/$PW_{12}O_{40}^{3-}$ o PES-PPy/AQSA resultara satisfactorio, se podría plantear la polimerización en fase gaseosa para la obtención de hilos conductores de forma continua. De esta forma se podría crear un método para realizar tejidos conductores de forma continua, con la síntesis de los polímeros conductores sobre los hilos de poliéster en fase gaseosa [1-3] y el posterior tejido de los hilos para obtener los tejidos conductores.

3. Se debería llevar a cabo también el estudio del apantallamiento electromagnético de los tejidos conductores [4-7] para estudiar posibles aplicaciones en el campo de los tejidos inteligentes. También se podría estudiar la incorporación de LEDS y otros dispositivos electrónicos y estudiar su funcionamiento [8].

4. Uno de los problemas de los tejidos conductores es su pérdida de conductividad con el tiempo debido a la exposición atmosférica y degradación por parte del oxígeno. Por ello sería interesante estudiar la aplicación de recubrimientos que permitieran aislar a los polímeros conductores y preservar sus propiedades eléctricas con el tiempo [9].

5. Otra de las posibles líneas futuras podría ser la obtención de tejidos conductores a partir de otros polímeros conductores menos estudiados como la polianilina [10-12], politiofeno [13], etc. El caso del empleo de la polianilina ya lo hemos empezado a estudiar; se han obtenido los primeros resultados como por ejemplo el cambio de color en los tejidos de polianilina (tejido electrocrómico). El tejido de polianilina presenta color verde amarillento a potenciales de reducción (-1 V vs Ag/AgCl) y un color verde oscuro a potenciales de oxidación (+ 2 V vs Ag/AgCl) (Fig. 14.1).
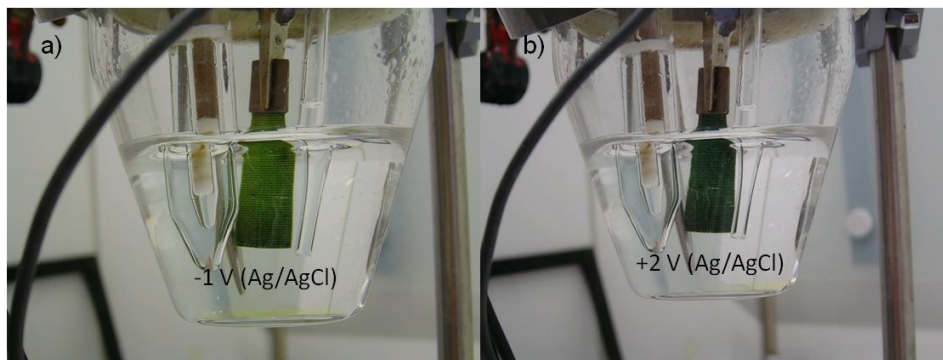

Fig. 15.1. Tejido de poliéster recubierto con polianilina a -1 V (Ag/AgCl) (a) y +2 V (Ag/AgCl) (b); en disolución de H_2SO_4 0.5 M.

6. Se está llevando a cabo también un estudio sobre la síntesis de Platino disperso sobre polímeros conductores depositados sobre diferentes sustratos (electrodos de Pt, tejidos conductores, etc.) con el fin de mejorar las propiedades catalíticas de los electrodos. Con una dispersión de Pt (<100 µg cm^{-2}) se puede alcanzar el mismo efecto que con un electrodo completamente de Pt [14]. El Pt disperso sobre los polímeros conductores ha demostrado aumentar la electroactividad de los recubrimientos frente a la oxidación de moléculas pequeñas como el metanol [15-21], sobre todo pensando en su empleo en células de combustible. El envenenamiento del Pt por adsorción de especies CO, también es menor cuando se encuentra dispersado respecto del metal en su forma normal [15].

El fin del estudio de la dispersión de Pt sería conseguir electrodos con suficiente actividad catalítica y probarlos en la degradación de moléculas de colorantes orgánicos.

BIBLIOGRAFÍA:

[1] S.S. Najar, A. Kaynak, R.C. Foitzik, Synth. Met. 157 (2007) 1.

[2] L. Dall'Acqua, C. Tonin, A. Varesano, M. Canetti, W. Porzio, M. Catellani, Synth. Met. 156 (2006) 379.

[3] A. Kaynak, S.S. Najar, R.C. Foitzik, Synth. Met. 158 (2008) 1.

[4] E. Hakansson, A. Amiet, S. Nahavandi, A. Kaynak, Eur. Polym. J. 43 (2007) 205.

[5] E. Håkansson, A. Amiet, A. Kaynak, Synth. Met. 156 (2006) 917.

[6] M. S. Kim, H. K. Kim, S. W. Byun, S. H. Jeong, Y. K. Hong, J. S. Joo, K. T. Song, J. K. Kim, C. J. Lee, J. Y. Lee, Synth. Met. 126 (2002) 233.

[7] A. Kaynak, E. Håkansson, A. Amiet, Synth. Met. 159 (2009) 1373.

[8] R.F. Service, Science 301 (2003) 909.

[9] L. Dall'Acqua, C. Tonin, R. Peila, F. Ferrero, M. Catellani, Synth. Met. 146 (2004) 213.

[9] D.C. Trivedi, S.K. Dhawan, J. Mater. Chem. 2 (1992) 1091.

[10] R. Fryczkowski, M. Rom, B. Fryczkowska, Fibres Text. East. Eur. 13 (2005) 141.

[11] K.W. Oh, S.H. Kim, E.A. Kim, J. Appl. Polym. Sci. 81 (2001) 684.

[12] S.K. Dhawan, N. Singh, S. Venkatachalam, Synth. Met. 125 (2002) 389.

[13] C.Y. Wang, A.M. Ballantyne, S.B. Hall, C.O. Too, D.L. Officer, G.G. Wallace, J. Power Sources 156 (2006) 610.

[14] M.J. Croissant, T. Napporn, J.-M. Léger, C. Lamy, Electrochim. Acta 43 (1998) 2447.

[15] L. Niu, Q. Li, F. Wei, X. Chen, H. Wang, Synth. Met. 139 (2003) 271.

[16] K. Bouzek, K.-M. Mangold, K. Jüttner, J. Appl. Electrochem. 31 (2001) 501.

[17] L. Niu, Q. Li, F. Wei, S. Wu, P. Liu, X. Cao, J. Electranal. Chem. 578 (2005) 331.

[18] J. Li, X. Lin, J. Electrochem. Soc. 154 (2007) B1074.

[19] H. Laborde, J.-M. Léger, C. Lamy, J. Appl. Electrochem. 24 (1994) 219.

[20] L. Li, Y. Zhang, J.-F. Drillet, R. Dittmeyer, K.-M. Jüttner, Chem. Eng. J. 133 (2007) 113.

[21] S. Domínguez-Domínguez, J. Arias-Pardilla, A. Berenguer-Murcia, E. Morallón, D. Cazorla-Amorós, J. Appl. Electrochem. 38 (2008) 259.

17.- APORTACIONES DE LA TESIS DOCTORAL

17. APORTACIONES DE LA TESIS DOCTORAL

Artículos publicados:

1. J. Molina, A.I. del Río, J. Bonastre, F. Cases. Chemical and electrochemical polymerisation of pyrrole on polyester textiles in presence of phosphotungstic acid. **European Polymer Journal 44 (2008) 2087-2098.**

2. J. Molina, A.I. del Río, J. Bonastre, F. Cases. Electrochemical polymerisation of aniline on conducting textiles of polyester covered with polypyrrole/AQSA. **European Polymer Journal 45 (2009) 1302-1315.**

3. J. Molina, A.I. del Río, J. Bonastre, F. Cases. Influence of the scan rate on the morphology of polyaniline grown on conducting fabrics. Centipede-like morphology. **Synthetic Metals 160 (2010) 99-107.**

4. J. López, F. Parres, I. Rico, J. Molina, J. Bonastre, F. Cases. Monitoring the polymerization process of polypyrrole films by thermogravimetric and X-ray analysis. **Journal of Thermal Analysis and Calorimetry 102 (2010) 695-701.**

5. J. Molina, J. Fernández, A.I. del Río, R. Lapuente, J. Bonastre, F. Cases. Stability of conducting polyester/polypyrrole fabrics in different pH solutions. Chemical and electrochemical characterization. **Polymer Degradation and Stability 95 (2010) 2574-2583.**

Artículos enviados:

1. J. Molina, J. Fernández, A.I. del Río, J. Bonastre, F. Cases. Chemical, electrical and electrochemical characterization of hybrid organic/inorganic polypyrrole/$PW_{12}O_{40}^{3-}$ coating deposited on polyester fabrics. **Artículo enviado a Applied Surface Science**.

2. J. Molina, J. Fernández, A.I. del Río, J. Bonastre, F. Cases. Electrochemical synthesis of polyaniline on conducting fabrics of polyester covered with polypyrrole/$PW_{12}O_{40}^{3-}$. Chemical and electrochemical characterization. **Artículo enviado a Synthetic Metals.**

3. E. Romero, J. Molina, A.I. del Río, J. Bonastre, F. Cases. Synthesis of PPy/$PW_{12}O_{40}^{3-}$ organic-inorganic hybrid material on polyester yarns and posterior weaving for obtaining conducting fabrics. **Artículo enviado a Textile Research Journal.**

4. J. Molina, J. Fernández, J.C. Galván, J. Bonastre, F. Cases. Chemical, physical and electrochemical characterization of polypyrrole doped with organic and inorganic counter ions. **Artículo enviado a Materials Letters.**

Artículos en preparación:

1. J. Bonastre, J. Molina, J. C. Galván, F. Cases. Study of the electrical properties of novel hybrid organic-inorganic conducting textiles of polypyrrole-phosphotungstate-polyester using Electrochemical Impedance Spectroscopy.

2. J. Molina, J. C. Galván, J. Bonastre, F. Cases. Characterization of polypyrrole/phosphotungstate films in different pH solutions by electrochemical impedance spectroscopy.

Capítulos de libro:

1. J. Molina, A.I. del Río, F. Cases, J. Bonastre. Textiles conductores. Modificación superficial con bicapas de polipirrol sintetizadas químicamente y electroquímicamente. **Nuevos desarrollos en materiales para ingeniería. I.S.B.N. 978-84-268-1437-1, pág. 69-82 (2008).** Editorial Marfil S.A.

2. J. Molina, A.I. del Río, F. Cases, J. Bonastre. Electropolimerización de anilina sobre textiles conductores de poliéster recubiertos de polipirrol/$PW_{12}O_{40}^{3-}$. **Nuevos desarrollos en materiales para ingeniería. I.S.B.N. 978-84-268-1437-1, pág. 83-96 (2008).** Editorial Marfil S.A.

Participación en proyectos de investigación:

1. **Proyecto CTM2010-18842-C02-02** del Ministerio de Ciencia y Tecnología. **Título del proyecto:** Tratamiento electroquímico de disoluciones de colorantes reactivos empleados en la industria textil y desarrollo de nuevos materiales electródicos.

2. **Primeros Proyectos de Investigación** de la Universidad Politécnica de Valencia (PAID-06-10).
Título del proyecto: Síntesis química y electroquímica de polímeros conductores intrínsecos sobre poliéster con actividad electrocatalítica mejorada.

Congresos:

1. J. Molina, A.I. del Río, J. Bonastre, F. Cases. Polimerización de pirrol sobre tejidos de poliéster. Inserción de $PW_{12}O_{40}^{-3}$ como contraión en la estructura. **XXIX Reunión del Grupo de Electroquímica**, Lleida (2007).

2. J. Molina, A.I. del Río, J. Bonastre, F. Cases. Synthesis and characterization of conducting textiles of polyester covered with polypyrrole. **21st IFATCC International Congress**, Barcelona (2008).

3. J. Molina, A.I. del Río, J. Bonastre, F. Cases. Electrochemical polymerization of polypyrrole and polyaniline onto conducting textiles of poliéster/polypyrrole. **59th Annual Meeting of the International Society of Electrochemistry**, Sevilla (2008).

4. J. Molina, A.I. del Río, J. Bonastre, F. Cases. Electropolimerización de anilina sobre tejidos de PES/PPy-AQSA. Influencia del método de síntesis. **V Congreso "La Investigación ante la Sociedad del Conocimiento". Sostenibilidad y Medioambiente**, Alcoy (2008).

5. J. Molina, A.I. del Río, J. Bonastre, F. Cases. Electrochemical impedance spectroscopy and X-ray photoelectron spectroscopy study of conducting textiles. **12ª Jornadas de Análisis Instrumental**, Barcelona (2008).

6. J. Molina, A.I. del Río, J. Bonastre, F. Cases. Nanoscale monitoring of morphology during electrochemical growth of polyaniline on conducting fabrics. **5th European Summer School on Electrochemical Engineering**, Almagro (2009).

7. A. García, J. Bonastre, J. Molina, A.I. del Río, F. Cases. Aplicación de materials híbridos polipirrol/polianilina para la protección del acero frente a la corrosión. **VI Congreso "La Investigación ante la Sociedad del Conocimiento". Sostenibilidad y Medioambiente**, Alcoy (2009).

8. J. Molina, J. Fernández, A.I. del Río, J. Bonastre, F. Cases. Electrochemical characterization of polypyrrole-based conducting fabrics in different pH media. **XII Iberic Meeting of Electrochemistry and XVI Meeting of the Portuguese Electrochemical Society**, Lisboa (2010).

Proyectos dirigidos:

1. Trabajo fin de Máster en Ingeniería Textil.

   Título: Elaboración de prototipos textiles capaces de conducir electricidad a través de la síntesis química del polipirrol sobre sustratos textiles.

   Autor: Eduardo Romero Senabre.

   Directores: Francisco Cases Iborra, Javier Molina Puerto.

   Calificación: Matrícula de honor.

2. Trabajo fin de carrera en Ingeniería de Materiales.

   Título: Aplicación de materiales hibridos bicapa de polipirrol/polianilina para la protección frente a la corrosión.

   Autor: Ángel García Ramos.

   Directores: José Antonio Bonastre Cano, Javier Molina Puerto.

   Calificación: Pendiente de presentar.